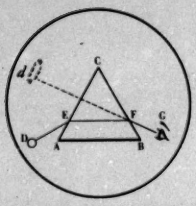

optics and spectroscopy

volume ix
number 2
august 1960

OPTICAL SOCIETY OF AMERICA

USSR ACADEMY OF SCIENCES

RUSSIAN EDITORIAL STAFF FOR
OPTIKA I SPEKTROSKOPIYA sponsored by
USSR ACADEMY OF SCIENCES

Editor: S. E. FRISH

Assistant Editor: P. P. FEOFILOV
Corresponding Secretary: L. S. SAZONOV

Associate Editors:

M. M. GUREVICH M. A. EL'IASHEVICH A. A. LEBEDEV V. P. LINNIK
S. L. MANDEL'SHTAM I. V. OBREIMOV V. K. PROKOF'EV
N. N. SOBOLEV A. N. TERENIN A. I. TUDOROVSKII

Translated from *OPTIKA I SPEKTROSKOPIYA* on the initiative of THE OPTICAL SOCIETY OF AMERICA, INC. with a grant-in-aid from THE NATIONAL SCIENCE FOUNDATION. *Optics and Spectroscopy* is a cover-to-cover translation of *Optika i Spektroskopiya* and no attempt is made to edit the material other than to correct obvious misprints. The views are those of the original authors and do not represent the Optical Society of America.

TRANSLATION EDITORIAL STAFF

Scientific Editors

CYRUS FELDMAN, *Oak Ridge National Laboratory*

CARL W. GARLAND, *Massachusetts Institute of Technology*

MATHEW G. GIBBONS, *Oakland, California*

Administrative Editor: PATRICIA R. WAKELING, *OSA*

Published monthly by the Optical Society of America, Inc. Executive office: 1155 Sixteenth Street, N.W., Washington, D.C. Subscriptions for one year to members of the Society: Associates $13.00; Regular members and Fellows $17.00. Subscriptions for non-members of the Society: One year U. S. and Possessions, $25.00; Foreign $28.00. Back numbers: $3.00 per copy. Subscriptions, changes of address and undeliverable copies should be referred to the Executive offices in Washington, D.C. The office of publication is 2500 South State Street, Ann Arbor, Michigan. Second class postage paid at Ann Arbor, Michigan.

Printed in the U.S.A. by Edwards Brothers, Inc., Ann Arbor, Michigan.

HYPERFINE STRUCTURE AND ISOTOPIC SHIFT IN THE SPECTRUM OF Tl I

A. I. Odintsov

Received 7 December 1959

The Tl I lines 5110, 5350, 5528, 5584, 6550, and 6714 A were investigated using an atomic beam and a Fabry-Perot etalon. The hyperfine splitting and isotopic shifts were determined for the levels $6^2P_{3/2}$, $8^2P_{1/2}$, $8^2P_{3/2}$, $9^2P_{1/2}$, $9^2P_{3/2}$, $10^2P_{3/2}$, and $7^2S_{1/2}$. An improvement was made in the accuracy of normalization of isotopic shifts. On the basis of an analysis of hyperfine structure, conclusions were drawn regarding the interaction of configurations in the thallium atom.

INTRODUCTION

Together with lead and mercury, thallium was one of the first elements whose spectra were used for investigation of the theory of the hyperfine structure (hfs) of spectral lines and the volume effect in the isotopic shift. The spectrum of neutral thallium is of special interest in connection with this theory, because effects such as the mutual perturbation of different configurations and the screening of inner electrons of the atom by the optical electron are strongly pronounced. An increasing amount of attention is being paid to these factors at the present time in the theoretical interpretation of isotopic shifts and the hfs of elements.

The hyperfine and isotopic structure of the Tl I spectrum was investigated in detail by optical methods in refs. 1-5. The hyperfine splittings of the lower levels $6^2P_{1/2}$ and $6^2P_{3/2}$ of this atom were also measured by microwave spectroscopy.[6,7] All of these optical measurements were made using Fabry-Perot etalons whose plates were thin and therefore had low resolving powers. Naturally, many details in the structure of the levels remained unclarified. Thus, the low accuracy of the measurements of the isotopic shifts of the upper P levels of the Tl atom in the work of Schüler and Keyston,[3] and the lack of other investigations which might support their data, made it impossible to perform a reliable correlation of shifts and terms (normalization of shifts[8]). The hyperfine splittings of the P levels of the atom, with the exception of the lower level $6^2P_{1/2}$, also remained unresolved. (An estimate of the splitting of the $6^2P_{3/2}$ level was made,[3] but this disagreed with the results of microwave measurements.)

The goal of the present work is to measure the isotopic shifts in Tl I lines, corresponding to the transitions from higher P levels to the $7^2S_{1/2}$ level (these shifts were not resolved in earlier publications) and to measure the hyperfine splittings of these levels and the $6^2P_{3/2}$ level. Because of the tightness of these structures, it was deemed necessary not only to use very thick Fabry-Perot etalons, but to use an atomic beam as the light source as well. Although thallium is a heavy element, and the Doppler broadening of its lines is not very great, the use of an atomic beam gives a considerably lower limit of resolution than can be obtained with other light sources, such as the hollow cathode. The accuracy of measurement of isotopic shifts obtained using an atomic beam and the natural mixture of thallium isotopes is undoubtedly considerably higher than that obtained with a hollow cathode and separated isotopes.

Table 1. Thickness of Etalons and Number of Interference Patterns Processed

Line (A)	5350	6550	6714	5584	5528	5110
Thickness of etalons (mm)	70 Multiplex 20×100	70	65	70	70	80
		80	70	78	80	
No. of patterns processed	3	3	2	2	2	1

EXPERIMENT AND RESULTS

The light source used in this investigation was an atomic beam excited by electrons. A detailed description is given in ref. 9. Collimations of the beam of 1:6 and 1:10 were used. Some gain in light intensity was obtained in investigating weak lines by placing a spherical mirror behind the beam, as in ref. 10. A Fabry-Perot etalon with dielectric-coated plates was used (reflection coefficient about 90%). Etalons 65-100 mm thick were used. The 5350 A line was also recorded using the compound etalon (multiplex) with 20 mm and 100 mm plates. Preliminary monochromatization of light was performed by means of an ISP-51 spectrograph.

Table 1 shows the thicknesses of the etalons and the number of interference patterns processed for each line.

As an example, the illustration contains the interference pattern of the 5350 A line, obtained using a 20 × 100 mm multiplex.

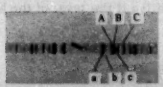

Interference pattern of thallium 5350 A line, obtained using multiplex with 20 and 100 mm thick etalons. A, B, C—components of Tl^{205} isotope; a, b, c—components of Tl^{203} isotope (the components A, B, a, b and the components C, c belong to different orders of interference).

The orders of interference close to the center were used for measurement. The average error of individual measurement was below 0.5×10^{-3} cm^{-1}.

Measurement of the intensity of the components was not the goal of this work. Approximate photometric measurements of intensities were performed only on the 5350 and 6714 A lines. These measurements (as well as the visual evaluation of other lines) showed that the intensities of the hfs components of the lines investigated correspond approximately to their theoretical values.

From the interference pattern of the 6714 A line, obtained using a 70 mm etalon at a 1:10 collimation of the atomic beam, the half-width of the interference rings corresponding to individual components was determined. This value was $5.2 \pm 0.5 \times 10^{-3}$ cm^{-1}. This is equal to the degree of resolution achieved, a fact which is also evident in the resolution of closely neighboring components in the photographs. (Thus, components which were 6×10^{-3} cm^{-1} apart were still resolved fairly well.)

In the 5584 A line, one of the components of the Tl^{203} isotope could not be resolved because of the superimposition of a component of the Tl^{205} isotope. In the 5528 and 5110 A lines, the components corresponding to the splitting of the $9^2P_{3/2}$ and $10^2P_{3/2}$ levels were not resolved. In each case, a weak component, whose intensity (theoretical) was about 20% of the neighboring strong component, remained unresolved. The slight shift suffered by the strong component when an unresolved weak component was superimposed was taken into consideration by introducing the necessary corrections (not exceeding 0.5×10^{-3} cm^{-1}). The value of this shift was determined by graphic addition of contours with corresponding intensities and half-widths, separated by a distance equal to the distance between components. Contours having the form of dispersion curves with half-widths from 5×10^{-3} to 7×10^{-3} cm^{-1} were used (depending on the thickness of the etalon and the collimation of the atomic beam). The intensities of the components were assumed to be equal to the theoretical values. The distance between components could be determined in all cases with sufficient accuracy from the previously measured values of level splitting. Similar corrections for the shift of a weak component in the vicinity of a strong one were introduced in working up the interference patterns of 6550 and 6714 A, although in this case, as with 5350 A, all components were resolved.

The results obtained are presented in Table 2.

All levels investigated exhibited the normal order of distribution of hfs levels. When the splitting of the $9^2P_{3/2}$ and $10^2P_{3/2}$ levels was determined from 5528 and 5510 A the splitting values of the $7^2S_{1/2}$ level found from other lines were used.

The isotopic shift was determined from the displacement of the centers of gravity of the components of the Tl^{203} and Tl^{205} lines, using the theoretical values for component intensities. In correlating shifts with terms, the shift of the $10^2S_{1/2}$ level was assumed to be zero. The shift was called positive if the level of the heavier isotope was higher.

Table 2. Values of Isotopic Shifts and Hyperfine Splittings of Levels of Tl I (10^{-3} cm^{-1})

Level	Isotopic shift $Tl^{205}-Tl^{203}$	Hyperfine splitting		Lines used (A)
		Tl^{205}	Tl^{203}	
$7^2S_{1/2}$	+14.9	406.4	410.0	5350, 6550, 6714, 5584
$6^2P_{3/2}$	−44.0	17.3	17.5	5350
$8^2P_{1/2}$	− 0.4	25.9	26.3	6714
$8^2P_{3/2}$	− 0.8	8.8	8.7	6550
$9^2P_{1/2}$	+ 1.1	—	13.1	5584
$9^2P_{3/2}$	− 0.1	3.8	3.5	5528
$10^2P_{1/2}$	0	2.3	2.3	5110

DISCUSSION OF RESULTS

Isotopic shift. In general, our measurements confirm the data of Schüler and Keyston,[3] although the differences amount to as much as 15×10^{-3} cm^{-1} for some lines. In addition to establishing more accurate values of the relative shifts of levels, the accurate values obtained for the shifts of higher P levels make possible a correct normalization of shifts. The fact that the shifts of the $8^2P_{1/2}$, $8^2P_{3/2}$, $9^2P_{1/2}$, $9^2P_{3/2}$, and $10^2P_{3/2}$ levels appear, with a high degree of accuracy, to be equal, shows that the shifts on these levels are not distorted by perturbations and consequently are close to the shift caused by the atomic residue $5d^{10}6s^2$, which can be assumed to be zero. Assuming the shift of the $10^2P_{3/2}$ level to be zero is somewhat arbitrary.

Out normalization of isotopic levels agrees in general with that given by Schüler and Keyston. At first glance, this normalization contradicts the theory of volume effect in isotopic shift, which predicts a positive sign for the shift of the levels. According to the theory of volume effect, the shift of the $6p_{1/2}$ electron should be close to zero, while the shift of the 7s electron should be approximately $+27 \times 10^{-3}$ cm^{-1} (the latter value was obtained by using the isotopic shift constant of thallium found from Tl II and Tl III spectra[11]). After the theory of volume effect was formulated, doubts were expressed concerning the correctness of Schüler and Keyston's normalization. It was shown later, however, that consideration of the screening of inner electrons (mainly $6s^2$ electrons) by the optical electron, made it possible to explain the shift observed.[12]

Hyperfine structure. Our hyperfine splitting values for the $7^2S_{1/2}$ level are considerably more accurate than previous values. (For instance, in comparison with ref. 3 the discrepancies reach 11×10^{-3} cm^{-1}.) Our values for the splitting of the $6^2P_{3/2}$ level agree within experimental error with microwave data.[7] Splitting of the other levels investigated was not measured in earlier publications.

Table 2 shows that the splitting values for the levels are somewhat different for the two isotopes. For all levels except $7^2S_{1/2}$, and possibly $6^2P_{3/2}$ and $8^2P_{1/2}$, these differences are within experimental error. For the $7^2S_{1/2}$ level, which possesses a high degree of splitting, a proportionality may be established between the splitting and the magnetic moments of the isotope nuclei. The value of the splitting ratio is

$$\frac{\Delta\nu(203)}{\Delta\nu(205)} = 0.9912 \pm 0.001,$$

while the ratio of magnetic moments[13]

$$\frac{\mu(203)}{\mu(205)} = 0.9903.$$

It is interesting to note that on the lower levels, $6^2P_{1/2}$ and $6^2P_{3/2}$, which were investigated by microwave methods, a deviation from this proportionality between splitting and magnetic moments was observed. This deviation was explained by influence of the size of nucleus.[6,7] The expected value of this deviation for the $7^2S_{1/2}$ level is about 0.03% of the splitting ratio (this value is beyond the limits of accuracy of our measurements). The values obtained for the splitting of the $8^2P_{1/2}$ and $9^2P_{1/2}$ levels are in good agreement with theoretical values calculated from the usual formulas for hfs.[12]

In the hfs of lower levels of Tl I, a well-known anomaly is observed; namely, the ratio of the values of splitting of the $6^2P_{1/2}$ and $6^2P_{3/2}$ levels differs considerably from the ratio predicted by the theory (40.25 against 6.04).[7] A similar anomaly, although less pronounced, is

observed in the spectra of Al, Ga, and In.[12] The opinion has been expressed[14] that the hfs of the $6^2P_{1/2}$ level is badly distorted because of perturbation by the levels of the 6s6p7s configuration, which are somewhat above the ionization potential of the atom. A calculation of this disturbance, performed for the gallium atom, gave satisfactory agreement with experimentally observed ratio of splittings.[15] In the case of the higher levels of thallium, 8^2P, 9^2P, and 10^2P, which are located considerably nearer to the levels of the 6s6p7s configuration than the lower levels 6^2P, considerable distortion of the hfs (even the reversal of hfs levels) might be expected. However, according to our measurements, the ratio of the splitting values

$$\frac{\Delta\nu(P_{1/2})}{\Delta\nu(P_{3/2})}$$

is 3.0 for 8^2P levels and 3.6 for 9^2P levels, while the theoretical value of ratio of splittings is 4.6 in both cases.[12] Thus, the anomaly observed in the hfs of the 6^2P levels does not exist here; on the contrary, the splitting ratio is somewhat lower than the theoretical value. From this it follows that the 8^2P and 9^2P levels, and apparently the $10^2P_{3/2}$ level, are not appreciably disturbed by the 6s6p7s configuration.

One of the causes of the decreased value of the ratio of the splitting ratio

$$\frac{\Delta\nu(P_{1/2})}{\Delta\nu(P_{3/2})}$$

of higher levels may be the perturbation of these levels by the lower atomic levels $6^2P_{1/2}$ and $6^2P_{3/2}$. Such perturbations, caused by spin-orbital interaction, were first studied by Fermi in order to explain the abnormal value of ratio of intensities in the doublets of the main series of alakline metals.[16] The method of calculation of perturbations used by Fermi would lead to large errors when applied to heavy atoms. Nevertheless, it may be used for obtaining an approximate evaluation of the degree of effect of the perturbation on the hfs of higher P levels of Tl I. We performed such a calculation for the 8^2P and 9^2P levels. The calculation indicated that these perturbations should decrease the value of the ratio

$$\frac{\Delta\nu(P_{1/2})}{\Delta\nu(P_{3/2})}$$

for these levels by a factor of approximately 1.4.

Unfortunately, the $7^2P_{1/2}$ and $7^2P_{3/2}$ levels could not be examined in this investigation, since their lines fall in the infrared region. The characteristics of the isotopic shift and hyperfine structure of these levels should have values falling between those of the lower and higher levels.

In conclusion, the author wishes to express his gratitude to F. A. Korolev for selection of the topic and direction of this work.

REFERENCE

1. H. Schüler and H. Bruck, Z. Physik **55**, 578 (1929).
2. J. Wulf, Z. Physik **69**, 70 (1931).
3. H. Schüler and I. E. Keyston, Z. Physik **70**, 1 (1931).
4. O. A. Jackson, Z. Physik **75**, 233 (1932).
5. H. Kopfermann and W. Walcher, Z. Physik **122**, 465 (1944).
6. A. Lurio and A. G. Prodell, Phys. Rev. **101**, 79 (1956).
7. G. Go, Phys. Rev. **101**, 1828 (1956).
8. G. Breit, Phys. Rev. **42**, 348 (1932).
9. A. I. Odintsov, Opt. i Spektr. **6**, 398 (1959), Optics and Spectroscopy **6**, 250 (1959).
10. L. G. Mundie and K. W. Meissner, Phys. Rev. **65**, 265 (1944).
11. P. Brix and H. Kopfermann, Revs. Modern Phys. **30**, 517 (1958).
12. H. Kopferman, "Kernmomente." Frankfurt am Main, 1956.
13. H. S. Gutowsky and B. R. McGarvey, Phys. Rev. **91**, 81 (1953).
14. E. Fermi and E. Segre, Z. Physik **82**, 729 (1933).
15. G. F. Koster, Phys. Rev. **86**, 148 (1952).
16. E. Fermi, Z. Phys. **59**, 680 (1929).

A SPECTROSCOPIC DETERMINATION OF THE ISOTOPIC COMPOSITION OF CARBON

A. N. Zaidel and G. V. Ostrovskaya

Received 18 November 1959

A spectral method for the determination of isotopic composition of carbon was worked out, based on photoelectric measurement of the intensities of $C^{13}O$ and $C^{12}O$ bands produced in an electrodeless high frequency discharge. The range of concentrations studied was 1.1-58% C^{13}. In the determination of low concentrations of C^{13} (1-5%), the coefficient of variation was 5-7%. When the C^{13} content was 5-60%, the coefficient of variation was 2-3%. Gas consumption per analysis was 0.1-0.2 cm^3; the time required for an analysis, 10-15 min.

The carbon isotope C^{13} was observed in 1929 by King[1] in the Swan bands of the C_2 molecule. It was not until 1956, however, that Ferguson and Broida utilized these bands for a spectral determination of the isotopic composition of carbon.[2] The analysis was performed by comparing the intensities of the 1,0 band heads in the $^3\Pi-^3\Pi$ Swan system of the molecules $C^{12}C^{12}$ and $C^{12}C^{13}$. The spectrum was produced in the flame of an acetylene burner and was recorded photoelectrically. The apparatus used in our spectral determination of the isotopic composition of carbon was the same as that used earlier for the isotopic analysis of hydrogen.[3,4] In this apparatus the spectrum is produced by an electrodeless high frequency discharge and is registered by a grating monochromator and photomultiplier.

DESCRIPTION OF EXPERIMENTS

Carbon, enriched in the heavy isotope, was available to us as gaseous methane containing about 18% air. In the spectrum of a discharge tube filled with methane, all of the C_2 and CH bands which are suitable for the determination of the isotopic composition of carbon are weak and are not free of the superimposed rotational structure of other molecular bands. In addition to this, as a result of operating the discharge in methane, the discharge tube blackens rapidly because of deposition of carbon on its walls. This not only decreases the quantity of radiation emitted, but also considerably increases the "memory" of the discharge tube (i.e., distortion of results of the analysis because of contamination of the tube by the preceeding portions of gas.) In order to avoid this, oxygen was introduced into the tube along with the methane. In this case, the discharge tube remained transparent for a considerable length of time, and intense CO bands (Angstrom system) appeared in the spectrum. Among the CO bands, the $C^{12}O$ band at 4123.6 A is the most convenient one for spectral analysis, especially when the C^{13} content is low, since the head of the corresponding band of the $C^{13}O$ molecule is displaced 8.2 A toward the red from the $C^{12}O$ band and is free from its superimposed rotational structure (the Angstrom bands are degraded to the violet).

The work was done in the second order of a diffraction grating having 600 lines/mm, using a spectral width of 0.8 A for both the input and output slits of the monochromator. The discharge tube, cooled by running water, was a glass capillary of 2 mm inner diameter equipped with external electrodes.

In order to reduce the "memory" of the discharge tube, the analysis was done in a flowing stream of gas. The time needed for rinsing out the discharge tube from the previous sample was about 2 min. The flow system and the apparatus for the excitation and photoelectric registration of the spectrum were similar to those we used in our isotopic analysis of hydrogen.[3,4] In determining low concentrations of C^{13}, the sensitivity of the amplifier was reduced on changing from the $C^{13}O$ band to the $C^{12}O$ band. This improved our accuracy in measuring the intensity ratio of these bands. Examples of recordings of bands at different concentrations are given in Fig. 1. The recording shows a band of N_2, λ = 4141.8 A, caused by contamination of methane by air. In order to compensate for the overlapping of the nitrogen band with the CO band, the necessary correction was applied. In order to do this, we investigated the intensity distribution of this nitrogen band in pure nitrogen. The intensity of this band was measured at the position of the heads of the $C^{13}O$ (a) and $C^{12}O$ (b) bands as a function of the intensity of the head of the N_2 band. This ratio was measured under conditions identical to those prevailing during the recording of the spectrum in isotopic analysis (using the same dispersion and slit width). The intensity was always measured from the minimum between the nitrogen band and the head of the $C^{13}O$ band. The scheme used for measuring the correction factors a and b and the intensities is shown in Fig. 2, in which the broken line signifies the wing of the nitrogen band. In principle,

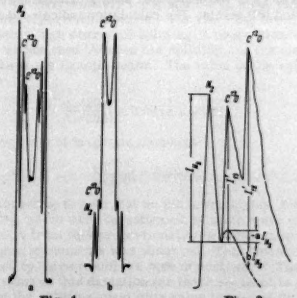

Fig. 1

Fig. 2

Fig. 1. Examples of recordings of CO bands at C^{13} concentrations 58% (a) and 22% (b).
Fig. 2. Diagram of measurements of correction factors, a and b, and intensities.

it is immaterial whether the intensity is measured from the above-mentioned minimum or from the background. The reproducibility of results is better, however, when the intensity is measured from the minimum between the N_2 band and the $C^{12}O$ band-head than when it is measured

from the background. This probably is explained by the fact that the intensity, inhomogeneity, and instability of the continuous spectrum are lower in this region than in front of the head of the N_2 band. The relationship between the corrections a and b obtained in this manner and the gas pressure in the discharge tube is presented in Fig. 3. The change of sign of correction factor a near 1.5 mm Hg is caused by a redistribution of intensity in the nitrogen band with changing pressure. It was shown that the correction factor a depends on the total gas pressure in the discharge tube, not on the partial pressure of nitrogen.

The intensity ratio I_{13}/I_{12} was calculated by means of the formula:

$$\frac{I_{13}}{I_{12}} = \frac{I'_{13} + aI_{N_2}}{I'_{12} + bI_{N_2}}$$

where I_{13}, I_{12}, and I_{N_2} are the intensities of the $C^{13}O$, $C^{12}O$, and N_2 bandheads, calculated from the valley between N_2 band and the $C^{13}O$ edge (see Fig. 2). The justification for the introduction of the correction factor for the overlapping of the nitrogen band is given in the Table, which lists the ratios of the intensities of the bands of the isotopic molecules without correction for the overlapping of the nitrogen band (a) and with this correction (b). The Table shows that when the correction factor is used, the ratio I_{13}/I_{12} remains constant within experimental error (~3%) even in the presence of 33% nitrogen. Under these conditions the intensity of the nitrogen band is 50 times greater than the intensity of the $C^{13}O$ edge. In our experiments, which were performed in the presence of 18% air in methane enriched in C^{13}, the intensity of the N_2 band was approximately equal to the intensity of the edge of $C^{13}O$ band. Thus the error due to any inaccuracy in the correction factors a and b was considerably lower than incidental errors in the measurement of the intensity ratio.

Concentration of N_2	$\frac{I_{13}}{I_{12}}$	
	a	b
0	0.036	0.036
0.8	0.037	0.036
1.7	0.039	0.037
3.4	0.037	0.035
4.2	0.038	0.035
7.2	0.041	0.037
12.0	0.045	0.037
33	0.079	0.038

Because of the simultaneous presence in the discharge tube of methane, nitrogen, and oxygen, a strong and uneven background existed in the region of the CO bands. Irregularity of the background under $C^{13}O$ and $C^{12}O$ bands is probably the main reason for the deviation of the intensity ratio I_{13}/I_{12} from the isotopes concentration ratio C_{13}/C_{12}, which is especially significant in the low C^{13} concentration range. The change of background associated with the change of conditions of analysis is produced by the dependence of I_{13}/I_{12} on the gas pressure in the discharge tube and on the concentration of oxygen in the gas mixture. At low C^{13} concentrations, the ratio I_{13}/I_{12} has a minimum at 2.2 mm Hg. The maximum emission intensity is obtained at the same pressure. It was shown that when the oxygen concentration in the gas mixture is higher than 50%, the ratio I_{13}/I_{12} is independent of oxygen concentration. In the presence of a deficiency of oxygen, the intensity of the CO bands decreases while the background remains almost constant, which leads to an increase in I_{13}/I_{12}. For this reason, all measurements were done at 2.2 mm pressure and an oxygen concentration higher than 50%.

At intermediate concentrations of C^{12} and C^{13}, the irregularity of the background has less of an effect on I_{13}/I_{12}; however, even in this case this ratio is not equal to C^{13}/C^{12}, since the $C^{13}O$ band overlaps the edge of the $C^{12}O$ band and increases the intensity of the latter. It is probably the change of the shape of bands associated with pressure changes in the discharge tube which leads to the dependence of I_{13}/I_{12} on pressure (Fig. 4). For this reason, the pressure in the discharge tube was kept constant to within 0.1 mm Hg during all measurements. Maintaining the pressure within the above accuracy limits was achieved by changing the capillaries of the flow system and by choosing the proper inlet pressure for the gas (about 3-5 mm). The pressure was measured with an oil manometer, permitting readings accurate to 0.05 mm Hg.

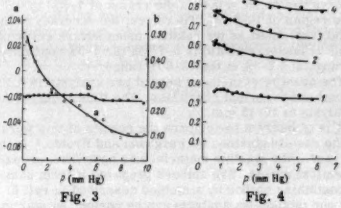

Fig. 3

Fig. 4

Fig. 3. Relationship between correction factors a and b and gas pressure in the discharge tube.
Fig. 4. Relationship between I_{13}/I_{12} and gas pressure in the discharge tube. Concentrations of C^{13} (in %): curve 1—31; curve 2—43; curve 3—51; curve 4—58.

EXPERIMENTAL RESULTS AND DISCUSSION

Because of the uneven background and the overlapping of the $C^{13}O$ and $C^{12}O$ bands, the determination of the isotopic composition of carbon was performed using a calibration graph prepared from standard mixtures. The standard mixtures were prepared by mixing enriched methane containing 58% C^{13} with natural methane containing 1.11% C^{13}. The incidental error in preparation of standards, caused by inaccuracy in volume and pressure measurements, was approximately 1%. The error in the determination of the C^{13} concentration in the starting material and the inaccuracy in the determination of the air impurity led to a systematic error in preparation of standards of approximately 2%. This systematic error, producing a displacement of calibration curve, could have been avoided if we had had available a more accurately analyzed starting mixture of isotopes.

The calibration curve, made from standards, is shown in Fig. 5. This figure shows that interpolations can be carried out over the entire region investigated, by means of two straight lines. Therefore it appears to be convenient to use 2 separate graphs for analysis: one corresponding to C^{13} concentrations of 1-5% and another one corresponding to concentrations of 5-60% C^{13}, each made from 3 or 4 points.

The accuracy of the concentration measurements is determined by the slope of the graph and by the accuracy of the measurements of the intensity ratio of the isotope

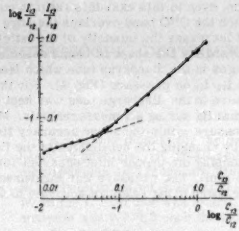

Fig. 5. Calibration curve.

bands. The accuracy of measurements of intensities is 2-3% over the whole concentration range, but the slope of the curve varies from 0.4 (in the region of 1-5%) to 0.9 (in the region of 10-60%). Therefore, the accuracy of the method, expressed as the relative mean square error of individual measurements, is 5-7% in the 1-5% concentration range and 2-3% in the 10-60% range.

The quantity of methane needed per analysis is 0.10-0.20 cm³ under normal conditions. The time required for an analysis is 10-15 min.

It is of interest to compare the results of this work with the results obtained by Ferguson and Broida.[2] In the latter work, the starting material was acetylene, prepared by chemical means. The authors prepared it from samples containing carbon by a method described in ref. 5. Using our method, an analysis can be performed starting with any gaseous carbon compound, since CO bands are readily produced in a high frequency discharge when oxygen and carbon-containing compounds are present. Obviously, when methane is replaced by another gas, the calibration curve may be distorted because of changes in the background under the bands of CO molecules. For this reason, a new calibration graph should be constructed whenever a new starting gas is used. The question of the stability of the calibration graph will be investigated in the future. It should be mentioned that there is a considerable consumption of enriched acetylene (about 100 cm³ per analysis) by the method of Broida and Ferguson, as well as possible errors (especially at low C^{12} concentrations) because of the inconsistent CO_2 content in air. When the method described here is used, the latter error is excluded completely and gas consumption may be limited to 0.1 cm³. The accuracy of the determinations of isotopic composition achieved in both publications is approximately equal.

In conclusion, the authors express their gratitude to I. G. Gvartsitel for supplying C^{13}-enriched methane.

REFERENCES

1. A. S. King and R. T. Birge, Nature **124**, 127 (1929).
2. R. E. Ferguson and H. P. Broida, Anal. Chem. **28**, 1436, (1956).
3. G. V. Veinberg, A. N. Zaidel, and A. A. Petrov, Opt. i Spektr. **1**, 972 (1956).
4. A. N. Zaidel and G. V. Ostrovskaya, Vestnik Leningrad. Gosudarst. Univ., No. 16, Ser. Fiz. i Khim. 39 (1959).
5. Calvin, "Isotopic Carbon," p. 205. Wiley, New York, 1949.

INTENSITY DISTRIBUTION IN THE BANDS OF THE α-SYSTEM OF THE TiO MOLECULE

F. S. Ortenberg

Received 24 October 1959

The dependence of the electronic transition moment R_e on the internuclear separation in the limits $1.58\ A < r < 1.72\ A$ was established for the α-system of TiO using a semiempirical method. More accurate values of relative transition probabilities $p_{v'v''}$ were determined for this band system. Pyrometric formulas are obtained for the determination of the gas temperature from the relative intensity of the TiO α-system bands.

The work of Canadian astrophysicists[1-4] shows that it is possible to find relative transition probabilities of the electronic-vibrational spectra of diatomic molecules taking account of the dependence of the electronic transition moment R_e on the internuclear separation. Using their method we computed the Franck-Condon factors $q_{v'v''}$ and the r-centroids for the α-system of the TiO molecule. Using Phillips' experimental data[5] we determined the dependence of R_e on r and also the "smoothed" transition probabilities for this band system.

When one cannot assume that the electronic transition moment is independent of the internuclear separation, the formula for the relative transition probability of the band may be written in the form

$$p_{v'v''} = \left| \int \psi_{v'} R_e(r)\, \psi_{v''} dr \right|^2, \qquad (1)$$

where $\psi_{v'}$ and $\psi_{v''}$ are the vibrational wave functions. However, in many cases[3,4] some average internuclear distance $\overline{r}_{v'v''}$ called the r-centroid can be assigned to each band, thus Eq. (1) becomes considerably simpler. The r-centroid for the $v' - v''$ transition is defined as follows:

$$\overline{r}_{v'v''} = \frac{\int \psi_{v'} r \psi_{v''} dr}{\int \psi_{v'} \psi_{v''} dr}. \qquad (2)$$

and has the following important property

$$\int \psi_{v'} f(r)\, \psi_{v''} dr = f(\overline{r}_{v'v''}) \int \psi_{v'} \psi_{v''} dr. \qquad (3)$$

Using the property (3) in Eq. (1) we have

$$p_{v'v''} = R_e^2(\overline{r}_{v'v''}) \left| \int \psi_{v'} \psi_{v''} dr \right|^2$$

or

$$p_{v'v''} = R_e^2(\overline{r}_{v'v''})\, q_{v'v''}, \qquad (4)$$

where $q_{v'v''}$ and are the Franck-Condon factors.

If experimental values of probabilities $p_{v'v''}{}_{exp.}$ are available, the dependence of R_e on $\overline{r}_{v'v''}$ can be found

with the help of (4), if $q_{v'v''}$ and $\bar{r}_{v'v''}$ are first computed for the whole band system.

We calculated the Franck-Condon factors $q_{v'v''}$ for the system $C^3\Pi - X^3\Pi$ of the TiO molecule using the Morse "simplified" potential method.[6] The following values of the molecular constants (taken from ref. 7) were used

	ω_e	$\omega_e\chi_e$	r_e
$C^3\Pi$	837.86	4.546	1.695
$X^3\Pi$	1008.4	4.61	1.620

Table 1 shows the results of these calculations. They are in good agreement with numerical integration results based on Morse potentials since the expression

$$\frac{|a_1 - a_2|}{a_1 + a_2} \cdot |r_{e1} - r_{e2}| \cdot 100,$$

which characterizes the size of the error of the simplified potential method, is sufficiently small (0.03%).

Table 1

v' \ v''	0	1	2	3	4
0	0.366	0.358	0.162	0.045	0.008
1	0.327	0.003	0.228	0.243	
2	0.161	0.164	0.076		
3	0.059	0.172			
4	0.018				

r-Centroids are determined graphically.[3] In order to do this the right side of the equation

$$E_{v'} - E_{v''} = D_1[1 - e^{-a_1(r'_{v'v''} - r_{e1})}]^2 - D_2[1 - e^{-a_2(r'_{v'v''} - r_{e2})}]^2 \quad (5)$$

was calculated and plotted as a function of $\bar{r}_{v'v''}$.

The value of the energy difference found for each band allowed us to find the corresponding value of the r-centroid from the graph. Figure 1 shows obtained results in the form of a graph of r-centroids versus band wavelength $\lambda_{v'v''}$.

Equation (4) shows that the quantities $(p_{v'v''}/q_{v'v''})^{1/2}$ plotted as a function of the corresponding $r_{v'v''}$ values will give the direction of the change of R_e with the change of the internuclear separation. In order to find $(p_{v'v''}/q_{v'v''})^{1/2}$ we used experimental values of transition probabilities $p_{v'v''}$ exp. for the α-system of the TiO molecule, obtained with the help of the photoelectric method in a King's oven.[5] The dots on Fig. 2 show the values of $(p_{v'v''}$ exp.$/q_{v'v''})^{1/2}$ for the seven most intensive bands of this system. The function

$$R_e(r) = e^{4.98 - 2.57r} \quad (6)$$

is a good representation of the dependence of the electronic transition moment of the α-system of the TiO molecule on the internuclear distance within the limits $1.58 \text{ A} < r < 1.72$ A. The constants in Eq. (6) are determined by fitting the curve $\ln(p_{v'v''}$ exp.$/q_{v'v''})^{1/2}$ versus $\bar{r}_{v'v''}$ to a straight line using the least squares method.

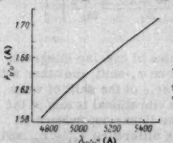

Fig. 1

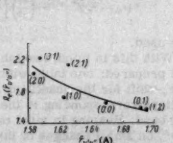

Fig. 2

Fig. 1. Dependence of $\bar{r}_{v'v''}$ on the wavelength.

Fig. 2. Dependence of the electronic transition moment on the internuclear separation.

The maximum value of the relative deviation of the electronic transition moment from the mean, $\Delta R/\bar{R}$, is equal to 0.17. This shows that it is necessary to take account of the dependence of R_e on r in a relative probabilities calculation. To account for this dependence "smoothed" values of $R_e^2(\bar{r}_{v'v''})$ determined from Eq. (6) were multiplied by the corresponding Franck-Condon factors $q_{v'v''}$. "Smoothed" relative values of transition probabilities $p_{v'v''}$ obtained in this way are shown in the last column of Table 2 on a scale such that $p_{00} = 1.000$. These values of $p_{v'v''}$ were used to obtain pyrometric formulas which determine the gas temperature from relative band intensities in the progressions $\Delta v = -1$, $\Delta v = +1$, and $\Delta v = +2$ of the α-system. According to ref. 8, the following relationship holds for the Boltzmann distribution of molecules over the vibrational levels

$$0.624 \cdot \frac{E_1(v') - E_2(v')}{T} = 4 \lg \frac{\lambda_2}{\lambda_1} + \lg \frac{p_1}{p_2} + \lg \frac{I_1}{I_2}, \quad (7)$$

where λ_1, p, and I are respectively wavelengths, relative probability values, and intensities of the two bands of a given system, and $E_1(v') - E_2(v')$ is the difference of the vibrational energies corresponding to the initial levels of the same bands.

Table 2

v', v''	$\lambda_{v'v''}$ (in Å)	$\bar{r}_{v'v''}$ (in Å)	$p_{v'v''}$ (exp.)	$p_{v'v''}$ (calc.)
0,0	5167	1.659	1.000	1.000
0,1	5448	1.703	0.877	0.781
1,2	5497	1.711	0.550	0.476
1,0	4954	1.625	0.962	1.063
2,1	5003	1.632	0.740	0.514
2,0	4761	1.588	0.652	0.633
3,1	4804	1.596	0.829	0.849

Substituting the values of ω_e, $\omega_e\chi_e$, λ, and p, given above, into Eq. (7) we obtain the following formulas for pairs of bands corresponding to transitions (1, 2) and (0, 1), (2, 1) and (1, 0), and (3, 1) and (2, 0).

$$\frac{517}{T} = -0.231 + \lg \frac{I_{5448}}{I_{5497}}, \quad (8)$$

$$\frac{512}{T} = -0.333 + \lg \frac{I_{4954}}{I_{5003}}, \quad (9)$$

$$\frac{506}{T} = -0.004 + \lg \frac{I_{4761}}{I_{4802}}. \quad (10)$$

In conclusion let us note that when the vibrational temperature is measured from the relative intensity of these bands (in the interval up to 2500°K), the relative error in the temperature determination does not exceed twice the error of the intensity measurement.[9]

REFERENCES

1. R. W. Nicholls, Proc. Phys. Soc. **A69**, 741 (1956).
2. R. G. Turner and R. W. Nicholls, Can. J. Phys. **32** 475 (1954).
3. R. W. Nicholls and W. R. Jarmain, Proc. Phys. Soc. **A69**, 253 (1956).
4. P. A. Fraser, Can. J. Phys. **32**, 515 (1954).
5. J. G. Phillips, Astrophys. J. **118**, 274 (1953).
6. P. A. Fraser and W. R. Jarmain, Proc. Phys. Soc. **A66**, 1145 (1953).
7. G. Herzberg, "Molecular Spectra and Molecular Structure I. Diatomic Molecules. Van Nostrand, New York, 1950.
8. L. V. Leskov, Opt. i Spektr. **4**, 168 (1958).
9. L. V. Leskov and L. P. Vasil'eva, Izvest. Akad. Nauk Ser. Fiz. **22**, 696 (1958).

CALCULATION OF THE RELATIVE TRANSITION PROBABILITIES FOR CERTAIN BAND SYSTEMS OF OXIDES AND HYDRIDES OF THE GROUP II ELEMENTS

F. S. Ortenberg

Received 20 November 1959

The relative transition probabilities of the following systems of oxides and hydrides of the elements of group II in the periodic system were calculated using the Bates' method and the Morse "simplified" potential method:

$B^1\Sigma^+ \longrightarrow X^1\Sigma^+$ BeO,
$B^1\Sigma \longrightarrow X^1\Sigma$ MgO,
$A^1\Sigma \longrightarrow X^1\Sigma$ BaO,
$A^2\Pi \longrightarrow X^2\Sigma$ MgH,
$A^2\Pi \longrightarrow X^2\Sigma$ CaH.

The electronic-vibrational spectra of diatomic molecules are particularly interesting in connection with the study of the physical processes which take place in various light sources. The radiation of diatomic molecules is observed in the spectra of gas discharge plasma and shock waves, in the laboratory and technical flames, and in star atmospheres. Many quantitative measurements on these sources require the knowledge of transition probabilities. However, the electronic-vibrational transition probabilities for diatomic molecules are known only for a small number of compounds. We lack data on transition probabilities for many molecules, the spectra of which were observed in various sources and have therefore been thoroughly investigated. The oxides and hydrides of the group II elements of Mendeleev's periodic system are among these molecules. These oxides and hydrides are undoubtedly interesting, however, with the exception of Leskov's calculation[2] on the second infrared system of CaO, there are no theoretical or experimental studies on the optical transition probabilities for these compounds.[1]

In this work the Franck-Condon factors $q(v'v'')$ were calculated for certain band systems of BeO, MgO, BaO, MgH, and CaH. The Franck-Condon factors $q(v', v'')$ are equal to the square of the overlap integral

$$(v', v'') = \int \psi_1^{(v')} \psi_2^{(v'')}\, dr, \tag{1}$$

where $\psi_1^{(v')}$ and $\psi_2^{(v'')}$ are the vibrational wave functions of the molecule in the levels v' and v'' of the electron states 1 and 2, such that the transition $1 \rightarrow 2$ takes place between these two states. If one assumes that the electronic transition moment R_e depends but slightly on r, then the magnitudes of the Franck-Condon factors are approximately equal to the values of the relative transition probabilities in the band system which corresponds to the given electronic transition.

We calculated the quantities $q(v', v'')$ using two methods: the perturbation method of the harmonic wave functions and the Morse "simplified" potential method.

In the perturbation method the values of the Franck-Condon factors are determined using Bates' tables.[3] In the simplified potential method[4] the overlap integrals were calculated with the help of the following formulas:

$$\frac{(v', v'')}{(0, 0)} = (-1)^{(v'+v'')} \cdot \frac{N_1^{(v')} N_2^{(v'')}}{N_1^{(0)} N_2^{(0)}} \sum_{n=0}^{v'+v''} (-1)^n \frac{\Gamma(k-1-v)}{\Gamma(k-1)} \times \sum_{m=0}^{n} C_{v'}^{m} C_{v''}^{n-m} \rho_1^{m} \rho_2^{n-m} \frac{\Gamma(k_1-v'-1)\,\Gamma(k_2-v''-n+m)}{\Gamma(k_1-v'-n)\,\Gamma(k_2-v''-n+m)} \tag{2}$$

and

$$(0, 0) = \left(\frac{1}{\rho_1}\right)^{\frac{k_1-1}{2}} \left(\frac{1}{\rho_2}\right)^{\frac{k_2-1}{2}} \frac{\Gamma(k-1)}{\left(\Gamma(k_1-1)\,\Gamma(k_2-1)\right)^{1/2}}. \tag{2}$$

The magnitudes of the ratios of the normalizing factors $N_i^{(v)}$ were determined from the ratio of the adjacent normalizing factors and given by the formula

$$\frac{N_i^{(v)}}{N_i^{(v-1)}} = \left[\frac{k_i - v}{v} \cdot \frac{k_i - 2v - 1}{k_i - 2v + 1}\right]^{1/2}. \tag{3}$$

Gamma functions were calculated using Stirling's formula. All calculations were carried out on a ten key semiautomatic calculating machine.

The most reliable values of the molecular constants which were used to calculate probabilities are given in Table 1. The sources of these constants are also given in this table. The constants α_i, k_i, ρ_i used to calculate transition probabilities with the method of α-averaging of the Morse potential function, and the quantities

$$\frac{|\alpha_1 - \alpha_2|}{|\alpha_1 - \alpha_2|} \cdot |r_{e1} - r_{e2}| \cdot 100,$$

which characterize the accuracy of the method are also given in Table 1. For the values

$$\frac{|\alpha_1 - \alpha_2|}{|\alpha_1 + \alpha_2|} \cdot |r_{e1} - r_{e2}| \cdot 100 < 0.25\%\ \text{A}$$

results of the calculations are in good agreement with the numerical integration data based on the Morse potential.

Results were improved for BaO when the r_e-shift was accounted for and Pillow's formulas[5]

$$\left.\begin{aligned} b_{\alpha i}^{(v)} &= \left(\frac{3v+2}{2k_i}\right)\left(\frac{b\alpha_i}{a^2}\right), \\ \delta\,(r_{e1} - r_{e2})^{(v', v'')} &= \left(\frac{b\alpha}{a^2}\right)\left\{\frac{3v'+2}{2k_1} + \frac{3v''+2}{2k_2}\right\}. \end{aligned}\right\} \tag{4}$$

were used.

With this in mind, two tables of overlap integrals were prepared: one table with no r_e-shift, the other with the r_e-shift for the quantities δr_{e1} of the shift of wave functions corresponding to the vibrational levels of the (2, 2) band. Bearing in mind the linear dependence of (v', v'') on small changes of the difference $r_{e1} - r_{e2}$ and using the formula (4), improved values of the overlap integrals for the whole band system[6] were determined with the help of these tables by means of interpolation and extrapolation.

Tables 2-6 give the results of these calculations. In these tables the values of the Franck-Condon factors

Table 1. Values of the Molecular Constants Used in These Calculations

Molecule	μ	State	ω_e (cm^{-1})	$\omega_e x_e$ (cm^{-1})	r_e (A)	Reference	κ_e (Λ^{-1})	k_e	N	$\left\|\frac{\omega_1-\omega_2}{\omega_1+\omega_2}\right\| \cdot \left\|r_{e_1}-r_{e_2}\right\|$ (% A)
BeO	5.76612	$B^1\Sigma^+$	1370.817	7.7455	1.3022	[7]	1.83732	141.61	1.01221	0.33
		$X^1\Sigma^+$	1487.323	11.8297	1.3308		2.02346	153.65	0.98808	
MgO	9.59888	$B^1\Sigma$	824.08	4.76	1.737	[8]	1.65607	105.88	0.98611	0.03
		$X^1\Sigma$	785.06	5.18	1.749		1.72759	158.03	1.01429	
BaO	14.3311	$A^1\Sigma$	500	1.6	2.133	[9]	1.17318	274.74	1.02611	1.20
		$X^1\Sigma$	669.81	2.054	1.940		1.33925	368.05	0.97518	
MgH	0.96748	$A^2\Pi$	1611.3	40.5	1.6795	[10]	1.53361	44.935	0.99964	0.31
		$X^2\Sigma$	1495.7	31.5	1.7306		1.35252	47.711	1.00035	
CaH	0.983332	$A^2\Pi$	1333	20	1.99	[7]	1.08650	67.096	0.99361	0.01
		$X^2\Sigma$	1299	19.5	2.002		1.07284	65.775	1.00647	

Table 2. BeO; $B^1\Sigma^+ - X^1\Sigma^+$ (Blue Green System)

v' \ v''	0	1	2	3	4
0	0.994 (0.885)	0.001 (0.111)	0.001 (0.005)	0.000 (0.000)	0.000 (0.000)
1	0.001 (0.107)	0.984 (0.675)	0.001 (0.146)	0.003 (0.014)	— (0.002)
2	0.000 (0.000)	0.001 (0.173)	0.968 (0.500)	— (0.277)	— —
3	0.000 (0.000)	0.002 (0.022)	— (0.231)	— (0.363)	— —
4	0.000 (0.000)	— (0.000)	— —	— —	— —

Table 3. MgO; $B^1\Sigma - X^1\Sigma$ (Green System)

v' \ v''	0	1	2	3
0	0.980 (0.934)	0.017 (0.015)	0.000 (0.000)	0.000 (0.000)
1	0.018 (0.017)	0.943 (0.901)	0.038 (0.034)	0.000 (0.000)
2	0.000 (0.000)	0.036 (0.033)	0.912 (0.860)	— (0.086)
3	0.000 (0.000)	0.002 (0.001)	— (0.053)	— (0.326)

Table 4. BaO; $A^1\Sigma - X^1\Sigma$ (System 5976 A)

v' \ v''	0	1	2	3	4	5	6
0	0.009 (0.009) [0.010]	0.044 (0.046) [0.047]	0.102 (0.112) [0.114]	0.158 (0.175) [0.178]	0.180 (0.229) [0.199]	0.158 (0.182) [0.166]	0.113 (0.139) [0.132]
1	0.040 (0.038) [0.039]	0.121 (0.119) [0.121]	0.151 (0.145) [0.150]	0.088 (0.081) [0.085]	— (0.025) [0.021]	— —	— —
2	0.094 (0.083) [0.085]	0.155 (0.144) [0.151]	0.073 (0.061) [0.057]	— (0.009) [0.019]	— —	— —	— —
3	0.147 (0.132) [0.135]	0.102 (0.088) [0.101]	— (0.005) [0.009]	— —	— —	— —	— —
4	0.181 (0.150) [0.161]	— (0.004) [0.010]	— —	— —	— —	— —	— —
5	0.184 (0.142) [0.165]	— —	— —	— —	— —	— —	— —
6	0.160 (0.182) [0.177]	— —	— —	— —	— —	— —	— —

obtained with the Bates' method and with the Morse simplified potential method are shown without brackets and in round brackets, respectively. In Table 4 the quantities in square brackets are calculated taking account of the r_e-shift.

Table 5. MgH; $A^2\Pi - X^2\Sigma$ (System 5211 A)

v' \ v''	0	1	2	3	4
0	0.939 (0.942)	0.056 (0.055)	0.005 (0.004)	0.000 (0.000)	0.000 (0.000)
1	0.060 (0.059)	0.832 (0.822)	0.102 (0.100)	0.001 (0.044)	— (0.001)
2	0.001 (0.000)	0.121 (0.096)	0.719 (0.725)	— (0.136)	— —
3	0.001 (0.000)	0.012 (0.001)	— (0.172)	— (0.590)	— —
4	0.000 (0.000)	— 0.000	— —	— —	— —

Table 6. CaH; $A^2\Pi - X^2\Sigma$ (System 6946 A)

v' \ v''	0	1	2	3
0	0.988 (0.992)	0.003 (0.001)	0.000 (0.000)	0.000 (0.000)
1	0.003 (0.003)	0.978 (0.985)	0.007 (0.007)	0.000 (0.000)
2	0.000 (0.000)	0.007 (0.006)	0.962 (0.979)	— (0.012)
3	0.000 (0.000)	0.001 (0.000)	— (0.008)	— (0.732)

REFERENCES

1. V. I. Kolesnikov and L. V. Leskov, Uspekhi Fiz. Nauk **65**, 3 (1958).
2. L. V. Leskov, Opt. i Spektr. **4**, 168 (1958).
3. D. Bates, Monthly Notices Roy. Astron. Soc. **112**, 614 (1952).
4. P. A. Fraser and W. R. Jarmain, Proc. Phys. Soc. **A66**, 1145 (1953).
5. M. E. Pillow, Proc. Phys. Soc. **A64**, 772 (1951).
6. W. R. Jarmain and P. A. Fraser, Proc. Phys. Soc. **A66**, 1153 (1953).
7. G. Herzberg, "Molecular Spectra and Molecular Structure I. Diatomic Molecules." Van Nostrand. New York, 1950.
8. A. Lagerquist and U. Uhler, Arkiv. Fysik **1**, 459 (1949).

9. A. Lagerquist, E. Lind, and R. F. Barrow, Proc. Phys. Soc. **A63**, 1132 (1950).
10. R. Barrow, A. Caunt, D. Downie, R. Herman, E. Huld, A. Mekellar, E. Miescher, B. Rosen, and K. Wieland, Constantes selectionnes Donnes Spectroscopiques concernant les molecules diatomiques. Paris, 1951.

ROTATIONAL ANALYSIS OF BORON MONOXIDE BANDS LOCATED IN THE VACUUM ULTRAVIOLET

Yu. Ya. Kuzyakov, V. M. Tetevskiy, and L. N. Tunitsky

Received 23 November 1959

This paper presents a rotational analysis of the bands (1,0) and (2,0) of the transition $^2\Pi \rightarrow {}^2\Sigma$ of the BO molecule. The rotational constants for the state $^2\Pi$ are $B_0 = 1.4759$, $\alpha = 0.0170$.

An investigation of the discharge spectrum in BF_3 in the region from 1300 to 2100 A was carried out by Chretien[1] on a vacuum spectrograph with a grating having a radius of curvature of 1 meter and dispersion of 8.3 A/mm. Chretien found bands in the region from 1700 to 1900 A having limits, numeration, and relative intensity as shown in Table 1.

Table 1. Numeration v′ and v″, Relative Intensity of the Bands j, and Wave Number of the Limit ($\nu_{lim.}$), of the BO Molecule as Discovered by Chretien

v′, v″	j	$\nu_{lim.}$ (cm^{-1})	v′, v″	j	$\nu_{lim.}$ (cm^{-1})
(2,3)	0	53422	(0,0)	4	56376
(1,2)	0	53952	(2,1)	0	57030
(0,1)	2	54517	(1,0)	3	57647
(2,2)	0	55222	(3,1)	1	58231
(1,1)	1	55790	(2,0)	1	58865

The limits of the bands satisfy the formula

$$\nu_{lim.} = 56870 + 1300\left(v'' + \frac{1}{2}\right) - 15\left(v'' + \frac{1}{2}\right)^2 - 1886\left(v'' + \frac{1}{2}\right) + 14\left(v'' + \frac{1}{2}\right)^3$$

with vibration constants ω_e'' and $\omega_e''x_e''$ approximately equal to the vibration constants of the ground state of the BO molecule. On this basis, Chretien predicted the existence of a new state of the molecule BO, and conditionally assigned the band to the transition $^2\Pi \rightarrow x^2\Sigma$ of the BO molecule, where $x^2\Sigma$ is the ground state of the molecule. In the work of Zelenskaya and Tunitskiy[2] the arc spectrum was obtained in the vacuum ultraviolet on a DFS-5 spectrograph with resolving power 120,000 and dispersion of 2.7 A/mm. As a source of light, the authors used an impulse discharge tube. The photography of the spectrum was carried out on Schumann plates. The known lines in BI and BII were used as internal standards for determination of the wavelengths. The authors erroneously assumed that the bands in the region 1700-1900 A, which were conditionally assigned by Chretien to the transition $^2\Pi \rightarrow x^2\Sigma$ of the BO molecule, belonged to a hydrogen compound. A more detailed investigation of the bands concerned has confirmed the accuracy of Chretien's assignment.

This research presents an analysis of the fine structure of the (0,0) and (1,0) bands according to Chretien's numeration. On the basis of research done in our laboratory by A. A. Mal'tsev and V. M. Tatevskiy on the isotope shift in the BO bands, it was shown that the numeration given by Chretien should be corrected by 1, so that the bands investigated in our work are in fact the bands (1,0) and (2,0). That is, this paper concerns the interpretation of the bands (1,0) and (2,0) of the transition $^2\Pi \rightarrow x^2\Sigma$ of the BO molecule, located in the region from 1300 to 2100 A, and the determination of the rotational constants of the $^2\Pi$ state.

METHOD OF INTERPRETATION OF THE SPECTRUM

The interpretation of the spectrum was carried out on the basis of the assumption that the band considered belongs to the transition $^2\Pi \rightarrow x^2\Sigma$ of the BO molecule. The state $^2\Pi$ corresponds to a coupling intermediate between the cases Hund (a) and Hund (b). The formulas for the branches in this case have the form:[3,4]

$$\left.\begin{aligned}
R_2(K-1) &= \nu_0 - B' + B''K + \frac{B'}{2}\sqrt{4K^2 + \lambda(\lambda-4)} \\
&\quad + (B'-B'')K^3 + 2(D'+D'')K^3 + (D'-D'')K^4, && \text{(a)}\\
R_1(K-2) &= \nu_0 - B' - 2B'' + 3B''K - \frac{B'}{2}\sqrt{4K^2 + \lambda(\lambda-4)} \\
&\quad + (B'-B'')K^2 - 2(D'-3D'')K^3 + (D'-D'')K^4, && \text{(b)}\\
Q_2(K) &= \nu_0 - B' - B''K + \frac{B'}{2}\sqrt{4K^2 + \lambda(\lambda-4)} + (B'-B'')K^2 \\
&\quad + (D'-D'')K^3, && \text{(c)}\\
Q_1(K-1) &= \nu_0 - B' + B''K - \frac{B'}{2}\sqrt{4K^2 + \lambda(\lambda-4)} \\
&\quad + (B'-B'')K^2 + (D'-D'')K^3, && \text{(d)}\\
P_2(K+1) &= \nu_0 - B' - 2B'' - 3B''K + \frac{B'}{2}\sqrt{4K^2 + \lambda(\lambda-4)} \\
&\quad + (B'-B'')K^3 + 2(D'-3D'')K^3 + (D'-D'')K^4, && \text{(e)}\\
P_1(K) &= \nu_0 - B' - B''K - \frac{B'}{2}\sqrt{4K^2 + \lambda(\lambda-4)} + (B'-B'')K^2 \\
&\quad - 2(D'+D'')K^3 + (D'-D'')K^4. && \text{(f)}
\end{aligned}\right\} \quad (1)$$

The $Q_1(K)$ and $Q_2(K)$ branches are especially intense. In the band (1,0) the branches $Q_1(K)$ and $Q_2(K)$, far from the limits, were separated directly. Close to the limits (for small K), where the lines were poorly resolved, the Loomis-Wood diagram[5] was used for separating the branches. The branches $R_2(K)$, $R_1(K)$, $P_2(K)$, and $P_1(K)$, and the numeration in the branches were determined from the condition of the coincidence of the first and second combination differences

$$\Delta_1 F''(K) = R(K) - Q(K+1) = Q(K) - P(K+1), \quad (2)$$

$$\Delta_2 F''(K) = R(K-1) - P(K+1), \quad (3)$$

with the respective combination differences known from the literature.[6] The magnitude of the splitting λ was

found to be so small that it could not be observed because of the resolving power of the spectrograph. In the (2,0) band the $Q_1(K)$ and $Q_2(K)$ branches could be singled out directly for small K. However, the determination of the numeration in the $Q_1(K)$ and $Q_2(K)$ bands was found to be difficult for two reasons. On the one hand, the first and second combination differences may be satisfactorily identified with the values known from the literature for more than one system of numeration; on the other hand, the position of the limit of the $R_2(K)$ branch cannot be determined by reason of its low intensity (the limit of the $R_2(K)$ branch is formed from lines with $K \leqslant 4$) and the fact that the lines of neighboring bands are superposed. Therefore the numeration of the lines in the band (2,0) was established in the following manner. Using the formulas

$$Q_2(K) - Q_1(K-1) = -2B''K + B'\sqrt{4K^2 + \lambda(\lambda-4)}, \qquad (4)$$

$$\frac{Q_2(K) + Q_1(K-1)}{2} = \nu_0 - B' + (B' - B'')K^2, \qquad (5)$$

obtained from Eqs. (1c) and (1d), the wave numbers of the lines of the $Q_1(K)$ and $Q_2(K)$ branches of the (1,0) band, and the value $B_2'' = 1.77229$ taken from ref. 7, the value of the rotational constant B′ was computed by a method of averaging, and also the magnitude of the doublet splitting λ. The value of $\lambda(\lambda - 4)$ was found to be equal to 944.6. We took the same value of $\lambda(\lambda - 4)$ for the (2,0) band. Furthermore, we give an approximate numeration to the lines of the $Q_1(K)$ and $Q_2(K)$ branches of the (2,0) band. In such a numeration, using formulas (1) for $Q_1(K)$ and $Q_2(K)$, for several of the lines located as far as possible from one another and the value found for $\lambda(\lambda - 4)$, determinations were made of the constants $\nu_0 - B'$, $B' - B''$, and $D' - D''$. From the values of $\nu_0 - B'$, $B' - B''$, $D' - D''$, $(B'/2)\sqrt{4K^2 + \lambda(\lambda-4)}$ and B'', it is possible to compute the probable branch completely. Numeration was selected on the basis of a satisfactory agreement of the computed and experimentally determined branch. In the case of an incorrectly chosen numeration, the discrepancy between computed and experimental wave numbers of the lines was found to be considerable.

After the determination of the numeration for the $Q_2(K)$ branch, and with the known combination differences $\Delta_1F''(K)$, the position of the limit of the $R_2(K)$ branch was determined. Comparison of the microphotograms of the (1,0) and (2,0) bands showed that the intensity of the limit of the (2,0) band corresponds to that of the limit of the (1,0) band. Furthermore, the wave number of the limit found for the $R_2(K)$ branch, $\nu_{R_2\,\mathrm{lim.}}$, is equal to 57,646.9 cm^{-1}, in agreement with the data of Chretien. According to his data, the wave number of that limit is equal to 57,647 cm^{-1}. Chretien obtained the spectra in a gas discharge tube, from a water cooled glow discharge; therefore the fine structure was missing, and only the first lines forming the limit were present. Thus one should conclude that the position of the limits and their wave numbers were accurately determined in the work of Chretien. From the Q(K) branches and the combination differences $\Delta_1F''(K)$ and $\Delta_2F''(K)$ the lines of the $R_1(K)$, $R_2(K)$, $P_1(K)$, and $P_2(K)$ branches were determined. The results of the interpretation of the fine structure of the (1,0) and (2,0) bands are presented in Tables 2 and 3.

Table 2. Wave Numbers of the Lines of the (1,0) Band (in cm^{-1})

K	$R_1(K)$	$Q_1(K)$	$P_1(K)$	$Q_1(K)$ computed	$R_2(K)$	$Q_2(K)$	$P_2(K)$	$Q_2(K)$ computed
2	56342.6	56331.8	—	56332.6	56377.9	—	—	
3	345.7	331.8	56320.7	331.8	377.9	56366.7	—	56367.5
4	345.7	330.3	317.3	330.4	377.9	364.1	56351.5	363.8
5	345.7	327.9	312.5	328.2	375.8	360.1	345.7	359.6
6	345.7	324.9	307.4	325.4	374.5	354.6	339.8	354.9
7	345.7	322.6	301.0	321.8	371.0	351.5	330.3	349.6
8	345.7	317.3	293.8	317.5	371.0	342.6	322.6	343.8
9	342.6	312.6	286.0	312.6	368.7	338.0	312.5	337.4
10	338.0	306.2	275.6	306.9	361.8	330.3	301.0	330.4
11	335.0	299.8	267.5	300.6	356.8	322.6	291.6	323.3
12	330.3	293.8	256.4	293.7	351.5	314.1	280.7	314.3
13	324.9	284.9	247.9	286.0	345.7	306.2	267.5	305.5
14	320.7	275.6	235.5	277.7	339.8	295.8	256.4	296.3
15	315.0	267.5	224.4	268.7	331.8	286.0	243.7	286.9
16	307.4	259.1	211.6	259.0	324.9	275.6	230.6	276.5
17	301.0	247.9	195.9	247.7	317.8	264.1	217.6	265.4
18	291.6	237.1	185.0	237.7	307.4	254.4	202.0	253.7
19	281.5	224.4	169.6	226.0	299.8	243.7	185.8	241.4
20	275.6	211.6	153.7	213.7	288.0	230.6	170.1	228.4
21	264.1	202.0	139.2	200.7	277.7	211.6	153.7	213.7
22	254.2	185.8	123.8	187.1	267.5	202.0	136.9	200.5
23	243.7	171.7	105.2	172.8	256.4	185.0	119.6	185.6
24	230.6	158.9	088.9	157.9	243.7	169.6	100.9	170.5
25	217.3	142.6	070.3	142.3	230.6	154.2	082.7	154.5
26	203.3	126.0	051.2	126.0	217.6	136.9	062.7	137.1
27	190.0	108.4	030.9	108.2	202.0	120.6	043.3	120.1
28	174.8	092.6	010.0	091.7	185.8	102.2	022.6	102.7
29	158.9	073.1	55991.7	073.1	170.1	083.8	001.1	084.7
30	142.6	054.4	968.3	054.4	154.2	064.6	55979.0	065.0
31	128.8	034.4	945.4	035.1	136.9	045.2	956.2	045.2
32	110.3	015.3	922.1	014.9	119.6	025.3	933.1	024.8
33	092.9	55994.1	901.4	55994.1	102.2	003.9	908.6	003.7
34	073.1	972.9	874.7	972.6	082.7	55982.6	884.0	55982.0
35	054.4	950.3	849.9	950.5	062.7	959.8	858.8	958.6
36	035.4	927.5	824.3	927.7	043.3	936.6	832.8	936.1
37	013.3	905.1	798.6	904.2	022.6	911.9	807.1	912.9
38	—	879.9	770.9	880.0	001.1	888.4	779.7	888.5
39	—	855.4	—	855.4	55979.0	863.6	751.3	863.5
40	—	830.4	—	829.7	956.2	838.3	—	838.3
41	—	804.2	—	803.6	933.1	811.9	—	811.6
42	—	776.5	—	776.8	908.6	784.8	—	784.8
43	—	—	—	—	—	756.1	—	756.9

Table 3. Wave Numbers of the Lines of the (2,0) Band (in cm^{-1})

K	$R_1(K)$	$Q_1(K)$	$P_1(K)$	$Q_1(K)$ computed	$R_2(K)$	$Q_2(K)$	$P_2(K)$	$Q_2(K)$ computed
2	—	—	—	—	57646.9	57639.9	—	57639.8
3	57615.9	—	—	—	646.9	636.2	57629.1	636.6
4	615.9	57601.0	—	—	646.9	633.3	623.3	632.9
5	615.9	597.7	57583.0	57597.4	644.3	628.1	615.9	628.5
6	615.9	595.4	574.1	594.3	644.3	623.3	607.4	623.6
7	615.9	590.4	571.1	590.5	639.9	618.0	597.7	618.0
8	611.4	586.8	561.1	586.0	636.2	611.4	590.4	611.0
9	607.4	580.2	554.8	580.7	633.3	606.2	580.2	605.7
10	57605.1	57574.1	57545.3	57574.7	57629.1	57597.7	57571.1	57598.0
11	603.2	566.7	535.0	568.0	623.3	589.0	559.7	580.1
12	597.7	559.7	524.2	560.7	618.0	580.2	545.3	581.6
13	592.6	547.4	512.5	552.5	611.4	571.1	535.0	572.5
14	589.0	543.1	501.0	543.7	605.1	561.1	520.8	562.8
15	580.2	535.0	490.3	534.2	597.7	551.4	506.4	552.4
16	574.1	525.3	480.2	524.1	589.0	540.3	495.8	541.4
17	566.5	512.5	461.5	513.0	580.2	529.1	480.5	529.8
18	559.7	501.0	448.2	501.4	571.1	515.9	465.2	517.3
19	545.3	490.3	432.1	488.1	561.1	503.0	448.2	504.4
20	535.0	475.8	416.5	476.0	551.4	490.3	432.1	490.7
21	526.0	461.1	400.9	462.4	540.1	475.8	416.5	476.7
22	512.5	448.2	383.3	447.6	529.1	461.1	399.0	461.8
23	501.0	432.1	365.8	432.9	515.9	444.6	380.4	446.7
24	490.3	416.5	347.2	417.2	501.0	430.0	361.2	429.9
25	475.8	400.9	327.6	400.7	485.8	412.7	341.4	413.1
26	461.1	382.3	307.5	383.6	471.5	395.4	319.4	395.9
27	448.2	365.8	288.2	365.8	457.7	376.4	298.6	377.5
28	430.0	347.3	265.8	347.1	441.8	357.7	278.5	358.5
29	412.7	327.6	244.9	327.9	424.0	336.1	256.0	339.0
30	395.4	307.5	222.0	308.0	406.6	319.4	231.8	318.8
31	378.7	286.9	199.1	287.5	388.5	298.6	209.1	298.0
32	361.2	265.8	174.7	266.5	373.7	278.5	185.3	276.5
33	341.4	224.9	148.4	244.6	—	256.0	161.5	254.3
34	325.2	222.0	124.4	222.0	333.0	231.8	135.5	232.4
35	303.4	199.1	087.8	198.6	312.5	209.1	109.4	207.8
36	278.5	174.7	070.9	174.7	289.1	184.7	082.0	183.6
37	258.2	149.4	044.3	149.9	269.6	158.8	055.1	158.5
38	234.4	124.4	015.0	124.3	244.9	133.3	024.0	132.9
39	212.0	097.6	986.0	098.3	219.3	105.3	—	106.7
40	185.3	070.9	956.4	071.4	195.0	078.5	—	079.7
41	161.5	043.3	925.2	043.9	170.5	051.4	—	052.0
42	130.4	015.4	893.8	015.4	144.4	022.8	—	023.6
43	109.4	56986.0	862.3	56986.7	118.4	56994.2	—	56994.4
44	082.5	956.4	—	957.0	56091.4	964.2	—	964.1
45	—	—	—	—	063.2	933.3	—	934.2
46	—	—	—	—	036.3	901.4	—	903.1
47	—	—	—	—	009.4	869.2	—	871.2

COMPUTATION OF ROTATIONAL CONSTANTS

The rotational constants of the upper state, $^2\Pi$, were computed by two methods. In the first method, the rotational constants were determined from the formula for the branches $Q_1(K)$ and $Q_2(K)$ by an averaging procedure,

Table 4. Rotational Constants of the $^2\Pi$ State of the BO Molecule

From band (1, 0).	From band (2, 0)
$\nu_0 = 354.3$ cm^{-1}, $\lambda = +32.8$ cm^{-1} for the normal term,	$\nu_0 = 623.8$ cm^{-1}, $\lambda = +32.8$ cm^{-1} for the normal term,
$\lambda = -28.8$ cm^{-1} for the inverse term,	$\lambda = -28.8$ cm^{-1} for the inverse term.
$B' = 1.4589$, $D' = -8.3 \cdot 10^{-6}$,	$B' = 1.4419$, $D' = -8.2 \cdot 10^{-6}$,
$B_0 = 1.4759$ $\alpha = 0.0170$, $D'_0 = -8.3 \cdot 10^{-6}$	

using the wave numbers of all the lines of the branches. The values $B''_0 = 1.77229$ and $D''_0 = -6.4 \times 10^{-6}$, used in computing the rotational constants of the upper state, are known to a high precision; they were obtained from ref. 7. The computation also permitted the determination of ν_0 in formulas (1).

In the second method, the rotational constants of the upper state B' were determined from the combination relations $\Delta_2 F(K)$. In this computation the lines having values of K from 23 to 40 were used. The values of the rotational constants computed from the combination relations agreed within the limits of experimental accuracy with the values computed from the branches Q(K). In view of the fact that the lines of the branches $Q_1(K)$ and $Q_2(K)$ are more intense than the lines of R(K) and P(K), and the wave numbers of the lines of the branches Q(K) were determined with higher precision, the rotational constants as presented in Table 4 include only those values obtained by using the first of the two methods mentioned.

Tables 2 and 3 show a comparison of the experimental values of the wave numbers of the branches $Q_1(K)$ and $Q_2(K)$, with values as computed by use of our rotational constants. It is evident that the experimental and calculated values of the wave numbers are in excellent agreement.

REFERENCES

1. M. Chretien, Helv. Phys. Acta **23**, 259 (1950).
2. L. G. Zelenskaya and L. N. Tunitskiy, Mater. X Vses. soveshch. po spektr. (Proceedings of the 10th All Union Conference on Spectroscopy). Vol. 1, p. 289, 1957.
3. F. A. Jenkins, Phys. Rev. **35**, 315 (1930).
4. R. S. Mulliken, Revs. Modern Phys. **3**, 89 (1931).
5. G. Herzberg, "Molecular Spectra and Molecular Structure. I. Spectra of Diatomic Molecules," 2nd ed., Van Nostrand, New York, 1950.
6. J. Funke and C. F. E. Simons, Proc. Acad. Sci. Amsterdam **38**, 142 (1935).
7. A. A. Mal'tsev, Yu. Ya. Kuzyakov, and V. M. Tatevskiy, Mater. X. Vses. soveshch po spectr. (Proceedings of the 10th All Union Conference on Spectroscopy). Vol. 1, p. 475, 1957.

THE ENERGY LEVELS AND WAVE FUNCTIONS OF THE DISUBSTITUTED BENZENE MOLECULE CALCULATED BY THE METHOD OF THE "METAL" MODEL

A. F. Terpugova

Received 11 November 1959

In a previous paper[1] we considered the energy levels of the monosubstituted benzene molecule. It was found that the longest wavelength absorption band with substitution of the first kind arises as a consequence of the transition from the substituted level to the split level of the benzene ring. In the nitrobenzene molecule the longest wavelength transition arises because of the transition from the benzene level to the substituted level.

It was of interest to clarify how the second substituent introduces changes in the energy spectrum of these compounds, and also to determine the origin of the longest wavelength bands in the spectra of these compounds. In addition, it was necessary to explain the influence of the position of the substituent on the electronic spectra. The experimental data show that the observed spectra of disubstituted benzene differ little from the spectra of monosubstituted.

In the present paper the energy levels, frequencies of the longest wavelength transitions, and the distributions of the electron density in three molecular isomers $C_6H_4Cl_2$, $C_6H_4Br_2$ and $C_6H_4(NO_2)_2$ are calculated by means of the "metal" model. The comparison of the energy spectra of these molecules with the corresponding spectra of monosubstituted benzene permits deductions concerning the origin of long wavelength absorption bands in the electronic spectrum. Here we put to use the same method of calculation as in the earlier work.[1] The computational results are shown in Figs. 1 and 2, where the

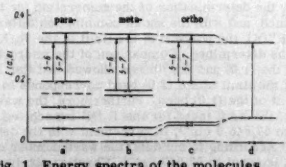

Fig. 1. Energy spectra of the molecules $C_6H_4Cl_2$ (a-c) and C_6H_6 (d).

spectrum of benzene[2] is also shown for comparison. We shall consider first the spectrum of the molecule $C_6H_4Cl_2$ (Fig. 1). As is evident from comparison with the benzene spectrum, part of the energy levels of the given molecules may be interpreted as the split benzene levels, and the others (levels 4 and 5) as the result of the presence of branch substitutent groups. The difference between this spectrum and the spectrum of the C_6H_5Cl consists only in that the given molecules have two levels which are required by their original substitution (4th and 5th), but in the C_6H_5Cl molecule there is only one such level (its level is marked in Fig. 1 with a dashed line). As far as the electronic spectra of these molecules is concerned, in both this and the preceding case they occur as a result of transitions from the substituted levels to the ben-

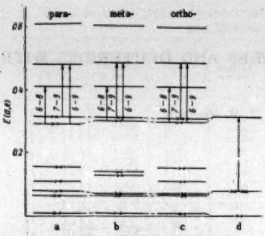

Fig. 2. Energy spectra of the molecules $C_6H_4(NO_2)_2$ (a-c) and C_6H_6 (d).

zene ring levels. Consequently, the origin of the spectra of these compounds is identical. From the comparison of the energy spectra of different isomers for the case of substitution of the first kind, it is evident that the spectrum of the meta form differs markedly from the two other forms. We note that this difference does not harmonize with the experimental data on the location of the absorption bands of the meta-isomers.

Calculated values of the frequencies of the longest wavelength transitions of all the studied molecules are presented in the Table and compared with experiment.

Frequencies of the Maxima of the Longest-Wavelength Absorption Bands for the Molecules $C_6H_4Cl_2$, $C_6H_4Br_2$, $C_6H_4(NO_2)_2$ (in cm^{-1})

Transition	$C_6H_4Cl_2$					
	Theory			Experiment[3]		
	para-	ortho-	meta-	para-	ortho-	meta-
5—6	28000	30000	37000	35000—37000	38000—38000	36000—38000
5—7	34000	32000	40000	37000—	38000	38000

Transition	$C_6H_4Br_2$					
	Theory			Experiment[3]		
	para-	ortho-	meta-	para-	ortho-	meta-
5—6	29000	29000	35000	35700—43000	36000—43000	36000—43000
5—7	30000	30000	44000	43000	43000	43000

Transition	$C_6H_4(NO_2)_2$					
	Theory			Experiment[4]		
	para-	ortho-	meta-	para-	ortho-	meta-
6—8	24900	24200	24400	33000—25000	30000—25000	32000—25000
6—9	40500	45440	41079	35700	41860	41860
7—9	35700	42980	39170	33000	33000	34000

The energy spectrum of the $C_6H_4(NO_2)_2$ molecule is markedly different from the spectra of those molecules in which the substituents are of the first kind. In the given case together with levels dependent on the presence of the C—N bond (4th and 5th), there appeared levels related to the N—O bond (8th and 9th levels). The close spacing of the indicated levels with respect to the split ones of benzene guarantees in these compounds the appearance of transitions in the visible regions of the spectrum (in contrast to molecules like $C_6H_4Cl_2$). The energy spectrum of dinitrobenzene differs from the spectrum of nitrobenzene only in the presence of two extra levels E_8 and E_9. The results of the calculation appear in Fig. 2, where the arrows indicate the transitions, and also in the Table. Unfortunately, the data appearing in the last column of the Table belong to a solution of dinitrobenzene in water, and make a comparison of the computed and experimental data difficult.

A comparison of the calculated and experimental data shows that, on the whole, qualitative agreement is found while the quantitative discrepancy in individual cases amounts to 7000 cm^{-1}. In spite of such large discrepancies, there is nevertheless a possibility of unique interpretation of the spectra of the considered compounds.

The wave functions ψ_i for all states of the corresponding molecules and the calculated curves of $\sum_i |\psi_i|^2$ which determine the distribution of the electron density in the molecule were also obtained. Such curves are shown in Fig. 3 for the para-isomers of the molecules $C_6H_4Cl_2$ and $C_6H_4(NO_2)_2$. From a comparison of these curves it is evident that in the molecules with substituents of the first and second kinds the electrons are distributed so that the minimum of one curve occurs above the maximum of the other. The experimental data on the orienting effect of the substituent corroborate this fact.

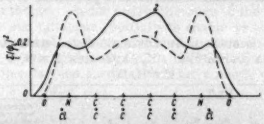

Fig. 3. Curves of the distribution of electron density in the molecules $C_6H_4Cl_2$ (curve 1) and $C_6H_4(NO_2)_2$ (curve 2).

In conclusion, I express my deep gratitude to N. A. Prilezhaeva for constant help with the problem, and to N. N. Ignatova for help received in the calculations.

REFERENCES

1. A. F. Terpugova, Opt. i Spektr. 7, 581 (1959), Optics and Spectroscopy 7, 359 (1959).
2. M. V. Vol'kenshtein and L. A. Borovinskii, Doklady Akad. Nauk SSSR 85, 737 (1952).
3. Landolt-Börnstein, "Zahlenwerte und Funktionen." Berlin 1950.
4. G. Kortüm, Z. physik. Chem. B42, 39 (1939).

PARTIAL FREQUENCIES OF PYRAMIDAL HYDRIDES AND DEUTERIDES WITH SYMMETRY C_{3v}

G. I. Rybakova, B. I. Naugol'nikov, and V. P. Morozov

Received 20 June 1959

We have considered the application of the method of partial frequencies to the study of the vibrations of nonplanar pyramidal molecules of the type RX_3 (X = H, D; R = N, P, As, Sb).

On the introduction of symmetry coordinates, the expression for the vibrational energy of an RX_3 molecule breaks down into parts which correspond to two-dimensional vibrations of symmetry A_1 and E. To each of these symmetry types, arguments analogous to those developed previously for the two-dimensional vibrations of an RX_2 molecule[1] may be applied.

The application of the method of partial frequencies[1] to the construction of a zero-order approximation to the characteristic vibration frequencies of RX_3 molecules (X = H, D; R = N, P, As, Sb) is illustrated by the data of Table 1. Here the following symbols are introduced: ω_1 and ω_1' are the zero-order frequencies of the RH_3 and RD_3 molecules, the values of which are taken from reference 2; $\bar{\omega}_{1\varepsilon}$, $\bar{\omega}_{1\varepsilon}'$ and $\bar{\omega}_{1\psi}$, $\bar{\omega}_{1\psi}'$ are the partial frefrequencies of these molecules in the coordinate and momentum representations respectively, evaluated with the use of the dynamic coefficients presented in reference 3.

Table 1. Results of Approximate Calculations of the Frequencies (in cm^{-1}) of RX_3 Molecules (R = N, P, As, Sb; X = H, D)

R	Symmetry	i	X = H			X = D				
			ω_i	$\bar{\omega}_{i\varepsilon}$	$\bar{\omega}_{i\psi}$	ω_i'	$\bar{\omega}_{i\varepsilon}'$	$\bar{\omega}_{i\psi}'$	Approximate value of ω_i' according to ref. 2	Approximate value of ω_i' according to ref. 3
N	A_1	1	3461	3453	3461	2484	2464	2483	2470	2483
		2	1099	1100	1102	832.9	832.3	838.8	831.6	836.1
	E	3	3621	3612	3621	2668	2643	2668	2650	2668
		4	1669	1671	1675	1213	1212	1223	1210	1219
P	A_1	1	2424	2422	2424	1738	1733	1736	1734	1736
		2	1028	1028	1029	749.0	748.7	750.8	748.5	750.2
	E	3	2442	2442	2442	1756	1754	1756	1754	1756
		4	1148	1148	1148	818.7	818.8	819.5	818.8	819.5
As	A_1	1	2199	2199	2198	1565	1565	1565	1564	1565
		2	960.0	960.0	960.0	687.9	688.0	688.1	687.8	688.1
	E	3	2209	2209	2207	1573	1573	1573	1573	1573
		4	1013	1013	1013	719.1	719.3	719.2	719.0	719.1
Sb	A_1	1	1969	1968	1968	1398	1398	1397	1398	1398
		2	799.9	800.0	799.9	570.5	570.5	570.8	570.4	570.5
	E	3	1974	1974	1970	1402	1402	1400	1402	1402
		4	847.8	849.2	847.8	601.0	602.0	601.1	601.0	601.0

It can be seen from the table that the partial frequencies of the pyramidal hydrides and deuterides of the type RX_3 are very close to the corresponding eigenfrequencies. They may therefore be considered as zero-order approximations to the eigenfrequencies.

In the same Table 1 are presented the results of approximate calculations of the frequencies of the pyramidal deuterides using relations of the form

$$\omega_i' = \rho_i \omega_i \quad (i = 1, 2, 3, 4), \tag{1}$$

where ρ_i is determined on the basis of the considerations described in reference 1.

The expressions for ρ_i have the following form: in the coordinate representation—

$$\left.\begin{aligned}
\rho_1 &= \left[\frac{m}{m_1}\,\frac{M+3m_1}{M+3m}\,\frac{M+2am}{M+2am_1}\right]^{1/2},\\
\rho_2 &= \left[\frac{m}{m_1}\,\frac{M+3m_1}{M+3m}\,\frac{M+bm}{M+bm_1}\right]^{1/2},\\
\rho_3 &= \left[\frac{m}{m_1}\,\frac{cM+3am_1}{cM+3am}\,\frac{cM+a^2m}{cM+a^2m_1}\right]^{1/2},\\
\rho_4 &= \left[\frac{m}{m_1}\,\frac{cM+3am_1}{cM+3am}\,\frac{M+am}{M+am_1}\right]^{1/2},
\end{aligned}\right\} \tag{2}$$

and in the momentum representation—

$$\left.\begin{aligned}
\rho_1 &= \left[\frac{m}{m_1}\,\frac{M+bm_1}{M+bm}\right]^{1/2},\\
\rho_2 &= \left[\frac{m}{m_1}\,\frac{M+2am_1}{M+2am}\right]^{1/2},\\
\rho_3 &= \left[\frac{m}{m_1}\,\frac{M+am_1}{M+am}\right]^{1/2},\\
\rho_4 &= \left[\frac{m}{m_1}\,\frac{cM+a^2m_1}{cM+a^2m}\right]^{1/2}.
\end{aligned}\right\} \tag{3}$$

Here m, m_1, and M are the masses of the atoms of H, D, and R respectively,

$$a = 1 - \cos\varphi,\ b = 1 + 2\cos\varphi,\ c = 2 + \cos\varphi,$$

and φ is the equilibrium angle between the bonds.

It can be seen from the data of Table 1 that the accuracy of the calculations of the zero-order frequencies of the RD_3 molecules according to formulas (1)-(3) is quite high. Let us now turn to the problem of constructing a zero-order approximation to the force coefficients. The secular equation of the RH_3 molecule enables us to set up, for each symmetry type, two equations in the three reduced force constants. We shall take as additional equations the approximate equalities between the stretching partial frequencies and the eigenfrequencies to which they correspond. The solutions of the sets thus obtained for the reduced force constants will be designated as zero-order approximation I. Zero-order approximation II is obtained in an analogous manner if we take as our third equations the approximate equalities between the deformation partial frequencies and the corresponding eigenfrequencies.

Zero-order approximation I is represented by the following formulas:
for symmetry A_1

$$\left.\begin{aligned}
v_1 &= \frac{m[M+2ma]}{M+3m}\lambda_1,\\
v_2 &= \frac{m^2\sin\varphi}{M+3m}\lambda_1,\\
v_3 &= \frac{m\sin^2\varphi}{M+2ma}\left[\frac{m^2\lambda_1}{M+3m} + \frac{M\lambda_2}{2(d-2\cos^2\varphi)}\right]
\end{aligned}\right\} \tag{4}$$

and for symmetry E

$$\left.\begin{aligned}
v_4 &= \frac{m[ma^2+Mc]}{3ma+Mc}\lambda_3,\\
v_5 &= -\frac{am^2\sin\varphi}{3ma+Mc}\lambda_3,\\
v_6 &= \frac{md}{ma^2+Mc}\left[\frac{m^2a^2\lambda_3}{3ma+Mc} + M\lambda_4\right].
\end{aligned}\right\} \tag{5}$$

Table 2. Zero-Order Approximations to the Reduced Force Constants (in millidynes/A) and Interaction Coefficients (in A/millidyne)

R	Symmetry	i	Value of ν_i according to ref. 3	Error $\Delta\nu_i$	Zero-order approximation I	Discrepancy with the data of ref. 3	Zero-order approximation II	Discrepancy with the data of ref. 3	Value of u_i according to ref. 3	Error Δu_i	Zero-order approximation I	Discrepancy with the data of ref. 3	Zero-order approximation II	Discrepancy with the data of ref. 3
N	A_1	1	6.904	0.094	6.937	0.033	6.909	0.005	0.1448	0.0008	0.1448	—	0.1507	0.006
		2	0.0164	0.50	0.402	0.39	0.0406	0.02	−0.00437	0.14	−0.0113	0.007	−0.112	0.11
		3	0.5198	0.022	0.5389	0.020	0.5189	0.001	1.939	0.090	1.928	0.005	1.936	0.013
	E	4	7.125	0.098	7.161	0.036	7.130	0.005	0.1404	0.0036	0.1404	—	0.1436	0.0032
		5	−0.0721	0.38	−0.349	0.28	−0.0741	0.002	0.0157	0.083	0.0161	0.0004	0.0761	0.060
		6	0.8448	0.011	0.8567	0.012	0.8433	0.002	1.552	0.045	1.556	0.004	1.563	0.011
P	A_1	1	3.393	0.060	3.398	0.005	3.393	—	0.2949	0.012	0.2948	0.0001	0.2970	0.002
		2	0.0287	0.45	0.103	0.07	0.0186	0.01	−0.0289	0.42	0.0174	0.01	−0.0968	0.07
		3	0.3146	0.012	0.3170	0.002	0.3144	0.0002	3.181	0.20	3.181	—	3.186	0.005
	E	4	3.424	0.059	3.424	—	3.423	0.001	0.2922	0.014	0.2922	—	0.2922	—
		5	−0.0252	0.76	−0.0597	0.03	−0.0132	0.01	0.0198	0.60	0.0104	0.009	0.0469	0.027
		6	0.3720	0.0094	0.3729	0.0009	0.3721	0.0001	2.690	0.15	2.687	0.003	2.689	0.001
As	A_1	1	2.836	0.031	2.836	—	2.835	0.001	0.3529	0.025	0.3527	0.0002	0.3533	0.0004
		2	0.0258	0.91	0.0371	0.01	0.00707	0.02	−0.0332	1.2	−0.0091	0.02	−0.0478	0.01
		3	0.2741	0.020	0.2744	0.0004	0.2740	0.0001	3.651	0.49	3.649	0.002	3.651	—
	E	4	2.858	0.021	2.858	—	2.857	0.001	0.3504	0.052	0.3494	0.001	0.3498	0.001
		5	−0.0345	1.7	−0.0199	0.01	−0.00418	0.03	0.0405	2.0	0.0049	0.03	0.0233	0.02
		6	0.2985	0.034	0.2984	0.0001	0.2982	0.0003	3.355	0.84	3.353	0.002	3.353	0.002
Sb	A_1	1	2.283	0.020	2.284	0.001	2.284	0.001	0.4366	0.082	0.4378	0.001	0.4382	0.0004
		2	0.0224	1.3	0.0186	0.004	0.00307	0.019	−0.0512	3.0	−0.00899	0.04	−0.0424	0.009
		3	0.1921	0.034	0.1921	—	0.1919	0.0002	5.212	1.6	5.211	0.001	5.211	0.001
	E	4	2.293	0.12	2.294	0.001	2.293	—	0.4375	0.19	0.4359	0.002	0.4370	0.0005
		5	−0.0394	2.3	−0.00863	0.06	−0.00181	0.04	0.0820	4.8	0.00377	0.078	0.0194	0.062
		6	0.2103	0.091	0.2096	0.0007	0.2096	0.0007	4.770	3.9	4.768	0.002	4.771	0.001

where

$$d = 1 + \cos\varphi, \quad \lambda_i = \omega_i^2.$$

Zero-order approximation II is obtained analogously:

$$\left.\begin{aligned}
v_1 &= \frac{Mm}{M+mb}\left[\frac{2m^2(d-2\cos^2\varphi)\lambda_2}{M(M+3m)} + \lambda_3\right],\\
v_2 &= \frac{m^2\sin\varphi}{M+3m}\lambda_2,\\
v_3 &= \frac{md(M+mb)}{2b(M+3m)}\lambda_2,\\
v_4 &= \frac{m}{M+ma}\left[\frac{m^2a^2\lambda_4}{3ma+Mc} + M\lambda_3\right],\\
v_5 &= -\frac{am^2\sin\varphi}{3ma+Mc}\lambda_4,\\
v_6 &= \frac{md(M+ma)}{3ma+Mc}\lambda_4.
\end{aligned}\right\} \quad (6)$$

It should be noted that expressions (4)-(6) give a simpler dependence of the force coefficients on the molecular and spectral parameters than do expressions (2)-(7) of reference 3.

The problem of zero-order approximations to the reduced interaction coefficients (u_i) is solved in a similar way. The results of the numerical calculation of the values of the dynamic coefficients v_i and u_i with the help of the above-described approximate method are represented in Table 2. From a comparison with the known values of v_i and u_i,[3] it can be seen that the discrepancies do not go beyond the limits of error of the evaluation of the dynamic coefficients by exact methods.[3]

Thus the zero-order approximations to the force constants and influence coefficients enable us to obtain, by a fairly simple method, sufficiently exact information about the dynamic structure of the molecule on the basis of the molecular and spectral data for a single compound.

REFERENCES

1. V. P. Morozov, Opt. i Spektr. 7, 289 (1959), Optics and Spectroscopy 7, 188 (1959).
2. N. K. Morozova and V. P. Morozov, Opt. i Spektr. 5, 535 (1958).
3. G. I. Rybakov, D. S. Koval'chuk, and V. P. Morozov, Opt. i Spektr. (in press).

INTENSITIES AND DEPOLARIZATIONS IN THE RAMAN SPECTRA OF POLYMETHYLBENZENES
II. Numerical Calculation for Toluene

M. A. Kovner and B. N. Snegirev

Received 25 November 1959

A numerical calculation of the intensities and depolarizations in the Raman spectra of toluene is carried out, and the question of their characteristic nature in the Raman spectra of monoalkylbenzenes is discussed.

I. METHOD OF CALCULATION

In a previous paper[1] formulas were introduced expressing the components of the tensor T of the derivatives of the polarizability with respect to the normal coordinates of toluene through the electro-optical parameters (linear combinations of the bond polarizabilities and their derivatives, abbreviated e.o.p.) and the elements of the matrix L of the normalized coefficients of the vibrational modes. A method has been described[2] for the direct determination of the e.o.p. from experimental values of the isotropic and anisotropic parts of the intensities (I^a and I') and from the elements of the matrix L^{-1}. However, we could not utilize this method for the following reasons:

(1) The formulas for the e.o.p. in ref. 2 assume a summation over all the values of the trace b′ and the anisotropy g′ of the tensor T, found from the experimental values of I^a and I' for all of the fundamental frequencies of each given symmetry type. But L_{ik} of many Raman lines was not measured.

(2) Even in those cases where L_{ik} is measured, it is necessary to know the true values of the depolarization coefficients ρ for the individual determination of I^a and I'. In ref. 3 values of $\rho > 0.86$ and also $\rho < 0.86$ for noncompletely symmetric vibrations are encountered; and, therefore, it is not expedient to use these values of ρ for the determination of the e.o.p.

(3) The formulas from ref. 2 allow one to determine easily the e.o.p. if the quantity g′ can be expressed linearly in terms of the e.o.p. (for example, the degenerate or completely symmetric vibrations of benzene). In the case of toluene, as seen in ref. 1, this condition is not observed.

(4) From the experimental data for one molecule only the absolute values of b′ and g′ can be determined, and not their signs. For the determination of the signs of b′ and g′ it is necessary to measure L_{ik} and ρ in the Raman spectra of deuterated derivatives of the substance investigated. Such data are absent in the case of toluene.

As a result we were forced to start from the assumption that the e.o.p. of the ring and of the aromatic CH bonds in toluene are the same as in benzene, and that the e.o.p. of the methyl groups are the same as in paraffin hydrocarbons. The first determinations in ref. 4 are on the basis of experimental values of $S = K^2(5b'^2 + 7g'^2)$; in ref. 5, for benzene, $K^2 = 0.028$ A^{-4}. Calculation of the e.o.p. of benzene from the experimental values of S in ref. 6 and the formulas in ref. 2 leads, as seen from Table 1, to insignificant differences, and so we used the e.o.p. values from ref. 4. The values of the e.o.p. of the methyl group are known from ref. 7.

Thus, the only remaining derived quantities are the e.o.p. of the C–C bond, and these were determined from the experimental values of S from ref. 6. From the values of S for the lines relating to the symmetry type A_1, by experimenting with a very large number of variations, we succeeded in establishing that $\alpha'_{Q10} + \alpha'_{Q20} + \alpha'_{Q30} \cong 3.03$ A^2 and $\alpha'_{Q10} \gg \alpha'_{Q20}, \alpha'_{Q30}$. From the value of S for the 1586 cm^{-1} line of symmetry type B_1 it was found that $\alpha_{Q10} - \alpha_{Q30} = 1.18$* A^2. This value agrees well with the value obtained for the C–C bond in ethane from quantum chemical calculations[8] (1.26 A^2).

Table 1. Comparison of the Values of the e.o.p. Found from Experimental Data Obtained in Refs. 5 and 6

Parameter	Numerical value of parameter	
	From ref. 5	From ref. 6
a'_{Q1}	4.70 A^2	4.98 A^2
a'_{Q2}	1.21 »	1.04 »
a'_{Q3}	0.80 »	0.81 »
a'_{q1}	3.04 »	3.14 »
a'_{q2}	0.83 »	0.65 »
a'_{q3}	0.11 »	0.11 »
$a_{Q1} - a_{Q2}$	0.80 A^2	0.97 A^2
$a_{q1} - a_{q2}$	0.14 »	0.19 »
$a'_{Q1} + a'_{Q2} + a'_{Q3}$	6.71 A^2	6.83 A^2
$a'_{q1} + a'_{q2} + a'_{q3}$	3.98 »	3.89 »

Finally, from the value of S for the 217 cm^{-1} line of symmetry type B_2 we found that $\alpha_{Q10} + \alpha_{Q20} - 2\alpha_{Q30} = 1.27$ A^2. This value can be considered reasonable since then $\alpha_{Q20} > \alpha_{Q30}$. However, it is not very certain since the 217 cm^{-1} line appears on the intense background of the PRK-2 lamp,[6] as a result of which the value of S can be inaccurate. All of the values of the e.o.p. shown above were used for the calculation of the values of S and ρ for all of the lines of symmetry A_1 and values of S for all of the lines of symmetry B_1, A_2, and B_2. The L matrices necessary for the calculation are presented in Table 2.*

*In the case of the 623 cm^{-1} frequency the coefficient for the desired e.o.p. is small, and therefore the value of S for this line was not used in the determination of the e.o.p.

*The authors express their thanks to A. M. Bogomolov for the L matrices, calculated by him on an electronic computer.

The calculated results are given in Table 3, where for B_1, A_2, and B_2 we used $\rho_{calc.} = 0.86$, and the $\rho_{obs.}$ from ref. 3 are not shown.

II. DISCUSSION OF THE RESULTS

We will examine separately the results relating to the different symmetry types.

Table 2. Normalized Coefficients of the Vibrational Form in the C_{2v} Symmetry Coordinates**

Symmetry Type A_1

ν(cm^{-1}) / No.	1 521	2 786	3 1004	4 1030	5 1181	6 1211	7 1380	8 1504	9 1605	10 2920	11 3064	12 3067	13 3067	Vibration
1	0.026	0.037	0.130	0.047	0.095	0.128	0.006	0.094	0.349	0	0.041	0.041	0.017	CC
2	−0.005	0.015	0.151	0.189	−0.052	−0.002	−0.007	−0.214	−0.150	0	−0.007	0.028	0.076	CC
3	0.023	0.115	0.104	−0.105	−0.068	0.085	−0.004	0.168	−0.236	0.002	0.015	0.042	−0.020	CC
4	0.003	0	0.007	−0.006	−0.004	0.003	0	0.012	−0.008	0.002	−0.279	−0.545	0.341	CH
5	0.003	−0.001	0.003	0.010	−0.004	0.005	0	−0.012	−0.002	0	−0.756	−0.033	−0.718	CH
6	−0.004	0.002	0.006	0.007	0.006	−0.003	0	−0.018	0.008	−0.002	0.684	−0.452	−0.676	CH
7	0.073	0.161	−0.025	−0.027	0.028	−0.286	0.143	−0.134	0.129	−0.053	−0.004	−0.001	0.003	C—C
8	−0.182	0.303	−0.218	0.055	0.015	0.140	0.006	0.178	0.193	0	0.134	−0.049	−0.021	CCC
9	−0.230	0.047	0.205	−0.072	0.059	−0.246	0.009	−0.134	0.300	−0.005	0.016	0.077	−0.022	CCC
10	−0.122	0.028	0.159	0.076	0.655	−0.441	0.012	0.613	−0.457	0	−0.028	0.054	−0.074	CCH
11	−0.088	0.210	−0.172	−0.094	0.582	0.389	−0.042	−0.784	−0.264	0	0.021	−0.056	0.076	CCH
12	0.012	0.012	−0.002	0.005	−0.009	−0.037	−1.112	0.026	0.027	0.041	0	0	−0.001	CCH / CH_3
13	0.004	0.007	−0.001	−0.001	0	−0.014	−0.038	−0.005	0.006	1.014	0.042	0.001	−0.002	CH / CH_3

Symmetry Type B_1

ν(cm^{-1}) / No.	14 366	15 823	16 970	17 1041	18 1155	19 1278	20 1311	21 1439	22 1460	23 2866	24 2930	25 3032	26 3074	Vibration
1	0.008	−0.011	0.053	0.171	0.178	0.088	0.257	0.038	0.053	−0.313	0	0.028	0.035	CC
2	0.018	0.028	0.107	−0.005	0.066	0.140	0.252	0.114	−0.003	0.330	0.003	−0.027	0.035	CC
3	−0.002	0.006	0.004	0.013	0.007	0.002	0	0.017	0.009	−0.007	−0.011	0.735	−0.741	CH
4	0.002	−0.006	0.006	0.008	0.003	0.006	0	0.020	0.009	0.006	0.003	−0.741	0.735	CH
5	−0.006	0.321	−0.102	−0.101	−0.011	−0.063	0.004	−0.163	−0.034	−0.279	−0.001	0.120	−0.048	CCC
6	0.039	−0.338	−0.006	−0.132	−0.037	−0.025	−0.008	−0.100	−0.102	0.281	0.001	−0.120	−0.047	CCC
7	0.056	−0.185	0.065	−0.332	0.131	0.702	−0.576	0.406	0.347	−0.132	−0.001	−0.037	0.054	CCH
8	−0.026	0.202	−0.071	−0.133	0.539	−0.684	−0.213	0.593	0.231	0.100	−0.001	0.037	−0.054	CCH
9	−0.008	0.073	0.075	0.305	0.789	−0.270	−0.613	−0.804	−0.368	0.527	0.001	−0.046	−0.060	CCH
10	0.297	0.098	0.024	−0.186	−0.045	−0.259	−0.089	−0.269	−0.049	−0.260	0.089	0.040	−0.054	CC—C
11	0.039	0.014	−0.345	0.078	0.047	0.225	0.190	0.731	−1.411	−0.187	−0.075	−0.002	0.001	HCH
12	−0.061	−0.000	0.869	−0.208	−0.087	−0.243	−0.135	0.012	−0.437	−0.293	0.102	0.001	−0.005	CCH / CH
13	0.007	0.002	−0.040	0.007	0.004	0.014	0.012	0.024	−0.040	0.002	−1.057	−0.010	0.006	CH

Symmetry Type B_2

ν(cm^{-1}) / No.	30 217	31 465	32 630	33 730	34 895	35 993	36 1041	37 1460	38 2980	Vibration
1	0.130	0.182	−0.102	0.496	0.802	0.045	0.060	0.004	0.035	β
2	−0.057	−0.071	−0.486	−0.450	0.528	1.245	−0.314	0.021	−0.023	β
3	−0.022	−0.036	1.225	0.712	−0.305	−0.667	0.351	−0.055	−0.005	π
4	0.141	0.255	0.487	−0.771	0.149	0.015	−0.010	0.010	0.025	β
5	0.021	0.437	−0.075	0.285	−0.818	0.760	0.362	−0.017	0.054	β
6	−0.193	0.776	−0.064	0.147	0.311	0.270	0.231	−0.008	−0.003	π
7	−0.011	−0.021	−0.012	−0.042	0.063	0.001	0.431	1.585	0.073	HCH
8	−0.017	−0.055	−0.055	−0.116	0.149	−0.002	0.970	−0.472	0.101	CCH / CH_3
9	0.002	0.004	0.002	0.006	−0.008	0	−0.047	−0.045	−1.057	CH

*Note. The horizontal column headings give the number and value of the frequency from Table 3 of ref. 1. The left-hand column gives the number of the symmetry coordinate from Table 1 of ref. 1.

Symmetry A_1. From Table 3 it is seen that for the lines 1, 2, 3, and 9 we obtained completely satisfactory coincidence of the calculated and observed values of S. It is well known that line 8, particularly intense in the infrared spectrum, has in the Raman Spectrum an insignificant intensity. As follows from ref. 9, the lines of the CH stretching vibrations are characterized by a high intensity. The results of the calculation also agree well with these properties.

Let us dwell briefly on line 7. From the structure of the secular equation of A_1 of toluene and from the L matrix, it obviously follows that it is related to the completely symmetric vibration of the methyl group, and its value of ρ should be low. As is clear from refs. 7 and 9, this line is very weak in the Raman spectra of the higher monoalkylbenzenes and the paraffins. On the other hand, from ref. 9 we see that the 1380 cm^{-1} line is intense and less polarized in the Raman spectra of toluene and the xylenes. From these data we can draw the conclusion that in those cases when the methyl group is located close to the phenyl ring its e.o.p. undergo significant changes, brought about by strong interactions. The latter can be considered as changes of the e.o.p. of the methyl group or as an equivalent introduction of corrections of the first approximation. There can also be resonance interaction with the combination frequencies 217 + 1156, 346 + 1031, 405 + 970, and 690 × 2.

To explain the discrepancy between the calculated and observed values of S of lines 4 and 6, it is possible to make the following assumptions:

(1) There occur resonance interactions with the combination frequencies 346 + 690, 405 + 623, 521 × 2 and 217 + 993, and 521 + 690.

(2) Since the values of S are very sensitive to a change of the elements of the L matrix, then there may be an effect of a certain inevitable inaccuracy in the solution of the mechanical problem.

(3) A series of authors (cf. the bibliography in ref. 10 devoted to this question) have shown that the dependence of L_{ik} on temperature does not correspond to that which follows from the theoretical formula for L_{ik}. Therefore, the values of S, calculated in ref. 6 from the theoretical formula relating S and L_{ik},[5] can differ from the true values, and these differences will not be identical for the different lines.

(4) The substitution H → CH_3 on transition from benzene to toluene can bring about some change (probably not large) of the state of the electronic cloud of the phenyl group due to the inductive effect of the methyl group. This change can have a greater effect on the magnitudes of the derivatives of the bond polarizabilities than on the polarizabilities themselves. From this, it follows that the e.o.p. introduced into the tensor T of symmetry type A_1 can have several differences in toluene and in benzene. However, as has already been noted above, a complete determination of all of the e.o.p. for toluene cannot be made in practice at the present time.

Symmetry B_1. In spite of the fact that the experi-

Table 3. The Observed and Calculated Values of the Intensities and Depolarizations in the Raman Spectrum of Toluene

No.	Symmetry type	ν (cm^{-1})	$S_{obs.}$ from ref. 6	$S_{calc.}$	$\rho_{obs.}$ from ref. 3	$\rho_{calc.}$
1		521	0.240	0.177	0.61	0.50
2		786	1.070	0.863	0.09	0.13
3		1004	2.540	2.541	0.07	0.11
4		1030	0.710	0.277	0.10	0.11
5		1181	—	0.240	0.54	0.84
6		1211	1.050	0.276	0.13	0.13
7	A_1	1380	—	0.014	0.42	0.20
8		1504	—	0.002	—	0.74
9		1605	1.190	0.885	0.70	0.86
10		2920	—	1.818	—	0.06
11		3054	—	3.273	0.33	0.53
12		3067	—	8.549	—	0.21
13		3067	—	3.869	—	0.23
14		346	—	0.014		
15		623	0.215	0.095		
16		970	—	0.036		
17		1081	—	0.056		
18		1155	—	0.096		
19	B_1	1278	—	0.005		
20		1311	—	0.002		
21		1439	—	0.020		
22		1460	—	0.051		
23		1586	0.520	0.520		
24		2980	—	0.273		
25		3032	—	2.771		
26		3074	—	0.000		
27		405 *	—	0.000		
28	A_2	849	—	0.105		
29		970 *	—	0.000		
30		217	0.070	0.070		
31		465	—	0.000		
32		690	—	0.005		
33		730	—	0.010		
34	B_2	895	—	0.021		
35		993	—	0.000		
36		1041	—	0.022		
37		1460	—	0.044		
38		2980	—	0.273		

*Note. Lines having an insignificant intensity in the Raman spectrum of toluene.

mental values of S for 11 of the 13 lines are absent, interesting conclusions can be drawn from Table 3. The Raman spectrum of toluene has been studied repeatedly, and its relative line intensities are sufficiently well known. In particular, it is known that lines 14, 16, 17, 19, 20, and 21 have low intensities, which completely agrees with the results of our calculation. Line 26 usually is not observed at all. On the other hand, lines 18, 24, and 25 are intense, and this also is in agreement with the results of the calculation.

Symmetry A_2. To this symmetry type belong the lines 405, 970, and 843 cm^{-1}. As follows from refs. 1 and 4 the values of S for them should accurately coincide with the values of S of the corresponding lines of benzene. For the first two of them S = 0, they are inactive in the Raman spectrum of benzene and have an insignificant intensity in the Raman spectrum of toluene. Using the formula relating S and L_∞[8] it is easy to compute the magnitude of the ratio of the values of L_∞ for the lines with frequencies 843 and 850 cm^{-1} in the spectra of benzene and toluene. This equals 1.25, compared with 80/50 = 1.6 obtained in ref. 9. This discrepancy lies within the limits of error of the measured L_∞ for weak lines. It is interesting to note, however, that if the values of L_∞ were measured with greater accuracy, then, by the degree of divergence from 1.25 of the measured ratio of the L_∞ values for these two lines in benzene and toluene, it would be possible to judge the difference in the values of the e.o.p. in these two molecules.

Symmetry B_2. Numerous experimental data, cited in our preceding studies on the mechanics of the vibrations of toluene, show that all lines of symmetry type B_2, except for 30, 37, and 38, have very low intensities. Many of them in general are almost not observed and are known only from infrared spectra. Lines 30, 37, and 38 are more intense. The results of our calculation completely agree with these experimental data.

III. THE CHARACTERISTIC NATURE OF THE INTENSITY AND DEPOLARIZATION IN THE SPECTRA OF MONOALKYLBENZENES

As has been conclusively shown[11] the quantities b′ and g′ morefundamentally characterize the optical properties of molecules than L_∞ and ρ. In refs. 11 and 12 an idea about characteristic lines was formulated. Thus, from the point of view developed in these studies, there appear lines for which the quantities b′ and g′ maintain constant values in a homologous series of compounds (for the same characteristic frequency in this series). If it is considered that the e.o.p. of the ring maintain constant values in a series of monoalkylbenzenes, then lines, characteristic according to vibrational form, will be characteristic. This has been established in ref. 13 on the basis of a calculation of the L matrix, of a computation of the shifts of the atoms, and of a graphical presentation of those vibrations which are characterized by the following frequencies: 405, 623, 690, 849, 895, 970, 993, 1004, 1030, 1155, 1181, 1211, 1311, 1504, 1586, and 1605 cm^{-1}.

Thus, the calculation leads to some broadening of the number of characteristic lines of monoalkybenzenes by comparison with the data of refs. 9 and 12. The list of characteristic lines includes very weak or even unobserved Raman lines, the intensities of which naturally cannot be measured. An extraordinarily low intensity (and, consequently, a low value of S) indeed is their characteristic property. However, some of them have a high intensity in the infrared spectra of monoalkylbenzenes and are characteristic for these spectra.

They will be examined in our succeeding work.

REFERENCES

1. M. A. Kovner and B. N. Snegirev, Opt. i Spektr. 7, 487 (1959), Optics and Spectroscopy 7, 309 (1959).
2. T. Yoshino and H. J. Bernstein, J. Mo. Spectroscopi, 2, 241 (1958).
3. M. R. Fenske, W. G. Braun, R. V. Wiegand, D. Q. R. H. McCormick, and D. H. Rank, Anal. Chem. 19, 700 (1947).
4. M. A. Kovner and B. N. Snegirev, Opt. i Spektr. 5, 239 (1959).
5. G. Allen and H. J. Bernstein, Con. J. Chem. 33, 1137 (1955).
6. N. I. Rezaev, Kand. Diss., Moskov. Gosudarst. Univ., 1958.
7. M. V. Vol'kenshtein, M. A. El'yashevich, and B. I. Stepanov, "Kolebaniya Molekul" (Molecular Vibrations), Vol. 1, p. 2. Gosudarst. Izd. Tekh.-Teoret. Lit., 1959.
8. M. G. Veselov and V. N. Filipovich, Vestnik Leningrad. Gosudarst. Univ. No. 2, 107 (1953).
9. G. S. Landsberg, P. A. Bazhulin, and M. M. Sushchinskii, "Osnovye Parametry Spektrov Komblinatsionnogo Rasseyaniya Uglevodorodov," (Fundamental Parameters of the Raman Spectra of Hydrocarbons). Izd. Akad. Nauk SSSR, 1956.
10. N. I. Rezaev and N. S. Andreev, Opt. i Spektr. 7, 119 (1959), Optics and Spectroscopy 7, 72 (1959).
11. M. M. Sushchinskii, Dokt. Diss. Fiz. Inst., Akad. Nauk SSSR, 1957.
12. M. M. Sushchinskii, Izd. Akad. Nauk SSSR Ser. Fiz. 17, 608 (1953).
13. A. M. Bogomolov, Opt. i Spektr. (in press).

CALCULATION OF INTENSITIES AND POLARIZATIONS IN THE VIBRATIONAL ABSORPTION SPECTRA OF POLYATOMIC MOLECULES. II

L. A. Gribov

Received 23 November 1959

With molecules of the ethylene and ammonia types as examples, a method is demonstrated for calculating the intensities and polarizations in the vibrational absorption spectra of polyatomic molecules, based on a vector representation of the change in the dipole moment.

In the previous communications,[1,2] a method was set forth for calculating the intensities and polarizations in the infrared absorption spectra of polyatomic molecules, based on a vector representation of the change in the dipole moment during a vibration of a given form. In this we succeeded in avoiding the difficulties associated with the calculation of the derivatives of the dipole moment of the molecule with respect to the normal coordinates. A general formula was derived expressing the transition probability factor during absorption in terms of the electro-optical and mechanical parameters of the molecule, and also the frequency and form of the vibration. All the derivatives of the dipole moments of the separate bonds with respect to the internal coordinates are brought together into a single matrix, which significantly facilitates the transition to the first approximation of the valence-optical scheme.

In the work here offered, two examples are presented which clearly demonstrate the pattern of calculations according to the new method.

THE X_2Y_4 MOLECULE OF THE ETHYLENE TYPE

The ethylene molecule belongs to the point group V_h and has vibrations of the following symmetry types:

$$\Gamma = 3A_g + A_u + 2B_{1g} + B_{1u} + 2B_{2u} + B_{2g} + 2B_{3u}.$$

The vibrations B_{1u} (nonplanar), B_{2u}, and B_{3u} are active in the infrared region. The set of internal coordinates and coordinate vectors is shown in Fig. 1.

Let us first consider the planar vibrations. The matrix

$$\left\| \left(\frac{\partial \mu}{\partial q}\right)_0, \left(\frac{\partial \mu}{\partial \gamma}\right)_0 \right\|$$

in this case will have the form

$$\left\| \begin{array}{cccccccccc} \left(\frac{\partial \mu_1}{\partial q_1}\right)_0 & \left(\frac{\partial \mu_1}{\partial q_2}\right)_0 & 0 & 0 & \left(\frac{\partial \mu_1}{\partial \alpha_1}\right)_0 & \left(\frac{\partial \mu_1}{\partial \beta_1}\right)_0 & 0 & 0 & 0 & 0 \\ \left(\frac{\partial \mu_2}{\partial q_1}\right)_0 & \left(\frac{\partial \mu_2}{\partial q_2}\right)_0 & 0 & 0 & \left(\frac{\partial \mu_2}{\partial \alpha_1}\right)_0 & 0 & \left(\frac{\partial \mu_2}{\partial \beta_2}\right)_0 & 0 & 0 & 0 \\ 0 & 0 & \left(\frac{\partial \mu_3}{\partial q_3}\right)_0 & \left(\frac{\partial \mu_3}{\partial q_4}\right)_0 & 0 & 0 & 0 & \left(\frac{\partial \mu_3}{\partial \alpha_2}\right)_0 & \left(\frac{\partial \mu_3}{\partial \beta_2}\right)_0 & 0 \\ 0 & 0 & \left(\frac{\partial \mu_4}{\partial q_3}\right)_0 & \left(\frac{\partial \mu_4}{\partial q_4}\right)_0 & 0 & 0 & 0 & \left(\frac{\partial \mu_4}{\partial \alpha_2}\right)_0 & 0 & \left(\frac{\partial \mu_4}{\partial \beta_1}\right)_0 \end{array} \right\|$$

In drawing this up, the entirely natural assumption has been made that the derivatives of the bond dipole moments with respect to the coordinates of the opposite bonds and angles are equal to zero. The columns corresponding to the derivatives of the bond dipole moments with respect to the nonplanar coordinates have been canceled, inasmuch as these coordinates take no part in vibrations of the types under consideration. Furthermore, in the B_{2u} and B_{3u} vibrations the length of the C=C bond

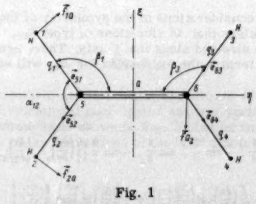

Fig. 1

and its direction in space do not change, while the displacements of all the remaining atoms and the deflections of the bonds are such as must lead to symmetric changes in the electric charge density at the ends of the C=C bond. Therefore, there is no basis for supposing that the derivatives of μ_{CC} (in the equilibrium state, $\mu_{CC} = 0$) with respect to the vibrational coordinates will be different from zero. Consequently, the row $(\partial \mu_{CC}/\partial q_i)_0$ and the column $(\partial \mu_i/\partial Q)_0$ may also be cancelled. From symmetry considerations it follows that

$$\left(\frac{\partial \mu_1}{\partial q_1}\right)_0 = \ldots = \left(\frac{\partial \mu_4}{\partial q_4}\right)_0 = \left(\frac{\partial \mu}{\partial q}\right)_0; \quad \left(\frac{\partial \mu_1}{\partial q_2}\right)_0 = \left(\frac{\partial \mu_2}{\partial q_1}\right)_0 = \left(\frac{\partial \mu_3}{\partial q_4}\right)_0 = \left(\frac{\partial \mu_4}{\partial q_3}\right)_0;$$

$$\left(\frac{\partial \mu_1}{\partial \alpha_1}\right)_0 = \left(\frac{\partial \mu_2}{\partial \alpha_1}\right)_0 = \left(\frac{\partial \mu_3}{\partial \alpha_2}\right)_0 = \left(\frac{\partial \mu_4}{\partial \alpha_2}\right)_0 = \left(\frac{\partial \mu}{\partial \alpha}\right)_0;$$

$$\left(\frac{\partial \mu_1}{\partial \beta_1}\right)_0 = \left(\frac{\partial \mu_2}{\partial \beta_2}\right)_0 = \left(\frac{\partial \mu_3}{\partial \beta_2}\right)_0 = \left(\frac{\partial \mu_4}{\partial \beta_1}\right)_0 = \left(\frac{\partial \mu}{\partial \beta}\right)_0.$$

The matrix **B** connecting the vibrational coordinates with the displacements of the atoms of the molecule is written down in the form

$$\left\| \begin{array}{c|cccccc} q_1 & e_{s1} & 0 & 0 & 0 & -e_{s1} & 0 \\ q_2 & 0 & e_{s2} & 0 & 0 & -e_{s2} & 0 \\ q_3 & 0 & 0 & e_{s3} & 0 & 0 & -e_{s3} \\ q_4 & 0 & 0 & 0 & e_{s4} & 0 & -e_{s4} \\ \alpha_1 & -\sigma l_{12} & -\sigma l_{21} & 0 & 0 & F_{12} & 0 \\ \beta_1 & -\sigma l_{1Q} & 0 & 0 & 0 & F_{1Q} & -\sigma_Q l_{Q1} \\ \beta_2 & 0 & -\sigma l_{2Q} & 0 & 0 & F_{2Q} & -\sigma_Q l_{Q2} \\ \alpha_2 & 0 & 0 & -\sigma l_{34} & -\sigma l_{43} & 0 & F_{34} \\ \beta_3 & 0 & 0 & -\sigma l_{3Q} & 0 & -\sigma_Q l_{Q3} & F_{3Q} \\ \beta_4 & 0 & 0 & 0 & -\sigma l_{4Q} & -\sigma_Q l_{Q4} & F_{4Q} \end{array} \right\| \left\| \begin{array}{c} r_1 \\ r_2 \\ r_3 \\ r_4 \\ r_5 \\ r_6 \end{array} \right\|$$

Going over to symmetry coordinates by multiplying the matrix **B** on the left by the matrix for the transition

from the original vibrational coordinates to symmetry coordinates, we obtain

$$B_{2u}\left\|\begin{matrix}q^1\\ \alpha^2\\ \beta^2\end{matrix}\right\| = \left|\begin{matrix}\frac{1}{2}e_{21} & \frac{1}{2}e_{22} & -\frac{1}{2}e_{23} & -\frac{1}{2}e_{24} & -\frac{1}{2}(e_{21}+e_{23}) & \frac{1}{2}(e_{23}+e_{24})\\ \frac{-\sigma}{\sqrt{2}}f_{12} & \frac{-\sigma}{\sqrt{2}}f_{21} & \frac{\sigma}{\sqrt{2}}f_{34} & \frac{\sigma}{\sqrt{2}}f_{43} & \frac{1}{\sqrt{2}}F_{12} & -\frac{1}{\sqrt{2}}F_{34}\\ \frac{-\sigma}{2}f_{1Q} & \frac{-\sigma}{2}f_{2Q} & \frac{\sigma}{2}f_{3Q} & \frac{\sigma}{2}f_{4Q} & \frac{\sigma}{2}(f_{1Q}+f_{2Q}) & \frac{-\sigma}{2}(f_{3Q}+f_{4Q})\end{matrix}\right| \cdot \left\|\begin{matrix}r_1\\ r_2\\ \cdot\\ \cdot\\ r_6\end{matrix}\right\|$$

$$B_{2u}\left\|\begin{matrix}q^1\\ \beta^2\end{matrix}\right\| = \left|\begin{matrix}\frac{1}{2}e_{21} & -\frac{1}{2}e_{22} & \frac{1}{2}e_{23} & -\frac{1}{2}e_{24} & -\frac{1}{2}(e_{21}-e_{23}) & -\frac{1}{2}(e_{23}-e_{24})\\ \frac{-\sigma}{2}f_{1Q} & \frac{\sigma}{2}f_{2Q} & \frac{-\sigma}{2}f_{3Q} & \frac{\sigma}{2}f_{4Q} & \frac{\sigma}{2}(f_{1Q}-f_{2Q}) & \frac{\sigma}{2}(f_{3Q}-f_{4Q})\end{matrix}\right| \cdot \left\|\begin{matrix}r_1\\ r_2\\ \cdot\\ \cdot\\ r_6\end{matrix}\right\|$$

From considerations of the symmetry of the vibrations it is clear that, in vibrations of type B_{2u}, the vector $\Delta\mu$ will be directed along the ξ-axis. Therefore the stretching term in the expression for $\Delta\mu$ will equal (see ref. 1)

$$\frac{1}{2}\left\{\sin\frac{\theta}{2},\ -\sin\frac{\theta}{2},\ \sin\frac{\theta}{2},\ -\sin\frac{\theta}{2}\right\}\left\|\left(\frac{\partial\mu}{\partial q}\right)_0,\ \left(\frac{\partial\mu}{\partial\gamma}\right)_0\right\| \cdot \left\|\begin{matrix}q^1\\ -q^1\\ q^1\\ -q^1\\ 0\\ \beta^1\\ -\beta^1\\ 0\\ \beta^1\\ -\beta^1\end{matrix}\right\|$$

$$= 2\left[\left(\frac{\partial\mu}{\partial q}\right)_0 q^1 - \left(\frac{\partial\mu}{\partial q_2}\right)_0 q^1 + \left(\frac{\partial\mu}{\partial\beta}\right)_0 \beta^1\right]\sin\frac{\theta}{2}\cdot$$

In a vibration of type B_{2u}, $\Delta\mu$ will be directed along the η-axis, and in this case the product

$$(e_i)\left\|\left(\frac{\partial\mu}{\partial q}\right)_0,\ \left(\frac{\partial\mu}{\partial\gamma}\right)_0\right\| \cdot \left\|\frac{q}{\gamma}\right\|$$

is found to equal

$$2\left[\left(\frac{\partial\mu}{\partial q}\right)_0 q^2 + \left(\frac{\partial\mu_3}{\partial q_2}\right)_0 q^2 + 2\left(\frac{\partial\mu}{\partial\beta}\right)_0 3\beta^2\right]\cos\frac{\theta}{2}\cdot$$

Here it is taken into account that $\alpha = -2\beta$ and

$$z = -2\beta \text{ and } \left(\frac{\partial\mu}{\partial z}\right)_0 = \left(\frac{\partial\mu}{\partial\beta}\right)_0\frac{d\beta}{dz} = -\frac{1}{2}\left(\frac{\partial\mu}{\partial\beta}\right)_0.$$

Let us now turn to the evaluation of the expression

$$(\mu_i)\,\sigma\,(\Delta\varepsilon\mathbf{B}\mathbf{T} - \mathbf{E})\left\|\frac{q}{\gamma}\right\|.$$

For vibrations of type B_{2u}, it takes the following form in symmetry coordinates:

$$\frac{1}{2}(\mu_i)\left\|\begin{matrix}\sigma&0&0&0\\ 0&\sigma&0&0\\ 0&0&\sigma&0\\ 0&0&0&\sigma\end{matrix}\right\|\left\|\begin{matrix}\varepsilon_n&0&0&0&-\varepsilon_c&0\\ 0&\varepsilon_n&0&0&-\varepsilon_c&0\\ 0&0&\varepsilon_n&0&0&-\varepsilon_c\\ 0&0&0&\varepsilon_n&0&-\varepsilon_c\end{matrix}\right\| \cdot \left\|\begin{matrix}\sin\frac{\theta}{2}\ /\ -\sigma\cos\frac{\theta}{2}\\ \sin\frac{\theta}{2}\ /\ -\sigma\cos\frac{\theta}{2}\\ \sin\frac{\theta}{2}\ /\ -\sigma\cos\frac{\theta}{2}\\ \sin\frac{\theta}{2}\ /\ -\sigma\cos\frac{\theta}{2}\\ -2\sin\frac{\theta}{2}\ /\ 2\sigma\cos\frac{\theta}{2}\\ -2\sin\frac{\theta}{2}\ /\ 2\sigma\cos\frac{\theta}{2}\end{matrix}\right\| \times T^q_{2u}\left\|\begin{matrix}q^1\\ \beta^1\end{matrix}\right\| - \left\|\begin{matrix}\sin\frac{\theta}{2}&0&0&0\\ 0&-\sin\frac{\theta}{2}&0&0\\ 0&0&\sin\frac{\theta}{2}&0\\ 0&0&0&-\sin\frac{\theta}{2}\end{matrix}\right\|\left\|\begin{matrix}q^1\\ -q^1\\ q^1\\ -q^1\end{matrix}\right\| = -2\mu_{CH}\cos\frac{\theta}{2}\beta^1;$$

$$T^q_{2u} = \left|\begin{matrix}\frac{(\varepsilon_n+\varepsilon_c+\varepsilon_c\cos\theta)\sigma^2}{(\varepsilon_n^2+2\varepsilon_c\varepsilon_n)\sigma^3} & \vdots & \frac{\varepsilon_c\sin\theta\sigma}{(\varepsilon_n^2+2\varepsilon_c\varepsilon_n)\sigma^3}\\ \cdots\cdots & \vdots & \cdots\cdots\\ \frac{\varepsilon_c\sin\theta\sigma}{(\varepsilon_n^2+2\varepsilon_c\varepsilon_n)\sigma^3} & \vdots & \frac{(\varepsilon_n+\varepsilon_c-\varepsilon_c\cos\theta)}{(\varepsilon_n^2+2\varepsilon_c\varepsilon_n)\sigma^3}\end{matrix}\right|$$

In just the same way, we find for vibrations of type B_{2u}

$$(\mu_i)\,\sigma\,(\Delta\varepsilon\tilde{\mathbf{B}}^*_q T^q - \mathbf{E}_\gamma) = 2\mu_{CH}\sin\frac{\theta}{2} - \beta^1,$$

the column corresponding to the dependent coordinate α being cancelled in the matrix $\tilde{\mathbf{B}}^*_q$. Thus we have obtained the following expressions for the changes in the dipole moment vector during the planar vibrations of the ethylene molecule:

$$\Delta\mu_i^{2u} = 2\left[\left(\frac{\partial\mu}{\partial q}\right)_0 - \left(\frac{\partial\mu_3}{\partial q_2}\right)_0\right]\sin\frac{\theta}{2}\cdot q^1$$

$$+ 2\left[\left(\frac{\partial\mu}{\partial\beta}\right)_0\sin\frac{\theta}{2} - \mu_{CH}\cos\frac{\theta}{2}\right]\beta^1;$$

$$\Delta\mu_i^{2u} = 2\left[\left(\frac{\partial\mu}{\partial q}\right)_0 + \left(\frac{\partial\mu_3}{\partial q_2}\right)_0\right]\cos\frac{\theta}{2}\cdot q^1$$

$$+ 2\left[2\left(\frac{\partial\mu}{\partial\beta}\right)_0\cdot\cos\frac{\theta}{2} + \mu_{CH}\sin\frac{\theta}{2}\right]\beta^1.$$

All that remains is to substitute into them the normalized quantities q^1 and β^1, which are found from the solution of the mechanical problem. On evaluation of the matrix $\sigma(\Delta\varepsilon\mathbf{B}\mathbf{T} - \mathbf{E})$, the rows determining the projections of the Δe vector of the CH bonds onto the coordinate axes are found to be identical, which is explained by the symmetry properties of the bond deflection vectors in vibrations of the types under consideration. This circumstance may be used either to shorten the calculations

or to check their accuracy.

The nonplanar vibrations of type B_{1u} are described by the coordinates ρ_1 and ρ_2 of the departure of the C=C bond from the planes of the two CH_2 groups. It is easy to see that in this case the vector $\Delta\mu$ will be directed along an axis perpendicular to the $\xi\eta$-plane. Therefore the stretching term will be entirely absent from the expression for $\Delta\mu$.

The internal coordinates ρ are connected with the displacements of the corresponding atoms in the following way:

$$\begin{vmatrix}\rho_1\\ \rho_2\end{vmatrix} = \begin{vmatrix} -c\mathfrak{h} & -c\mathfrak{h} & 0 & 0 & (s_Q - 2s)\,\mathfrak{h} & -s_Q\mathfrak{h} \\ 0 & 0 & -c\mathfrak{h} & -c\mathfrak{h} & -s_Q\mathfrak{h} & (s_Q + 2s)\,\mathfrak{h}\end{vmatrix} \| r \|,$$

where $\mathfrak{h}$ is a vector perpendicular to the $\xi\eta$-plane. For symmetry coordinates,

$$\rho^s = \frac{1}{\sqrt{2}} \{ -c\mathfrak{h} - c\mathfrak{h} - c\mathfrak{h} - c\mathfrak{h} 2s\mathfrak{h} 2s\mathfrak{h} \} \| r \|.$$

To simplify the calculations, we take advantage of the property that the projections of all the bond deflection vectors onto the h-direction are identical. Then

$$\Delta\mu_{\mathfrak{h}} = 4\mu_1 \Delta e_1 = 4\mu_1 s \left(\| \tau_H - \tau_C \| \cdot \begin{vmatrix} -s\frac{1}{\sqrt{2}} \\ \frac{+2}{\sqrt{2}} c \end{vmatrix} T'_{1u} \rho^s \right) = -\sqrt{2}\mu_1 \beta^s,$$

where

$$T_1 = \frac{1}{2s^2 (\tau_H + 2\tau_C)}.$$

To describe the electro-optics of the vibrations, we have made use of the four parameters $-\mu_{CH}$, $(\partial\mu/\partial q)$, $(\partial\mu_1/\partial q_A)$, and $(\partial\mu/\partial\beta)$. The intensities of five absorption bands may be found from experiment. Therefore all the unknowns may be determined. The dipole moment of the CH bond may be calculated most precisely from investigation of the nonplanar vibrations.

We note one more advantage associated with the evaluation of $\Delta\mu$ in vector form. In some cases, when the atom displacements are known from the solution of the mechanical problem, the bond deflections may be found without any calculations. In fact, in the B_{3u} vibrations of ethylene the C=C bond does not change its direction in space. Consequently, the deflection of the CH bond is simply equal to the change in the HCC angle during the vibration, i.e., to the coordinate β. For the nonplanar B_{1u} vibrations, it may also be concluded without any calculation (solely from the condition that the C=C direction in space does not change) that $|\Delta e| = \rho \cos\vartheta/2 = \frac{1}{2}\rho$.

THE PYRAMIDAL XY_3 MOLECULE OF THE AMMONIA TYPE

Calculation of the intensities of nonplanar molecules is made difficult by the fact that in this case the process of finding the projections of the unit coordinate vectors onto the chosen coordinate axes is definitely complex. However, the calculations may be substantially facilitated if we take into account the fact that the coordinate vectors $\mathfrak{f}_{ij}$ and $\mathfrak{h}$ may be expressed, as is well known, in terms of the unit bond vectors. Furthermore, in a number of cases it is advantageous to introduce an oblique three-dimensional coordinate system in place of a rectangular one.

Let us consider the ammonia molecule as an example. This molecule belongs to the point group C_{3v} and has two

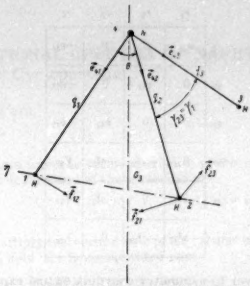

Fig. 2

totally symmetric and two doubly degenerate vibrations. The set of vibrational coordinates and unit vectors usually used for ammonia is shown in Fig. 2. Let us write down the matrix of the derivatives of the bond dipole moments in the form

$$\begin{vmatrix} \left(\frac{\partial\mu_1}{\partial q_1}\right)_0 & \left(\frac{\partial\mu_1}{\partial q_2}\right)_0 & \left(\frac{\partial\mu_1}{\partial q_3}\right)_0 & 0 & \left(\frac{\partial\mu_1}{\partial\tau_{12}}\right)_0 & \left(\frac{\partial\mu_1}{\partial\tau_{13}}\right)_0 \\ \left(\frac{\partial\mu_2}{\partial q_1}\right)_0 & \left(\frac{\partial\mu_2}{\partial q_2}\right)_0 & \left(\frac{\partial\mu_2}{\partial q_3}\right)_0 & \left(\frac{\partial\mu_2}{\partial\tau_{11}}\right)_0 & 0 & \left(\frac{\partial\mu_2}{\partial\tau_{13}}\right)_0 \\ \left(\frac{\partial\mu_3}{\partial q_1}\right)_0 & \left(\frac{\partial\mu_3}{\partial q_2}\right)_0 & \left(\frac{\partial\mu_3}{\partial q_3}\right)_0 & \left(\frac{\partial\mu_3}{\partial\tau_{11}}\right)_0 & \left(\frac{\partial\mu_3}{\partial\tau_{12}}\right)_0 & 0 \end{vmatrix}$$

Here the assumption has been made that the derivatives of the bond dipole moments with respect to the coordinates of the opposite angles equal zero. By virtue of the symmetry of the molecule,

$$\left(\frac{\partial\mu_1}{\partial q_1}\right)_0 = \left(\frac{\partial\mu_2}{\partial q_2}\right)_0 = \left(\frac{\partial\mu_3}{\partial q_3}\right)_0 = \left(\frac{\partial\mu}{\partial q}\right)_0;$$

$$\left(\frac{\partial\mu_1}{\partial q_2}\right)_0 = \left(\frac{\partial\mu_1}{\partial q_3}\right)_0 = \left(\frac{\partial\mu_2}{\partial q_1}\right)_0 = \dots = \left(\frac{\partial\mu_3}{\partial q_2}\right)_0;$$

$$\left(\frac{\partial\mu_1}{\partial\tau_{12}}\right)_0 = \left(\frac{\partial\mu_1}{\partial\tau_{13}}\right)_0 = \dots = \left(\frac{\partial\mu_3}{\partial\tau_{12}}\right)_0 = \left(\frac{\partial\mu}{\partial\tau}\right)_0.$$

In the case of the totally symmetric vibrations, the vector $\Delta\mu$ will be directed along the C_3-axis. $q_1 = q_2 = q_3 = (1/\sqrt{3})q^A$ and $\gamma_1 = \gamma_2 = \gamma_3 = (1/\sqrt{3})\gamma^A$. The stretching term will equal

$$\sqrt{3}\left\{\left[\left(\frac{\partial\mu}{\partial q}\right)_0 + 2\left(\frac{\partial\mu_1}{\partial q_2}\right)_0\right] q^A + 2\left(\frac{\partial\mu}{\partial\tau}\right)_0 \tau^A\right\} \cos\alpha.$$

Here α is the angle between the C_3-axis and an NH bond; $\sin\alpha = (2/\sqrt{3})\sin(\vartheta/2)$. For the degenerate vibrations, we have

$$q_1 = -q_2 = \frac{1}{\sqrt{2}} q^E;\ \gamma_1 = -\gamma_2 = \frac{1}{\sqrt{2}} \tau^E;\ q_3 = 0 \text{ and } \gamma_3 = 0.$$

The vector $\Delta\mu$ will be directed along the η-axis. By calculating the projections of the e_i vectors onto the η-axis and taking into account the form of the matrix of the derivatives of the bond dipole moments and the values of the internal coordinates, we obtain the following expression for the stretching term:

$$\sqrt{\frac{3}{2}}\left\{\left[\left(\frac{\partial\mu}{\partial q}\right)_0 - \left(\frac{\partial\mu_1}{\partial q_2}\right)_0\right] q^E - \left(\frac{\partial\mu}{\partial\tau}\right)_0 \tau^E\right\} \sin\alpha.$$

The B matrix for the ammonia molecule has the form

	r_1	r_2	r_3	r_4
q_1	e_{41}	0	0	$-e_{41}$
q_2	0	e_{42}	0	$-e_{42}$
q_3	0	0	e_{43}	$-e_{43}$
$\gamma_1 = \gamma_{23}$	0	$-\sigma l_{23}$	$-\sigma l_{22}$	F_{23}
$\gamma_2 = \gamma_{13}$	$-\sigma l_{13}$	0	$-\sigma l_{31}$	F_{13}
$\gamma_3 = \gamma_{12}$	$-\sigma l_{12}$	$-\sigma l_{21}$	0	F_{12}

Going over to symmetry coordinates and expressing the vectors f_{ij} in terms of the unit vectors e_i according to the formula

$$f_{ij} = \frac{1}{\sin\theta}(e_j - e_i\cos\theta),$$

we get

$$\begin{vmatrix} \sqrt{3}\,q^A \\ \sqrt{3}\,\gamma^A \\ \sqrt{2}\,q^E \\ \sqrt{2}\,\gamma^E \end{vmatrix} = \begin{vmatrix} e_{11} & e_{12} & e_{13} & -(e_{11}+e_{12}+e_{13}) \\ \frac{-\sigma}{\sin\theta}(e_{11}+e_{12} & \frac{-\sigma}{\sin\theta}(e_{11}+e_{12} & \frac{-\sigma}{\sin\theta}(e_{11}+e_{12} & 2(e_{11}+e_{12} \\ -2e_{13}\cos\theta) & -2e_{13}\cos\theta) & -2e_{13}\cos\theta) & +e_{13})\cdot\tau\,\mathrm{tg}\frac{\theta}{2} \\ e_{11} & -e_{12} & 0 & -e_{11}+e_{12} \\ \frac{\sigma}{\sin\theta}(e_{11} & \frac{\sigma}{\sin\theta}(e_{12} & \frac{\sigma}{\sin\theta}(e_{11}-e_{13}) & \frac{\sigma}{\sin\theta}[(e_{13}-e_{11}) \\ -e_{11}\cos\theta) & -e_{12}\cos\theta & & -(e_{12}-e_{11})\cos\theta] \end{vmatrix} \cdot \begin{vmatrix} r_1 \\ r_2 \\ r_3 \\ r_4 \end{vmatrix}$$

Hence, taking account of the symmetry properties of the Δe_i vectors and the direction of the $\Delta\mu$ vector, we find for the totally symmetric vibrations the following expression for the deformation term:

$$\sqrt{3}\mu_3\cos\alpha\cdot\left[(\varepsilon_H,\ -\varepsilon_N)\cdot\left|\begin{array}{c|c} 1 & -2\sigma\tan\frac{\theta}{2} \\ \hline -3 & 6\sigma\tan\frac{\theta}{2} \end{array}\right|\cdot\left|\begin{matrix}\tau_{11}\tau_{12}\\ \tau_{21}\tau_{22}\end{matrix}\right|\cdot\left|\begin{matrix}q^A\\ \gamma^A\end{matrix}\right| - q^A\right]$$

$$= \sqrt{3}\mu_3\cos\alpha\left(\varepsilon_H + 3\varepsilon_N\right)\left(\tau_{12} - 2\sigma\tan\frac{\theta}{2}\cdot\tau_{22}\right)\gamma^A,$$

where θ if the HNH angle. The matrix

$$T = \left|\begin{matrix}\tau_{11}\tau_{12}\\ \tau_{21}\tau_{22}\end{matrix}\right|.$$

In the present case, the inversion of the matrix T^{-1} was not carried out in the general form, since it leads to unduly awkward calculations. In the practical conduct of the calculations, the T^{-1} matrix is always written down in numerical form, and therefore the calculation of the inverse matrix presents no serious difficulties, especially if we consider that this operation may be performed on electronic computers.

In the case of the degenerate vibrations, it is easy to show that Δe_3 will equal zero, as also follows from the symmetry properties of the bond deflection vectors. Furthermore, $\| \Delta e_1 \| \Delta e_2 \|$. The sum $\mu(\Delta e_1 + \Delta e_2)$ will be directed along the η-axis, in consequence of which

$$(\mu_\eta)\cdot(\Delta_1\widehat{\mathbf{B}}\gamma - \mathbf{E})\left|\begin{matrix}q\\ \gamma\end{matrix}\right| = \sqrt{\frac{3}{2}}\mu_3\sin\alpha\left[(\varepsilon_H - \varepsilon_N)\right]\left|\begin{matrix}1 & -\sigma\cot\theta\\ -2 & -2\sigma\cdot\tan\frac{\theta}{2}\end{matrix}\right|$$

$$\times\left|\begin{matrix}\tau_{11}\tau_{12}\\ \tau_{21}\tau_{22}\end{matrix}\right|\cdot\left|\begin{matrix}q^E\\ \gamma^E\end{matrix}\right| - q^E\Big] = \sqrt{\frac{3}{2}}\mu_3\sin\alpha\Big\{\Big[(\varepsilon_H + 2\varepsilon_N)\tau_{11}$$

$$-\sigma\Big(\varepsilon_H\cot\theta - 2\varepsilon_N\tan\frac{\theta}{2}\Big)\tau_{21} - 1\Big]q^E + \Big[(\varepsilon_H + 2\varepsilon_N)\tau_{12} - \sigma\Big(\varepsilon_H\cot\theta - 2\varepsilon_N\tan\frac{\theta}{2}\Big)\tau_{22}\Big]\gamma^E\Big\}.$$

For ammonia, the coefficient for q^E is significantly less than that for γ^E, but nevertheless, as in the case of a symmetrical nonlinear triatomic molecule, the action of the coordinates q leads to deflection of the corresponding bonds.

Finally, for the totally symmetric vibrations,

$$\Delta\mu_{\eta_1} = \sqrt{3}\cos\alpha\left\{\left[\left(\frac{\partial\mu_1}{\partial q}\right)_0 + 2\left(\frac{\partial\mu_1}{\partial q_2}\right)_0\right]q^A + \left[2\left(\frac{\partial\mu}{\partial\gamma}\right)_0 + \mu_3(\varepsilon_H + 3\varepsilon_N)\right.\right.$$
$$\left.\left.\times\left(\tau_{12} - 2\sigma\tan\frac{\theta}{2}\tau_{22}\right)\right]\gamma^A\right\}$$

and for the degenerate vibrations,

$$\Delta\mu_\eta = \sqrt{\frac{3}{2}}\sin\alpha\left\{\left[\left(\frac{\partial\mu}{\partial q}\right)_0 - \left(\frac{\partial\mu}{\partial q_2}\right)_0 + \mu_3\left\{(\varepsilon_H + 2\varepsilon_N)\tau_{11}\right.\right.\right.$$
$$\left.\left.\left. - \sigma\left(\varepsilon_H\cot\theta - 2\varepsilon_N\tan\frac{\theta}{2}\right)\tau_{21} - 1\right\}\right]q^E - \left[\left(\frac{\partial\mu}{\partial\gamma}\right)_0\right.$$
$$\left. - \mu_3\left\{(\varepsilon_H + 2\varepsilon_N)\tau_{12} - \sigma\left(\varepsilon_H\cot\theta - 2\varepsilon_N\tan\frac{\theta}{2}\right)\tau_{22}\right\}\right]\gamma^E\Big\}.$$

Thus we have obtained, in explicit form, expressions for the transition probability factor during absorption. We have still to substitute the normalized values of q^A, γ^A and q^E, γ^E for the corresponding normal vibrations and the magnitudes of the elements of the T matrix for the totally symmetric and degenerate vibrations.

From the examples presented, the advantages of the method here analyzed can be clearly seen: the clarity and routineness of all the calculations, the possibility of performing the calculations directly in the first approximation of the valence-optical scheme, the absence of intermediate steps (the introduction of valence-optical coordinates and the finding of the center of mass). If the solution of the mechanical problem is carried as far as the determination of the magnitudes of the atomic displacements, the evaluation of the intensities becomes a thoroughly simple task.

REFERENCES

1. L. A. Gribov, Doklady Akad. Nauk SSSR 127, 788 (1959).
2. L. A. Gribov, Opt. i Spektr. 8, 769 (1960), Optics and Spectroscopy 8, 404 (1960).

CALCULATION AND INTERPRETATION OF THE VIBRATIONAL SPECTRA OF NAPHTHENES
IV. The Influence Constants of Cyclopentane

L. M. Sverdlov and N. I. Prokof'eva

Received 28 November 1959

A calculation of the complete system of influence constants (inverse force constants) of the cyclopentane molecule is carried out. The particulars of the force field of the molecule are clarified.

1. In a previous study[1] we made a calculation of the frequencies and gave an interpretation of the vibrational spectra of cyclopentane and deuterocyclopentane. At the same time the system of symmetry force constants k^{s}_{ij} of cyclopentane was computed. These constants are complicated combinations of the force constants of the natural coordinates k_{ij} due to the presence of numerous complementary relations among the coordinates (16 relations among 55 coordinates). Therefore, it is impossible to determine a large majority of the constants k_{ij}; the number of constants k_{ij} (97) is many more than the number of symmetry constants k^{s}_{ij} (52). True, it is possible by putting a portion of the constants k_{ij} equal to zero to calculate the remaining. However, in the given case such a method will be too uncertain since, due to the rather strong bonds between different atoms of the molecule resulting from the cyclic conditions, it is difficult to say in advance which of the constants can be equated to zero.

In order to avoid this difficulty, it is necessary to calculate the system of influence constants[2] (i.e., inverse force constants k^{-1}_{ij}), invariant to coordinate variation and giving a more complete characterization of the particulars of the force field than the force constants. Using the circumstance that the influence constants are related by the same complementary conditions as the coordinates themselves,[2] it is possible to calculate the complete system of influence constants k^{-1}_{ij} of cyclopentane.

2. Inversion of the symmetry matrices of the force constants was performed by the well-known matrix method of line reorganization.[3] This method appears to be more effective than the method of determinants, generally applied for this purpose. This method is particularly valuable in the inversion of matrices of high order.

We will demonstrate the application of this method with the example of the inversion of the force matrix, belonging to the A'_1 symmetry type

$$[k_{ij}]^{A'_1} = \begin{bmatrix} 8.03 & 0 & 0.2424 \\ 0 & 7.22 & -0.4388 \\ 0.2424 & -0.4388 & 0.99 \end{bmatrix}. \qquad \text{A}$$

Inverse to this will be that matrix $[k^{-1}_{ij}]^{A'_1}$, such that

$$[k_{ij}]^{A'_1} \cdot [k^{-1}_{ij}]^{A'_1} = \begin{bmatrix} 1 & 0 & 0 \\ 0 & 1 & 0 \\ 0 & 0 & 1 \end{bmatrix}. \qquad (1)$$

We apply to the right and left parts of the equality (1) the following operation. We multiply the first row on the left by 1/8.03 and subtract termwise from the second and third rows

$$\begin{bmatrix} 1 & 0 & 0.0302 \\ 0 & 7.22 & -0.4388 \\ 0 & -0.4388 & 0.9827 \end{bmatrix} [k^{-1}_{ij}]^{A'_1} = \begin{bmatrix} 0.1245 & 0 & 0 \\ 0 & 1 & 0 \\ -0.0302 & 0 & 1 \end{bmatrix}. \qquad (2)$$

We multiply the second row of Eq. (2) on the left by 1/7.22 and subtract from the third row

$$\begin{bmatrix} 1 & 0 & 0.0302 \\ 0 & 1 & -0.0608 \\ 0 & 0 & 0.956 \end{bmatrix} [k^{-1}_{ij}]^{A'_1} = \begin{bmatrix} 0.1245 & 0 & 0 \\ 0 & 0.1385 & 0 \\ -0.0302 & 0.0608 & 1 \end{bmatrix}. \qquad (3)$$

Multiplying the third row on the left by 1/0.956 and subtracting termwise from the second and third rows, we obtain the desired matrix $[k^{-1}_{ij}]^{A'_1}$

$$\begin{bmatrix} 1 & 0 & 0 \\ 0 & 1 & 0 \\ 0 & 0 & 1 \end{bmatrix} [k^{-1}_{ij}]^{A'_1} = \begin{bmatrix} 0.1255 & -0.0019 & -0.0316 \\ -0.0019 & 0.1424 & 0.0636 \\ -0.0316 & 0.0636 & 1.046 \end{bmatrix}. \qquad (4)$$

Using the derived system of linearly independent symmetry influence constants and introducing the complementary relations among the symmetry coordinates, we obtain the linearly-dependent influence constants.

For example, for the symmetry type E''_2 we have a system of six equations for the determination of the linearly-dependent coefficients $[k^{-1}_{ij}]^{E''_2}$ of the following form

$$k^{-1}_{\varphi^{s}_{2}1\varphi^{s}_{2}1} = -\left[0.4966 \cdot k^{-1}_{\varphi^{s}_{2}1\rho^{s}_{2}1} + 0.5102 \cdot k^{-1}_{\rho^{s}_{2}1\rho^{s}_{2}1}\right]; \qquad \text{B}$$

$$k^{-1}_{\varphi^{s}_{2}1\varphi^{s}_{2}1} = -\left[0.4966 \cdot k^{-1}_{\varphi^{s}_{2}1\tau^{s}_{2}1} + 0.5102 \cdot k^{-1}_{\varphi^{s}_{2}1\varphi^{s}_{2}1}\right]$$

etc.

Then, using the table of symmetry coefficients of the D_{5h} group, given in ref. 1, we transform from the symmetry influence coefficients to the influence coefficients to the influence coefficients k^{-1}_{ij}. These transformation formulas have a particularly complicated form, so we will not present them here.

3. The complete system of influence constants obtained from the complicated calculations is given in the Table. Comparison of the influence constants of cyclopentane and ethane,[4] and also an analysis of the data obtained, permits us to draw the following conclusions about the character of the force field of the cyclopentane molecule.

a. The influence constants of the CH_2 group—k^{-1}_{r}, k^{-1}_{α}, h^{-1}_{13}, a^{-1}_{α}—practically coincide with the corresponding constants in paraffins. The smallness of the influence constants h^{-1}_{13}, h^{-1}_{14}, b^{-1}_{13}, b^{-1}_{14}, $U^{-1}_{12,34}$, $U^{-1}_{12,56}$ bear witness to the weak interaction between the CH_2 groups.

b. In comparison with ethane, the stiffness of the CCH angle increases only very slightly by 3%, in all. The interaction of the CCH angles of type (a1, e1), (a1, e2), (a1, a2) (i.e., adjacent angles) has a significant magnitude, while the interaction of nonadjacent angles is several times smaller (but this interaction must be taken into account).

c. The C-C bond in cyclopentane is approximately 15% weaker than in ethane. The interaction between neighboring C-C bonds is rather significant (H^{-1}_{45} is $\sim 11\%$ k^{-1}_{C}).

Influence Constants of Cyclopentane (in Units of 10^{-6} cm²)

Generalized forces	$f_{(q_i)}$	$f_{(Q_{2i})}$	$f_{(\varkappa_{1i})}$	$f_{(\tau_{2ai})}$	$f_{(\tau_{3ai})}$	$f_{(\tau_{3ci}^{a})}$	Generalized forces	$f_{(\delta_{1i})}$	$f_{(Q_{2i})}$	$f_{(\varkappa_{1i})}$	$f_{(\tau_{2ai})}$	$f_{(\tau_{3ci})}$	$f_{(\tau_{3ci}^{a})}$
$f_{(q_1)}$	0.1284	0.0007	−0.0261	0.0097	−0.0121	−0.0038	$f_{(\delta_{1i})}$	0.0085	−0.0281	−0.031	0.058	−0.0967	0.0559
$f_{(q_2)}$	−0.0023	0.0007	−0.0261	0.0097	0.0206	0.0038	$f_{(\delta_{2i})}$	−0.0143	0.0396	0.0035	0.0068	+0.0480	−0.0554
$f_{(q_3)}$	0.0001	0.0007	0.0023	−0.0064	−0.0055	0.0049	$f_{(\delta_{3i})}$	0.0154	0.0396	0.0035	0.0068	−0.0351	0.0554
$f_{(q_4)}$	−0.0005	0.0007	0.0023	−0.0064	0.0085	−0.0049	$f_{(\delta_{4i})}$	−0.0094	0.0096	0.0095	−0.0108	+0.0511	0.0445
$f_{(q_5)}$	0.0003	−0.0002	−0.0005	0.0016	−0.0094	−0.0041	$f_{(\delta_{5i})}$	0.0084	0.0096	0.0095	−0.0108	−0.0544	−0.0445
$f_{(q_6)}$	−0.0002	−0.0002	−0.0005	0.0016	0.0084	0.0041	$f_{(\varkappa_{1i})}$	0.0102	−0.0415	−0.0025	−0.0054	−0.0001	0.049
$f_{(q_7)}$	0.0003	−0.0025	−0.0005	0.0016	0.0102	0.0018	$f_{(\varkappa_{2i})}$	−0.0103	−0.0415	−0.0025	−0.0054	−0.0034	−0.049
$f_{(q_8)}$	−0.0002	−0.0025	−0.0005	0.0016	−0.0103	−0.0018	$f_{(\varkappa_{3i})}$	0.0102	0.0041	−0.0025	−0.0054	0.0598	−0.0161
$f_{(q_9)}$	0.0001	−0.0002	0.0023	−0.0064	−0.0143	0.0013	$f_{(\varkappa_{4i})}$	−0.0103	0.0041	−0.0025	−0.0054	−0.0407	0.0161
$f_{(q_{10})}$	−0.0005	−0.0002	0.0023	−0.0064	0.0154	−0.0013	$f_{(\varkappa_{5i})}$	−0.0094	0.0041	0.0095	−0.0108	−0.0001	−0.0238
$f_{(Q_{1i})}$	0.0007	0.1814	−0.003	0.0402	−0.0281	0	$f_{(\varkappa_{6i})}$	0.0084	0.0041	0.0095	−0.0108	−0.0034	0.0238
$f_{(Q_{2i})}$	−0.0002	−0.0202	0.0075	−0.004	0.0096	0	$f_{(\varkappa_{7i})}$	−0.0143	−0.0415	0.0035	0.0068	+0.0095	−0.0185
$f_{(Q_{3i})}$	−0.0025	0.0096	0.0544	−0.0729	0.0041	0	$f_{(\varkappa_{8i})}$	0.0153	−0.0415	0.0035	0.0068	0.0132	0.0185
$f_{(Q_{4i})}$	−0.0002	0.0096	0.0075	−0.004	−0.0415	0	$f_{(\varkappa_{9i})}$	−0.0055	0.0096	−0.031	0.058	0.0480	−0.0104
$f_{(Q_{5i})}$	0.0007	−0.0202	−0.003	0.0402	0.0396	0	$f_{(\varkappa_{10i})}$	0.0085	0.0096	−0.031	0.058	−0.0351	0.0104
$f_{(\tau_{12i})}$	−0.0361	−0.003	1.0926	−0.1305	−0.2463	0	$f_{(\varkappa_{11i})}$	−0.0121	0.0396	−0.2463	−0.0484	−0.1732	0.0459
$f_{(\tau_{23i})}$	0.0023	−0.003	−0.0257	0.0818	−0.031	0	$f_{(\varkappa_{12i})}$	0.0296	0.0396	−0.2463	−0.0484	−0.2542	−0.0459
$f_{(\tau_{34i})}$	−0.0005	0.0075	0.0024	−0.0166	0.0095	0	$f_{(\tau_{1ci}^{a})}$	−0.0038	0	0	0	0.0407	1.1222
$f_{(\tau_{45i})}$	−0.0005	0.0544	0.0024	−0.0166	−0.0025		$f_{(\tau_{1ci}^{s})}$	0.0013	0	0	0	−0.0104	−0.9079
$f_{(\tau_{51i})}$	0.0025	0.0075	−0.0257	0.0818	0.0035	0	$f_{(\tau_{2ai}^{a})}$	0.0018	0	0	0	−0.0238	0.3468
$f_{(\tau_{1ai})}$	0.0097	0.0402	−0.1305	0.3291	−0.0484	0	$f_{(\tau_{2ai}^{s})}$	−0.0041	0	0	0	0.049	0.3468
$f_{(\tau_{2ai})}$	−0.0064	0.0402	0.0818	−0.2142	0.058	0	$f_{(\tau_{3ci}^{a})}$	0.0049	0	0	0	−0.0554	−0.9079
$f_{(\tau_{3ai})}$	0.0016	−0.004	−0.0166	0.0497	−0.0108	0	$f_{(\tau_{3ci}^{s})}$	0.0049	0	0	0	−0.0559	−0.8347
$f_{(\tau_{4ai})}$	0.0016	−0.0723	−0.0108	0.0497	−0.0054	0	$f_{(\tau_{1ai}^{a})}$	−0.0041	0	0	0	0.0445	1.1162
$f_{(\tau_{5ai})}$	−0.0064	−0.004	0.0818	−0.2142	0.0066	0	$f_{(\tau_{1ai}^{s})}$	0.0018	0	0	0	−0.0161	−0.9713
$f_{(\tau_{a1})}$	−0.0121	−0.0281	−0.2463	−0.0484	0.0156	0.0407	$f_{(\tau_{2ci}^{a})}$	0.0013	0	0	0	−0.0185	0.4555
$f_{(\tau_{a2})}$	0.0206	−0.0281	−0.2463	−0.0484	−0.1816	−0.0407	$f_{(\tau_{2ci}^{s})}$	−0.0038	0	0	0	0.0459	0.2343
$f_{(\tau_{a3})}$	−0.0025	−0.0281	−0.031	0.058	−0.0179	−0.0559							

d. Comparison of the influence constants k^{-1} (C-C) and k^{-1} (CCC) shows that the stiffness of the CCC angle in cyclopentane is much greater (it is about 50% of the strength of the C-C bond) than in acyclic hydrocarbons. The interaction of the elements of the ring also has a significant magnitude.

4. In conclusion, we will examine the work of Lebedev and Sechkarev,[5] devoted to a calculation of the force constants of cyclopentane. In the calculation of the force constants these authors made a series of unfounded assumptions: they arbitrarily put 72 of the 97 constants equal to zero; they did not completely take account of the symmetry force constants $k_{\beta A_2''}$, $k_{\beta A_2''}$, $k_{\beta E_2''\tau_a}$, $k_{\beta E_2''\tau_b}$, $U_{\beta E_2''\tau_a\beta E_2''\tau_b}$, forming individual combinations of the force constants among the coordinates β, not met with in the symmetry force constants of the other symmetry types. As a result, their system of force constants must be regarded with considerable doubt. For example, their increase of the force constant k_δ by 40% in comparison with paraffins is unreasonable. In addition, obvious errors are assumed in ref. 5. As in a preceding study,[6] they use for the interaction (qq) in the matrix of the kinematic coefficients A_2'', the value 1.0604 instead of the correct value of 1.1208, as a result of which for the frequency $\nu A_2''$ (C-H) they obtained a lower value (by 73 cm^{-1} in comparison with $\nu E_1'$ (C-H)). Further, the values of the frequencies ν(C-H) of the symmetry types A_1', E_2'', and E_1' should be close to one another (the difference should not exceed 15-20 cm^{-1}), while in ref. 5 the calculated value of the frequency $\nu A_1'$ (C-H) is greater than the frequency $\nu E_2''$ (C-H) by 93 cm^{-1}.

Finally, these authors[5] distorted the results obtained in ref. 4. There it was shown that the strength of the C-C bond in cyclopropane is greater than in paraffins, while the authors in ref. 5, quoting the value of the symmetry constant $k_{OA_1'}$ and having identified it with the force constant k_O affirm that the force constant k_O in cyclopropane is lower than in paraffins.

REFERENCES

1. L. M. Sverdlov and N. I. Prokof'eva, Opt. i Spektr. 7, 588 (1959), Optics and Spectroscopy 7, 363 (1959).
2. L. S. Mayants, Trudy Fiz. Inst. Akad. Nauk SSSR 5, 63 (1950).
3. R. R. Fraser, V. Duncan, and A. Kollor, "Teoriya Matritz i ee Prilozheniya" (The Theory of Matrices and its Application). Izd. Inostrannoi Lit., Moscow, 1950.
4. L. M. Sverdlov and E. P. Krainov, Opt. i Spektr. 3, 54 (1957).
5. R. S. Lebedev and A. V. Sechkarev, Opt. i Spektr. 7, 164 (1959), Optics and Spectroscopy 7, 104 (1959).
6. R. S. Lebedev, Opt. i Spektr. 6, 154 (1959), Optics and Spectroscopy 6, 101 (1959).

EFFECT OF TEMPERATURE ON THE INTENSITIES OF THE VIBRATIONAL ABSORPTION BANDS OF LIQUID BROMOFORM

M. P. Lisitsa and Yu. P. Tsyashchenko

Received 14 December 1959

Quantitative data are presented on the temperature variations of the intensities of the absorption bands corresponding to the fundamental vibrations ν_1, ν_4, and ν_5 of liquid bromoform, their first overtones, and the combination frequency $\nu_1 + \nu_4$. For most of the bands the measurements were carried out in the temperature range 18-130°C. A discussion of the results obtained is set forth.

INTRODUCTION

Those temperature changes in the infrared absorption spectra of liquids which are associated with the presence of a hydrogen bond or of rotational isomerism are satisfactorily well known at the present time. However, the influence of temperature on the intensities of vibrational absorption bands corresponding to vibrations which are not subject to the influence of a hydrogen bond or are not associated with the presence of various isomeric forms of the molecule has been considerably less well investigated.[1-6] Most of the works devoted to the solution of this problem are of a haphazard character and contain chiefly qualitative information on the diminution of the integrated absorption of vibrational bands with an increase in temperature. It is true that in one work[3] the reverse effect is noted; that is, an increase of absorption in the bands of the fundamental vibrations ν_1, ν_2, and ν_5 of liquid CH_3I. This fact, however, is in contradiction with the more reliable quantitative data of Bazhulin and Smirnov,[7] which confirm in this case also the general tendency to a diminution of the absorption with an increase in temperature.

A more systematic study of the phenomenon was recently begun,[5-6] and only in the latest publications are there quantitative data which enable one to judge the regularities of this decrease[5,6,8] and of the presence of a connection—insufficiently clearly expressed, to be sure—between the observed temperature dependence and the magnitude of the dipole moment of the molecule.[7]

There are very few quantitative investigations in which the effect under discussion could be more fully studied on the spectrum of one and the same liquid possessing certain fundamental frequencies and bands corresponding to vibrations of different order, form, and intensity. At the same time, just such investigations are necessary to clarify the influence of the properties of the vibration itself on the temperature dependence. The present work, in which the effect of temperature on the integrated absorption of various vibrational bands of bromoform has been studied, is a continuation of our investigations in this direction.

PROCEDURE AND ERRORS OF THE MEASUREMENTS

Under ordinary conditions, bromoform is a liquid in the temperature range 8-148°C,* which is sufficient for the solution of the problem before us.

One of the basic difficulties in temperature studies of the infrared absorption of a liquid consists in the construction of an appropriate cell. Various designs of temperature cells have previously been described.[7, 10-14] However, some of them are complicated to make and cannot be reproduced in every laboratory, while others do not satisfy all the requirements which confront quantitative measurements. The cell used in the present work is in our view easier to construct and sufficiently reliable over a wide temperature range.

A cross section of the cell is represented in Fig. 1. Between the well-polished (to within 1-2 interference bands) salt plates 1 is clamped a rectangular gasket 2 of the required thickness, cut from lead or silver foil.*

*Lead gaskets with a minimum thickness of 15-20μ may be obtained by rolling between aluminum facings. For the thinnest cells, silver foil with a minimum thickness of ~3-4μ, obtained by rolling between brass facings, was used.

The copper capillaries 3 with an internal diameter of 0.3 mm and an external diameter of 1 mm, which serve for filling the cell, were introduced into openings in the window together with lead packings 4. The places of possible leaks were sealed with glyptal 5, which, after polymerization (1.5-2 hr at 180-200°C followed by slow cooling), has good vacuum properties, sufficient mechanical strength, and chemical inertness. For the sealing and polymerization, the cell was fastened in a metal holder. After it was filled, the ends of the capillaries were flattened, whereby the cell was hermetically sealed. After the measurement, the flattened part of the ends could be removed and the cell could be refilled with the liquid under study through the openings thus formed. If the original length of the copper tubes is 5 cm, the cell may be used at least 15 times.

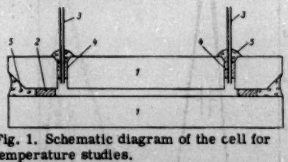

Fig. 1. Schematic diagram of the cell for temperature studies.

The heating of the liquid was conducted in special cylindrical electric furnaces, the end openings of which were tightly closed with rock-salt windows. The temperature was controlled with an EMV-21 thermoregulator. The copper-constantan thermocouple which served to measure the temperature was inserted into a notch in one of the cell windows. The error in determining the temperature did not exceed ±2°. There was no thermal gradient along the layer studied.

The cell thickness was determined by the interference method with an error of 1-2%. The thinnest cells,

which were used to study the bands of the fundamental vibrations ν_4 and ν_5, were calibrated with an error of 10-20% on the basis of the absorption known for these bands at room temperature.[15] Visual inspection by reflected light of the interference figure from the unfilled thinnest cells (~4-8μ) established the constancy of their thickeness with temperature on heating to 120-130°. A check of this sort was not made for the thicker cells, but there is no reason to suppose that they behave differently in response to temperature change. The thickness of the cells was selected so as to achieve maximum contrast in transmission for the greatest possible part of the band,[16] but even so the temperature-controlled changes at the base of the band (transmission of the order of 90%) may not be detected. The transmission at the minimum usually did not exceed 20%, and the ratio of the magnitude of the spectral slit width of the apparatus,* calculated according to ref. 17, to the observed half-width did not go beyond the limits 0.25-0.35. Under such conditions the correction for the spectral slit width in the value of the integrated absorption amounts to 1-2%[18,19] and is insignificant for practical purposes. No correction for the wings was introduced, since the range of integration remained unchanged during the temperature changes; consequently, the influence of this correction[7] on the relative temperature change of the integrated absorption could hardly exceed the random experimental error, which amounted (average of 5-6 measurements) to 5-7%.

*The measurements were carried out on an ISK-6 instrument.

A direct test and certain indirect considerations, described in a following article, did not detect in our case (at least within the limits of random errors) any effect of dilation of the cells in consequence of the temperature variation of the vapor pressure of bromoform.[7] However, even if such a dilation were present, it could not affect the accuracy of the measurements carried out in the present work with two cells of different thickness,[20] by means of which the effect under consideration was eliminated as not dependent on the thickness.

At each temperature point, the results of the measurements were corrected for the change in density of bromoform with temperature, which reaches 15-16% over the whole range of existence of the liquid phase.

Selective radiation of the liquid was not detected. The thermal background from the furnaces and cells was excluded in calculating the absorption coefficients.

The experimental conditions described above permitted in most cases a measurement of the integrated absorption with an error of 10-15%. The band of the vibration ν_5, for which the error may reach 25%, is an exception. We note, however, that the error in the determination of the relative temperature variation of the integrated absorption was in all cases not greater than 5-7%.

Experimental results and their discussion

EXPERIMENTAL RESULTS AND THEIR DISCUSSION

The infrared spectrum of bromoform has previously been studied in detail by us.[15] The molecule $CHBr_3$ is relatively simple, it forms no associations, and it does not possess rotational isomers. Consequently, bromoform is a good material for the study of the temperature dependence of the intensities of vibrational absorption bands. We have completed studies of such a dependence from the bands of the fundamental vibrations ν_1, ν_4, and ν_5, their overtones $2\nu_1$, $2\nu_4$, and $2\nu_5$, and the combination frequency $\nu_1 + \nu_4$. The remaining bands in the spectrum of liquid $CHBr_3$ (in the spectral region accessible for our temperature measurements, 1-15μ) as a rule are of low intensity and overlap both one another and the wings of the more intense bands, which makes them inconvenient for temperature measurements. Furthermore, in a number of cases they are not unequivocally identified, and this rules out the possibility of establishing a connection between the shape of the vibration and the order of the tone, on the one hand, and the effect of temperature, on the other. The temperature variations observed in the intensities of the bands of the fundamental vibrations ν_1, ν_4, and ν_5 are represented in Fig. 2. It should first of all be noted that the magnitude of the temperature shift of the maxima of the bands studied did not, in general, go beyond the limits of the errors in the calibration of the apparatus and indeed, as a test showed, was brought about by an uncom-

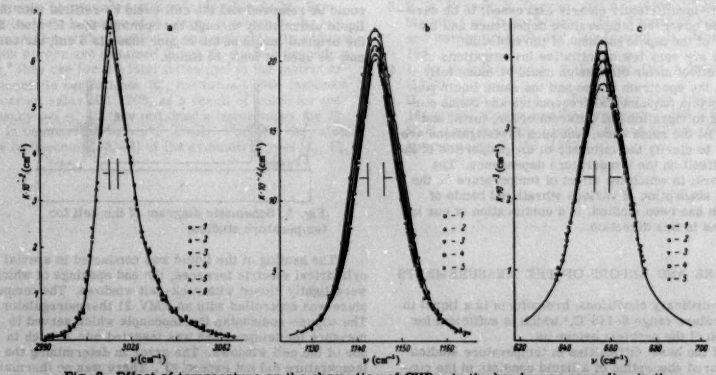

Fig. 2. Effect of temperature on the absorption of $CHBr_3$ in the bands corresponding to the fundamental vibrations ν_1 (a), ν_4 (b), and ν_5 (c). Temperature (in °C): 1—20; 2—40; 3—60; 4—80; 5—100; 6—130.

pensated change in the refractive index of the prisms as a result of the heating of the spectrometer. Accordingly, the curves corresponding to different temperatures have been brought, on the graphs, to the same position of the maximum.

The course of the temperature dependence of the integrated absorption in the region of the three bands mentioned is shown in Fig. 3, from which it follows that the absorption diminishes linearly with an increase in temperature. Thus the regularity established during the investigation of carbon tetrachloride[8] and tetrabromide[8] is confirmed in the present case also. The intensity of the band which corresponds to the doubly degenerate deformation vibration of the C—H bond, ν_4, changes most significantly, its integrated absorption diminishing by 18%. The intensities of the bands of the totally symmetric valence vibration of the C—H bond, ν_1, and of the doubly degenerate vibration of the C—Br bonds, ν_5, diminish insignificantly and to almost the same degree (8-9%) as the temperature increases.

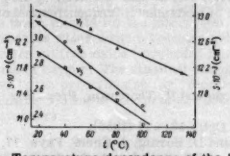

Fig. 3. Temperature dependence of the integrated absorption in the bands of the fundamental vibrations ν_1, ν_4, and ν_5 of $CHBr_3$. Scale for the ordinate axis: for ν_1 at the right, for ν_5 at the left, for ν_4 in the middle.

The fact that deformation vibrations are more strongly subject to temperature dependence was noted earlier by Bobovich,[21] who was investigating the effect of temperature on Raman spectra. Similar parallelism was not detected in ref. 7, in which a greater temperature dependence was observed for the C—H valence vibrations of chloroform and the C≡N vibration of acetonitrile in comparison with the corresponding deformation vibrations of the same molecules. As far as the former vibration is concerned, the same result as in ref. 7 has been obtained qualitatively by the authors of the present work as a result of their temperature studies of the infrared spectrum of chloroform.* All this testifies to the extremely complex character of the influence of the intermolecular force field on the intramolecular vibrations. This influence must indisputably add its contribution to the temperature variation of the intensity. The difficulties in revealing it are explained by the presence of other factors which are reflected in the temperature course of the vibrational intensities. The first of these is the Boltzmann factor, and the second the interaction of the fundamental vibrations of the molecule. The simultaneous action of even these three factors is sufficient to complicate to a considerable degree the solution of a second question, namely, the establishment of a connection between the temperature variation in the intensity of a vibration and its frequency. If in all cases—i.e., independently of the form of the vibration—the intermolecular force field made itself felt in the same way, and there were no interaction of the vibrational levels, then as the frequency of the transition increased (the role of the factor $\exp(-h\nu/kT)$ would thereby diminish), the effect of a lowering of the intensity of the absorption band with an increase in temperature would show itself more distinctly. The fact is that the change in the intermolecular force field with an increase in temperature must lead (apparently in all cases, so long as we are dealing with a liquid, a solution, or an insufficiently rarefied gas) to a lowering of the intensity of the vibrational absorption bands.[8]

Practically no effect of temperature on the bands corresponding to the overtones $2\nu_1$, $2\nu_4$, and $2\nu_5$ and the combination frequency $\nu_1 + \nu_4$ was detected.* One can note only a certain tendency toward a diminution of absorption with an increase in temperature (Fig. 4,a) in

*The data on these studies will be written up in a subsequent communication.

*The points corresponding to the temperature 100°C are not entered in Fig. 4.

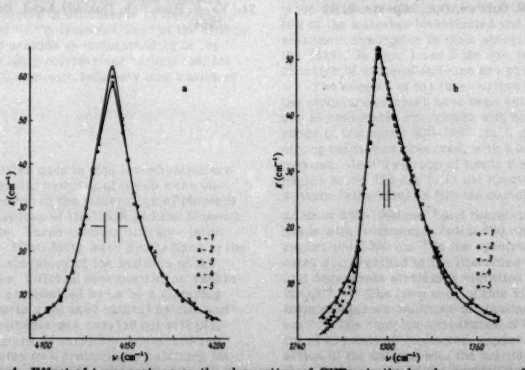

Fig. 4. Effect of temperature on the absorption of $CHBr_3$ in the bands corresponding to the combination frequency $\nu_1 + \nu_4$ (a) and to the overtone $2\nu_5$ (b). Temperature (in °C): 1—20; 2—40; 3—60; 4—80; 5—130.

the region of the maximum of the band corresponding to the vibration $\nu_1 + \nu_4$, and an increase in the absorption in the wings of the band belonging to the overtone $2\nu_3$ (Fig. 4,b). It is interesting to note that the effect of temperature on the intensity of the two-quantum transition $\nu_1 + \nu_4$ is considerably weaker than in the case of the fundamental transitions ν_1 and ν_4 which compose it. Such behavior of the overtones $2\nu_1$, $2\nu_4$, and $2\nu_3$, and of the combination frequency $\nu_1 + \nu_4$, is explained apparently by the weak temperature dependence of the intensities of the fundamental vibrations corresponding to them, and by the large contribution (in the case of additive combinations of frequencies) of the Boltzmann factor, which acts in the direction of increasing the intensity. As a result of such an action, the diminution of intensity brought about by the weakening of the intermolecular interactions with an increase in temperature may be completely compensated. For the same reason, no change was detected in the intensities of certain combination frequencies and the $2\nu_3$ overtone of liquid CBr_4.[5] However, in the case of carbon tetrachloride,[6] certain additive combinations of the fundamental frequencies have a fairly strong temperature dependence. Inasmuch as only the one fundamental frequency ν_3 can be studied in the infrared spectrum of this compound, no comparison of the dependence observed for the fundamentals and for the combinations formed by them can be carried out; accordingly, CCl_4 does not belong to the materials which enable us to verify the above-stated assumption.

CONCLUSIONS

1. An increase in temperature is accompanied by a diminution in the intensities of the fundamental vibrations ν_1, ν_4, and ν_3 of liquid bromoform. This diminution follows a linear law and is most significant for the deformation vibration ν_4.

2. For the overtones $2\nu_1$, $2\nu_4$, and $2\nu_3$ and the combination $\nu_1 + \nu_4$, temperature variations are practically absent, which is apparently explained by the weak temperature dependence of the fundamental vibrations which compose them and by the increase in the role of the Boltzmann factor and of anharmonicity in the case of combinations of fundamental frequencies and of overtones.

REFERENCES

1. B. Bloch and O. Errera, J. phys. radium **6**, 154 (1935).
2. J. Mador and R. Quinn, J. Chem. Phys. **20**, 1837 (1952).
3. E. Slowinsky and G. Clawer, J. Opt. Soc. Am. **45**, 396 (1955).
4. U. Liddel and E. Becker, J. Chem. Phys. **25**, 173 (1956).
5. G. Dijkstra, Proc. Colloq. Spectrosc. Internat. **6**, 618, London, 1957.
6. M. P. Lisitsa and V. N. Malinko, Izvest. Akad. Nauk SSSR, Ser. Fiz. **22**, 1117 (1958).
7. P. A. Bazhulin and V. N. Smirnov, Opt. i Spektr. **6**, 745 (1959), Optics and Spectroscopy **6**, 485 (1959).
8. M. P. Lisitsa, V. N. Malinko, and I. N. Khalimonova, Opt. i Spektr. **7**, 638 (1959), Optics and Spectroscopy **7**, 386 (1959).
9. A. Vaisberger, "Organicheskie rastvoriteli" (Organic Solvents). Izd. Inostrannoi Lit., Moscow, 1958.
10. I. I. Novak and E. S. Solv'ev, Opt. i Spektr. **2**, 62 (1957).
11. R. Richards and H. Thompson, Proc. Roy. Soc. **A195**, 1 (1948).
12. E. Funk, Optik **13**, 524 (1956).
13. R. Mair and D. Hornig, J. Chem. Phys. **17**, 1236 (1949).
14. L. Brown and P. Holliday, J. Sci. Instr. **28**, 27 (1951).
15. N. E. Gaponova, M. P. Lisitsa, and Yu. P. Tsyashchenko, Opt. i Spektr. **8**, 465 (1960), Optics and Spectroscopy **8**, 245 (1960).
16. V. M. Chulanovskii and N. P. Penkin, Izvest. Akad. Nauk SSSR, Ser. Fiz. **9**, 206 (1945).
17. A. N. Aleksandrov and V. A. Nikitin, Uspekhi Fiz. Nauk **56**, 3 (1955).
18. J. Willis, Australian J. Sci. Research, Ser. A **4**, 172 (1951).
19. V. N. Smirnov, Vestnik Moskov. Gosudarst. Univ., Ser. Fiz.-Khim. No. 1, 61 (1959).
20. M. P. Lisitsa and Yu. P. Tsyashchenko, Opt. i Spektr. **6**, 605 (1959), Optics and Spectroscopy **6**, 396 (1959).
21. Ya. S. Bobovich, Doklady Akad. Nauk SSSR **98**, 39 (1954).

VIBRATION SPECTRA OF THE SILICATES
I. Infrared Spectra of Silicates with Anions of the Type $(Si_2O_7)^{-6}$

A. N. Lazarev

Received 14 November 1959

The infrared absorption spectra of silicates containing complex anions of the type $(Si_2O_7)^{-6}$ were investigated. The "internal" vibrations of these ions were considered, and an attempt was made to derive a spectroscopic criterion for identification of the silicate group $(Si_2O_7)^{-6}$ in crystals, and to arrive at some indication of their shape.

INTRODUCTION

In our previous communications[1,2] we described changes in the spectra of polyalkoxyloxanes resulting from a transition from separate tetrahedra of SiO_4 to chains of 2, 3, and more tetrahedra. Hence it is interesting to use those results for the interpretation of the spectra of silicates which contain complex anions consisting of several silicon oxide tetrahedra joined by common atoms of oxygen. The simplest example of such silicates is the pyrosilicates (or "diorthosilicates" (containing anions in the form of "double" silicon oxide tetrahedra

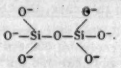

X-ray research, in particular the work of N. V. Belov and co-workers over the past years, has established that silicates with anions of the type $(Si_2O_7)^{-6}$ are rather widespread as a class of compounds, although previously such structures had been considered rare. However x-ray research on crystals is very laborious, and a complete deciphering of the structure is sometimes difficult. Therefore it is justifiable to attempt even a partial indication of structure—say the structure of the anion—by methods of molecular spectroscopy. Further, as has been already reported in the literature,[3] investigation of the spectra of silicates with ions $(Si_2O_7)^{-6}$ containing a low order of "polymerization" of the silicon oxide tetrahedra may provide an understanding of the spectra of the more highly polymerized structures, for example, the metasilicates with infinitely long chains of tetrahedra.

METHOD

Many of the silicates used in this investigation are found in natural minerals, samples of which were obtained from the collection of the Mineralogical Museum of the Academy of Sciences of the USSR and the Museum of the Mining Institute. Three calcium silicates (alite $3CaO.SiO_2$, β- and γ - $2CaO.SiO_2$) were synthesized in the Physical-Chemical Laboratory of the Institute of the Chemistry of Silicates. Calcium diorthosilicate, rankinite ($3CaO.2SiO_2$) was synthesized by us by a sintering method. As raw materials we used natural calcite and rock crystal. The synthesis was carried out in a platinum crucible. A mixture of carefully pulverized raw materials was subjected to a preliminary calcining for 4-5 hr at a temperature of 900°C., after which the samples were pressed and fired repeatedly for 5-6 hr at 1350°C in a silicate furnace. After 3 to 5 firings homogeneous samples of rankinite were obtained. Identification and control of the homogeneity of the compounds investigated were effected by means of microscopic and x-ray phase analysis.

The infrared absorption spectra were investigated with a VIKS-MZ spectrometer (with NaCl prism) and an ISP-14b spectrometer (with KBr prism). The mineral samples were prepared in the form of pressed disks made up of a mixture of potassium bromide with the material under investigation. (Diameter of the disks was 25 mm; the amount of the mixture was 2 gm, of concentration 0.1-0.5%). Other samples consisted of a suspension of the material investigated, in liquid paraffin. No difference was observed in the spectra of samples prepared by these two methods.

SPECTRA OF ORTHO- AND PYROSILICATES

We investigated the absorption spectra of a number of silicates in which x-ray analysis shows that $(Si_2O_7)^{-6}$ ions are present or where such ions might be presumed to be present on the basis of the chemical composition. In some cases we also investigated the spectra of orthosilicates (with ions $(SiO_4)^{-4}$) with the object of determining with more precision the frequency of the vibrations of the oxide polyhedra of metals (M-O bonds) which play the role of cations in the silicates of interest to us. We also wished to clarify the character of the influence of these cations on the internal vibrations of the anions. A list of the silicates investigated and the frequencies of maximum absorption in their spectra are presented in the Table. In figs. 1 and 2 the spectra of a number of silicates of calcium and zinc are presented.

The spectra of the three orthosilicates of calcium, the structure of which have been established by x-rays, are in reasonable agreement with each other. In the range of frequency 800-1000 cm^{-1}, a group of several strong bands was observed, with a series of weaker maxima. Another group of bands lies in the frequency region below 550 cm^{-1}. In the spectrum of zinc orthosilicate (willemite) an intense complex band is observed at about 850-1000 cm^{-1} and there are fairly strong bands with frequencies below 620 cm^{-1}. Bands in the region 800-1000 cm^{-1} in the spectra of the orthosilicates are ascribed in the literature as due to a threefold degenerate stretching vibration of the group $(SiO_4)^{-4}$.[3,14] The frequency of this vibration in the spectrum of aqueous solutions of alkaline silicates is 935 cm^{-1}.[15] The complex appearance of the bands in spectra of crystals is connected, apparently, with the interaction of the cations with the anions, which for lower than T_d symmetry of the crystal field leads to a removal or reduction of the degeneracy. Additional complication of the spectra in this region may be as-

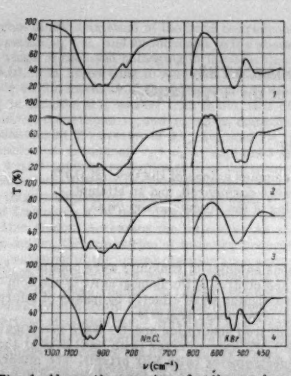

Fig. 1. Absorption spectra of ortho- and pyrosilicates of calcium. Curves 1—$Ca_3O(SiO_4)$; curves 2—γ-Ca_2SiO_4; curves 3—β-Ca_2SiO_4; curves 4—$Ca_2Si_2O_7$. Samples were prepared by the method of pressing in KBr (concentration 0.25%).

cribed to resonance interactions of the complex ions in the elementary cell, and composite transitions due to simultaneous excitation of vibrations of the lattice and the internal vibrations of the SiO_4 ion.

Completely symmetrical stretching vibrations of the SiO_4 group, observed in the Raman spectrum of the SiO_4 ion in aqueous solution at 775 cm^{-1},[16] are apparently not observed in absorption spectra of crystalline orthosilicates, in spite of the possibility of a change in the selection rule on transition from the isolated ion to the crystal.* In the absorption spectra of orthosilicates,

*Ryskin[16] showed that this vibration may have a noticeable intensity in absorption for the "asymmetrization"

Frequencies of Maxima in the Infrared Absorption Spectra Investigated

Mineral	Origin	Type of anion structure	Frequencies of maxima in absorption spectra (cm^{-1})	References: X-ray work	References: Spectroscopic work
$Ca_3O(SiO_4)$ (elite)	Synthetic	$[SiO_4]^{4-}$	933, 901, 883, 812, 525, 464, 452	[4]	—
γ-Ca_2SiO_4	Synthetic	»	1120 (w.), 952, 933, 855, 818, 852 (w.), 582, 516, 492, 442	[15]	—
β-Ca_2SiO_4 (larnite)	Synthetic	»	1120 (w.), 996, 941, 917, 901, 872, 845, 529	[5]	[12, 13]
Zn_2SiO_4 (willemite)	Natural	»	976, 930, 902, 868, 616, 574, 499 (w.), 460	[7]	[12, 14]
$Ca_2Si_2O_7$ (rankinite)	Synthetic	$[Si_2O_7]^{6-}$	1002, 980, 950, 903, 847, 652, 580, 538, 482	—	—
$Zn_4(OH)_2(Si_2O_7)H_2O$ (calamine)	Natural	»	~3200, 1604, 1092, 1007, 958—930, 862, 872, 603, 562, 542, 498 (w.), 448	[9, 8]	[14]
$Ca_2ZnSi_2O_7$ (hardystonite)	Natural	»	1035—1000, 970, 918—891, 836, 677, 618, 596, 547, 498, 462	[10]	—
$CaFe_2^{II}O(Si_2O_7)OH$ (ilvaite)	Natural	»	~3400, 1038, 945, 901, 818, 754 (w.), 697, 570, 538, 494, 452	[11]	—

Note. Designation of the intensity of the band (in parentheses): w—weak.

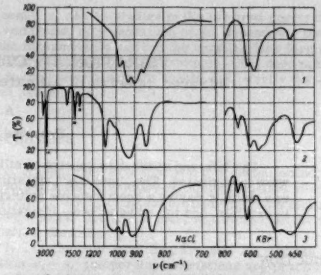

Fig. 2. Absorption spectra of the ortho- and pyrosilicates of zinc. Curves 1—Zn_2SiO_4 (pressed in KBr, concentration 0.25%); curves 2—$Zn_4(OH)_2(Si_2O_7).H_2O$ (immersed in paraffin oil; asterisks indicate absorption bands of the paraffin); curves 3—$Ca_2ZnSi_2O_7$ (pressed in KBr; concentration 0.25%).

of the SiO_4 group (with formation of a substantial dipole moment), in the hydrated ion SiO_3OH. In an aqueous solution, the SiO_4 ion may also be partially hydrated, which leads to a change in frequency. However, for elements of group IV, silicon in this case, the change is negligible.

shown in Figs. 1 and 2, this vibration is likewise not observed. Bands in the region of 600 cm^{-1} in the spectrum of zinc orthosilicate, and near 500 cm^{-1} in the spectrum of calcium silicate, and also the lower frequency bands, can be ascribed to vibrations of the metal-oxide polyhedra (the bonds Zn-O and Ca-O) and partly ascribed to deformation of the SiO_4 group, the bands of which occur primarily outside the region of the spectra investigated.[3]

Transition from the orthosilicates to the pyrosilicates leads to a characteristic change in the spectrum. Thus, in the spectrum of rankinite, $3CaO.2SiO_2$, the composition of which permits one to expect the appearance of ions of the type $(Si_2O_7)^{-6}$ ($Ca_2Si_2O_7$), bands appear in the region 800-1000 cm^{-1} and below 550 cm^{-1}, and, in addition, a single band which is rather narrow with a symmetrical contour and of medium intensity appears at 652 cm^{-1}. In the spectra of the calcium orthosilicates, absorption is missing in this region.* For the spectra

*The appearance of a very weak band with frequency of 652 cm^{-1} in the spectrum of synthetic γ-Ca_2SiO_4 is ascribed to a small admixture of rankinite, which is supported by a microscopic phase analysis.

of zinc pyrosilicate (calamine), in which the existence of $(Si_2O_7)^{-6}$ ions is established by x-ray analysis, and in hardystonite, also apparently a pyrosilicate ($Ca_2ZnSi_2O_7$), a band of the same character appears near 670-680 cm^{-1}.

For interpretation of the results obtained, we turn to the results of a consideration of the vibrations of the SiO_4 and Si_2O_7 groups carried out in a previous communication.[3] On transition to the "double" tetrahedron of Si_2O_7 a splitting of the normal vibrations of the SiO_4 group occurs.*

*In such a consideration of the Si_2O_7 groups the vibrations separate into two torsional vibrations of the SiO_3 groups and one bending vibration of SiOSi.

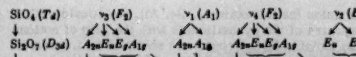

In addition, the completely symmetrical stretching vibration of the tetrahedron, ν_1, splits to a greater extent than does the threefold degenerate vibration; and this splitting increases in proportion to the approach of the SiOSi angle to 180°.

Computation based on these considerations permits a an explanation of the change in the spectrum on transition from the ortho- to the pyrosilicates (Fig. 3). The band in the region 650-680 cm^{-1} which appears on transition from orthosilicates to pyrosilicates may be ascribed to a vibration of type A_1 (or A_{1g}) which arises on the splitting of the completely symmetrical vibration of the SiO_4 group. The band corresponding to the other component of this vibration (type B_1 or A_{2u}) apparently falls in the region near 900 cm^{-1}, a circumstance that makes its identification difficult. In this same region either 4 or 6 bands are to be observed (depending on the symmetry of the Si_2O_7 group), generated by splitting of the threefold degenerate vibration of the SiO_4 group. However, inasmuch as the splitting of this vibration is small (not more than the splitting in orthosilicates due to interaction with the cations), identification of the different components, other than the vibration of type A_1 (or A_{1g}) lying near 850 cm^{-1}, is difficult. No detailed consideration of the vibrations of Ca-O and Zn-O, or of δ_{SiO_4} or $\delta_{Si_2O_7}$ interacting with them is possible within the range of approximations used.

It should be noticed that the spectrum of calamine permits a check of the data of the x-ray analysis as to the state of the water in that silicate. In addition to the OH stretching band near 1600 cm^{-1}, a band is observed due to bending vibration of a molecule of water of crystallization. The band at 1092 cm^{-1} is related, probably, to the bending vibration of the OH group in the structure, since its frequency is the same as the frequency δ_{HO} in crystalline $Zn(OH)_2$.[17] Thus the spectroscopic results permit verification of the presence in the structure both of a molecule of H_2O, and the group $(OH)^-$

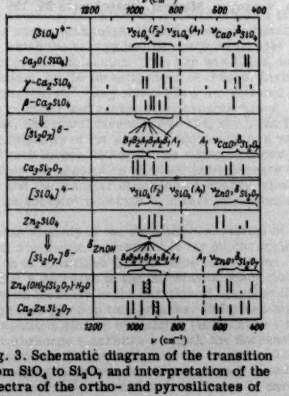

Fig. 3. Schematic diagram of the transition from SiO_4 to Si_2O_7 and interpretation of the spectra of the ortho- and pyrosilicates of calcium and zinc.

VIBRATION SPECTRUM AND CONFIGURATION OF THE Si_2O_7 GROUP

In addition to the possibility of identifying the Si_2O_7 groups in silicates by use of spectroscopic data, there is some interest in the attempt to reach a conclusion, though possibly a very tentative one, as to the configuration of those groups, that is, the magnitude of the SiOSi angle. The first problem in this direction is the choice between a bent and linear (SiOSi angle equal 180°) oxygen "bridge" (the highest symmetry of the Si_2O_7 group in these cases corresponds to C_{2v} and D_{3d}). The use of a computation of a number of frequencies in the region of the threefold degenerate stretching vibration of the SiO_4 tetrahedron is difficult as a rule. Somewhat more interesting would be the use of the change in selection rules on transition from the symmetry of D_{3d} to C_{2v}. The completely symmetric stretching vibration of the SiO_4 tetrahedron splits, on transition to the Si_2O_7 group, into two vibrations, a symmetric one and an antisymmetric one, in which the latter (with symmetry D_{3d}) is inactive in the absorption spectrum (although in the crystal, this condition is not necessarily valid). For magnitudes of the SiOSi angle less than 180°, this vibration becomes active in the infrared spectrum. The degree of splitting of the completely symmetrical vibration of the tetrahedron is especially sensitive to change in the SiOSi angle, as has been mentioned, the splitting increasing in proportion to the size of the angle.

For a rough evaluation of the possible values of the SiOSi angle in the pyrosilicates investigated by us, we used the results of approximate calculations of the frequencies of the Si_2O_7 group for SiOSi angles equal to 120 and 180°.[2,3,18] Since the precise identification of the high frequency component is difficult, it was assumed that the splitting takes place approximately symmetrically with respect to the frequency $\nu_{SiO_4}(A^1) = 775$ cm^{-1}. (This corresponds to the assumption that $K_{Si-O-} \simeq K_{Si-O(Si)}$ in $Si_2O_7^{-6}$ ions; such an assumption for the quadrivalent atom, silicon, is reasonably justifiable.[3] In the absorption spectrum of rankinite, the band with frequency 652 cm^{-1} has fairly high intensity, which in the computation of the relative magnitude of the splitting of the symmetrical vibration permits the conclusion that the SiOSi angle lies in the interval 160° to 170°.*

*It should be noticed that for large values of the SiOSi angle (near 180°), the dependence of the magnitude of the splitting on the size of angle should not be very marked.

Analogous remarks applicable to the calamine and hardystonite spectrum, in which the band is displaced toward higher frequencies (670-680 cm^{-1}), lead to a probable value of the SiOSi angle of about 145°. It must be noted that the original x-ray structure investigation of calamine led to the value for the SiOSi angle of 180°,[8] which is in disagreement with recent work,[9] but in which, however, precise values of the angle were not obtained.

In this connection it is interesting to turn to the spectrum of ilvaite, in which, according to the data of Belov,[11] the SiOSi angle is not large (122°). The spectrum of ilvaite (Fig. 4) is similar to those of other pyrosilicates; but of interest to us is the fact that the band has a higher frequency (about 700 cm^{-1}); that is, the splitting of the symmetrical vibration of the SiO_4 group is less. The relative magnitude of the splitting leads, according to our evaluation, to a value for the SiOSi angle of 130-140°. This agrees satisfactorily with the x-ray structure data, particularly in the light of the circumstance that ilvaite contains iron ions, which are capable of bonding with oxygen with bonds having a considerable degree of co-

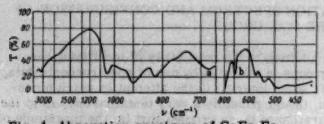

Fig. 4. Absorption spectrum of $CaFe_2FeO(Si_2O_7)OH$ (pressed in KBr, concentration: curve a—0.25; curve b—0.5%).

valency, and on that account, having a rather strong influence on the spectrum of the anion.

In ref. [19] the absorption spectrum of synthetic cuspidine $Ca_4(Si_2O_7)F_2$ in the region up to 16 μ is presented without interpretation. It may be assumed that the rather weak band near 15.3 μ (653 cm^{-1}) is analogous in origin to the band in the region 650-700 cm^{-1} in the spectra of other pyrosilicates. From this, using the data on the relative magnitude of the splitting, we arrive at a value for the SiOSi angle lying in the interval 160° to 170°, as in the case of rankinite. X-ray structure analysis gives for cuspidine an SiOSi angle of about 180° [20] Thus, in this case also, there is apparently qualitative correlation in the determination of the value of the SiOSi angle as between the x-ray structure and spectroscopic methods. It may be presumed that the accumulation of experimental data will permit ultimately an increase in the reliability of the spectroscopic evaluations.

CONCLUSIONS

1. Transition from orthosilicates to pyrosilicates causes characteristic changes in the vibration spectrum, dependent primarily on changes in the normal vibrations of the SiO_4 tetrahedra due to their combination in the "double" group Si_2O_7.

2. The vibrational spectra can be used for conclusions as to the existence of the Si_2O_7 group in crystals of the silicates, and for an approximate evaluation of the magnitude of the SiOSi angle in these groups.

3. In the presence of relatively light cations capable of strong interactions (with large degree of covalency) with the anion (as for example, Be, Al), the consideration of the spectra of the pyrosilicates with the help of notions as to the isolated Si_2O_7 groups are shown to be impossible by virtue of the strong interactions of the vibrations.

The author extends his thanks to E. F. Gross and N. A. Toropov for their continued interest in the work, and to A. I. Boykov and Yu. G. Sokolov for their assistance in the microscopic and x-ray analysis of samples.

REFERENCES

1. A. N. Lazarev, Opt. i Spektr. **4**, 805 (1958).
2. A. N. Lazarev and M. G. Voronkov, Opt. i Spektr. **8**, 614 (1960), Optics and Spectroscopy **8**, 325 (1960).
3. H. Siebert, Z. anorg. u. allgem. Chem. **275**, 225 (1954).
4. J. W. Jeffery, Acta Cryst. **5**, 26 (1952).
5. W. L. Bragg and G. B. Brown, Z. Krist. **63**, 538 (1926).
6. C. M. Midgley, Acta Cryst. **5**, 307 (1952).
7. W. L. Bragg and W. H. Zachariasen, Z. Krist. **72**, 518 (1930).
8. T. Ito and J. West, Z. Krist. **83**, 1 (1932).
9. G. A. Barclay, E. Cox, and H. Linton, Chem. & Ind. (London) 178, (1956).
10. B. E. Warren and O. R. Trautz, Z. Krist. **75**, 525 (1930).
11. N. V. Belov and V. I. Mokeeva, Doklady Akad. Nauk. SSSR **81**, 581 (1951).
12. P. J. Launer, Am. Mineralogist **37**, 764 (1952).
13. Ya. I. Ryskin, Trudy V Soveshch. po Eksperim. i Tekhnich. Mineralogii i Petrografii (Papers of the Fifth Conference on Experimental and Technical Mineralogy and Petrography), p. 55. Moscow, 1958.
14. F. Matossi and H. Krüger, Z. Physik **99**, 1 (1936).
15. D. Fortnum and J. O. Edwards, J. Inorg. & Nuclear Chem. **2**, 264 (1956).
16. Ya. I. Ryskin and G. P. Stavitskaya, Opt. i Spektr. **8**, 606 (1960), Optics and Spectroscopy **8**, 326 (1960).
17. E. Hartert and O. Glemser, Z. Elektrochem. **60**, 746 (1956).
18. F. Matossi, J. Chem. Phys. **17**, 679 (1949).
19. A. van Valkenburg and G. E. Rynders, Am. Mineralogist, **43**, 1195 (1958).
20. R. F. Smirnova, I. M. Rumanova, and N. V. Belov, Zap. Vsesoyuz. Mineral. Obshchestva **84**, 159 (1955).

SENSITIZED FLUORESCENCE IN SOLUTIONS

B. Ya. Sveshnikov, P. I. Kudryashov and L. A. Limareva

Received 9 December 1959

The work was carried out in order to obtain new data concerning the mechanism of sensitized fluorescence in solutions. Changes in the absorption and luminescence spectra and the yield and duration of luminescence of solutions of rhodamine B and trypaflavine and mixed solutions of these dyes were studied as a function of the concentration of the dyes. It was shown that the effect of sensitization of fluorescence was complicated to a considerable degree by the trivial absorption of trypaflavine fluorescence by rhodamine. Nevertheless, at concentrations higher than 2×10^{-4} mol/liter (the concentrations of the two in solution were equal), there is a very intensive radiationless transfer of excitation energy from trypaflavine to rhodamine with a yield close to 0.7. At concentrations greater than 2×10^{-3} mol/liter, quenching of the excited rhodamine molecules by trypaflavine molecules is observed, together with a transfer of energy from trypaflavine to rhodamine.

Shortly after Frank and Cario[1] discovered sensitized fluorescence in vapors, Perrin and Choucroun[2] found a similar effect in solutions. For two decades these papers were the sole evidence for the existence of sensitized fluorescence in solutions, although as Pringsheim pointed out in his book,[3] "the evidence is rather unconvincing."

Beginning at the end of the past decade, a series of papers have appeared devoted to the study of sensitized fluorescence in solutions. The first attempt was made by Förster[4]. He demonstrated that if, in mixtures containing energy donors and acceptors in the same proportion, the concentration of both solutes is increased, the fluorescence of the donor is greatly weakened. This effect cannot be explained as an increase in the absorption of donor fluorescence by the acceptor. Through experiments on the quenching of donor fluorescence by foreign substances, Förster established that the quenching of donor molecules by acceptor molecules is dynamic in character and leads to a reduction in the duration of donor fluorescence. His calculations indicated that migration of energy between molecules occurs over considerable distances.

Unfortunately, there are no quantitative data in Förster's work which might permit determination of the extent to which the energy lost by donor molecules is used by acceptor molecules. This gap was filled, to a certain extent, by the investigations of Bowen, Livingston, and Brocklenhurst.[5] They showed that for selected combinations of donor and acceptor (chloroanthracene + perylene, chloroanthracene + rubrene, etc.), the fluorescence intensity of the acceptor increases to a value several times larger than would be expected if one considered only the absorption of donor luminescence by the acceptor and the transfer of excitation energy from a donor to an acceptor molecule by direct (diffusion) collision.

Galanin's[6] study of the time characteristics of the effect was a valuable supplement to the photometric investigation of sensitized fluorescence in solutions. He showed that a decrease in the duration of donor fluorescence and an increase in the duration of acceptor fluorescence takes place in this process. Unfortunately, for the combinations studied by Galanin (anthracene + benzoflavine, anthracene + acridine orange), the decrease in duration of donor fluorescence and the increase in duration of acceptor fluorescence did not exceed 20-30%. The author correctly noted that the increase in duration of acceptor luminescence may be largely explained by absorption of donor luminescence by the acceptor.*

*In Galanin's work, measurements of the duration of fluorescence were performed with fairly thick layers.

Schmillen[7] observed a greater increase in the duration of acceptor fluorescence on studying changes in the duration of fluorescence of rhodamine B, dissolved together with trypaflavine (donor) in methyl alcohol. Unfortunately, in Schmillen's work, the effect of trivial absorption of trypaflavine luminescence by rhodamine on the duration of rhodamine fluorescence is not evaluated.

It follows from the foregoing that the papers mentioned, which were devoted to the experimental proof of individual steps in the proposed mechanism of sensitized fluorescence, and the results presented therein, were qualitative rather than quantitative. We therefore considered it necessary to carry out a more thorough quantitative investigation of sensitized fluorescence in solutions, even if only in one instance paying more attention, if possible, to the change in the luminescent properties of the acceptor.

For the study, we selected the mixture of trypaflavine and rhodamine B in methyl alcohol* which Förster investigated. The combination of these two dyes is very convenient, because there is a deep minimum in the absorption spectrum of rhodamine B in the region of the mercury line 436 mμ, and this line is strongly absorbed by trypaflavine.

*As in Förster's experiments, the concentrations of the two dyes in the mixture were equal.

First of all, we compared the absorption spectra of mixed solutions of the dyes with the absorption spectra of separate solutions of the dyes at concentrations from 1×10^{-5} to 1×10^{-3} mol/liter. The purpose of this study was to show that compound dimers do not form in a solution containing a mixture of the dyes. The formation of such dimers is known from the literature, and Schmillen proposed that they are responsible for sensitized fluorescence.

Although this hypothesis is inconsistent with Förster's experiments on the quenching of sensitized fluorescence by potassium iodide and is refuted by the experiments of Bowen and Livingston, who showed that the absorption spectrum of chloroanthracene does not change when perylene is added to the solution, we considered it necessary to establish the additivity of the absorption spectrum of the mixture of trypaflavine and rho-

damine B which we studied, since both dyes are inclined to associate under certain conditions.

From our curves, presented in Fig. 1, it follows that (a) the absorption spectrum of trypaflavine is practically unchanged between 1×10^{-3} and 5×10^{-3} mol/liter; (b) the absorption spectrum of rhodamine B, for the same concentration change, is slightly displaced to the red; and (c) the absorption spectrum of a solution containing a mixture of the two dyes, in the same concentration range, may be obtained by simply superimposing the absorption spectra of solutions of the separate substances. This result contradicts the hypothesis of the formation of compound dimers from molecules of trypaflavine and rhodamine.

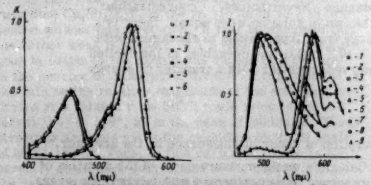

Fig. 1. Absorption spectra of solutions. Rhodamine B ($1-1 \times 10^{-5}$ mol/liter; $2-5 \times 10^{-3}$ mol/liter), trypaflavine ($3-1 \times 10^{-3}$ mol/liter; $4-5 \times 10^{-3}$ mol/liter), and the mixture ($5-C_t = C_r = 1 \times 10^{-3}$ mol/liter; $6-C_t = C_r = 5 \times 10^{-3}$ mol/liter) in methyl alcohol. (K is in relative units.)

Fig. 2. Luminescence spectra of solutions. Rhodamine B ($1-1 \times 10^{-5}$ mol/liter; $2-5 \times 10^{-3}$ mol/liter), trypaflavine ($3-1 \times 10^{-5}$ mol/liter; $4-5 \times 10^{-5}$ mol/liter), and their mixture ($5-C_t = C_r = 5 \times 10^{-7}$ mol/liter; $6-C_t = C_r = 5 \times 10^{-3}$ mol/liter) in cuvettes 10 mm thick. Fluorescence spectra of rhodamine B ($7-5 \times 10^{-3}$ mol/liter), trypaflavine ($8-5 \times 10^{-3}$ mol/liter), and the mixture ($9-5 \times 10^{-3}$ mol/liter) in cuvettes 0.05 mm thick. (I is in quanta.)

We also studied the luminescence spectra of rhodamine B, trypaflavine, and a mixture of the two in methyl alcohol, at concentrations from 5×10^{-7} to 2×10^{-2} mol/liter in thick (10 mm) cuvettes and from 1×10^{-4} to 5×10^{-3} mol/liter in thin (0.1–0.05 mm) cuvettes, making observations from the excitation side at a small angle to the exciting light.

The results obtained are presented graphically in Figs. 2 and 3. The purpose of Fig. 2, which gives the luminescence spectra of solutions of the pure substances and their mixtures for two concentrations of dye in thick and thin layers, is to show that the luminescence spectra of the pure solutions is not appreciably changed,* apart from absorption of luminescence. The luminescence spectra of mixed solutions may be obtained from the luminescence spectra of trypaflavine and rhodamine, if one takes account of the distortion of the luminescence spectrum of trypaflavine in the mixture brought about by absorption of its luminescence by rhodamine. The figure also shows that the luminescence bands of the individual components in the mixture are sharply separated.

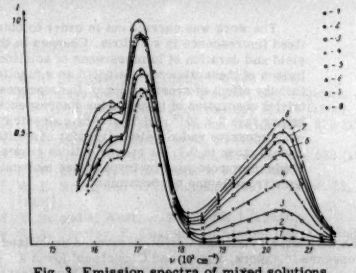

Fig. 3. Emission spectra of mixed solutions at different dye concentrations. $1-1 \times 10^{-2}$ mol/liter; $2-5 \times 10^{-3}$ mol/liter; $3-2.5 \times 10^{-3}$ mol/liter; $4-1.25 \times 10^{-3}$ mol/liter; $5-6.25 \times 10^{-4}$ mol/liter; $6-3.12 \times 10^{-4}$ mol/liter; $7-1.56 \times 10^{-4}$ mol/liter; $8-7.8 \times 10^{-5}$ mol/liter. (I is in quanta.)

Figure 3 presents energy distribution curves of the emission spectra of mixed solutions at concentrations from 2.5×10^{-4} to 1×10^{-2} mol/liter.* It is apparent from the figure that the distortions of the luminescence spectra in the emission bands of trypaflavine and rhodamine, the first of which occurs as a result of an increase in the absorption of trypaflavine luminescence by rhodamine, and the second as a result of reabsorption of its own luminescence by rhodamine, are small in the given concentration range, and may be calculated. In the calculation of these corrections, it is not difficult to determine the changes in the fluorescence yields of the two components as a function of concentration by the usual method of calculating the area bound by the corresponding energy distribution curve in the emission spectrum.

To further our investigation, it is desirable to obtain curves of the change in fluorescence yield of donor and acceptor produced by energy migration only, and free from the effects of the absorption of trypaflavine luminescence by rhodamine B.

The fastest and most convenient way to detect the reabsorption of fluorescence is to measure the duration of the fluorescence of a substance as a function of concentration and cuvette thickness. Figure 4 shows the duration of trypaflavine and rhodamine B fluorescence in cuvettes 10 mm thick for dye concentrations from 1×10^{-6} to 5×10^{-2} mol/liter. It is evident from the figure that under the experimental conditions, the duration of fluorescence of solutions of pure dyes attains a maximum at concentrations from 5×10^{-4} to 2×10^{-3} mol/liter, when reabsorption of luminescence becomes particularly strong. The duration decreases slightly at concentrations from 2×10^{-3} to 1×10^{-2} mol/liter, and then falls rapidly between 1×10^{-2} and 5×10^{-2} mol/liter.

*The fluorescence of the solution of pure rhodamine in these studies was excited by the mercury line 546 mμ. We considered that excitation with this line corresponds more closely to the conditions of excitation of rhodamine B fluorescence in the mixed solution than excitation by the weakly absorbed mercury line 436 mμ. Control experiments indicated that exceptionally severe distortion of the fluorescence spectra of concentrated rhodamine B solutions is observed when the 436 mμ line is used for excitation.

*In this concentration range, the exciting light is sure to be absorbed within a relatively thin layer.

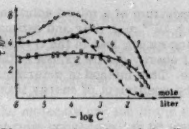

Fig. 4. Change in duration of the fluorescence τ of solutions of trypaflavine and rhodamine B as a function of the concentration of dye in cuvettes 10 mm thick upon excitation by the mercury lines 436 mμ, for trypaflavine (curve 1), and 546 mμ for rhodamine B (curve 2). Change in duration of luminescence of the mixed solution in the emission bands of trypaflavine (curve 3) and rhodamine B (curve 4) on excitation by the 436 mμ line in similar cuvettes.

In thin cuvettes (0.05-0.1 mm), the duration of trypaflavine fluorescence at concentrations from 5×10^{-3} to 5×10^{-4} mol/liter is the same as it is at low concentrations.

In mixed solutions, the duration of luminescence in the emission bands of the dyes changes according to other laws. At low concentrations of both dyes, the duration of luminescence in the emission band of trypaflavine is equal to the duration of fluorescence of a solution of trypaflavine, but at concentrations greater than 1×10^{-4} mol/liter, a rapid decrease begins in the duration of fluorescence in the emission band of trypaflavine. At a dye concentration of 3×10^{-3} mol/liter, the duration is 0.22×10^{-9} sec, and the duration of luminescence of a pure trypaflavine solution at the same concentration is 2.65×10^{-9} sec.

It is obvious that such a rapid decrease in the duration of trypaflavine fluorescence in mixed solutions can be caused only by quenching of the trypaflavine fluorescence by rhodamine B. We verified this assertion through experiments in which for a constant rhodamine concentration of 5×10^{-3} mol/liter, the concentration of trypaflavine was changed from 1.25×10^{-3} to 5×10^{-3} mol/liter. The durations of luminescence of trypaflavine and rhodamine were 0.95 to 1.05×10^{-9} and 2.95 to 2.87×10^{-9} respectively; i.e., they remained unchanged within the limits of experimental error.

The curve showing the change in the duration of luminescence in the radiation band of rhodamine is completely unlike the previous one. In the first place, under the conditions of our experiment, it begins not at the value of the duration of rhodamine fluorescence, but at a value a little larger than the duration of trypaflavine fluorescence. This is quite understandable. The coefficient of absorption of the mercury line 436 mμ by rhodamine B is considerably less than the coefficients of absorption of trypaflavine luminescence by rhodamine; therefore, at low concentrations of the dyes in mixed solutions, a large proportion of the radiating rhodamine molecules will be excited as a result of absorption of trypaflavine fluorescence. Since the duration of trypaflavine fluorescence is 1.5 times greater than that of rhodamine B fluorescence, the duration of luminescence of the mixed solution in the emission band of rhodamine will be determined mainly by the duration of trypaflavine fluorescence. On increasing the concentration of both dyes, the absorption of trypaflavine fluorescence by rhodamine will increase, but the fraction of the total emission contributed by rhodamine molecules excited directly by the source will decrease. Moreover, reabsorption of its own fluorescence by rhodamine also starts to play a noticeable role. As a result of both factors, the duration of luminescence in the rhodamine band will increase rapidly. This explanation of the observed effect is confirmed by experiments with thin layers. Let us cite one example: when the component concentration in a mixture is 1×10^{-4} mol/liter, the duration of luminescence in the rhodamine band, in a cuvette 10 mm thick, is 5.7×10^{-9} sec. In a cuvette, 0.05 mm thick, the duration is 4.3×10^{-9} sec, i.e., equal to the duration of luminescence in this band when the component concentration in the mixture is 1×10^{-3} mol/liter.

When the concentrations of the components in the mixture are greater than 1×10^{-4} mol/liter, as we pointed out above, excitation energy begins to migrate, reducing the time needed to supply energy to the rhodamine molecule. This must lead to a reduction in the duration of luminescence in the rhodamine band, in such a manner that at high concentrations of dye in the mixed solution, the duration of fluorescence must approach that of a solution of rhodamine B. However, in reality, the duration of luminescence in the rhodamine band at high dye concentrations becomes less than the duration of fluorescence of a pure solution of rhodamine (see Fig. 4) at the same dye concentrations. We consider the most plausible explanation of this effect to be the assumption that, at sufficiently high concentrations of both dyes in mixed solutions, trypaflavine may act as a quencher of the excited rhodamine molecules.

Having explained the concentration range in which the processes of migration of excitation energy occur, and possible distortions of this process as a result of the effects of other factors, we may plot a curve of the change in yield (light sum) in a mixture of dyes in both emission bands. The curves of the change of luminescence yields in both radiation bands of mixed solutions, calculated from Fig. 3 (making use of the above-mentioned corrections) are presented in Fig. 5.

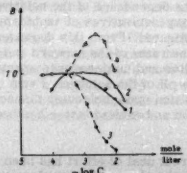

Fig. 5. Curves of the change of luminescence yield of trypaflavine (curve 1) and rhodamine B (curve 2) in pure solutions, and also trypaflavine (curve 3) and rhodamine B (curve 4) in mixed solutions.

The curves in Fig. 5 start from a concentration of 2.5×10^{-4} mol/liter, i.e., approximately from the concentration at which, judging by the reduction in duration of luminescence in the trypaflavine band, the migration of energy from trypaflavine to rhodamine begins. Since the experiments were carried out in cuvettes 10 mm thick and the concentrations were fairly high, complete absorption of the exciting light was ensured and there was no increase of the trivial absorption of trypaflavine luminescence by rhodamine. This is demonstrated by the fact that at a concentration of 2.5×10^{-4} mol/liter, the duration of luminescence in the rhodamine band in a mixed solution is noticeably less than the duration at a dye concentration of 1×10^{-4} mol/liter, when it attains a maximum value. The decrease in the duration of luminescence in the rhodamine band is greater than the decrease in the duration of the donor (trypaflavine);

therefore, it may be supposed that at a concentration of 2.5×10^{-4} there is already a certain decrease in the trivial absorption of trypaflavine luminescence by rhodamine.

From a comparison of Figs. 5 and 3, it is evident that the change in the yield of the emission band of trypaflavine is noticeably larger than the change in the duration of luminescence of the same band, which is consistent with recent theories of resonance quenching. Also, Fig. 5 shows graphically that the energy lost by trypaflavine molecules in this quenching process is converted, with great efficiency, into energy of excitation of rhodamine molecules, in any case with an efficiency not less than that obtained in the trivial absorption of trypaflavine luminescence by rhodamine. Actually, at the same time as the luminescence yield of trypaflavine is decreasing tenfold, the decrease in the luminescence yield in the emission band of rhodamine is very small. There are two probable reasons for this decrease: concentration quenching of rhodamine fluorescence and the quenching of excited rhodamine molecules by trypaflavine molecules.

It is also possible to estimate the coefficient of transfer of a quantum during energy migration by the more direct method of comparing the energy distribution curves in the emission spectrum of a mixed solution at 2.5×10^{-4} mol/liter and 2.5×10^{-3} mol/liter and estimating the number of radiation quanta lost in the trypaflavine band, and the number of energy quanta gained in the emission band of rhodamine. This method of determination gives a value of 0.7 for the coefficient of energy transfer.

REFERENCES

1. J. Frank and G. Cario, Z. Physik 11, 161 (1922); 17, 202 (1923).
2. J. Perrin and Choucroun, Compt. Rend. Acad. Sci. 184, 1097 (1927); 189, 1213 (1929).
3. P. Pringsheim, "Fluorestsentsiya i fosforestsentsiya" (Fluorescence and Phosphorescence). Izd. Inostrannoi Lit., Moscow, 1951.
4. Th. Förster, Z. Elektrochem. 53, 93 (1949).
5. E. Bowen and B. Brocklenhurst. Trans. Faraday Soc. 49, 1131 (1953); E. Bowen and K. Livingston, J. Amer. Chem. Soc. 76, 6300 (1954).
6. M. D. Galanin, Izvest. Akad. Nauk SSSR, Ser. Fiz. 15, 543 (1951); Diss., Fiz. Inst. Akad. Nauk, 1955.
7. A. Schmillen, Z. Physik 135, 294 (1953).

VARIATION IN THE FLUORESCENCE OF NAPHTHALENE DERIVATIVES AS A FUNCTION OF THE CONCENTRATION OF HYDROGEN IONS IN SOLUTION

L. D. Derkacheva

Received 23 November 1959

The dependence of the relative luminescence outputs of the molecular and ionic forms of nine hydroxy-derivatives of naphthalene on the concentration of hydrogen ions in solution has been investigated. From this dependence the values of the dissociation constants in the excited state and the rates of the forward and reverse protolytic reactions have been determined. The absorption and luminescence spectra of these compounds have been measured for various values of the pH of the solution. From the magnitude of the displacement of the zero-point electronic transition upon molecular dissociation the difference between the dissociation constants in the ground and excited states has been determined.

Recently a great deal of effort has been directed toward explaining the changes taking place in molecules undergoing transitions to excited states. The magnitudes of dipole moments in the excited state have been investigated in detail, experiments have been performed to determine the changes in radius of the excited molecules, and the interactions of molecules in the excited state have been studied.[1-3] Förster[4] and Weller[5] have indicated a way to determine yet another characteristic of a molecule in an excited state, namely, the dissociation constant, an important parameter which characterizes the bond strengths in a molecule.

In the present work we have undertaken the measurement of the dissociation constants in the excited state of nine different hydroxy-derivatives of naphthalene and determined their differences from the dissociation constants in the ground state.

The choice of the hydroxy-derivatives of napthalene as objects of investigation was decided by the fact that Förster had reported an interesting peculiarity characteristic of a difference in the dissociation processes of molecules in ground and excited states, for the case of β-naphthol and 2,5-naphthol sulfonic acid. For a given change in the pH of the solution the fluorescence spectrum of these compounds changes, whereas the absorption spectrum remains constant; the change in the spectrum of the latter first appears in a completely different range of pH values. The fluorescence spectrum begins to show signs of the dissociated form at much smaller values of pH than the absorption spectrum.

According to Förster, a molecule of naphthol in aqueous solution can take part in two concurrent processes during the lifetime of the excited state: on the one hand luminescence or a radiationless transformation of the excitation energy into heat can occur, on the other there can be a dissociation of the molecule, i.e., transfer of a proton from the excited molecule to the water. The ion so formed can, in its turn, either radiate or associate with a proton.

The reaction mechanism can be presented in the following form:

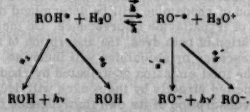

Here n_1 and n_2 are the probabilities of spontaneous

deactivation of the molecule with emission and without emission of light; n_1' and n_b' are the same probabilities for the ion; **k** is the rate constant for the forward protolysis reaction in the excited state; **−k** is the rate constant for the reverse reaction.

If we use ρ and ρ' to symbolize the probabilities of residence of the molecule and ion in the excited state, then the equilibrium conditions can be expressed by the following equations:

$$-\frac{d\rho}{dt} = (n_1 + n_b + k)\rho - kC_{H_3O^+}\rho',$$

$$-\frac{d\rho'}{dt} = (n_1' + n_b' + kC_{H_3O^+})\rho' - k\rho.$$

Solving this system and taking into account that

$$\frac{n_1}{n_1 + n_b} = \eta_0 \text{ and } \frac{1}{n_1 + n_b} = \tau,$$

where η_0 is the luminescence output of the molecule in the absence of a dissociation process, and τ is the lifetime of a molecule in the excited state, it is possible to obtain expressions for the relative luminescence output of the molecules and ions in solution

$$\frac{\eta}{\eta_0} = \frac{1 + k\tau' C_{H_3O^+} f^2}{1 + k\tau + k\tau' C_{H_3O^+} f^2},$$

$$\frac{\eta'}{\eta_0'} = \frac{k\tau}{1 + k\tau + k\tau' C_{H_3O^+} f^2}.$$

The ratio of the relative outputs is written in the form

$$\frac{\eta}{\eta_0} \cdot \frac{\eta_0'}{\eta'} = \frac{1}{k\tau} + \frac{1}{K}\frac{\tau'}{\tau} C_{H_3O^+} f^2,$$

where $K = k/-k$ is the dissociation constant, and f is the activity coefficient of the ions, which depends on the concentration of the hydrogen ions.

It is evident that one can determine the value of the dissociation constant in the excited state by measuring the relative luminescence outputs of the molecules and ions of naphthol as a function of the hydrogen-ion concentration of the solution and by knowing the lifetime of the excited states of the molecules and ions. At the same time we have the possibility of determining the rates of the forward and reverse protolysis reactions **k** and **−k**, which is difficult to do by other methods because of the extreme speed of the reaction.

Weller[5] has made a detailed study of the rates of the protolysis reactions in β-naphthol. We have repeated Weller's experiments on β-naphthol and also undertook the determination of the dissociation constants in the excited state for eight other hydroxyl-derivatives of naphthalene and the determination of the changes in the reaction rates as a function of the kind of naphthol.

First of all, the absorption and luminescence spectra of the hydroxy-derivatives of naphthalene were measured for various values of pH* in order to see whether a change in the luminescence spectra with concomitant stability of the absorption spectra could be observed in the selected compounds, and where in the spectrum it took place, and also to ascertain the best conditions for excitation.

*We had studied the absorption spectra of naphthols in a neutral medium earlier.[6]

The absorption spectra were measured in a CF-4 spectrophotometer. The luminescence spectra were measured with the same spectrophotometer used as a monochromator. The receiver was a FEU-18 photomultiplier, the signal from which was amplified and registered by a EPPV-51 recording potentiometer provided with a wavelength marker connected to the drum of the monochromator. A SVDSh-1000 mercury lamp served as a source of excitation, the light from which was monochromatized by a special glass filter for the isolation of a wavelength of 313 mμ, by a UFS-2 (2mm) filter, by a 1 cm-thick film of potassium biphthalate solution, and by a heat-absorbing filter SZS14.

It was found that the luminescence and absorption spectra of all nine of the hydroxy-derivatives of naphthalene studied changed when the pH of the solution was changed. In basic media (pH ≈ 13), in which only the ionic form of the naphthols exists, one observes a marked shift of the spectra to the long wavelength side and in the majority of cases a disappearance of structure and a widening of the spectra.

The ratios of the relative luminescence outputs of the undissociated molecules and ions $(\eta/\eta_0) \cdot (\eta_0'/\eta')$ as a function of pH were also determined. For this the relative intensity η/η' of luminescence of the solution (under complete absorption) was measured at two wavelengths, one of which is located in the molecular spectrum, the other in the spectrum of the ions, for a given value of pH. Values of η_0'/η_0 were determined by means of a measurement of the intensity of luminescence for the wavelengths mentioned in base and in acid.

Special attention was given to a careful separation of the molecular and ionic parts of the luminescence spectrum, for which the monochromator was used in lieu of filters; the measurements of η and η' were carried out on the edges of the bands, where the mutual overlapping of the spectra is absent.

Figures 1 and 2 show the results of experiments for measuring the ratio of the relative outputs of the molecular and ionic forms of the naphthols as a function of the hydrogen-ion concentration for the various naphthols. Values of $(\eta/\eta_0) \cdot (\eta_0'/\eta')$ are plotted along the ordinate axis, and the values of $C_{H_3O^+} \cdot f^2 10^3$ in moles per liter along the abcissa. The numbers close to the lines indicate the locations of the hydroxyl groups in the naphthalene molecule. For α-naphthol (Fig. 2), whose luminescence in water was hardly noticeable, values of $(\eta_0/\eta) - 1$ have been plotted along the ordinate.

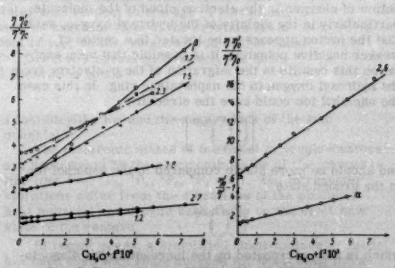

Fig. 1. Dependence of the ratio of the relative luminescence outputs of the molecular and ionic forms of the naphthols on the hydrogen-ion concentration.

Fig. 2. Dependence of the ratio of the relative luminescence outputs of the molecular and ionic forms of 2,6-naphthol and the relative output of the ionic form of α-naphthol on the hydrogen-ion concentration.

The fact that a rather good linear dependence is observed confirms the assumed mechanism of the reactions that take place in the excited state. The intercepts at $C_{H_3O^+} = 0$ determine the magnitude of $1/\mathbf{k}\tau$ in all cases, and the slope of the lines gives the magnitude of $(1/K)(\tau'/\tau)$.

For the calculation of the dissociation constant K in the excited state it is necessary to know the ratio τ'/τ. This ratio can be obtained to a first approximation from the ratio of the natural lifetimes, which can be calculated from the absorption spectra. The possibility of this approximation was checked for β-naphthol, for which the magnitudes of τ and τ' are known from the work of Weller. According to these data the ratio τ'/τ amounts to 0.735. From the absorption spectra we derived $\tau'_e/\tau_e = 0.75$. The deviation of approximately 2 percent indicates that the replacement of the ratio τ'/τ by the ratio τ'_e/τ_e is permissible. The values of τ'_e/τ_e determined from the absorption spectra for all nine hydroxy-derivatives of naphthalene are presented in Table 1. Values obtained for the dissociation constant K in the excited state are also given in this table.

Table 1

Compound	$\frac{\tau}{\tau_0}$	$\frac{1}{K}\cdot\frac{\tau'}{\tau}$	$\frac{\tau'_e}{\tau_e}$	$K\cdot 10^2$	log K
β-naphthol	0.444	825	0.75	9.09	−3.0414
α-naphthol	0.820	506	1.06	20.95	−2.6789
1,2-naphthol	1.785	96	0.424	44	−2.3565
1,5-naphthol	0.405	585	0.73	12.5	−2.9031
1,7-naphthol	0.318	600	0.438	7.3	−3.1367
1,8-naphthol	0.501	182	0.25	13.7	−2.8633
2,3-naphthol	0.281	484	0.29	6.0	−3.2218
2,6-naphthol	0.156	1385	0.525	3.79	−3.4214
2,7-naphthol	1.325	87	0.303	34.7	−2.4597

The magnitude of the dissociation constant in the excited state depends on the kind of naphthol and varies from 3.79×10^{-4} to 4.4×10^{-3} for the substances investigated. The difference between these constants and the dissociation constant in the ground state is striking. The latter are of the order of 10^{-10} for α- and β-naphthol. Consequently, the dissociation constants in the excited state exceed the dissociation constants in the ground state by six to seven orders of magnitude.

Evidently, excitation leads to a significant redistribution of charges in the electron cloud of the molecule, particularly in the vicinity of the hydroxyl oxygen, such that the proton appears to be located in a region of weaker negative potential. It is possible that upon excitation this results in the migration of the p-electron from the hydroxyl oxygen to the naphthalene ring. In this case the naphthol ion could have the structure

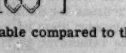

and should be more stable compared to the naphthol ion in the ground state

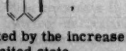

which is also corrobated by the increase in the dissociation constant in the excited state.

The difference between the dissociation constants in the ground and excited states can also be determined by several other methods considered by Förster.[7]

As was mentioned above, the absorption and luminescence spectra of naphthol ions are displaced toward longer wavelengths relative to the molecular spectra. The magnitude of the long wavelength shift of the zero-point transition can characterize the difference in energies necessary for the dissociation of the molecule in the ground and excited states. This is well illustrated by the following energy-level scheme (Fig. 3), from which it follows that $\Delta E - \Delta E' = D - D^*$.

As is known, the equilibrium constant of the reaction is determined from the expression

$$K = e^{\frac{-\Delta\Phi}{RT}} = e^{\frac{-\Delta H}{RT} + \frac{\Delta ST}{RT}},$$

where $\Delta\Phi$ is the free energy of thermodynamic potential, R is the universal gas constant, ΔH is the heat content (enthalpy), and ΔS is the entropy.

The difference in the dissociation energy in the ground and excited states equals

$$D - D^* = \Delta H - \Delta H^*.$$

Thus, if the entropy of the reaction in the ground and excited states is the same, then

$$\ln K - \ln K^* = -\frac{\Delta E - \Delta E'}{RT}$$

or

$$pK - pK^* = \frac{\Delta E - \Delta E'}{2.3RT}.$$

In Table 2 are presented the frequency shifts of the zero-point transitions upon molecular dissociation, obtained from the absorption and luminescence spectra of the substances investigated. These long wavelength shifts amount to 2400–3600 cm^{-1}. The calculated difference in the logarithms of the dissociation constants of the ground and excited states is given in this same table. It varies for the various naphthols from 5.2 to 7.65, i.e., when a molecule makes a transition to the excited state its dissociation constant changes by five to seven orders of magnitude. Thus, the results of such an energetic consideration of the process again confirms the fact that in the transition to the excited state the ability of the molecule to dissociate increases tremendously.

We shall now examine the rate constants for the forward (**k**) and reverse (**−k**) protolysis reaction for the different naphthols and how they change as a function of log K. Values of **kτ** obtained from the intercepts in Figs. 1 and 2 are shown in Table 1. For calculating **k** it is necessary to know τ. The value of τ for β-naphthol is 1.1×10^{-8} sec.[8] We have assumed that, in a first approximation, τ has the same order of magnitude for all the naphthols, and we take it equal to 1×10^{-8} sec. The values of **k** obtained for the various naphthols ranges from 1.6×10^7 to 1.8×10^8 sec^{-1}, and the values of **−k** = **k**/K are approximately the same $(3\text{–}5 \times 10^{-10})$ for all the naphthols. (See Table 3.)

Table 2

Compound	$\Delta E - \Delta E'$ (cm^{-1})	$pK - pK^*$
β-naphthol	3050	6.5
α-naphthol	2675	7.65
1,2-naphthol	2700	5.75
1,5-naphthol	2425	5.2
1,7-naphthol	3350	7.15
1,8-naphthol	3200	6.9
2,3-naphthol	3125	6.65
2,6-naphthol	2775	5.9
2,7-naphthol	3150	6.7

Table 3

Compound	$\log \vec{k}$	$\log \overleftarrow{k}$
β-naphthol	7.6474	10.6888
α-naphthol	7.9139	10.5927
1,2-naphthol	8.2517	10.6082
1,5-naphthol	7.6075	10.5106
1,7-naphthol	7.5024	10.6391
1,8-naphthol	7.6998	10.5631
2,3-naphthol	7.4487	10.6705
2,6-naphthol	7.1931	10.6145
2,7-naphthol	8.1222	10.5819

In Fig. 4 are presented log **k** and log **−k** as functions of log K. It is obvious that log **k** depends on the kind of naphthol and increases linearly with log K, but log **−k** remains approximately constant. The lack of change of the rate constants **−k** for the association of anions with protons for the different naphthols shows that this rate

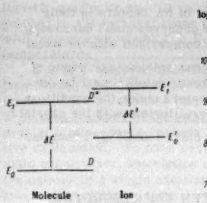

Fig. 3

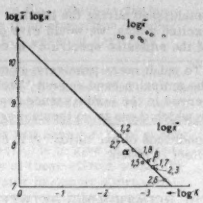

Fig. 4

Fig. 3. D is the dissociation energy of a molecule in the ground state; D* is the dissociation energy of a molecule in the excited state.
Fig. 4. Dependence of the rate constants of the protolysis reaction on the dissociation constant for the various naphthols.

is practically independent of the kind of anion, and the order of its magnitude 10^{10} shows that it is basically determined by the rate of diffusion. Actually, Weller has calculated the frequency of collisions of the charged particles according to the Debye formula (which is determined by the diffusion process) for the case of β-naphthol. The calculated value of $\log k_{diff.}$ is 10.837 at 20°C. This magnitude by itself determines the frequency of collisions between naphthol ions and protons. But not every collision can bring about an association reaction. The probability of establishing this reaction is determined by the ratio $\gamma = -k_{obs.}/k_{diff.}$. Assuming that the diffusion coefficients for all the investigated naphthols are the same to a first approximation, and therefore, taking $-k_{diff.}$ to be the same for all the naphthols, we calculated the value of γ. It turned out to vary between the limits 0.47 to 0.71 for the various naphthols. Consequently, two out of every three or four diffusion collisions should lead to capture of a proton by an ion.

REFERENCES

1. N. Mataga, J. Kaifu, and M. Koizumi, Bull. Chem. Soc. Japan, 29, 465 (1956).
2. E. Lippert, Z. Elektrochem. 61, 962 (1957).
3. T. Förster and K. Kasper, Z. Elektrochem. 59, 976 (1955).
4. T. Förster, Z. Elektrochem. 54, 531 (1950).
5. A. Weller, Z. Phys. Chem. 3, 238 (1955); Z. Elektrochem. 56, 662 (1952).
6. L. D. Derkacheva, Opt. i. Spektr. 5, 542 (1958).
7. T. Förster, Z. Elektrochem. 54, 42 (1950).

ELECTRONIC-VIBRATIONAL PROCESSES IN THE LUMINESCENCE CENTERS OF IONIC CRYSTALS*

*Presented at the VIII Conference on Luminescence, Minsk, October 1959.

Ch. B. Lushchik, N. E. Lushchik, and K. K. Shvarts

Received 30 November 1960

A study of the emission spectra, absorption spectra, and quantum yield of luminescence from alkali halide crystals as functions of the frequency of the exciting light ($\nu_{exc.}$) and temperature indicated that radiative and nonradiative transitions in luminescence centers take place after an equilibrium distribution of excited states with respect to storage of vibrational energy is established with the crystal. The luminescence quantum yield of the crystals has a steplike dependence on $\nu_{exc.}$. The yield is independent of $\nu_{exc.}$ in the neighborhood of individual fundamental electronic-vibrational absorption bands. Generally speaking, however, the quantum yields are different near different fundamental absorption bands.

INTRODUCTION

Electronic-vibrational processes in solutions and vapors of complex molecules have been investigated in detail by Vavilov, Terenin, Levshin, Neporent, Stepanov, Alentsev, and others (see refs. 1-6 for example).

We have made a detailed study of electronic-vibrational processes in the luminescence centers of the simplest ionic crystals—alkali halide salts activated with ions of atoms similar to mercury.[7-13]

It was spectroscopically proved in refs. 7, 8, 10 and 14 that the "cores" of luminescence centers in this class of luminors, as had also been suggested previously for thallium-activated phosphors,[15-17] are the mercurylike ions Ga^+, Ge^{++}, In^+, Sn^{++}, Tl^+, and Pb^{++} located at cation sites in the crystal lattice. The mercurylike ions interact with the nearest ions of the host material. A luminescence center may be considered as a quasimolecular subsystem located in a crystalline thermostat and including a mercurylike ion and the nearby ions of the host material.

The electronic states of the quasi molecule-centers are determined by the electronic states of the mercurylike ions ($^1S_0$, $^3P_0$, $^3P_1$, $^3P_2$, $^1P_1$ etc.). The intracenter vibrations differ from the vibrations of the phosphor host material and depend essentially on the electronic state of the centers.

In recent years, a simplified quasi-molecular model has been used with some success for describing intracenter phenomena. The model is a single oscillator harmonic approximation using a semiclassical version of the Franck-Condon principle.[18,19-21] We have investigated the applicability of this model to describe luminescence centers in alkali halide crystals.[8-13]

In the present paper, we are continuing our investigation of the fundamental principles which determine the character of the intracenter processes in alkali halide crystals activated with mercurylike ions.

THE DEPENDENCE OF LUMINESCENCE EMISSION SPECTRA ON THE FREQUENCY OF THE EXCITING LIGHT

In their electronic ground state, luminescence centers are in thermal equilibrium with the crystal-thermostat. When a center is excited, the inertial process is not able to rearrange the heavy ions, and at the initial moment after absorbing a light quantum, the luminescence center has a nonequilibrium supply of vibrational energy. Our experiments must tell us whether the vibrational energy distribution of the centers has time to come to equilibrium with the crystal while the centers remain in the excited state, and whether the process of establishing equilibrium will be accompanied by radiative and nonradiative transitions. We investigated the dependence of the emission spectra on the frequency of the exciting light $\nu_{exc.}$ for a large number of alkali halide phosphors (KCl-In, KBr-In, KCl-Ga, KBr-Ga, KCl-Tl, KBr-Tl, NaCl-Tl, KCl-Pb, KCl-Sn, KBr-Sn, and others). It was

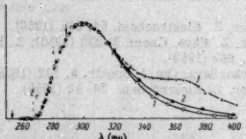

Fig. 1. Emission spectra of an NaCl-Tl phosphor (T = 550°K) during excitation by light from various mercury lines. $\lambda_{exc.}$ (in mμ): curve 1—254; curve 2—280; curve 3—289 (indicated by the arrows). The spectral sensitivity of the photomultiplier and the dispersion of the spectrophotometer were not taken into account.

found that at room temperature, the emission spectra of all of these phosphors were independent of $\nu_{exc.}$ when excited in the region of the absorption band of one kind of activator center. This radiation corresponds to $^3P \rightarrow {}^1S_0$ electron transitions in the mercurylike ions.[7,8] Therefore the vibrational energy distribution of centers has time to reach equilibrium with the crystal during the lifetime τ of the luminescence centers if the ^3P state,*

*According to Piyavin',[22] in alkali halide crystals τ (^3P) is $\sim 10^{-8}$ sec for Ga^+ ions, $\sim 3 \times 10^{-6}$ sec for In^+ ions, and $\sim 10^{-9}$–10^{-7} sec for Tl^+ ions.

and it is only after this that radiative transitions take place.

The shape of the fundamental emission band is independent of $\nu_{exc.}$ even under the most unfavorable excitation conditions. Emission spectra of the phosphor NaCl-Tl are shown in Fig. 1. They were measured during excitation in the anti-Stokes region ($\nu_{exc.} < \nu_{el.}$, where $\nu_{el.}$ is the frequency of the pure electronic transition) almost at the maximum of the emission band, and under the usual excitation conditions at the maximum of the absorption band. As is seen from the figure, these spectra coincide perfectly in the short wavelength region.*

*The differences in the long wavelength region are explained by the superposition of an emission band from a second type of centers during the anti-Stokes excitation.

Excitation in the region of the emission band maximum must lead to a minimum initial supply of vibrational energy in the excited centers. If in this situation equilibrium with the crystal had not had time to become established during the lifetime of the centers in their excited states, we would have observed some narrowing of the emission spectrum* in comparison with the usual

*To put it more precisely, in our opinion, narrowing of the emission band and not "Stokes cutoff" must be observed in the luminescence centers under the conditions in which there is no thermal equilibrium with the crystal.

conditions of excitation. It is clear from Fig. 1 that this effect is absent.

THE RELATIONSHIP BETWEEN THE ABSORPTION AND EMISSION SPECTRA OF IMPURITY CENTERS IN CRYSTALS

Because of the establishment of an equilibrium distribution of excited luminescence centers with respect to storage of vibrational energy, the emission spectra of the centers are connected with the absorption spectra in a relatively simple way. As is well known, an especially simple relationship (discovered by Levshin,[3] i.e., the mirror symmetry of the absorption and emission spectra with respect to the electronic transition energy E_0) exists for the case in which the vibrational frequency remains the same when the electronic state of the center is changed. We have measured the shapes of the related absorption and emission bands ($^1S_0 \rightleftarrows {}^3P$ transitions) of many alkali halide phosphors activated with mercurylike ions. Some of these are shown in Fig. 2 in $I/\nu^3 - \nu$ and $x/\nu - \nu$ coordinates. The absorption and emission spectra are normalized to equal areas. It follows from

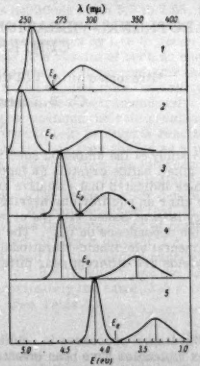

Fig. 2. Spectra of the associated absorption and emission bands for the $^1S_0 \rightleftarrows {}^3P$ electronic transition in the phosphors: NaCl-Tl (1), KCl-Tl (2), NaCl-Pb (3), KCl-Pb (4), and KBr-Pb (5).

these data that the mirror symmetry rule is not followed in our case. The deviations from mirror symmetry in the phosphors studied have a regular character: the half-widths of the absorption bands δ^a are appreciably less than the halfwidths of the emission bands δ^l. The intersection point of the spectra (E_m) lies nearer the absorption band maximum E_m^a than the emission band maximum E_m^l. The absorption band contours are asymmetrically broadened on the low frequency side. There is a charac-

teristic maximum energy value $E_{lim.}$ which is distinguished by the fact that there is no absorption of light with frequencies where $E > E_{lim.}$, even at very high temperatures.

If it is considered that the intracenter vibrational frequencies are lowered 30-40% on photoexcitation of the centers, then all of these and some other (see reference 9) special features of the spectral characteristics of ionic crystal luminescence centers will have a natural qualitative explanation. We have been able to give an approximate quantitative description of these effects within the framework of a single oscillator harmonic approximation, using a semi-classical version of the Franck-Condon principle.[7-9] The following relationships* occur among the optical characteristics of the luminescence centers at high temperatures:

*The relationship (2) was obtained by N. N. Kristoffel.

$$E_e - E_m^I = l\,(E_m^* - E_e), \tag{1}$$

$$E_n = E_e - \frac{kT}{2}\ln l, \tag{2}$$

$$E_m^* - E_m^I = \frac{1}{8kT\ln 2}\,\frac{l(l+1)}{2}\,(\delta^I)^2 = \frac{1}{8kT\ln 2}\,\frac{l+1}{2l}\,(\delta^I)^2, \tag{3}$$

$$E_{lim.} = E_e + \frac{1}{l-1}\,(E_e - E_m^I). \tag{4}$$

The parameter

$$l = \frac{\omega_1^2}{\omega_2^2} = \left(\frac{\delta^I}{\delta^*}\right)^2$$

represents the value of the ratio of the squares of the vibrational frequencies in the ground state ω_1 and the excited state ω_2. When $l = 1$, these formulas reduce to the well-known formulas of Pekar and Krivoglaz.[23,24] A comparison of the relationships (1)-(4) with the experimental data from Fig. 2 is shown in the Table.

Phosphor	l	$E_m^* - E_m^I$ (ev)		E_e (ev)		E_n (ev)	$E_{lim.}$ (ev)	
		From ref. 3	Exp.	From ref. 1	From ref. 2		From ref. 4	Exp.
NaCl-Tl	1.73	0.80	0.84	4.64	4.63	4.62	5.20	~5.10
KCl-Tl	2.00	0.89	1.01	4.68	~4.69	~4.68	5.45	5.20
NaCl-Pb	2.03	0.59	0.63	4.34	4.33	4.32	4.75	~4.75
KCl-Pb	2.00	0.61	0.96	4.25	~4.27	~4.26	4.87	4.80
KBr-Pb	2.05	0.53	0.76	3.86	3.88	3.87	4.38	~4.35

Our detailed comparison of the experimental data with relationship (3)[9,12] showed that there was good agreement between theory and experiment only for certain phosphors (crystals activated with thallium). For most of the crystals studied, there was a systematic discrepancy between theory and experiment. An analysis of the nature of these discrepancies indicated that one of the primary causes was the fact that the theory did not take account of the anharmonic aspects of intracenter vibrations.[9]

This effect is especially prominent in centers having large Stokes losses. Considering the fact that in all the phosphors we investigated, the anions surrounding the mercurylike ion are drawn nearer to it during excitation of the centers (this was shown by experiments on the compression of phosphors[25,26] from all sides), we concluded that the anharmonicity of intracenter vibrations is "normal." When the ions approach each other, the potential energy increases more rapidly than as the square, and decreases more slowly as they separate. This anharmonic property of the vibrations is a second, less essential cause of the lack of mirror symmetry in the absorption and emission spectra of luminescence centers having small radii in ionic crystals.

NONRADIATIVE TRANSITIONS IN LUMINESCENCE CENTERS

Bünger,[27] Morgenshtern,[28] and Shvarts[13] have shown that the quantum yield of intracenter luminescence in alkali halide phosphors is close to unity at sufficiently low temperatures. A sharply defined thermal quenching of luminescence is observed when the temperature is raised. This thermal quenching has been studied over a wide range of temperatures for the whole series of alkali halide crystals.[11,13] An analysis of the available experimental material indicates that the temperature dependence of the luminescence quantum yield is described very well by Mott's formula,[29]

$$\eta = \frac{1}{1 + \frac{d}{f}\exp\left(-\frac{Q}{kT}\right)}, \tag{5}$$

where f is the probability of radiative transitions and $d = d_0 \exp(-Q/kT)$ is the probability of nonradiative transitions. According to the theory of nonradiative transitions,[30,32] the function $d(1/T)$ is exponential at high temperatures. Such a form for the indicated function leaves no doubt that nonradiative transitions are accomplished by overcoming the activation barrier Q. It is generally accepted that the physical meaning of the latter is the difference between the minimum adiabatic potential of the excited state of the center and the area of convergence (intersection) of the adiabatic potentials of the ground state and the excited state. If this is so, then the value of Q must be connected in a relatively simple way with the optical characteristics of the center. We derived this relationship using the single oscillator harmonic approximation.[9] A comparison of our expression with experiment showed[9,13] that for centers with nearly harmonic vibrations, the experimental Q values agreed satisfactorily with the Q values calculated from the optical characteristics of the centers. We are inclined to regard this fact as a direct experimental verification of the mechanism proposed by Mott[29] for nonradiative transitions in luminescence centers. This proposed mechanism is based on Frenkel's idea[32] that the possibility of nonradiative transitions in crystals, as in molecules, is related to changes in the equilibrium conditions and vibrational frequencies of the heavy particles after a phototransition. As a result of this the activation barrier for nonradiative transitions has a finite height.

We have investigated the nonradiative transitions that take place after the equilibrium distribution of excited centers with respect to stored vibrational energy is established. It is legitimate to ask whether nonradiative transitions take place during establishment of the equilibrium. The idea was expressed in ref. 33 that when a center is optically excited to an energy level lying above the region where the adiabatic potentials of the ground state and the excited state approach each other, all of the excited states will undergo nonradiative transitions to the ground state. We conducted an experimental test of this idea.[13] The energy diagrams of a number of luminescence centers that we studied are shown in Fig. 3. They are plotted according to the optical and thermal characteristics of the centers. Relationships (1) and (2) were used to determine E_e. During excitation near the absorption band maximum, we did not approach the "dangerous level" $E_e + Q$ for most of the centers investigated. For this reason, "optical quenching" cannot be substantial in these cases. For phosphors activated with lead, the centers fall into the "dangerous" energy zone even after excitation in the region of the absorption band maximum. On excitation in the short wave-

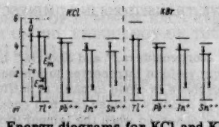

Fig. 3. Energy diagrams for KCl and KBr phosphors (for the electronic transition $({}^1S_0 \rightleftarrows {}^3P)$

length part of the absorption band, the centers shift to a region located 0.2-0.3 ev above the level $E_a + Q$. However, the experiments showed that for these phosphors as well, the quantum yield is close to one in the absence of thermal quenching. We think that because of the strong connection between intracenter and crystal vibrations, the thermal equilibrium of the excited centers and the crystal-thermostat is established so rapidly that for practical purposes nonradiative transitions cannot take place while the centers are passing through the "dangerous" energy zone. This is the situation not only for activator centers but also for F centers, as was shown by Zaitov[34] in our laboratory.

THE DEPENDENCE OF LUMINESCENCE QUANTUM YIELD ON THE FREQUENCY OF THE EXCITING LIGHT

The dependence of the luminescence quantum yield on the frequency of the exciting light $\nu_{exc.}$ has been investigated by Bünger[37] and Kato[38] for KCl-Tl, NaCl-Tl, and NaCl-Ag. One of us has carried out a detailed study of the function $\eta(\nu_{exc.})$ for a large number of alkali halide crystals activated with mercurylike ions. Some of the data are presented in ref. 13.

It has been shown that the intracenter luminescence quantum yield of crystals is independent of the frequency of the exciting light within the boundaries of all the long wavelength absorption bands of luminescence centers. The data for NaCl-Tl and KCl-Tl are shown in Fig. 4 as an example. The absorption and emission spectra of these phosphors overlap to such a marked degree at 500-600°K that even in the anti-Stokes region* the absence of any dependence of the luminescence quantum yield on $\nu_{exc.}$ can be established. The reason for this lies in the above-mentioned rapid "thermostating" of excited centers by the crystal lattice.

*The absence of any decrease in yield in the anti-Stokes region is not surprising. Theoretical studies in recent years[39] have shown that preservation of the high yield when $\nu_{exc.} < \nu_{el.}$ does not violate the laws of thermodynamics and is entirely possible.

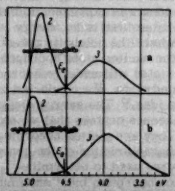

Fig. 4. The dependence of luminescence quantum yield (curve 1) on the frequency of the exciting light for the phosphors: (a) NaCl-Tl at 580°K; (b) KCl-Tl at 600°K. Curves 2 and 3 are the absorption and emission spectra of the phosphors respectively.

Thus far we have been discussing physical processes in luminescence excited to the ${}^3P$ level. At room temperature, the excitation ${}^1S_0 \rightarrow {}^1P_1$ gives rise to the appearance of luminescence corresponding to ${}^3P \rightarrow {}^1S_0$ electronic transitions, the intermediate transitions ${}^1P_1 \rightarrow {}^3P$ occuring nonradiatively. We were not successful in "freezing" these radiationless transitions at a temperature of 90°K.*

*We may be encountering the effect of "intracenter sensitizing," as in complex molecules.[37]

When the ${}^1S_0 \rightarrow {}^1P_1$ transition is excited, a weaker and longer-lived luminescence of the recombination type arises along with the short duration fluorescence. Electronic color centers (F-, M-, N-, and O-centers) are formed in the crystal at the same time.[38-42] At the suggestion of one of us, Yaek investigated the spectral dependence of the recombination phosphorescence quantum yield of some alkali halide phosphors.[43] It was shown that while the quantum yield of the steady state luminescence is practically independent of the frequency of the exciting light, the quantum yield of the phosphorescence increases with the frequency of the exciting light. The phosphorescence quantum yield is constant in the region of each fundamental electron-vibrational absorption band, but in going from one fundamental band to another the yield varies in a stepwise manner. The constancy of the yield in the region of each band confirms the fact that equilibrium with respect to storage of vibrational energy is established between centers and the surrounding medium during the lifetime of the centers in their excited states (${}^3P$, ${}^1P_1$, ...). Even after equilibrium has been established, thermal ionization of the excited center (or some other kind of process[38-42]) occurs, leading to the stimulation of recombination luminescence of the phosphor and to the creation in it of electronic color centers.

The excitation spectrum of activator luminescence in the region of the fundamental absorption band of the host material was studied quantitatively in our laboratory.[42,44,45] It was shown that the luminescence of activator ions is also excited in exciton absorption bands in "band-band" transitions. If the results obtained in refs. 43-45 are corrected for the spectral dependence of light reflected from the phosphors, it is evident that the luminescence yield depends slightly on $\nu_{exc.}$ in the region of each fundamental absorption band. However, this dependence is different for the various absorption bands of the host material. The luminescence is more effectively developed under "band-band" excitation than with "exciton excitation." It follows that equilibrium between (electrical) current and noncurrent excitation cannot be reached while fundamental excitation of the host material is occuring.[42,44]

Zaitov has investigated the spectral dependence of the quantum yield of the optical flare of luminescence of mercurylike ions in some x-rayed alkali halide phosphors.[34] In this case it turned out that the quantum yield has a steplike dependence on the frequency of the light stimulating the flare. The quantum yield is constant in the region of each fundamental band of stimulated absorption (F, M, Z,) but varies sharply on going from one band to another.

It seems to us that all of these phenomena obey a rule which has considerable generality:

The quantum yield of luminescence of ionic crystals is a steplike function of the frequency of the exciting light. It is independent of $\nu_{exc.}$ in the neighborhood of individual fundamental electronic-vibrational absorption bands. In general, the quantum yield is different for dif-

ferent fundamental absorption bands. The equality of the luminescence quantum yield in several fundamental absorption bands, which is observed in some cases, is a less general phenomenon in ionic crystals. In the future it will be necessary to check the applicability of these mechanisms to photoelectric and photochemical processes in ionic crystals.

REFERENCES

1. S. I. Vavilov, Sobr. Soch. (Collection of Papers) Vols. 1, 2. Izd. Akad. Nauk SSSR, Moscow, 1952, 1954.
2. A. N. Terenin, "Fotokhimiya krasitelei" (Photochemistry of Dyes). Izd. Akad. Nauk SSSR, Moscow-Leningrad, 1947.
3. V. L. Levshin, Zhur. Fiz. Khim. **2**, 641 (1931).
4. B. S. Neporent and B. I. Stepanov, Uzpekhi Fiz. Nauk **43**, 380 (1951).
5. B. I. Stepanov, "Lyuminestsentsiya slozhnykh molekul" (The Luminescence of Complex Molecules). Izd. Akad. Nauk Beloruss. SSR, Minsk, 1955.
6. M. N. Alentsev, Trudy Fiz. Inst. Akad. Nauk SSSR **5**, 499 (1950).
7. N. E. Lushchik and Ch. B. Lushchik, Trudy Inst. Fiz. Astron. Akad. Nauk Est. SSR **6**, 5 (1957).
8. Ch. B. Lushchik and N. E. Lushchik. Izvest. Adak. Nauk SSSR Ser. Fiz. **22**, 1347 (1958).
9. Ch. B. Lushchik, N. E. Lushchik and K. K. Shvarts. Trudy Inst. Fiz. i Astron., Akad. Nauk Eston. SSR **8**, 3 (1958).
10. N. E. Lushchik, Trudy Inst. Fiz. i Astron., Akad. Nauk Eston. SSR. **7**, 119, 134 (1958).
11. K. K. Shvarts, Trudy Inst. Fiz. i Astron., Akad. Nauk Eston. SSR. 7, 153 (1958).
12. N. E. Lushchik, Mater. VII. Soveshch. po lyuminests. (Proceedings of the VII Conf. on Luminescence). Tartu, 1959.
13. K. K. Shvarts, Mater. VII. Soveshch. po lyuminests. (Proceedings of the VII Conf. on Luminescence). Tartu, 1959.
14. N. E. Lushchik and Ch. B. Lushchik, Opt. i Spektr. **8**, 839 (1960), Optics and Spectroscopy **8**, 441 (1960).
15. F. Seitz, J. Chem. Phys. **1**, 150 (1938).
16. F. Williams, J. Chem. Phys. **19**, 457 (1951).
17. K. V. Shalimova, Doctor's dissertation. Fiz. Inst. Akad. Nauk SSSR, 1953.
18. C. Klick, Phys. Rev. **85**, 154 (1952).
19. M. Lax, J. Chem. Phys. **20**, 1752 (1952).
20. N. D. Potekhima, Opt. i Spektr. **2**, 388 (1957).
21. N. N. Kristoffel, Trudy Inst. Fiz. i Astron., Akad. Nauk Eston. SSR. **7**, 85 (1958); **10**, 3 (1959).
22. I. K. Plyavin', Candidate's dissertation, Fiz. Inst. Akad. Nauk SSSR, 1959.
23. S. I. Pekar, Zhur. Eksptl. i Teoret. Fiz. **22**, 641 (1952).
24. M. A. Krivoglaz, Zhur. Eksptl. i Teoret. Fiz. **25**, 191 (1953).
25. P. Johnson and F. Williams, Phys. Rev. **95**, 69 (1954).
26. Ya. Ya. Kirs and A. I. Laisaar, Trudy, Inst. Fiz. i Astron., Akad. Nauk Eston. SSR. **10**, 51 (1959).
27. W. Bünger, Z. Physik **66**, 311 (1930).
28. Z. L. Morgenshtern, Zhur. Eksptl. i Teoret. Fiz. **29**, 902 (1955).
29. N. Mott, Proc. Roy. Soc. (London) **A167**, 384 (1938).
30. R. Kubo, Phys. Rev. **86**, 929 (1952).
31. Yu. E. Perlin and V. A. Kovarskii, Uchenye Zapiski, Kishinev. Gosudarst. Univ., Fiz.-Matem. **21**, 81 (1954); and Yu. E. Perlin and M. M. Sharand, Uchenye Zapiski, Kishinev. Univ., Fiz.-Matem. **24**, 41 (1956).
32. Ya. I. Frenkel', Phys. Rev. **37**, 17, 1276 (1931).
33. D. Dexter, C. Klick, and G. Russel, Phys. Rev. **100**, 603 (1955).
34. F. N. Zaitov, Opt. i Spektr. **4**, 102 (1958).
35. M. Kato, Sci. Papers Inst. Phys. Chem. Research (Tokyo) **42**, 35 (1944).
36. V. V. Antonov-Romanovskii, B. I. Stepanov, M. V. Fok, and A. P. Khapalyuk, Doklady Akad. Nauk SSSR. **105**, 50 (1955).
37. V. L. Ermolaev and I. P. Kotlyar and K. K. Svitashov, Doklady na VIII Soveshch po lyuminests. (Proceedings of the VIII Conf. on Luminescence). Minsk, 1959.
38. Ch. B. Lushchik and V. I. Volin, Trudy Inst. Fiz. i Astron. Akad. Nauk Eston. SSR. **7**, 311 (1958).
39. Ch. B. Lushchik, Kh. F. Kyazmbre, and I. V. Yaek, Mater. VII Soveshch. po lyuminests. (Proceedings of the VII Conf. on Luminescence). Tartu, 1959.
40. I. V. Yaek, Trudy. Inst. Fiz. i Astron., Akad. Nauk Eston. SSR. **10**, 166 (1959).
41. Ch. B. Lushchik and E. S. Tiisler, Trudy Inst. Fiz. i Astron., Akad. Nauk Eston. SSR. **10**, 135 (1959).
42. Ch. B. Lushchik, G. G. Liid'ya, I. V. Yaek, and E. S. Tiisler, Opt. i Spektr. **9**, 70 (1960), Optics and Spectroscopy **9**, 35 (1960).
43. I. V. Yaek, Opt. i Spektr. **8**, 577 (1960), Optics and Spectroscopy **8**, 305 (1960).
44. I. V. Yaek and G. G. Liid'ya, Opt. i Spektr. **8**, 142 (1960), Optics and Spectroscopy **8**, 74 (1960).
45. Ch. B. Lushchik and G. G. Liid'ya, Mater. VII Soveshch. po lyuminests. (Proceedings of the VII Conf. on Luminescence), Tartu, 1959.

THE NATURE AND KINETICS OF RADIATION PROCESSES IN ZnS-Mn PHOSPHORS DURING EXCITATION

V. L. Levshin and V. F. Tunitskaya

Received 17 December 1959

An investigation was made of the effect of temperature on the blue and orange luminescence of ZnS-Mn phosphors excited by 312 and 366 mμ radiation. The processes of converting the excitation energy into blue luminescence, manganese luminescence, and heat were examined in relation to the experimental temperatures and manganese concentrations. A scheme for the development of the separate processes of luminescence and quenching is proposed which qualitatively explains the special features of the observed phenomena.

INTRODUCTION

In a previous paper[1] on the luminescence of ZnS-Mn phosphors, the authors studied the thermoluminescence and the origin of trapping levels of these phosphors. This paper is concerned with the luminescence of the same phosphors during excitation. In this case, when a steady state is attained, the number of recombining (radiating and nonradiating) electrons is equal to the number of newly generated electrons. The luminescence intensity can vary with temperature, both as a consequence of changes in the absorptive power of the phosphor and the process of transformation of one kind of radiation into another, and as a consequence of the development of thermal quenching. In this case however, the change in intensity takes place in an entirely different way than the thermoluminescence; as a matter of fact, this was pointed out in refs. 1-3.

This investigation was conducted on the same series of ZnS-Mn phosphors which were used previously.[1] The phosphors were prepared in the form of layers about 3.7μ thick (diameter of grains ~ 1μ) and excited through their entire thickness by 365 and 312 mμ Hg radiation. The quantum intensities of these lines were equalized with the aid of a wire gauge. An FEU-32 photomultiplier was used to measure the intensity of the luminescence.

I. THE ABSORPTION OF ZnS-Mn PHOSPHORS

Temperature-sensitive changes in the luminescence intensity of phosphors under excitation can be explained to a large degree by changes in their absorptive power. Semiquantitative information on absorption by powdered phosphors can be obtained by determining the coefficient of diffuse reflection (R) of light from the surface of a thick layer of phosphor ($R = I/I_0$, where I and I_0 are the intensities of the light reflected from the phosphor and from magnesium oxide, respectively). The values of 1 – R for the phosphor ZnS-Mn (10^{-3}), corresponding to various t° are shown in Fig. 1. It is easy to see that at $\lambda < 330\mu$ an increase in temperature does not change the absorption of the phosphor. Thus, in our experiments, the absorption of light at 312 mμ is practically independent of temperature. In the longer wavelength regions (near the edge of the absorption band of the phosphor) a great change in the reflection coefficient is observed. In our work, the change in absorption near λ = 365 mμ is obvious and substantial. Figure 1 indicates (using a slight extrapolation) that the absorption near 365 mμ is changed approximately 1.4-fold when the temperature is increased from –165° to +20°, and 1.8-fold when the phosphor is heated to +100°. These data also make it possible to estimate the changes in absorption of the phosphor at 365 mμ for intermediate temperatures.

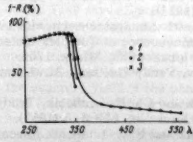

Fig. 1. The absorption of the phosphor ZnS-Mn (10^{-3}) at various temperatures. Temperature (in °C): 1—(–165); 2—(+20); 3—(+100).

In addition to this the absorption spectra depend on the manganese content in the phosphor. The values of 1 – R for a number of phosphors with different Mn concentrations are shown in Fig. 2. It is seen from the figure that absorptivity in the region of the fundamental band gradually decreases (by about 10%) as the manganese concentration increases from 0 to 6×10^{-3} gm/gm. Between 350 and 550 mμ, however, it begins to fall off somewhat, as in ref. 4, but after that significantly increases again.

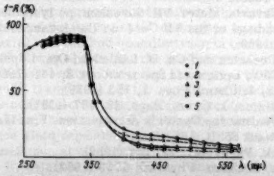

Fig. 2. The absorptivity of ZnS-Mn phosphors with different Mn concentrations (temperature + 20°C). Mn concentration (in gm/gm): 1–0; $2–10^{-3}$; $3–10^{-4}$; $4–10^{-3}$; $5–6 \times 10^{-3}$.

II. THE EMISSION SPECTRA OF ZnS and ZnS-Mn PHOSPHORS

A monochromator was used to study the intensity (energy) of the blue and orange luminescence bands of ZnS and ZnS-Mn phosphors in various portions of the spectrum. It is therefore essential to know the form of the emission spectra in order to determine the relationship of the integrated luminescence intensities at

various temperatures and concentrations. The emission spectra of the ZnS and ZnS-Mn (10^{-2}) phosphors are shown in Fig. 3 for temperatures from −196° to +170° when excited by 312 and 365 mμ radiation (the intensities at the maxima of the spectra are taken as unity in all cases). It is seen from the figure that the shape of the spectrum is independent of the wavelength of the exciting radiation. A change in the temperature from −196° to −72° leads to a shift in the ZnS emission maximum from 480 to 470 mμ. A further increase in temperature (from −72° to +90°) does not change the location of the blue band

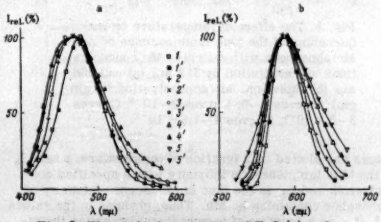

Fig. 3. The emission spectra of ZnS (a) and ZnS-Mn (10^{-2}) (b) excited by 366 mμ light (1-5) and 312 mμ light (1′-5′) at different temperatures. Temperature (in 0°C): 1,1′—(−196); 2,2′—(−72); 3,3′—(+20); 4,4′—(+90); 5,5′—(+170).

maximum. Raising the temperature also changes the half-width of the ZnS emission band, which is 32 mμ at −196°, 38 mμ at −70°, 43 mμ at +20°, and 45 mμ at +90°. The greatest rise in intensity was noted in the long wavelength part of the spectrum.

The location of the maximum of the orange emission band of Mn was practically unchanged over the entire temperature range studied. There was a change in the half-width of the emission spectrum, however; this amounted to 25 mμ at −196°, 29 mμ at −72°, 34 mμ at +20°, 39 mμ at +90°, and 44 mμ at +170°.

A large increase in intensity was noted at the edges of the spectrum. In the red region, for example, a new emission band was produced at the high temperatures.

III. THE LUMINESCENCE INTENSITY OF ZnS-Mn PHOSPHORS DURING EXCITATION

Measurements of the luminescence intensity of thin layers of ZnS-Mn phosphors as a function of temperature were made in two spectral regions—those of the blue band and the manganese band (Fig. 4). The Mn concentration of the phosphors ranged from 0 to 3×10^{-2} gm/gm. In the figure, curves I and I′ correspond to excitation by 312 mμ radiation, and curves II and II′ to excitation by 366 mμ radiation. Curves I and II, which pertain to the blue luminescence, are represented by continuous lines; the manganese luminescence curves I′ and II′ are shown as broken lines. The luminescence intensity values cited take into account the shapes of the emission spectra and the spectral sensitivity of the FEU-32 photomultiplier.

An examination of the data (Fig. 4) leads to several conclusions which are essential to an explanation of the luminescence kinetics and energetics.

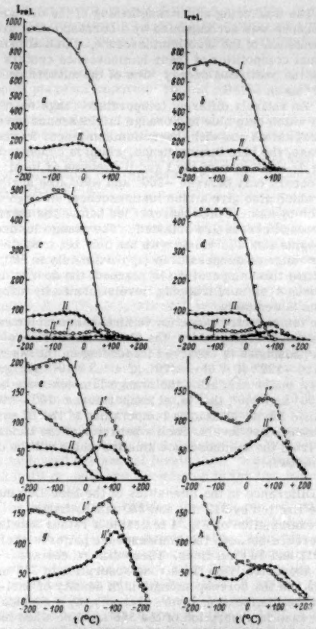

Fig. 4. The dependence of the luminescence intensity under excitation on temperature for ZnS-Mn phosphors having different Mn concentrations. Concentration of Mn (in gm/gm): a—0; b—10^{-4}; c—3×10^{-4}; d—10^{-3}; e—1.5×10^{-3}; f—4.5×10^{-3}; g—10^{-2}; h—3×10^{-2}. Solid curves I and II—blue luminescence; the dashed curves I′ and II′—Mn luminescence; I and I′—312 mμ exciting light; II and II′—similar curves for 366 mμ.

1. The Difference Between Luminescence Under Excitation and Thermoluminescence

(a) It is clear from a comparison of the curves of Fig. 4 with the thermoluminescence curves for the same phosphors[1] that the spectral compositions of the two types of luminescence at a given temperature are substantially different.

There are three maxima in the thermoluminescence curves (at −160°, −90°, and −30°). The latter is observed only in phosphors containing Mn, and is due to luminescence from manganese centers only; the other two maxima give both orange and blue luminescence in different proportions. Both luminescences were observed in the emission spectra during excitation at all of the temperatures specified; no effects due to discrete levels were apparent to any appreciable degree. Temperature quenching set in only at significantly higher temperatures, beginning with the blue and afterward the orange lumines-

cence. The weakening and strengthening of the orange luminescence was accompanied by a corresponding growth and attenuation of the blue luminescence, which attests to the mutual competition of these luminescence centers in utilizing the excitation energy. One of the authors described this in ref. 3.

(b) An entirely different temperature range must be noted in which both blue and orange luminescence develop during excitation and with thermoluminescence. In the latter case, the blue luminescence, which is connected with the de-excitation of the I and II systems of local levels, occurs only between −200° and −90° (the shallower levels, which also give a blue luminescence, undergo de-excitation by natural phosphorescence before the thermoluminescence curves are obtained). The orange luminescence begins simultaneously with the blue but extends to a higher range of temperatures (approximately to 10°). By the time this temperature is reached, the de-excitation of this deep system of trapping levels formed by manganese ions is complete.

The temperature range for luminescence under excitation is considerably wider: the blue luminescence of ZnS-Mn phosphors is observed (depending on the Mn content) up to −120° (C = 0) or +70° (C = 1.5×10^{-3} gm/gm). Similarly, under excitation the orange luminescence between 200° and 250°, that is, at temperatures 190°-240° higher than the de-excitation temperature of the III system of manganese levels. Such a behavior of the bands follows from the luminescence kinetics which will be discussed below.

2. The Difference in the Intensities of the Blue Luminescence Excited by 312 mμ and 360 mμ Radiation.

An examination of Fig. 4 indicates a rather substantial difference between the luminescence patterns excited by the 312 and 360 mμ lines. These differences are brought about firstly by the strong absorption of 312 mμ radiation and the correspondingly high density of excitation of the luminescent layer; secondly, by a considerable increase in absorption of the 366 mμ line when the temperature is raised (Fig. 2), while the absorption of the 312 mμ line, according to our experiments, remains practically unchanged; and thirdly, by a difference in the nature of the absorbing centers.

At −190°, the blue luminescence excitated by the 312 mμ radiation is seven times as intense as that excited by the 366 mμ radiation, which implies a correspondingly greater degree of absorption.

The increase in absorption of 366 mμ radiation associated with increasing temperature makes it difficult to detect the onset of temperature quenching, which develops at considerably higher temperatures in this case than when excited by 312 mμ radiation. On the other hand, owing to the high density of excitation by 312 mμ radiation, temperature quenching in this case must begin at higher temperatures than with excitation by the 366 mμ line.[8] This effect partially masks the stronger effect of the increased absorption of 366 mμ radiation at higher temperatures. The increasing absorption of 366 mμ radiation with increasing temperature also explains the crossing of the orange luminescence curves of the $C_{Mn} = 10^{-2}$ and 3×10^{-2} phosphors (Fig. 4) corresponding to excitation by 312 and 366 mμ radiation.

3. The Influence of Manganese Concentration on the Blue Luminescence Intensity

Figure 4 shows that the introduction of Mn sharply reduces the blue luminescence and enhances temperature quenching. In the absence of Mn, the luminescence is extinguished completely at temperatures around +120°, but with $C_{Mn} = 1.5 \times 10^{-3}$, this occurs at ~ + 60°. The curves shown in Fig. 5 were plotted to illustrate the effect of Mn on the blue luminescence more clearly. The I_b/I_{ob}

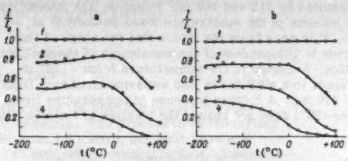

Fig. 5. The effect of temperature on the quenching of the blue luminescence of ZnS-Mn phosphors with different Mn concentrations and excitation by 312 mμ (a) and 366 mμ (b) radiation. Mn concentration (in gm/gm): Curves 1—0; Curves 2—10^{-4}; Curves 3—3×10^{-4}; Curves 4—1.5×10^{-3}.

values are plotted as a function of temperature, where I_b is the blue luminescence intensity with a specified concentration and I_{ob} is the blue luminescence intensity of a phosphor containing no Mn. Thus, changes in the values of I_b/I_{ob} as a function of temperature determine the effect of Mn at the various temperatures, the usual temperature quenching effect (at least in the first approximation) being excluded.

It is clear from Fig. 5 that even a small addition of Mn strongly quenches the blue luminescence. This quenching is apparently the summing up of several processes: between −190° and −40°, it depends very little on temperature, but when t > −40° a second process is added to the first, its effectiveness increasing rapidly as the temperature is raised. A discussion of these processes will be presented below.

4. The Development of the Manganese Luminescence

An examination of the temperature curve of the orange luminescence (dashed lines of Fig. 4) indicates first of all a direct connection between the growth of the orange luminescence and the diminishing of the blue (see also ref. 3). Some further increase in the orange luminescence intensity is observed when phosphers with $C_{Mn} < 4.5 \times 10^{-3}$ gm/gm are heated after the blue luminescence has completely disappeared. This behavior and the complex intensity curve of the orange luminescence from phosphors with $C_{Mn} < 4.5 \times 10^{-3}$ gm/gm are caused by a change in the absorption of the exciting light and an increased luminescence yield (temperature quenching starts to increase above +80°). Figure 4 also shows that the manganese luminescence output is not large. On the other hand in contrast to the luminescence under excitation, the light sums of the long-lived luminescences [the blue luminescence of the ZnS-phosphor and the orange luminescence of the ZnS-Mn (10^{-2}) phosphor] are approximately the same.[1]

5. On the Yield of the Blue and Orange Luminescence and the Quenching of ZnS-Mn Phosphors

The blue and orange luminescence output values are shown in Fig. 6 (the fine lines and the dashed curves), along with values for the loss due to quenching (the heavy curves). The data of Fig. 2 and Fig. 4 were used to obtain the curves in Fig. 6 with the following assumptions: the blue luminescence yield of ZnS at −196° is taken as 100% (this value may be too high[9]); the values of the blue and orange luminescence output for other concentrations and temperatures were calculated by comparison with I_o

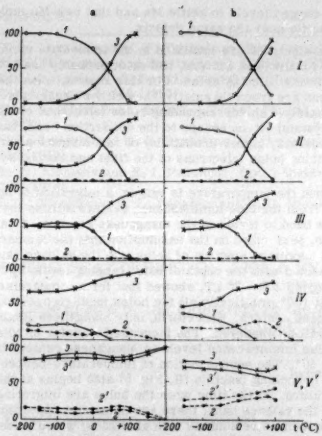

Fig. 6. The distribution of excitation energy among the blue luminescence (curves 1), the orange luminescence (curves 2,2′) and quenching (curves 3,3′) as it depends on temperature for ZnS-Mn phosphors with various Mn concentrations and excited by light at 312 mμ (a) and 366 mμ (b). Mn concentration (in gm/gm): I—0; II—10^{-4}; III—3×10^{-4}; IV—1.5×10^{-3}; V—4.5×10^{-3}; V′—10^{-2}.

(in %); and the degree of quenching ($100 \times I_q/I_0$) is found from the relationship

$$\frac{I_q}{I_0} = 1 - \frac{I_b}{I_0} - \frac{I_{or}}{I_0}.$$

The change in the absorptivity of the ZnS phosphor with increasing temperature was taken into consideration when calculating these same values for the case of excitation by 366 mμ radiation. The value of the correction coefficient varied from 1 (at −196°) to 1.8 (at 100°). We note that these coefficients are not very accurate.

It follows from Fig. 6 that the transformation of excitation energy into orange luminescence involves large losses. Quantitative data corresponding to two temperatures (−100° and +100°) are shown in the Table. They show that the decrease in blue luminescence is only slightly compensated by a growth in the orange luminescence.

The Spectral Composition of ZnS-Mn Phosphor Luminescence (Yield in %) Under Strong Excitation by Focused Light From a PRK-2 Lamp With Filter

λ_{exc} (mμ)	t°	C_{Mn} (gm/gm)											
		0			$3 \cdot 10^{-4}$			$1.5 \cdot 10^{-3}$			10^{-2}		
		b	or.	q	b	or.	q	b	or.	q	b	or.	q
312	−100	99	0	1	50	3	47	21	12	67	0	15	85
	+100	4	0	96	5	3	92	0	14	86	0	18	82
366	−100	100	0	0	52	5	43	33	17	50	0	25	75
	+100	13	0	87	1	4	95	0	20	80	0	38	62

Note: b—blue luminescence; or.—orange luminescence; q—quenching.

IV. ELECTRON TRAPPING LEVELS AND HOLES IN ZnS-Mn PHOSPHORS AND SOME CONSIDERATIONS CONCERNING THE LUMINESCENCE KINETICS

The distribution scheme of electron trapping levels and holes plays an important role in establishing the kinetics of luminescence.

For the phosphors which we studied by the thermoluminescence method, luminosity maxima were found* at approximately 115°, 180° and 245°K. The bands of the first two levels are observed in ZnS without Mn and belong to sulfur (115°K) and oxygen (180°K) vacancies, but the latter level (245°K) is produced by the intrusion of some of the manganese particles located near oxygen ions. The depth of the levels is calculated from the relationship $E = kT^2_{max}/\delta$, where δ is the half-width of the lower branch of the thermoluminescence peak,[9] and is equal to 0.04, 0.18, and 0.32 ev respectively. We note that the latter relationship is correct in our case, since the probability of re-trapping is less than the probability of recombination. The location of these levels is independent of Mn concentration up to $C_{Mn} = 4.5 \times 10^{-3}$ gm/gm. A further increase in concentration to 3×10^{-2} gm/gm displaces the I and III levels to the conduction band (in addition to this, level II fades out). Besides the three indicated systems of levels there is apparently a fourth (still deeper) now showing up in the thermoluminescence curves.

*The position of the first maximum may be too high owing to an insufficiently low temperature for the beginning of de-excitation (77°K).

The width of the forbidden zone changes only slightly with increasing concentration (Fig. 2) and is thought to be equal to 3.98 ev (λ of the primary absorption edge is 310 mμ[5]). However, the strong growth of impurity centers, whose levels lie considerably higher than the valence band, must be taken into consideration. It follows from an examination of the displacement of the absorption edge that when the temperature changes from −165° to 100°C, the band-width is changed by approximately 0.13 ev. As a consequence of this, these same shallow localization levels can merge with the conduction band at temperatures above room temperature.

We now turn to a consideration of the location (ΔE_H) of the hole trapping levels relative to the top of the valence band. Two systems of hole levels are clearly discernible—the blue luminescence center levels and the manganese levels. The value of ΔE_H can be estimated by two methods—by using absorption frequency values and by using the formula

$$\frac{I}{I_0} = \frac{1}{1 + ae^{-\frac{\Delta E}{kT}}}. \qquad (1)$$

A formula of this type was first used by Yastrebov[10] to describe external quenching of phosphors. In our case, the exponential term in the denominator takes account of the migration of holes from centers to the valence band, which leads to quenching. Taking the logarithms (1), we find a value of $\Delta E_b = 0.49$ ev for the blue luminescence and $\Delta E_{or.} = 0.78$ ev for the orange. Absorption at defects caused by blue luminescence centers and manganese centers extends gradually, weakening to 450 mμ[1,2,4,6]; that is, the limiting positions of the levels of these defects in the forbidden zone are higher than the valence band for blue luminescence centers and for manganese centers—by approximately 1.5 ev. Calculating the position of the blue centers from the location of the sharp absorption edge gives a value of 0.4 ev, which agrees with the value of 0.49 ev obtained by formula (1).

The level scheme for a ZnS-Mn (10^{-3}) phosphor at 20°C is shown in Fig. 7. When the concentration or temperature is changed, some shifting of levels takes place, within the above-mentioned limits. Making use of the above-mentioned scheme, one can attempt to give an approximate model of the development of luminescence in ZnS-Mn phosphors. We are assuming that the model must take the following main features of the luminescence into account: (a) the stable existence of blue and orange luminescence in temperature ranges in which the corresponding electron localization levels are completely emptied during thermoluminescence, and also the difference (at a given temperature) between the spectral composition of the luminescence during excitation and in thermoluminescence; (b) the existence of a tendency for electrons released from specific local levels to recombine only with particular luminescence centers; and (c) the existence of two temperature ranges of concentration quenching—a region where the blue luminescence quenching is independent of temperature and depends only on the manganese concentration, and a region where concentration quenching of the blue luminescence increases sharply with increasing temperature.

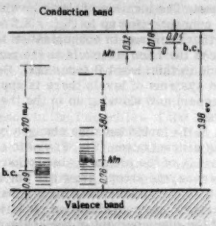

Fig. 7. The distribution scheme of electron and hole trapping levels in ZnS-Mn phosphors. Symbols: b.c.—blue luminescence centers.

The above-mentioned special features of the luminescence process can be interpreted in the following way: It follows from (a) that different systems of trapping levels, corresponding to a wide range of temperatures, participate in the luminescence which occurs during excitation. During excitation by 312 mμ radiation, electrons go from the valence band up to the conduction band. Their immediate recombination with holes in the valence band leads to quenching; however, the majority of the electrons have time to localize prior to recombining, and the holes succeed in going up to the levels of the blue and the manganese luminescence centers. When the electrons are subsequently released, their recombination with holes gives rise to the blue luminescence and the manganese luminescence.

It follows from (b) that the electrons which are released from different levels and migrate to the conduction band cannot be considered as absolutely free, inasmuch as electrons from the first system of levels (–120°) give the blue luminescence primarily, electrons from the system (–80°) formed by oxygen give a large percentage of the orange luminescence (because the manganese is localized next to the oxygen) and finally, electrons from the third system of levels (–30°), formed by manganese, give orange luminescence only.* Apparently it can be assumed that the electrons are localized in the immediate vicinity of hole localization centers, and most probably near centers already filled by holes. For this reason, when the electrons are freed thermally, they either recombine immediately with corresponding holes (electrons of the third system) or, on escape to the conduction band, have a considerably higher probability of recombination with neighboring holes (electrons of the first and second systems).

*The levels of the second and third systems merge at high Mn concentrations, which indicates the full utilization of oxygen levels to settle Mn and that new Mn molecules settle near the same defects.

When the temperature is raised, a migration of holes begins from the blue luminescence centers across the valence band to levels of the manganese centers. A calculation, performed on the assumption that the temperature of maximum ejection of holes into the valence band is connected with the depth of hole trapping levels by the relationship $\Delta E = 25$ kT, showed that for a temperature of about 100° practically all the holes must go over to the manganese centers. Henceforth, only manganese luminescence will be observed. The increased transfer of holes from blue luminescence levels to manganese centers begins at 40°. The second region of temperature-concentration quenching (section III, Fig. 5) also begins at this temperature. At the time when the holes are migrating across the valence band, there are numerous opportunities for them to recombine with electrons, which leads to quenching and reduces the orange luminescence yield. Since the depths of the electron trapping levels relative to the conduction band are close to the depths of the holes of the blue luminescence centers relative to the valence, the mechanism of hole migration under consideration can partially explain the changes in the composition that occur when electrons are freed from various trapping levels (see ref. 11, for example). However, the complete departure of holes from the blue centers at –30° is hardly possible.

Excitation by 366 mμ radiation gives a picture of the luminescence that is quite similar to excitation by 312 mμ light. For this reason it is quite probable that the luminescence kinetics under this excitation are for the most part the same as the former. The distinction lies only in the fact that electrons enter the conduction band from levels of the blue and manganese luminescence centers which absorb in the 366 mμ region, and not from the lattice.

It can be assumed, however, that part of the excitation energy transfers from the blue luminescence centers to manganese centers by resonance. The possibility of such a process cannot be excluded, because there is overlapping of the blue luminescence emission spectra and the manganese absorption spectra. The temperature independence of concentration quenching of the blue luminescence at low temperatures and the absence of nonlinearity in the luminescence intensity curve when the excitation intensity is increased are in agreement with the resonance model of energy transfer from blue luminescence centers to manganese luminescence centers. This explains the fact that quenching takes place in the first stage of the energy transfer process, before localization of the electrons in trapping levels, and that it subsequently proceeds without losses. At still higher temperatures, an even larger number of holes migrate from the manganese centers to the valence band, which leads to an increase in the thermal quenching of the manganese.

In conclusion, the authors express their gratitude to O. M. Agafonova for her help in conducting the study and to A. V. Lavrov for preparing the luminors.

REFERENCES

1. V. L. Levshin and V. F. Tunitskaya, Opt. i Spektr. 8, 663 (1960) Optics and Spectroscopy 8, 350 (1960).
2. V. L. Levshin, N. S. Borodin, and G. P. Neronova, Opt. i Spektr. 3, 258 (1957).
3. V. L. Levshin, Zhur. Eksptl. i Teoret. Fiz. 17, 675 (1947).
4. V. L. Levshin and B. D. Ryzhikov, Opt. i Spektr. 4, 358 (1958).
5. M. N. Alentsev and E. I. Panasyuk, Opt. i Spektr. 5, 207 (1958).
6. L. A. Vinokurov, V. L. Levshin, and E. G. Baronova, Zhur. Eksptl. i Teoret. Fiz. 21, 236 (1954).
7. M. N. Alentsev, Opt. i Spektr. 1, 240 (1956).
8. V. L. Levshin and V. N. Rebane, Opt. i Spektr. 7, 236 (1959), Optics and Spectroscopy 7, 149 (1959); M. D. Galanin and A. V. Raevskii, Izvest. Akad. Nauk SSSR Ser. Fiz. 23, 1280 (1959).
9. Ch. B. Lushchik, Doklady Akad. Nauk SSSR. 101, 641 (1955).
10. V. A. Yastrebov, Zhur. Eksptl. i Teoret. Fiz. 21, 164 (1951).
11. L. A. Vinokurov and M. V. Fok, Opt. i Spektr. 4, 118 (1958).

ON THE SCATTERING OF LIGHT BY DIELECTRIC ELLIPSOIDS COMPARABLE WITH THE WAVELENGTH

II. Dependence of the Indicatrix of the Scattering on the Size, Form, and Orientation of the Ellipsoid. The Scattering Coefficient

A. V. Shatilov

Received 16 October 1959

From an expression obtained earlier[1]

$$I = I_0 \frac{k^4}{r_1^2} \cdot \frac{P_{0\perp}^2}{E_0^2} \nu^2 f^2(q), \tag{1}$$

where

$$f(q) = \frac{3}{q^3}(\sin q - q\cos q);$$

$$q = 2\rho \sin\frac{\beta}{2}\sqrt{1+\cos^2\alpha_1};$$

$$I_0 = \frac{c}{8\pi}\sqrt{\varepsilon_1}\, E_0^2 \frac{1}{r^2}; \qquad \text{A}$$

$$\alpha = \frac{\varepsilon^2}{1-\varepsilon^2}, \quad \rho = 2\pi\frac{b}{\lambda},$$

the scattering indicatrix is determined by the parameters $P_{0\perp}$ and q, whose dependence on the dimensions, form, dielectric properties, and orientation of the scattering ellipsoid must be found (here ν is the volume of the ellipsoid, ϵ is its eccentricity, b is the semiaxis which is not the axis of symmetry, β is the scattering angle, α_1 is the cosine of the angle between the normal to the scattering layers and the symmetry axis of the ellipsoid, k is the wave vector, and r the distance to the particle). We recall that $P_{0\perp}$ is determined by the polarization of the ellipsoid and q by the number of waves contained within the dimensions of the particle in a direction normal to the "reflecting" layers.[1]

THE POLARIZATION OF AN ARBITRARILY ORIENTED ANISOTROPIC ELLIPSOID

The magnitude and direction of the vector $\mathbf{P}_{0\perp} = [\mathbf{R}_0[\mathbf{R}_0\mathbf{P}]]$ are determined by the orientation, eccentricity, and dielectric constants of the ellipsoid and medium, and also by the direction of the vector $\mathbf{R}_0$.

Indeed, if α_0, β_0, and γ_0 are the direction cosines of the vector $\mathbf{R}_0$ in the system of coordinates connected with the ellipsoid of rotation

$$\frac{\zeta^2}{a^2} + \frac{\eta^2}{b^2} + \frac{\delta^2}{b^2} = 1. \qquad \text{B}$$

then

$$P_{0\perp}^2 = P^2 - (\mathbf{PR})^2 = \left[P_\zeta^2(1-\alpha_0^2) + P_\eta^2(1-\beta_0^2) + P_\delta^2(1-\gamma_0^2)\right] - 2P_\zeta P_\eta \alpha_0\beta_0 - 2P_\eta P_\delta \beta_0\gamma_0 - 2P_\delta P_\zeta \gamma_0\alpha_0. \tag{2}$$

The direction of the δ axis in the case of an ellipsoid of rotation can always be taken perpendicular to the vector $\mathbf{E}_0$ (then the polarization P_δ equals zero, and expression (2) is simplified). Both components of the polarization which are different from zero, P_ζ and P_η, in the general case of an anisotropic ellipsoid of rotation are expressed in terms of the components of the internal field

$$P_\zeta = \frac{\varepsilon_\zeta - \varepsilon_1}{4\pi} E_\zeta; \quad P_\eta = \frac{\varepsilon_\eta - \varepsilon_1}{4\pi} E_\eta, \tag{3}$$

where

$$E_\zeta = \frac{E_{0\zeta}}{1 + A_\zeta \frac{\varepsilon_\zeta - \varepsilon_1}{\varepsilon_1}}; \quad E_\eta = \frac{E_{0\eta}}{1 + A_\eta \frac{\varepsilon_\eta - \varepsilon_1}{\varepsilon_1}}; \tag{4}$$

so that

$$P_\zeta = \alpha_\zeta E_{0\zeta}; \quad P_\eta = \alpha_\eta E_{0\eta}. \tag{5}$$

Here the quantities

$$\alpha_\zeta = \frac{\varepsilon_\zeta - \varepsilon_1}{4\pi} \frac{1}{1 + A_\zeta \frac{\varepsilon_\zeta - \varepsilon_1}{\varepsilon_1}}; \quad \alpha_\eta = \frac{\varepsilon_\eta - \varepsilon_1}{4\pi} \frac{1}{1 + A_\eta \frac{\varepsilon_\eta - \varepsilon_1}{\varepsilon_1}} \qquad \text{C}$$

represent the effective values of the polarizability of the ellipsoid in the direction of the axes, depending on the form factors A_ζ and A_η,[2] and on the components, $E_{0\zeta}$ and $E_{0\eta}$, of the vector $\mathbf{E}_0$. Finally,

$$P_{0\perp}^2 = E_0^2\left[\alpha_\zeta^2 l_\zeta^2(1-\alpha_0^2) + \alpha_\eta^2 l_\eta^2\left(1-\beta_0^2\right) - 2\alpha_\zeta\alpha_\eta l_\zeta l_\eta \alpha_0\beta_0\right], \tag{6}$$

where l_ζ and l_η are the direction cosines of the vector E_0 in the system, connected with the ellipsoid.

THE PARAMETERS P AND q IN THE SYSTEM CONNECTED WITH THE EXTERNAL FIELD

If now we go to the system connected with the vectors E and K (fig. 1), in which the direction of the symmetry axis of the ellipsoid is determined by the angles Δ and φ, and the direction of the vector R by the angles β and φ', then for the direction cosines of the vectors

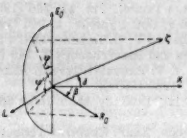

Fig. 1. The position of the symmetry axis of the ellipsoid ζ and the scattering vector **R** in the coordinate system connected with the vectors **E** and **K**.

R and **E** in the former system we obtain

$$\left.\begin{aligned} a_0 &= \sin\beta\sin\Delta\cos(\varphi-\varphi')+\cos\beta\cos\Delta,\\ \beta_0 &= \frac{1}{l_\eta}(\sin\beta\cos\varphi'-\sin\Delta\cos\varphi\, a_0),\\ l_\zeta &= \sin\Delta\cos\varphi,\\ l_\eta &= \sqrt{1-\epsilon_\zeta^2}. \end{aligned}\right\} \quad \text{D}$$

Thus, for known values of the effective polarizabilities α_ζ and α_η the component of the polarizability $\mathbf{P}_{0\perp}$ is determined, from (6), by the orientation of the symmetry axis of the ellipsoid relative to the vector **E** and by the direction of the scattering vector R relative to the axes ζ and η.

If we express α_1, defining the magnitude of the angle between the normal to the layers and the symmetry axis of the ellipsoid in this system we obtain

$$\alpha_1 = \cos\Delta\sin\frac{\beta}{2}-\sin\Delta\cos\frac{\beta}{2}\cos(\varphi'-\varphi). \qquad (7)$$

We will examine several particular cases.

1. The symmetry axis lies in a plane which includes the vectors **E** and **K**, i.e., $\varphi = \pi/2$, $l_\zeta = \sin\Delta$, $l_\eta = \cos\Delta$, and correspondingly

$$\left.\begin{aligned} a_0 &= \cos\Delta\cos\beta+\sin\Delta\sin\beta\cos\varphi',\\ \beta_0 &= \frac{1}{\epsilon_\eta}(\sin\beta\cos\varphi'-\sin\Delta\, a_0). \end{aligned}\right\} \quad \text{E}$$

In particular, if the symmetry axis is parallel to the vector **E**($\epsilon_\zeta = 1$), then expression (6) simplifies to

$$P_{0\perp}^2 = E_0^2\alpha_\zeta^2(1-\sin^2\beta\cos^2\varphi'). \qquad \text{F}$$

2. The symmetry axis lies in a plane perpendicular to the vector **E**, i.e., $l_\eta = 1$, and $\beta_0 = \sin\beta\cos\varphi'$. Then

$$P_{0\perp}^2 = E_0^2\alpha_\eta^2(1-\sin^2\beta\cos^2\varphi'). \qquad \text{G}$$

For the basic positions of the ellipsoid, we obtain

$$P_{0\perp}^2 = E_0^2\alpha_1^2(1-\sin^2\beta\cos^2\varphi'), \qquad (8)$$

where $\alpha_1 = \alpha_\zeta$, if (a) the axis ζ is parallel to **E**, (b) the axis ζ is perpendicular to **E** and **K**, and $\alpha_1 = \alpha_\eta$, if (c) the axis ζ is perpendicular to **K**.

The values of the parameter α_1 and of the q corresponding to it in these cases equal, from (7) and (1),

$$\left.\begin{aligned} &\text{a)}\quad \alpha_1 = -\cos\frac{\beta}{2}\cos\varphi';\quad q = 2\rho\sin\frac{\beta}{2}\sqrt{1+\sigma\cos^2\frac{\beta}{2}\cos^2\varphi'}\,.\\ &\text{b)}\quad \alpha_1 = \cos\frac{\beta}{2}\sin\varphi';\quad q = 2\rho\sin\frac{\beta}{2}\sqrt{1+\sigma\cos^2\frac{\beta}{2}\sin^2\varphi'}\,.\\ &\text{c)}\quad \alpha_1 = \sin\frac{\beta}{2};\quad q = 2\rho\sin\frac{\beta}{2}\sqrt{1+\sigma\sin^2\frac{\beta}{2}}\,. \end{aligned}\right\} \qquad (9)$$

Thus, in the calculation of the scattering indicatrix in the general case it is necessary to substitute for the parameters q and $\mathbf{P}_{0\perp}$ in expression (1).

Here q, in accordance with (1), depends on a series of quantities: $\alpha_1 = \cos\alpha$ is a parameter determined by the orientation of the symmetry axis of the ellipsoid relative to the normal to the conventional planes of reflection of the scattered wave and depending on the angles Δ, φ, β, and φ', and $\rho = 2\pi b/\lambda$ is a characteristic parameter calculated for the semiaxis b (ϵ is the eccentricity of the ellipsoid).

The other parameter $\mathbf{P}_{0\perp}$ depends, as seen from (6), on the magnitudes of the direction cosines l_ζ and l_η, which are determined by the orientation of the ellipsoid relative to the field vector $\mathbf{E}_0$, and on the quantities a_0 and β_0 which are determined by the orientation of the ellipsoid relative to the scattering vector and which depend on the angles Δ, φ, β, and φ'. In addition, $\mathbf{P}_{0\perp}$ depends on the values of the effective polarizabilities, α_ζ and α_η, determined by the magnitudes of the dielectric constant of the medium and the ellipsoid, and also by its eccentricity.

If, however, we use a cruder approximation for the internal field of the particle, i.e., we put the internal polarization field equal to the external (cf. ref. 1), then since from (5) α_ζ and α_η depend only on the dielectric properties of the ellipsoid and the medium (in the case of an isotropic ellipsoid they will be equal), the direction of the polarization vector coincides with the direction of the field vector, i.e., we obtain

$$P_{0\perp} = P_0\sin(\mathbf{E},\mathbf{R}) = P_0\cos\beta\cos\varphi'. \qquad (10)$$

THE SCATTERING COEFFICIENT

Starting from the expression for the scattering indicatrix (1), it is possible to define the scattering coefficient

$$K(\rho,\epsilon,\Delta,\varphi) = \int I(\omega)\,d\omega = I_0\frac{\omega^4}{c^4}v^2K_0, \qquad \text{H}$$

where

$$K_0 = \int\frac{P_{0\perp}^2}{E_0^2}f^2(q)\,d\varphi'\sin\beta d\beta. \qquad \text{J}$$

Also, taking account of the fact that the function $f^2(q)$ can be represented in series form

$$f^2(q) = 3^2\cdot 2^2\cdot\sum_{n=0}^{\infty}A_{n+2}(2q)^{2n}, \qquad \text{K}$$

where

$$A_n = \frac{(-)^n}{(2n)!}\cdot\frac{n-1}{n+1}, \qquad \text{L}$$

we obtain for the case most simply calculated, in which the symmetry axis of the ellipsoid is directed along the wave vector,

$$K_0 = C_0\sum_{n=0}^{\infty}A_{n+2}\sum_{j=0}^{n}D_n^j\tau_n^j. \qquad (11)$$

Here

$$D_n^j = C_n^j\left(\frac{1}{j+n+1}-\frac{2}{j+n+2}+\frac{2}{j+n+3}\right) \qquad \text{M}$$

and

$$C_0 = 3^2\cdot 2^4\cdot\pi\alpha_1^2, \qquad \text{N}$$

and $\tau_n = (4\rho)^{2n}\sigma$ is a quantity characterizing the size and form of the ellipsoid ($\sigma = \epsilon^2/1-\epsilon^2$).

The convergence of the series is guaranteed by the rapid decrease of the coefficient A_n. A more general expression for the scattering coefficient will be introduced in the following section.

The region of applicability for the approximation of the indicatrix and coefficient of scattering obtained in this

work should coincide approximately with the region of applicability of the Rayleigh-Gans approximation for a sphere with radius $r = \sqrt[3]{ab^2}$. In the case of a strongly elongated (compressed) ellipsoid, it is determined by the dimensions of the particle in the direction normal to the layers ($r_0 = x_0$) reflecting in the specified direction.

We recall that according to the evaluation of Shifrin,[9] who compared his data with results which follow from the exact formulae of Mie, the Rayleigh-Gans approximation permits one to determine the scattering indicatrix for water drops in air ($\rho = 0.8$, $m = 4/3$) with an error not greater than 12%. For the scattering coefficient the region of applicability is broad, even for $\rho = 5$ the error does not exceed 20%.

THE SCATTERING INDICATRIX FOR THE CASES OF ELONGATED AND COMPRESSED ELLIPSOIDS

For specified dielectric properties the scattering indicatrix of a particle is determined by the dimensions of the particle (compared with the wavelength), its form (eccentricity), and orientation in the external field. Since the number of parameters is necessarily large, we will restrict ourselves to an examination only of certain cases, which allow us to clarify the fundamental laws of scattering. In each of these cases, in order not to complicate the picture, we will consider the ellipsoid to be isotropic, the magnitude of its polarization being determined by formula (10).

We will examine the scattering indicatrix in the planes parallel to the light vector and to the wave vector ($\varphi' = 0$) and perpendicular to the light vector ($\varphi' = \pi/2$), for three basic orientations of elongated ($\epsilon_- = 0.8889$) and compressed ($\epsilon_+ = -80$) ellipsoids, having the volumes $v_1 = {}^4/_3\pi \times 0.1111$, $v_2 = {}^4/_3\pi \times 0.8889$, and $v_3 = {}^4/_3\pi \times 3$.

In these cases the corresponding magnitudes of the semimajor and semiminor axes are:
For the elongated ellipsoids

$$a_1 = 1 \quad a_2 = 2 \quad a_3 = 3$$
$$b_1 = 0.333 \quad b_2 = 0.666 \quad b_3 = 0.999. \qquad \text{O}$$

For the compressed ellipsoids

$$a_1 = 0.111 \quad a_2 = 0.222 \quad a_3 = 0.333$$
$$b_1 = 1 \quad b_2 = 2 \quad b_3 = 3. \qquad \text{P}$$

For convenience of comparison the volumes of the elongated and compressed ellipsoids are chosen the same, and the indicatrices corresponding to the different particles are given on a single scale, since, from (1), the absolute magnitude of the scattering intensity in an arbitrary direction is proportional to v^2 or r^6 and, accordingly,

$$I_1 : I_2 : I_3 = 1 : 64 : 729. \qquad \text{Q}$$

Taking account of (9) we obtain for the three specified orientations

a) $$q^2 = 4\rho^2 \sin^2 \frac{\beta}{2}\left(1 + \alpha \cos^2 \frac{\beta}{2}\right) \quad \text{for } \varphi' = 0, \qquad \text{R}$$

$$q^2 = 4\rho^2 \sin^2 \frac{\beta}{2} \quad \text{for } \varphi' = \frac{\pi}{2}; \qquad \text{S}$$

b) $$q^2 = 4\rho^2 \sin^2 \frac{\beta}{2} \quad \text{for } \varphi' = 0, \qquad \text{T}$$

$$q^2 = 4\rho^2 \sin^2 \frac{\beta}{2}\left(1 + \alpha \cos^2 \frac{\beta}{2}\right) \quad \text{for } \varphi' = \frac{\pi}{2}; \qquad \text{U}$$

c) $$q^2 = 4\rho^2 \sin^2 \frac{\beta}{2}\left(1 + \alpha \sin^2 \frac{\beta}{2}\right) \quad \text{for any } \varphi'. \qquad \text{V}$$

From this we can conclude that the coefficient

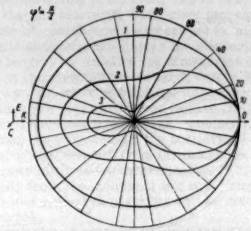

Fig. 2. The indicatrices of elongated ellipsoids (b/a = 1/3) with the symmetry axis ζ perpendicular to the plane of the vectors **E** and **K**. The semimajor axis a: curve 1—1; curve 2—2; curve 3—3 (here, as in all of the remaining cases, the unit of measurement is taken as $2\pi/\lambda$).

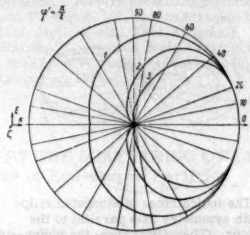

Fig. 3. The indicatrices of compressed ellipsoids (b/a = 9/1), with the symmetry axis ζ perpendicular to the plane of the vectors **E** and **K**. The semimajor axis b: curve 1—1; curve 2—2; curve 3—3.

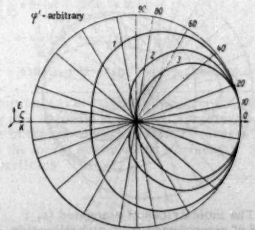

Fig. 4. The indicatrices of elongated ellipsoids (b/a = 1/3), whose symmetry axes are directed along the wave vector. The semimajor axis a: curve 1—1; curve 2—2; curve 3—3.

$I \sim f(q^2)v$, which determines the result of the interference of the waves scattered from the separate elements of the particle, is the same for case (a) for $\varphi' = 0$ and case (b) for $\varphi' = \pi/2$, and also for case (a) for $\varphi' = \pi/2$ and case (b) for $\varphi' = 0$.

Therefore, we can restrict ourselves to the exami-

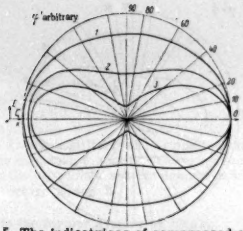

Fig. 5. The indicatrices of compressed ellipsoids (b/a = 9/1), whose symmetry axis are directed along the wave vector. The semimajor axis b: curve 1—1; curve 2—2; curve 3—3.

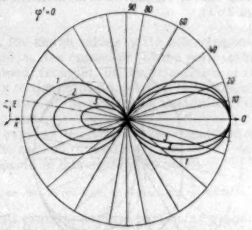

Fig. 6. The indicatrices of elongated ellipsoids with symmetry axis parallel to the light vector. (They differ from the indicatrices depicted in Fig. 2 only by the factor $\cos^2\beta$.)

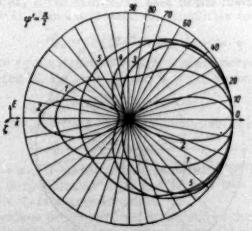

Fig. 7. The indicatrices of elongated (ϵ_{1-}; ϵ_{2-}) and of compressed (ϵ_{1+}; ϵ_{2+}) ellipsoids of equal volume with symmetry axis located perpendicular to the vectors **E** and **K**. Curve 1—ϵ^2_{1-} = 0.8889, b/a = 1/3; curve 2—ϵ^2_{2-} = 0.99, b/a = 1/10; curve 3—ϵ^2_{1+} = −80, b/a = 9/1; curve 4—ϵ^2_{2+} = −15, b/a = 4/1; curve 5—the indicatrix of a sphere of the same volume.

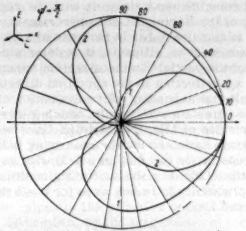

Fig. 8. The indicatrices of elongated (curve 1) and compressed (curve 2) ellipsoids, whose symmetry axes are perpendicular to the vector **E** and form an angle Δ = 45° with the wave vector **K**. Curve 1—ϵ^2 = 0.8889; curve 2—ϵ^2 = −80.

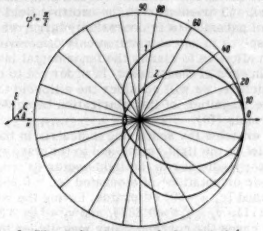

Fig. 9. The indicatrices of elongated (curve 1) and compressed (curve 2) ellipsoids whose symmetry axes lie in a plane parallel to the vectors **E** and **K** and form an angle with them of Δ = 45°. Curve 1—b/a = 1/3; curve 2—b/a = 9/1.

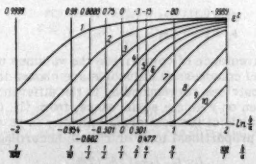

Fig. 10. Dependence of the ratio $I_{backward}/I_{forward}$ on the eccentricity (ratio of the semiaxes for ellipsoids having different sizes. Volume (radius) of the ellipsoid: curve 1—0.0625 (0.25); curve 2—0.125 (0.5); curve 3—0.422 (0.75); curve 4—1 (1); curve 5—1.953 (1.25); curve 6—3.375 (1.5); curve 7—8 (2); curve 8—27 (3); curve 9—64 (4); curve 10— 125 (5). (The dimensions of the particles are expressed in the same units in which the characteristic parameter ρ is measured.)

nation of only three types of indicatrix: case (a) for $\varphi' = \pi/2$, case (b) for $\varphi' = \pi/2$, and case (c) for any φ'.

For identical values of $f^2(q)$ the indicatrices for the planes $\varphi' = 0$ and $\varphi' = \pi/2$ will differ, as seen from (10), only by the factor $\cos^2\beta$.

The scattering indicatrices have their most characteristic form in the plane $\varphi' = \pi/2$ for the cases $\zeta \perp \mathbf{E}$, $\zeta \perp \mathbf{K}$, and $\zeta \parallel \mathbf{E}$. The indicatrices have the form of a leaf if the semimajor axis of the ellipsoid is directed along the wave vector (cf. Figs. 3 and 4), and a pear-shaped form if the semimajor axis of the ellipsoid is perpendicular to the wave vector (cf. Figs. 2 and 5). If the symmetry axis coincides with the direction of the light vector, then the indicatrix in the plane $\varphi' = \pi/2$ coincides with the indicatrix of a sphere which has a radius r = b. . .

The influence of the form (the eccentricity) on the indicatrix is shown in Fig. 7, where, for comparison, the indicatrix of a spherical particle of the same volume is given, and also in Fig. 10, where the dependence of the ratio of the scattering intensities, forward and backward, on the eccentricity for ellipsoids of different volumes is given.

In Figs. 8 and 9 are also presented indicatrices of obliquely oriented ellipsoids—their symmetry axes form an angle $\Delta = 45°$ with the direction of the wave vector **K**. They prove to be approximately symmetrical relative to the direction of the semimajor axis of the ellipsoid.

Already from the simple comparison of the indicatrices, corresponding to different values of ρ, we can conclude that the scattering coefficient increases more slowly than ρ^6, which would correspond to dipole scattering. This is understandable since the scattering coefficient is larger, the smaller the dimensions of the particles in the direction of the wave vector **K** (cf. Figs. 4 and 5), i.e., the more effectively, for a given volume, the particles are polarized in the field of the light wave. Note that for the case in which the symmetry axis is directed along the wave vector, the scattering coefficient can be calculated directly from the indicatrix.

The possibility of the determination of the size and eccentricity from the indicatrix and scattering coefficient of an oriented system of particles will be discussed in another article.

In conclusion, I express my deep thanks to N. A. Tolstoi for his attention and interest in the work.

REFERENCES

1. A. V. Shatilov, Opt. i. Spektr. 9, 86 (1960), Optics and Spectroscopy 9, 44 (1960).
2. J. A. Stratton, "Teoriya Elektromagnetisma" (Electromagnetic Theory) p. 193, Izd. Inostrannoi Lit., Moscow, 1948, McGraw-Hill, 1941 (Original).
3. K. S. Shifrin, "Rasseyanie Sveta v Mutnoi Srede" (Light Scattering in Turbid Media) pp. 140, 148, Moscow, Leningrad, 1951.

DETERMINATION OF THE SIZE OF PARTICLES BY THE SCATTERING OF LIGHT
Nomograms for the Determination of the Size of Rod-shaped Particles

I. Ya. Slonim

Received 30 November 1959

Nomograms for the calculation of the size of particles from the scattering of light applicable to particles of spherical (or nearly spherical) shape were given in previous communications.[1] In a number of cases (for example, viruses,[2] micelles of surface-active substances,[3] etc.) the particles are in the form of rods whose cross-sectional diameters are considerably smaller than, and whose lengths are of the same order as, the wavelength of light.

It is well known[4] that the indicatrix of scattering of randomly oriented rod-shaped particles differs from the indicatrix for small spherical particles by the factor $P(\theta)$ which is a function of the angular distribution

$$P(\theta) = \frac{1}{u}\int_0^{2u} \frac{\sin w}{w}\,dw - \left(\frac{\sin u}{u}\right)^2, \qquad (1)$$

where $u = (2\pi L/\lambda)\sin(\theta/2)$, L is the length of the particle, θ is the angle between the incident and the scattered rays, and λ is the wavelength of the light in the medium.

The indicatrix of scattering of rod-shaped particles is asymmetrical; it is elongated in the forward direction. The intensity of the light scattered at an angle of 45° is larger than that scattered at an angle of 135°. The asymmetry of the light scattering I_{45}/I_{135} is uniquely determined by the magnitude of the ratio L/λ.

The total light energy scattered from the original beam by the rod-shaped particles is 1/Q times smaller than that scattered by small spherical particles of the same volume. The magnitude of the coefficient of dissipation Q is given by the equation obtained from the integration of the angular distribution function[5]

$$Q = \frac{6}{x^2}\left\{\frac{11}{15}x\,\mathrm{Si}(x) + \mathrm{Ci}(x) - \ln(x) - \gamma + \frac{1}{15}\left(11 + \frac{8}{x^2} - \frac{36}{x^4}\right)\cos x - \frac{4}{15}\left(\frac{1}{x} + \frac{9}{x^3}\right)\sin x - \left(\frac{1}{2} - \frac{2}{3x^2} - \frac{12}{5x^4}\right)\right\}, \qquad (2)$$

where $x = 4\pi L/\lambda$ and γ is Euler's constant and is equal to 0.5772 . . . .

According to the Rayleigh equation the change in the turbidity of a suspension of small spherical particles for a change in the wavelength of light is inversely proportional to the fourth power of the wavelength. For rod-shaped particles

$$-\frac{d\lg\tau}{d\lg\lambda} = 4 - \beta, \qquad (3)$$

where τ is the turbidity of the suspension and β is the dissipation index. The magnitude of β is uniquely determined by the magnitude of the ratio L/λ.

The values of $1/P(90)$, $1/Q$, I_{45}/I_{135}, and β were calculated and tabulated for values of L/λ between 0.2 and 0.8 in ref. 6.

The calculation of the dimensions of the rod-shaped particles can be carried out in the following manner. From the values of the characteristic turbidity of the suspension or the characteristic intensity of scattering of light at an angle of 90°, the volume V_{eq} of the equivalent spherical particles can be calculated using the

Rayleigh equation. It is clear that the volume of the rod-shaped particles is larger than the volume of the equivalent particles by 1/Q or 1/P (90), respectively. For the determination of 1/Q the magnitude of τ is measured for two or more values of the wavelength, and thereupon one finds the value of β from Eq. (3) and the corresponding values of 1/Q and L/λ from tables. After this the real volume of the particles is calculated from $V_{real} = V_{eq.}/Q$, the magnitude of L is determined from the values of L/λ and λ, and the thickness of the particles is calculated from the real volume and the length. The correction 1/P (90) and the quantity L/λ can of course be determined from the measured asymmetry of the light scattering I_{45}/I_{135}.

We constructed appropriate nomograms (Figs. 1 and 2) to facilitate the calculations. The following symbols were adopted for this purpose: τ represents the characteristic turbidity (the limit of the ratio of the turbidity of the system (in cm^{-1}) to the volume concentration (volumetric fraction) of the particles when the concentration tends to zero); I_{90} is the characteristic intensity of the light scattered at an angle of 90° (the limit of the ratio of the intensity of the light scattered at the angle of 90° to the volume concentration when the concentration tends to zero and the intensity of the incident light is equal to one); $a_{eq.}$ is the radius of the equivalent spherical particles; λ is the wavelength of the light in the medium; m is the relative refractive index of the particles (the ratio of the refractive index of the particles to the refractive index of the medium*); β is the dissipation index (according to Eq. (3)); I_{45}/I_{135} is the asymmetry of the light scattering; L is the length and d is the thickness of the particles.

*If the refractive index of the particles is not known, it can be calculated from the values of the refractive indices of the pure solvent and of a suspension, using the specifications of the mixture.

The nomograms make possible the determination of the dimensions of the particles by two methods: from measurements on the transmitted light (from τ and β) and from measurements on the scattered light (from I_{90} and I_{45}/I_{135}).

The course of the calculation is as follows: using Nomogram 1, $Q_{eq.}$ is found from the known values of τ (or I_{90}), m, and λ. The desired values of L and d are then obtained from the value found for $Q_{eq.}$ and the known values of β (or I_{45}/I_{135}) and λ employing Nomogram 2.

To solve the inverse problem, i.e., to calculate the turbidity from the known dimensions of the particles, one first of all determines $Q_{eq.}$ from Nomogram 2 and then τ (or I_{90}) from Nomogram 1. The use of the nomograms is clear from the diagrams and from the examples.

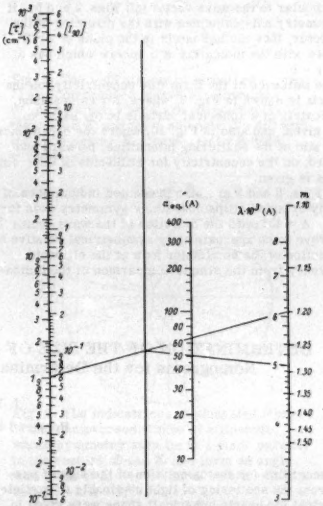

Fig. 1. Nomogram 1. Example: $I_{90} = 6.1 \times 10^{-2}$; $\lambda = 5 \times 10^3$A; m = 1.20; $a_{eq.} = 50$A.

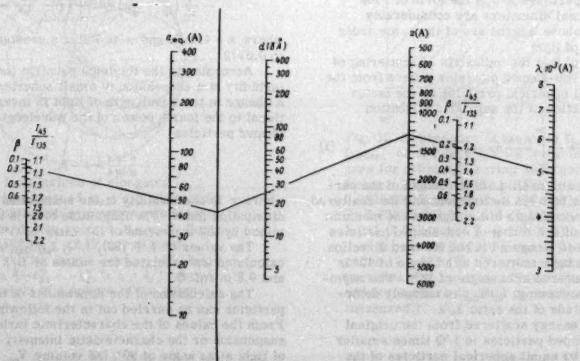

Fig. 2. Nomogram 2. Example: $a_{eq.} = 50$A; $I_{45}/I_{135} = 1.2$; $\lambda = 5 \times 10^3$A; z = 1250A; d = 25A.

REFERENCES

1. I. Ya. Slonim, Opt. i Spektr. **8**, 98, 243, 255 (1960), Optics and Spectroscopy **8**, 48, 124, 130 (1960).
2. G. Oster, P. Doty, and B. H. Zimm, J. Am. Chem. Soc. **69**, 1193 (1947).
3. P. Debye and E. W. Anacker, J. Phys. Coll. Chem. **55**, 644 (1951).
4. H. C. van de Hulst, "Light Scattering by Small Particles." Wiley, New York, 1957.
5. F Bueche, P. Debye, and W. M. Cashin, J. Chem. Phys. **19**, 803 (1951).
6. P. Doty and R. F. Steiner, J. Chem. Phys. **18**, 1211 (1950).
7. W. Heller, Phys. Rev. **68**, 5 (1945).

THEORY OF INCREASING THE TRANSPARENCY OF METALLIC COATINGS

P. G. Kard

Received 1 October 1959

With the help of simplified Vlasov formulas investigated in a preceding paper,[1] a theory is developed for the "clarifying" (increasing the transparency) of metallic coatings by the introduction between the coating and substrate of a properly matched many-layered dielectric film. The possibilities of the method are illustrated in an example.

INTRODUCTION

Semitransparent metallic coatings (usually monolayers) are widely used in optics. Among their defects is that of considerable absorption. Therefore the problem of improving the optical properties of such coatings arises. Depending on the specific objective, the change of optical properties of a metallic layer can proceed in different directions; however, in any case it is possible to formulate the problem as follows: the absorption coefficient A must be as small as possible, and the ratio R/D (of the reflection coefficient to the transmission coefficient) must initially have a given value. Thus the basic problem consists of clarifying a metallic coating; we understand "clarifying" to mean a decrease in the absorption coefficient whether it results in an increase in D or in R.

In this paper we will examine theoretically the problem of clarifying a metallic layer with the help of multilayer dielectric films. It is conceivable that in this way better results will be obtained than by the application of additional metallic layers (see reference 2).

The dielectric film can be deposited on the outside of the metallic layer or introduced between the substrate and the layer. In the first case, clarification is possible only accompanying an increase in the reflection coefficient. In the second case, the magnitude of the ratio R/D can take large or small values depending principally on the way in which the parameters of the dielectric film are chosen. Also, the magnitude of the ratio A/D is constant in the first case, while in the second case it can be significantly decreased. The second case consequently contains more possibilities, and so we will give it our principal attention.

In our theory we will use simplified Vlasov formulas, investigated in reference 1.

We will make use of the following designations:

$$a = \frac{r}{d}, \quad b = \frac{1}{d}, \tag{1}$$

where r and d are the amplitude reflection and transmission coefficients,

$$\alpha = knh, \quad \beta = kxh, \tag{2}$$

where K is the wave number in vacuum, n is the index of refraction or its real part, x is the imaginary part of the refractive index and h is the thickness of the layer. The subscripts used with the magnitudes a, b, n, x, h, α, and β will show to which coating, layer, or lumped subassembly of coatings they are related.

The incidence of the light will be assumed normal throughout.

DIELECTRIC PLATE OVER A METALLIC LAYER

We will designate the initial medium, metallic layer, and substrate, by indices 0, 1, 2, that of the dielectric coating adjacent to the metallic layer by index m, and its residual part by the index k. In this way the schematic of the coating will be (Okm 12). We will write the Vlasov formulas in the form

$$\left.\begin{aligned} a &= a_1 b_2 e^{i\alpha_m} + a_2 b_1^* e^{-i\alpha_m}, \\ b &= b_1 b_2 e^{i\alpha_m} + a_2 a_1^* e^{-i\alpha_m}, \end{aligned}\right\} \tag{3}$$

where a_1, b_1 are related to the layers (Okm) and a_2, b_2 to the layers (m 1 2). From these formulas we easily find

$$\frac{A}{D} = |b|^2 - |a^2| - 1 = \frac{A_2}{D_2} = Mn_2^{-1} + Nn_2 + P, \tag{4}$$

where

$$\left.\begin{aligned} M &= \frac{n_1 \sinh 2\beta_1 + \varkappa_1 \sin 2\alpha_1}{2}, \\ N &= \frac{n_1 \sinh 2\beta_1 - \varkappa_1 \sin 2\alpha_1}{2(n_1^2 + \varkappa_1^2)}, \\ P &= \frac{2(n_1^2 \sinh^2 \beta_1 - \varkappa_1^2 \sin^2 \alpha_1)}{n_1^2 + \varkappa_1^2}, \end{aligned}\right\} \tag{5}$$

are magnitudes depending only on the parameters of the metallic layer (and, of course, on the wavelength of the light). In the derivation of formula (4) it is necessary to use expressions for a_2 and b_2 computed in their turn from the Vlasov formulas.

From the second part of formula (4) it is seen that the magnitude of A_2/D_2 depends only on the properties of the metallic layer and substrate. This means that if the substrate and metallic layer are given, then the coating above the last dielectric film does not change the value of A/D. Consequently, the clarification is inevitably accompanied by a decrease in D and an increase in R. In fact we may obtain in this way a value of R very close to unity. We note that the indicated method is applied with

success for improving the quality of reflecting plates of a Fabry-Perot interferometer (see for example reference 3).

DIELECTRIC FILM UNDER A METALLIC LAYER

We will write the schematic of the coating as (01 mk 2), making use of the same designations used above. Insofar as the first coatings (01 m) are absorbing the Vlasov formulas must be taken in the following form (see reference 1):

$$\left.\begin{aligned} a &= a_1 b_2 e^{i\varphi_m} + a_2 \tilde{b}_1^* e^{-i\varphi_m}, \\ b &= b_1 b_2 e^{i\varphi_m} + a_2 \tilde{a}_1^* e^{-i\varphi_m}, \end{aligned}\right\} \tag{6}$$

where ~ means that the complex refractive index $n_1 - ix_1$ is to be replaced by the conjugate value $n_1 + ix_1$. We note that a_1, b_1 and a_2, b_2 are related in formulas (6) to the coatings (0 1 m) and (m k 2), and consequently do not coincide with the same designations in formulas (3). That, however, cannot lead to misunderstandings, since we will not make any more use of the old designations.

From formulas (6) arises

$$\frac{R}{D} = |a|^2 = \frac{1}{D_2}\left\{\frac{R_1}{D_1} + \frac{R_2}{D_1} + 2\sqrt{\frac{R_1 R_2}{D_1 D_1}}\cos(2\varphi_m + \mu_1 - \mu_2 + \tilde{\nu}_1 + \nu_2)\right\}, \tag{7}$$

where μ_1, μ_2, $\tilde{\nu}_1$, and ν_2 are the phases of the magnitudes a_1, a_2, $\tilde{b}_1$, and b_2. Further we find

$$\frac{A}{D} = |b|^2 - |a|^2 - 1 = \frac{1}{D_2} - \frac{A_1}{D_1} - \frac{R_2}{D_2}\frac{\tilde{A}_1}{\tilde{D}_1} + \frac{\sqrt{R_2}}{D_2}\left[(\tilde{a}_1 b_1 - a_1 \tilde{b}_1)\, e^{i(2\varphi_m - \nu_2 + \tilde{\nu}_1)} + (\tilde{a}_1 b_1 - a_1 \tilde{b}_1)^* e^{-i(2\varphi_m - \nu_2 + \tilde{\nu}_1)}\right]. \tag{8}$$

Here, in agreement with (4),

$$\frac{A_1}{D_1} = P + S. \tag{9}$$

where

$$S = M n_m^{-1} + N n_m. \tag{10}$$

$\tilde{A}_1/D_1$ differs from A_1/D_1 only by the sign of x_1 and β_1, i.e.,

$$\frac{\tilde{A}_1}{D_1} = P - S. \tag{11}$$

Further, we will designate

$$a_1 b_1 - a_1 \tilde{b}_1 = U e^{i\vartheta}. \tag{12}$$

A rather cumbersome calculation (with the use again of the Vlasov formulas for a_1 and b_1) leads to the following result:

$$U = \sqrt{S^2 - P(P+2)} \tag{13}$$

and

$$\cos\vartheta = \frac{M n_m^{-1} - N n_m}{U}, \quad \sin\vartheta > 0. \tag{14}$$

Substituting (9), (11), and (12) into (8), we find

$$\frac{A}{D} = P + S\frac{1+R_2}{1-R_2} + 2U\frac{\sqrt{R_2}}{1-R_2}\cos(2\varphi_m - \mu_2 + \nu_2 + \vartheta). \tag{15}$$

To obtain the best clarification, the magnitude of A/D must be as small as possible. With this objective we first of all choose the thickness of the intermediate layer such that

$$\cos(2\varphi_m - \mu_2 + \nu_2 + \vartheta) = -1.$$

Then

$$\frac{A}{D} = P + S\frac{1+R_2}{1-R_2} - 2U\frac{\sqrt{R_2}}{1-R_2}. \tag{17}$$

Further, we can require that A/D have a minimum relative to R_2. This minimum, equal to

$$\left(\frac{A}{D}\right)_{min} = P + \sqrt{P(P+2)}, \tag{18}$$

occurs for

$$R_2 = \frac{S - \sqrt{P(P+2)}}{S + \sqrt{P(P+2)}}. \tag{19}$$

It is possible to write formula (18) in a different form, namely,

$$\left(\frac{A}{D}\right)_{min} = e^{\Psi} - 1, \tag{20}$$

where

$$\operatorname{ch}\Psi = \frac{n_1^2\cosh 2\beta_1 + x_1^2\cos 2\varepsilon_1}{n_1^2 + x_1^2} \tag{21}$$

The results obtained show that the very smallest value which A/D can have depends only on the metallic layer which is being clarified. In order to realize this value, it is necessary only to satisfy conditions (16) and (19), of which the first fixes the thickness of the intermediate layer and the second the reflection coefficient of the dielectric film (designated above by the index k). Inasmuch as, in agreement with formulas (4) and (5), the magnitude of P is significantly less than M and N, the minimum value of A/D is less by far than that of an unclarified layer or a layer clarified by depositing a film above it. In particular the magnitude of $(A/D)_{min}$ is small in the case where the metallic layer is so thin that β_1 is markedly less than unity. Expanding $\cosh\varphi$ (formula (21)) in a series and considering that for most (if not all) metals of interest $x_1 \gg n_1$, we find for this case

$$\left(\frac{A}{D}\right)_{min} = \frac{2n_1\beta_1^2}{x_1\sqrt{3}}. \tag{22}$$

We shall return now to formula (7). On the basis of expression (16) we rewrite it in the form

$$\frac{R}{D} = \frac{1}{D_2}\left[\frac{R_1}{D_1} + \frac{R_2}{D_1} - 2\sqrt{\frac{R_1 R_2}{D_1 D_1}}\cos(\mu_1 + \tilde{\nu}_1 - \vartheta)\right]. \tag{23}$$

If R_2 is fixed (see equation (19)), the value of R/D depends on the thickness of the metallic layer and in a much lesser degree on the refractive index of the intermediate layer. However, as the calculation shows, the dependence on the thickness of the clarified layer is likewise rather weak. Thus with variation of the thickness in the interval from 0.01 to $0.1\lambda_0$ (λ_0 being the wavelength in vacuum) R varies within the limits 77-94%; (the minimum value of 77% occurs for $h_1 = 0.05\lambda_0$). See the example.)

EXAMPLE AND CONSIDERATION OF RESULTS

On the basis of the above, it can be shown that the clarified coatings cannot have an arbitrary desired value of reflection coefficient. However, this is not so. The fact is that the magnitude of R/D corresponding to

formula (23) depends very strongly on R_2. Up to this time we have taken this magnitude as fixed (in agreement with (19)), in order for A/D to have a minimum value. This minimum, with sufficiently small thickness of the clarified layer, is in fact very shallow, as one may readily verify by taking the second derivative of A/D with respect to R_2. Its value in the minimum is equal to $4\sqrt{P(P+2)}/D_1^2$ and the limit of this expression as $h_1 \to 0$ is $2n_1x_1\sqrt{3}/n_m^2$. If the largest possible value is chosen for n_m, then the second derivative of A/D will be small, and the magnitude of A/D will remain quite small even away from the minimum. Since $(A/D)_{min}$ for a sufficiently thin layer is very small, the clarification will remain good even without fulfillment of condition (19). In other words, we can in fact choose the value of R_2 in an arbitrary way, which gives the possibility of realizing any value of R in a wide interval.

We will give a numerical example. Let $n_0 = 1$ (air), $n_1 - ix_1 = 0.18 - i3.64$ (silver), and $n_m = 2.3$ (ZnS). Further, let $h_1 = 0.01\lambda_0$ (we assume, of course, condition (16) was fulfilled). Then $\mu_1 + \tilde{\nu}_1 - \sigma = 125°$, $P = 3.6 \times 10^{-6}$, $S = 0.0368$, $U = 0.0367$, $R_1/D_1 = 0.324$, and $1/D_1 = 1.239$. From these results it is easy to compute a table in which the dependence of the magnitudes of R, D, and A on R_2 is shown.

From the table it is seen that the clarification appears very good with large and medium values of R, but somewhat worse for small values. However, even in the latter case the result can be improved if a thinner metallic layer is taken. In this way our theory gives good possibilities for the synthesis of clarified metallic coatings, useful for a Fabry-Perot interferometer and for beam splitters.

R_2	R (%)	D (%)	A (%)
0.0	23.8	73.5	2.7
0.1	42.4	56.5	1.1
0.2	52.4	46.9	0.7
0.3	60.7	38.9	0.4
0.4	67.8	31.9	0.3
0.5	74.3	25.5	0.2
0.6	80.2	19.7	0.1
0.7	85.6	14.3	0.1
0.8	90.7	9.3	0.0
0.9	95.5	4.5	0.0
0.95	97.8	2.2	0.0

It is possible that even better results can be attained with the help of two clarifying films—one deposited above and the other below the metallic layer. However this question deserves individual examination. Also, we have not been concerned in this article with the question of achromatic coatings, i.e., the question of how much the magnitudes R and A characterizing the coating can be made only slightly dependent on the wavelength of the light. It appears probable that the proposed method will permit comparatively easy solution of this problem.

REFERENCES

1. P. G. Kard, Opt. i Spektr. 9, 95 (1960), Optics and Spectroscopy 9, 49 (1960).
2. I. N. Shklyarevskii and A. A. Avdeenko, Opt. i Spektr. 6, 678 (1959), Optics and Spectroscopy 6, 439 (1959).
3. K. I. Tarasov, Opt. i Spektr. 6, 96 (1959), Optics and Spectroscopy 6, 54 (1959).

THE SPECTROVISOR

M. M. Gurevich and K. I. Kolyadin

Received 23 March 1960

This paper describes a fast spectrophotometer for the visible part of the spectrum, which traces the transmission coefficient versus wavelength curves of the sample and a standard on the screen of a cathode-ray tube. Each of the curves is traced in 0.01 sec. A motion picture camera takes 12 photographs of the screen per second, thus making it possible to record the optical aspect of the kinetics of some chemical reactions.

The name "spectrovisor" has been given to a fast spectrophotometer which allows one to see (and photograph) undistorted optical transmission curves on the screen of a cathode ray tube. Its scanning time is short compared to the persistence of a visual image. By combining mechanical, optical, and electronic methods it turned out to be possible to construct such an apparatus primarily for the visible portion of the spectrum.

A schematic diagram of the apparatus is shown in Fig. 1. S is the light source (an incandescent lamp whose power was supplied by ferro-resonance stabilizer St), located inside a drum B which is rotated around an inclined axis by means of the synchronous motor Q at a rate of 50 rev/sec. A helical slot, which covered almost 180° of the circumference of the drum, was made on the side surface of the drum. Part of this slot, passing over the entrance slit of the monochromator R, was equivalent to a rapidly moving vertical entrance slit. During each revolution of the drum, the slit passed over the plane of the spectrum and a beam of light whose wavelength changed continuously came out of the fixed

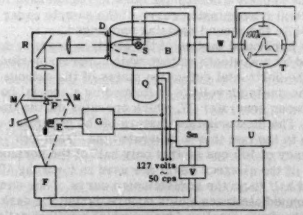

Fig. 1. Block diagram of the spectrovisor.

exit slit. During an interval of 0.01 sec, the wavelength of this beam passed through the complete available operating range of the spectrum. During the following one hundredth of a second, there was no light coming out of the monochromator, since the solid part of the drum B was

passing over the entrance slit of the monochromator.

The dispersing element of the monochromator was a replica of a diffraction grating (600 lines/mm), so that the dispersion of the apparatus (5mμ/mm) was almost constant over the whole spectrum. The apparatus utilized only the first order spectrum. In order to eliminate higher orders, a wedge-shaped light filter made from Zh S-12 glass was placed over the entrance window of the monochromator. A reflecting prism P, which acted as an optical commutator, was placed at the exit slit of the monochromator. The prism P, whose polished face was covered by a reflecting layer of aluminum, was placed on the upper end of a steel spring blade whose lower end was attached to the base of the apparatus. The electromagnet E, fed by an ac current of frequency 25 cps produced by the generator G, set the prism P into an oscillatory motion so that in one sequence the light output of the monochromator was reflected to the right at the exit part of the monochromator, and the other sequence to the left. In other words the optical commutator successively directed the beam into two light channels—a right and a left one—which after reflection from the plane mirror M converge upon the light sensitive surface of the photomultiplier F.

The output of the photomultiplier, whose power supply consists of the stabilized voltage from the circuit V, was amplified with the help of the dc amplifier (U) after which the voltage was applied to the vertical plates of a cathode ray tube T. Thus, the signal appearing at the vertical plates of the cathode ray tube and determining the vertical deflection of the electron beam depends on the intensity of the light beam and on the spectral response of the photomultiplier.

The irregularly shaped diaphragm D, located in the entrance port of the monochromator, permitted the effective height of the moving slit to be changed and set for different wavelengths in such a way that the vertical deflection of the electron beam was the same for all wavelengths. By horizontal displacement of the electron beam, a horizontal line corresponding to 100% transmission, is formed on the screen of the cathode ray tube. This line consists of two lines superimposed on each other, one of which is related to the right and the other to the left channel of the apparatus. If the sample under investigation J is placed in one of the channels (e.g., in the left channel), then the intensity of the transmitted beam will be decreased in proportion to the absorption constant of the sample and the vertical deflection of the electron beam is proportionately smaller. As a result one of the two 100% horizontal lines is transferred into the spectral transmission curve of the sample under study, while the second remains unchanged.

The horizontal motion of the electron beam is determined by a sawtooth voltage which appears periodically at the horizontal deflection plates of the cathode ray tube. The sawtooth voltage is formed by a special horizontal sweep generator W, which operates off the line voltage. The distinguishing feature of the generator circuit lies in the fact that it generates the "sawtooth" at a frequency of 100 cps so that only half of the horizontal motions of the electron beam are used to form the 100% line, and half form the transmission curve of the sample. The intermediate trace which occurs during the dark time of the drum rotation (during which vertical deflection is absent) produces the "zero" line on the screen. Thus, on the screen of the cathode ray tube, three lines are visible: the zero line, the 100% line, and the transmission curve of the sample located between the first and second.

It is convenient to place a plate of didymia glass, whose spectral curve has a very characteristic and constant form, in the right-hand channel. Then the 100% line changes into the transmission curve of didymia glass which allows one to orient oneself easily with regard to both the wavelength region and transmission range.

A complete realization of the possibilities of the apparatus can be achieved only with the aid of photographs which allow one to record each of the successive curves on the screen. The naked eye is not able to observe all the characteristics of the processes shown on the screen. It is easy to see that in order to record the 100% line as well as the light transmission curve on the photographs, it is necessary for the exposure time to be less than 0.04 sec. A motion picture frame requires approximately the same exposure time, i.e., the apparatus makes it possible to make about 12 photographs per second. Thus the spectrovisor makes it possible to follow the dynamics of processes connected with changes in the absorption in a layer of a substance.

Figure 2 shows the spectral characteristics of various stages of a reaction occurring between furfuryl and aniline in acetone (in the presence of hydrochloric acid.)*

*M. S. Barvinok pointed out this reaction, for which we wish to express our gratitude.

This reaction proceeds relatively slowly. Time intervals, subsequent to the introduction of the furfuryl solution into the aniline solution, are shown to an accuracy of the order of 0.2 sec. These intervals were marked by means of a timer and were recorded on the appropriate frames. The transmission curve of the didymia glass is shown on all the photographs. The two upper photographs show the transmission curves of furfuryl and aniline solutions.

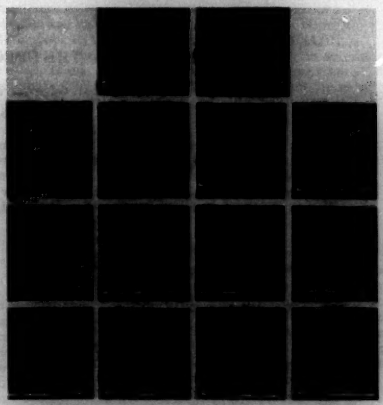

Fig. 2. Spectral characteristics of various stages of the reaction between solutions of furfuryl and aniline in acetone. 1—Transmission curve of a furfuryl solution; 2—the same for an aniline solution; 3—14, the same for various stages of the reaction. The time elapsed from the start of the reaction (in sec); 3—3.7; 4—5.2; 5—8.7; 6—13; 7—15; 8—21; 9—29.5; 10—51; 11—107.5; 12—144; 13—235; 14—368.

The subsequent 12 curves show the transmission of the cell at various times. The reaction occurred in a layer 5 mm thick at a temperature of 18 to 20°C.

Prospects for utilizing the spectrovisor are quite varied. The authors of this paper, who are working on improvements to this apparatus, will be very grateful to those readers of this journal who point out concrete cases of possible utilization of the apparatus and indicate requirements which it should satisfy.

SHORT COMMUNICATIONS

THE THEORY OF SPIN-LATTICE RELAXATION OF NUCLEAR SPINS SURROUNDED BY AN OCTAHEDRAL COMPLEX

B. I. Kochelaev

Received 26 October 1959

Previously, the theory of nuclear spin-lattice relaxation in solids was developed only for crystals of the NaCl and CsCl type. The present note reports calculations of spin-lattice relaxation times of nuclear spins for which the spin-lattice relaxation depends on quadrupolar interactions in complexes XY_6 (X is the atom with the relaxing nuclear spin). Thus we considered materials in which the binding of the atoms within the complex is appreciably stronger than with the other particles of the crystal. Cryolite (complex AlF_6), potassium alum (complex $Al(H_2O)_6$), and others might serve as examples of such materials. As in ref. 1 we assumed that the coupling of the nuclear spins to the lattice vibrations is brought about by the interaction between the quadrupole moment of the nucleus and an electric field gradient produced by the surroundings at a particular nucleus. As a consequence of the thermal vibrations, the field gradient varies with time and causes a flipping of the nuclear spins relative to the external magnetic field. In this case, one may write the operator for the spin-lattice interaction in the following form:

$$\mathcal{H}_{s-p} = \gamma \sum_{\mu} \hat{Q}_{\mu} (\Delta E)_{-\mu}$$

where $\hat{Q}_\mu$ are the components of the nuclear quadrupole moment operator, $(\Delta E)_{-\mu}$ are the components of the electric field gradient tensor produced by particles Y at the position of the nucleus of atom X, and γ is a coefficient which takes into account the enhancement of the electric field gradient because of polarization of the electron cloud of atom X in the field of the nucleus and its neighbors and also because of the possibility of partial covalent bonding between X and Y.

In case the particle Y possesses an electrical charge e, the components $(\Delta E)_\mu$ have the following form:

$$\Delta E_0 = 3\sqrt{3}eR_0^{-4}q_3, \quad \Delta E_{\pm 1} = \sqrt{6}eR_0^{-4}[q_5 \pm iq_4],$$
$$\Delta E_{\pm 2} = -\sqrt{6}eR_0^{-4}\left[\frac{3}{2}q_3 \pm iq_4\right],$$

where q_λ are the normal coordinates of XY_6 in the notation of Van Vleck.[2] When Y has only a dipole moment p, then

$$\Delta E_0 = 12\sqrt{3}pR_0^{-5}q_3, \quad \Delta E_{\pm 1} = 4\sqrt{6}pR_0^{-5}[q_5 \pm iq_4],$$
$$\Delta E_{\pm 2} = -4\sqrt{6}pR_0^{-5}\left[\frac{3}{2}q_3 \mp iq_4\right].$$

However, the exchange of energy between the natural vibrations of the complex and the spin can not take place, since the energy spectrum of the nuclear spin has a limit of 10^{-3} cm^{-1}; but the frequencies of the natural vibrations of XY_6 are the order of $\Omega \sim 10^3$ cm^{-1}. Therefore, it is necessary to take account of the interactions of the vibrations of the complex with the lattice whose spectrum is quasi-continuous and starts at zero. Expanding the interaction energy of the complex XY_6 with its surroundings in a series with respect to the normal coordinates of the complex, we find that the first nonzero term is the energy of the quadrupole moment of XY_6 in the field of the remaining particles of the crystal. Taking this interaction as a perturbation to the Hamiltonian which describes the natural vibrations of XY_6, we find the perturbed wave functions of the vibrating states of the complex. With the aid of the perturbed wave functions, it is easy to find the matrix elements for the operator of the spin-lattice interaction. Computing further the probability of a relaxation transition for two phonon processes by the usual method and taking account of the optical vibrations of the lattice[3] we obtain for the case that Y has only a dipole moment:

$$A(m+1, m) = 9.1 \cdot 10^{4} \pi \; cm + 1 \, |\hat{Q}_1| \, m\rangle^2 \frac{\gamma^2 p^4 E^2}{M_1^2 \omega_0^4 v^{10} R^{10}} \left(\frac{kT}{\hbar}\right)^4 \times \left\{\frac{1}{\omega_0^4 \Delta\omega_0}\left(\frac{M_2 + M_3}{M_2 M_3}\right)^2 + \frac{r^4}{5\sigma_0 v^5 (M_2 + M_3)^2}\right\}.$$

The formula for the $(m + 2) \rightarrow m$ transition is analogous. Here m is the magnetic quantum number, M_1 is the mass of the particles Y, M_2 the mass of the complex, M_3 the mass of the nearest neighbor of the complex, E is its charge, r is the distance to it from the complex, R is the equilibrium distance X – Y, σ_0 is the limiting length of the phonon wave vector, ω_0 is the frequency of the optical vibrations of the lattice when $\sigma = 0$, $\Delta\omega_0$ is the width of the optical vibration spectrum, and v is the average speed of sound in the crystal. The calculations were carried out for an alum-type lattice with the assumption that $kT > \hbar\omega_0$, $\hbar\sigma_0 v$.

Comparing this result with the well-known formulas of van Kranendonk,[1] we note that the probability of a relaxation transition for a nuclear spin inside a stable complex depends strongly on the frequency of the natural vibrations of the complex; whereupon, the spin-lattice relaxation time for such spins must be appreciably longer. The relaxation mechanism considered is the most essential for spin-lattice relaxation of electron spins of paramagnetic ions. We consider this question elsewhere.

In conclusion the author expresses deep thanks to S. A. Al'tshuler for interest in the work and discussion of the results.

REFERENCES

1. J. van Kranendonk, Physica **20**, 781 (1954).
2. J. H. van Vleck, J. Chem. Phys. **7**, 72 (1939).
3. B. I. Kochelaev, Zhur. Eksptl. i Teoret. Fiz. **37**, 242 (1959).

ON THE LIGHT ABSORPTION EDGE IN ALKALI-EARTH METAL OXIDES

V. P. Rombakh

Received 28 October 1959

It was shown in a series of papers[1-3] that the fundamental absorption bands in heteropolar crystals are closely related to the crystal lattice energy. Shamovskii[2] proposed the use of the following equation to calculate the position of the long wavelength edge of the fundamental absorption band of a crystal

$$h\nu = E - I + U$$

or what amounts to the same thing

$$h\nu = Q + S + \frac{1}{2}D,$$

where the quantities entering into the first parts of the equations are interconnected by the Born-Haber thermodynamic cycle.

Here $h\nu$ represents the long wavelength edge of the first optical absorption band in the ultraviolet; E is the electron affinity; I is the ionization energy; D is the dissociation energy of the halogen; Q is the total energy; U is the crystal lattice energy, and S is the heat of sublimation of the metal.

Both Shamovskii's equation and the Born-Haber cycle were in good agreement with experiment for all of the alkali halide compounds. Table 1, taken from ref. 2, shows the theoretically calculated and experimentally observed values of the energy corresponding to the beginning of the absorption band. As can be seen from this table, the disagreement between theory and experiment never exceeded 6.5%, and was usually considerably less.

The Born-Haber cycle was used with similar success to calculate the crystal lattice energies of the alkaline earth oxides MgO, CaO, SrO, and BaO. This follows from the fact that according to ref. 4, they, as well as all alkali halides in Table 1, have the rock salt crystal structure. Hence, it is logical to assume that the Shamovskii equation can be used in the case of this group of oxides.*

*Starting from this consideration, Weir[14] drew an analogy between the alkali halides and the oxides, sulfides, selenides, and tellurides of the alkaline earths. He derived the lattice energies of the alkaline earth—Group VI—compounds from the lattice energies of the alkali halides.

Table 2 shows the values of the energy of the long wavelength edge of the fundamental optical absorption band for the class of compounds indicated above. These values were calculated by us, using Shamovskii's equations. From this table, it is clear that the absorption bands of these oxides lie in wavelength ranges shorter than 118 mμ. Actually, in our previous work[5] on the compounds MgO, CaO, SrO and BaO, no strong absorption of light was observed over the visible and ultraviolet regions of the spectrum to 250 mμ. Later on we made an investigation up to 200 mμ and obtained the same results. Our data on MgO are in good agreement with a whole series of experimental investigations.[6-9] Thus, for example, Nelson[8] found a value of 10 ev for the fundamental absorption edge and Lempicki[10] assigned an approximate value of 11 ev to this quantity. Our value is 10.5 ev.

Table 1*

Salt	Edge of the first absorption band	
	ev (exp.)	ev (theory)
NaCl	7.05	6.84
KCl	6.93	6.74
RbCl	6.85	6.65
CsCl	6.70	6.69

Table 2

Salt	Edge of the first absorption band	
	ev	λ (A)
MgO	10.50	1180
CaO	11.23	1100
SrO	10.74	1150
BaO	10.69	1160

*Alkali bromides and iodides behave similarly but were omitted for the sake of brevity.

Barium oxide and strontium oxide have been studied by Jahoda,[11] Zollweg,[12] and others.[13] In these papers, it is shown that between 3200 and 2025 A, at low temperatures barium and strontium oxides have 3 to 5 absorption maxima whose intensities decrease rapidly with increasing temperature. At temperatures of 20°C and higher they disappear completely.

The shorter wavelength absorption maxima turn out to be insensitive to temperature changes. Jahoda pointed out that such maxima ought to be found in the region below 2000 A, as was the case in our work.

In conclusion the author expresses his indebtedness to G. A. Tikhov for his interest in this work.

REFERENCES

1. R. Hilsch and R. W. Pohl, Z. Physik **57**, 145 (1929); **59**, 812 (1929).
2. L. M. Shamovskii, "Absorption Spectra of Heteropolar Crystals and the Crystal Lattice Energy." GONTI, 1938.
3. E. K. Zavadovskaya, Doklady Akad. Nauk SSSR **98**, 547 (1954).
4. B. F. Ormont, "Structure of Inorganic Materials." Gosudarst. Izd. Tekh.-Teoret. Inst., 1950.
5. B. P. Rombakh, Bull. Crimean Pedagogic Inst. **29**, 306 (1957).
6. K. Larche, Licht **12**, 110 (1942).
7. K. Larche and R. Schulze, Z. tech. Physik **23**, 114 (1942).
8. G. R. Nelson, Phys. Rev. **99**, 1902 (1955).
9. H. Watanabe, Phys. Rev. **95**, 1684 (1954).
10. A. Lempicki, Proc. Phys. Soc. (London) **B66**, 278 (1953).
11. F. C. Jahoda, Phys. Rev. **107**, 1261 (1957).
12. R. J. Zollweg, Phys. Rev. **111**, 113 (1958).
13. J. Cunningham, J. Chem. Phys. **29**, 1196 (1958).
14. C. E. Weir, Phys. Rev. **108**, 19 (1957).

FREE EXCITON LUMINESCENCE IN A MOLECULAR CRYSTAL

Yu. M. Popov and A. S. Selivanenko

Received 23 November 1959

Free excitons in thermal equilibrium with the lattice of an ideal crystal cannot luminesce without the help of phonons. The momentum of a "thermal" exciton is 10^2-10^3 times greater than the momentum of a luminescence quantum which can be emitted according to the law of conservation of energy. The free exciton may give up its momentum to the lattice when luminescence takes place. Such a process is analogous to the "indirect" transitions in a semiconductor[1] and can be calculated in the second approximation of perturbation theory.

The expression for the probability of the disappearance of a free exciton with the simultaneous emergence of a photon and a phonon has the form

$$dw = \frac{2\pi}{\hbar}\left|\sum \frac{H_I H_{II}}{E_0 - E_\nu}\right|^2 \rho_F \delta\left(E_0 - E_F\right) dE_F. \qquad (1)$$

where ρ_F is the density of final states; E_0 and E_F are the energies of the initial and final states; E_ν is the energy of the intermediate state; H_I is the matrix element of the transition from the excited state of the crystal to the ground state with the emission of a photon[2]; H_{II} is the matrix element for the dissipation of an exciton into phonons[3], and δ is Dirac's symbol. The probability (1) is different from zero when $k - Q - q = 0$, where k, Q, and q are the momenta of the exciton, photon, and phonon respectively.

For a process with phonon emission,

$$E_0 = E' + D + \frac{k^2\hbar^2}{2\mu},$$
$$E_F = \hbar\omega + \hbar\Omega_q + E',$$

where E' is the energy of the ground state of the crystal, D is the energy of the lower boundary of the exciton band, measured from E', $\hbar\omega$ and $\hbar\Omega_q$ are the energies of the luminescence and phonon quanta, respectively, and $k^2\hbar^2/2\mu$ is the kinetic energy of the exciton which we will hereafter assume to be thermal, since according to ref. 3 the collision time of an exciton with phonons is of the order of 10^{-11} sec. This time, as we will show, is much less than the lifetime of the exciton with simultaneous emission of a photon and a phonon. Therefore the exciton comes to thermal equilibrium with the lattice before emission of a photon with a phonon. The thermal energies of the exciton justify the "effective mass" approximation.

The computations lead to the following expression for the probability of emission of a luminescence quantum by a free exciton within the solid angle $d\theta$ (assuming that $|Q| \ll |k|$).

$$dw = \frac{8\pi\,|e\,(\mathbf{xj})|^2 \left[\frac{(ex)^2}{a^3}\right]^2 (N_q + 1)\,\hbar^2 k^2\,(\hbar\omega)^3}{\hbar M\left[\frac{\hbar^2 k^2}{2\mu} - \hbar\Omega_q\right]^2 \hbar\Omega_q\,(2\pi\hbar c)^3}\,d\theta. \qquad (2)$$

Where ex is the matrix element of the dipole moment of a transition in a crystal molecule, j is the polarization vector of an electromagnetic field quantum, a is the lattice constant, N_q is the number of phonons with momentum q, M is the mass of a molecule in the crystal, and c is the velocity of light.

Integrating over all angles, we obtain the total probability of free exciton luminescence with the emission of a phonon in an ideal crystal. If $N_q > 1$ (i.e., temperatures not lower than helium) then the probability of luminescence with the absorption of a phonon also has the form (2) when $\hbar^2k^2/2\mu \gg \hbar\Omega_q$, which is almost always the case.

For $\mu \sim 10^{-27}$ gm, $\omega \sim 10^{15}$ sec^{-1}, $\hbar\Omega_q \sim 0.003$ ev, and $M \sim 5 \times 10^{-22}$ gm, we obtain $w \sim 10^7$ sec^{-1}.

In this evaluation we assumed that the oscillator strength of the electron transition in the molecule is approximately 0.01. The value of w increases in proportion to the cube of the oscillator strength. Therefore when the oscillator strength is greater than 0.1, multiphonon processes must apparently be taken into account.

For the case in which only acoustic phonons are emitted ($\Omega_q = uq$, where u is the velocity of sound, i.e., at crystal temperatures below the Debye temperature, it follows from (2) that $w \sim T^{-1}$ for a "thermal" exciton. This indicates that the probability of an exciton decaying to a photon and a phonon increases as the temperature decreases.

The effect of impurities on the luminescence of free excitons becomes appreciable if

$$w \sim vn\sigma, \qquad (3)$$

where v is the exciton velocity, n is the number of impurities or defects in 1 cm^3, and σ is the cross section for interaction of an exciton with an impurity (capture, with subsequent luminescent emission by the impurity, capture with nonradiative dissipation of the exciton energy etc.). When we apply numerical evaluation to our situation we obtain from the conditions of (3) for $T \sim 300°K$

$$n\sigma \sim 1\ \text{cm}^{-1}. \qquad (4)$$

We note in conclusion that the appearance of "impurity bands" in the luminescence spectrum associated with a known impurity concentration presents an opportunity, using formula (3), to find the cross section for capture of an exciton by an impurity with subsequent emission of a luminescence quantum.

REFERENCES

1. L. Hall, G. Bardeen, and F. Blatt, Phys. Rev. **95**, 559 (1954).
2. A. S. Davydov, "Teoriya poglosbcheniya sveta v molekulyarnykh kristallakh" (The Theory of Light Absorption in Molecular Crystals). Izd. Akad. Nauk. Ukrain. SSR., Kiev, 1956.
3. V. M. Agranovich and Yu. V. Konobeev, Opt. i Spektr. **4**, 242 (1959).

SUPERHIGH-FREQUENCY ABSORPTION OF CH_3GeF_3

N. A. Irisova and E. M. Dianov

Received 21 December 1959

The absorption spectrum of the CH_3GeF_3 molecule has been observed in the 10-30 kMc range. Records were obtained for absorption lines corresponding to the transitions $J = 1 \rightarrow 2$, $J = 2 \rightarrow 3$, and $J = 3 \rightarrow 4$. On the basis of the change in the relative intensities of the absorption lines with temperature, it was established that lines of both the ground and the excited states of internal rotation were observed.

According to preliminary measurements, the value of the rotational constant of the CH_3GeF_3 molecule is $B = 3257 \pm 1$ Mc, and the dipole moment equals $3.8 \pm 20\%$ Debye units.

The compound CH_3GeF_3 was synthesized for us by our scientific collaborator G. Ya. Zueva, to whom we express our sincere gratitude.

LUMINESCENCE OF ETHANOLAMINE COMPOUNDS OF PLATINUM

A. M. Tkachuk and N. A. Tolstoi

Received 29 February 1960

A study of the luminescence of platinicyanic compounds (particularly of the relaxation of their luminescence[1]) revealed several interesting rules, which makes further investigation into complex platinum salts desirable. In the course of this intensified study, it is expedient to consider data on other related classes of platinum compounds. Data concerning the steady-state and relaxation properties of the luminescence of several ethanolamine compounds of platinum (synthesized and described by Gil'dengershel'[2-4]) is presented for the first time in this article.

OBJECTS AND METHOD OF INVESTIGATION

We studied the following ethanolamine compounds of platinum: $[PtEtm_2I_2]$ trans- and cis- modifications, $[PtEtm_2Br_2]$ trans-modification, $[PtEtm_2Cl_2]$ trans- and cis- modifications, and the diethanolamine compounds $[PtDEtm_2I_2]$, $[PtDEtm_2Br_2]$, and $[PtDEtm_2Cl_2]$ trans-modifications. All these compounds contain divalent platinum with a coordination number of four. All complexes have a planar configuration.

The luminescence spectra of all the enumerated compounds were obtained using photoelectric equipment[5] consisting of a monochromator with a diffraction grating (relative operature of 1:4, and dispersion of 15A/mm in the second order), an FEU-22 photomultiplier, and an electronic recording potentiometer EPPV-51. Excitation of the luminescence was accomplished by a diffraction monochromator with light of the $\lambda 365$ mμ mercury line from a lamp SVDSh-250.

Measurements of the luminescence relaxation time τ were made using an ultratauometer with a mechanical light modulator.[6] The luminescent light was received by the FEU-22 photomultiplier. The sample was placed in a special apparatus which enabled one to change the temperature evenly throughout the interval from −183 to 150°C.

RESULTS OF MEASUREMENTS

The luminescence of all the ethanol- and diethanolamine compounds of platinum which we studied is characterized (as in the case of platinicyanides) by the following properties: (1) the intensity of the steady-state luminescence I_∞ is proportional to the intensity of the exciting light E; (2) the curves of growth and decay are symmetrical and exponential; (3) the value of τ does not depend on the intensity of the exciting light. Only in the case of trans- $[PtEtm_2I_2]$, when cooled below −150°C, does the relaxation of luminescence obey a law somewhat different from an exponential, as a consequence of the appearance of a second, slower process.

In Fig. 1, the luminescence spectra of all the studied compounds are given; they are broad bands with contours similar to a Gaussian distribution curve. On transition from diethanolamine to ethanolamine compounds with trans- and cis- modifications, the maxima of the bands are appreciably displaced only in the case of the compounds containing chlorine.

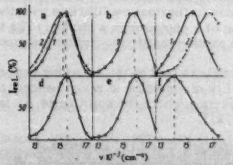

Fig. 1. Luminescence spectra of ethanolamine compounds of platinum at −196°C. a—$[PtEtm_2I_2]$; b—$[PtEtm_2Br_2]$; c—$[PtEtm_2Cl_2]$; d—$[PtDEtm_2I_2]$; e—$[PtDEtm_2Br_2]$; f—$[PtDEtm_2Cl_2]$. Curves 1—trans-, curves 2—cis- modifications.

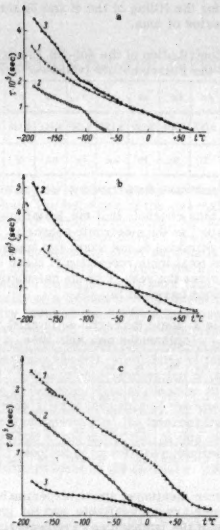

Fig. 2. Temperature dependences of the duration of luminescence τ. a—trans- $[PtEtm_2I_2]$ (curve 1); cis- $[PtEtm_2I_2]$ (curve 2); trans- $[PtDEtm_2I_2]$ (curve 3). b—trans- $[PtEtm_2Br_2]$ (curve 1); trans- $[PtDEtm_2Br_2]$ (curve 2). c—trans-$[PtEtm_2Cl_2]$ (curve 1); cis- $[PtEtm_2Cl_2]$ (curve 2), trans- $[PtDEtm_2Cl_2]$ (curve 3).

The temperature dependences of τ are illustrated in Fig. 2 (a, b, and c). Both the appearance of the graphs of $\tau(t)$, and plots of $\ln\tau$ versus $(1/t)$, show that the reduction of τ with temperature does not obey Mott's formula which is derived from a hypothesis concerning the increase of nonradiative transitions with temperature according to the Boltzmann law. A comparison of the nature of the temperature drop of τ with the temperature quenching of the intensity of luminescence I_∞ (which also does not obey Mott's formula) shows that, on heating, τ is reduced more quickly than I_∞. The foregoing indicates that the variations of τ are specified not only by a change in the probability of nonradiative transitions but also, to a considerable extent, by the probability of radiative transitions. The temperature changes in the probability of radiative transitions are apparently connected with the fact that the interaction of the luminescence center with the lattice surrounding it removes the prohibition on a radiative transition to a certain degree. The intensity of the interaction and the degree of prohibition removal depend on the thermal motion of the lattice.

The authors are extremely grateful to Kh. I. Gil'dengershel' for donating the above-mentioned compounds for investigation.

REFERENCES

1. N. A. Tolstoi, A. K. Trofimov, A. M. Tkachuk, and N. N. Tkachuk, Izvest. Akad. Nauk SSSR, Ser. Fiz. **20**, 583 (1955).
2. Kh. I. Gil'dengershel', Zhur. Neorg. Khim. **3**, 1328 (1958).
3. Kh. I. Gil'dengershel', Zhur. Neorg. Khim. **2**, 1077 (1957).
4. Kh. I. Gil'dengershel', Zhur. Neorg. Khim. **2**, 1070 (1957).
5. V. L. Ermolaev, Kand. diss. Gosudarst. Opt. Inst., 1959.
6. N. A. Tolstoi, A. M. Tkachuk, and N. N. Tkachuk, Izvest. Akad. Nauk SSSR, Ser. Fiz. **21**, 595 (1955).

APPLICATION OF PERTURBATION THEORY TO THE CALCULATION OF THE IONIC REFRACTIONS OF LANTHANIDES AND ACTINIDES

L. N. Mazalov and S. S. Batsanov

Received 3 March 1960

Knowledge of the ionic refractions is essential for the solution of a number of physico-chemical problems: the calculation of the electronic and atomic polarization of ionic crystals, the optical study of glasses and minerals, calculation of the ionic radii and diamagnetic susceptibilities of ions, etc. The least reliable values at the present time are the ionic refractions of the lanthanides and actinides. The experimental data available for this purpose are quite insignificant, and the theoretical evaluation is based on Kordes' formula[1] which lacks a solid foundation. This formula permits the calculation of ionic refractions from the ionic radii. The result of such a calculation is, therefore, strongly dependent on how accurately these radii are known. In the case of the lanthanides and actinides, the values of the ionic radii have undergone considerable revision during the last fifteen to twenty years; the present values are 0.12-0.15 A smaller than the ionic radii of Kordes (see refs. 2, 3). Such a change in the radii implies a sharp decrease of the ionic refractions of the lanthanides and actinides. Kordes gives the value $R = 2.65\ cm^3$ for La^{3+} while the calculation based on Zachariasen's more accurate values of the radii leads to the value $1.77\ cm^3$, etc. Considering that the experimentally determined value of the ionic refraction of lanthanum turns out to be $3.56\ cm^3$, it will be clear that it is desirable to formulate new methods for the accurate determination of the ionic refractions of the lanthanides and actinides.

According to perturbation theory,[2] the electronic polarizability of an ion with closed electron shells in a

homogeneous electric field is given by the expression

$$\alpha = \frac{4}{9Na_0}\left(\sum_i^k \overline{(r_i^2)}\right)^2, \qquad (1)$$

where N is the number of electrons in the ion, a_0 is the radius of the first Bohr orbit, and r_i is the radius of the i-th electron shell. To determine the quantity $\overline{r_i^2}$, one may use Slater's eigenfunctions[8]

$$\psi = Ar^{n^*-1}e^{-\frac{(Z-\sigma)r}{(n^*a_0)}}Y_{lm},$$

where A is a normalization factor, Z the nuclear charge, and σ the screening constant; the quantity Y_{lm} characterizes the angular dependence of the orbit. Since Y_{lm} is of no importance, we find that

$$\overline{r_i^2} = \frac{(2n_i^*+2)(2n_i^*+1)(n_i^*)^2}{4(Z-\sigma)^2}a_0^2,$$

In order to determine σ, the electrons are separated into groups according to Angus' rule.[7] Equation (1) can then be written in the form

$$\alpha = \frac{4a_0^3}{9N}\left(\sum_i \nu_i \frac{(2n_i^*+2)(2n_i^*+1)(n_i^*)^2}{4(Z-\sigma)^2}\right)^2 \qquad (2)$$

where ν_i is the number of electrons in the i-th group of electrons of the ion. We have also used this formula for the evaluation of the electronic polarizabilities of the lanthanides and actinides. However, a preliminary check was made by applying this formula to the ions of the alkali and alkaline earth metals for which one has the reliable experimental data of Fajans.[9]

Table 1 compares the results of the calculations with the experimental data. In accordance with customary usage in physical chemistry, the electronic polarizabilities are given in the form of refractions

$$R = \frac{4}{3}\pi N\alpha = 2.522\alpha.$$

It can be seen from the table that the mean relative error is about 10%, but this figure is reduced to about 5% if one disregards the cases of Li^+ and Be^{2+}, for which the relative error is large while the absolute difference is of the same order as the experimental uncertainty.

Table 1. Refraction (in cm^3) of the Ions of the Alkali and Alkaline Earth Metals

Ion	Li^+	Na^+	K^+	Rb^+	Cs^+	Be^{2+}	Mg^{2+}	Ca^{2+}	Sr^{2+}	Ba^{2+}
$R_{theor.}$	0.06	0.47	2.45	4.11	6.52	0.02	0.26	1.55	2.88	4.88
$R_{exp.}$	0.08	0.47	2.25	3.79	6.53	0.03	0.28	1.40	2.58	4.73

Going on to the trivalent lanthanides and actinides, we encounter cases of ions with a closed outer shell while the shell below it is not filled. It has been shown in several theoretical papers that the inner electron shells do not contribute much to the total polarizability of the ion (see, for instance, refs. 9 and 10); their influence is therefore frequently negligible. Besides, as has been shown by our calculations (see Table 2), the magnitude of the product $\nu_i\overline{r_i^2}$, which characterizes the polarizability of the 4df group in the case of the lanthanides, and of the 5df group for the actinides, remains practically constant during the filling of the 4f and 5f shells of the respective series of ions.

Table 2. Contribution of the 4df-5df Electron Groups to the Polarizability (values of $\nu_i\overline{r_i^2}$)

Ce	Pr	Nd	Pm	Sm	Eu	Gd	Tb	Dy	Ho	Er	Tu	Yb
9.024	9.175	8.961	9.047	9.104	9.140	9.156	9.156	9.141	9.116	9.080	9.036	8.986
Lu	Th	Pa	U	Np	Pu	Am	Cm	Bk	Cf	Es	Fm	Mv
8.930	11.571	11.780	11.938	12.052	12.129	12.176	12.197	12.196	12.177	12.143	12.096	12.038

One can thus conclude that the deviations from the "inert gas type" in the electronic subshells of the lanthanides and actinides do not exert any appreciable influence on the total ionic refraction of these elements.

Table 3 gives the results of the calculations of the ionic refractions based on Eq. (2).

Table 3. Ionic Refractions (in cm^3) of the Lanthanides and Actinides

Ce	Pr	Nd	Pm	Sm	Eu	Gd	Tb	Dy	Ho	Er	Tu	Yb
3.35	3.20	2.95	2.80	2.66	2.62	2.38	2.26	2.12	2.04	1.93	1.83	1.74
Lu	Th	Pa	U	Np	Pu	Am	Cm	Bk	Cf	Es	Fm	Mv
1.66	3.52	3.36	3.21	3.06	2.92	2.79	2.66	2.54	2.42	2.31	2.20	2.10

As has been mentioned above, experimental data for the actinides are not available, and the ionic refractions of some of the lanthanides have recently become known from measurements of the refractions of solutions of the respective nitrates. Thus, according to the data of Leipziger and Roberts,[4] the values of some of these refractions are: $La^{3+} = 3.56\ cm^3$, $Ce^{3+} = 3.34\ cm^3$, $Nd^{3+} = 3.05\ cm^3$; our calculations give the corresponding values 3.46, 3.35, and 2.95 cm^3. The mean relative error is in these cases about 2%. One can assume that for the remaining elements the deviations between theory and experiment will be just as insignificant.

REFERENCES

1. S. S. Batsanov, "Strukturnaya refrektometriya" (Structural Refractometry). Izd. Moskov. Gosudarst. Univ., 1959.
2. E. Kordes, Z. Physik. Chem. B48, 91 (1940).
3. W. Zachariasen, in "Aktinidy" (Actinides). Izd. Inostrannoi Lit., Moscow, 1955.
4. F. Leipziger and J. Roberts, J. Phys. Chem. 62, 1014 (1958).
5. P. Gombas, "Problema Mnogikh Chastits v Kvantovoi Mekhanike" (Problem of Many Particles in Quantum Mechanics). Izd. Inostrannoi Lit., Moscow, 1953.
6. J. C. Slater, Phys. Rev. 36, 57 (1930).
7. W. R. Angus, Proc. Roy. Soc. A136, 569 (1932).
8. N. Bauer and K. Fajans, J. Am. Chem. Soc. 64, 3023 (1942).
9. S. S. Batsanov, Zhur. Fiz. Khim. 30, 2640 (1956).
10. N. Sundbom, Arkiv Fysik 13, 539 (1958).

CONSIDERATION OF THE INTERNAL FIELD IN THE DETERMINATION OF RAMAN INTENSITIES

V. M. Pivovarov

Received 8 March 1960

There have been a number of studies[1-4] on the necessity of considering the influence of the internal field in the determination of Raman intensities. An investigation of the intensities of the Raman lines of binary liquid mixtures,[5] whose components differ substantially in refractive index, quite clearly confirmed the influence of the internal field. Two major facts were established:[5] first, the intensity of a Raman line increases (decreases) as the refractive index of the medium increases (decreases); and second, the intensity of depolarized lines changes more than that of polarized lines. A theoretical treatment, explaining the indicated shifts of intensity and first proposed,[3] is based on consideration of the internal field according to Onsager. Use of the valence-optical scheme in considering the influence of the internal field is based on the assumption that the internal field influences every bond in the molecule. In this case, it leads to the introduction of an effective derivative of the polarizability with respect to the normal vibrational coordinate.

$$\frac{\partial a_{i\,\text{eff.}}}{\partial q} = \frac{3n^2}{(2n^2+1)\left(1-\frac{2(n^2-1)}{2n^2+1}\frac{a_i}{r^3}\right)^2}\frac{\partial a_i}{\partial q}. \qquad (1)$$

where n is the refractive index of the medium, a_i is the principal value of the bond polarizability, $\partial a_i/\partial q$ is the derivative of the polarizability with respect to the normal vibrational coordinate, and r is the radius of the Onsager cavity, determined from experimental data. It is assumed in this case that the molecular constants a_i and $\partial a_i/\partial q$ do not depend on the magnitude of the internal field.

When the refractive index of the medium is changing, it is also necessary to take account of the influence of purely optical effects on intensity[4,5] leading to a dependence of the effective length of the cell and the brightness of the scattered light on the refractive index of the medium, and also to a focusing action of the cross section of the cell. The sign of the optical effect is opposite to that of the internal field effect. The line intensity observed experimentally depends on these two factors, and can be defined by the formula

$$I_{s\,\text{obs.}} \sim c\left(5b'^2_{s\,\text{eff.}} + 13g'^2_{s\,\text{eff.}}\right)\frac{1}{n_c}, \qquad (2)$$

where c is the volume concentration of the substance in per cent and n_c is the refractive index of the medium, corresponding to the concentration c. The factor $1/n_c$ takes account of the pure optical effect.[4] The effective trace of the tensor $b'_{c\,\text{eff.}}$ and the anisotropy $g'_{c\,\text{eff.}}$ are formed from the effective polarizability derivatives (1), in which $n = n_c$. From formula (2) it is possible to define a relative effective intensity coefficient.

$$k_{\text{eff. rel.}} = \frac{5b'^2_{s\,\text{eff.}} + 13g'^2_{s\,\text{eff.}}}{5b'^2_{s=100\,\text{eff.}} + 13g'^2_{s=100\,\text{eff.}}} = \frac{I_{s,\,c=\text{obs.}}}{I_{s,\,c=100\,\text{obs.}}} \cdot \frac{100}{c} \cdot \frac{n_s}{n_{s=100}}. \qquad (3)$$

To check equation (3), we calculated the concentration dependence of $k_{\text{eff. rel.}}$ for the lines 459, 313 and 217 cm^{-1} of carbon tetrachloride in mixtures with acetone, and for the lines 606, 992, 1176, 1605, and 3063 cm^{-1} of benzene in mixtures with acetone. The original data for the calculation of the value of $k_{\text{eff. rel.}}$ and the sources from which they are drawn are presented in the Table. For the calculation of the value of the effective polarizabilities of the trace $b_{c\,\text{eff.}}$ and of the anisotropy $g_{c\,\text{eff.}}$ of the vibrations of benzene indicated above, we used the corresponding data of the first variant in the paper by Kovner and Snegirev.[6] Then, to find all six values of the principal polarizabilities of the C-C(Q) and C-H(q) bonds, we added two equations to the four independent equations in this work: $a_{Q_3} + a_{q_3} = 1.06$ A^3 [7] (the polarizability of the benzene molecule in the direction perpendicular to the ring) and $a_{q_1} = 0.79$ A^3 [8] (the value of the CH bond polarizability for paraffins). The latter circumstance, together with the use of a $\partial a_i/\partial q$ value calculated to a first approximation in the computation of the effective bond polarizability derivatives, introduces a certain inaccuracy. Nonetheless, keeping in mind the approximate character of the solution of the mechanical and electro-optical problems, and also the coarseness of the Onsager model, this lack of rigor cannot influence the results substantially. The magnitudes of the radii r were chosen to give the best fit of theory with experiment for the polarized lines 459 cm^{-1} of CCl_4 and 992 cm^{-1} of C_6H_6.

Original Data for the Calculation of the Value of $k_{\text{eff. rel.}}$

CCl_4		C_6H_6	
The C–Cl bond from ref. 9		C–H bond	
a_i (A^3)	a'_i (A^3)	a_i (A^3)	a'_i (A^3) [8]
$a_1 = 3.67$	$a'_1 = 2.82$	$a_1 = 0.79$ [8]	$a'_1 = 0.86$
$a_2 = 2.08$	$a'_2 = 0.68$	$a_2 = 0.75$	$a'_2 = 0.24$
$r = 2.30$ A		$a_3 = 0.65$	$a'_3 = 0.00$
		C–C bond	
		$a_1 = 1.395$	$a'_1 = 1.32$
		$a_2 = 1.175$	$a'_2 = 0.34$
b'_{459} and g'_{217} from ref. 9		$a_3 = 0.43$	$a'_3 = 0.23$
g'_{313} from ref. 10		$r = 1.89$ A	
		b'_{992}, g'_{992}, b'_{3063}, g'_{3063}, g'_{606}, g'_{1176}, g'_{1605} from ref. 6	

The concentration dependence of the quantities $k_{\text{eff. rel.}}$ was determined from the data in ref. 5. The quantities of interest to us, $I_{c\,\text{obs.}}/I_{c=100\,\text{obs.}}$, can easily be determined from the graphs given in the reference, since the ordinates represent quantities characterizing the deviation of the intensity from proportionality to the concentration of the liquid in the mixture,

$$\Delta = \frac{I_{s\,\text{obs.}} - I'_{s\,\text{obs.}}}{I_{s=100\,\text{obs.}}} = \frac{I_{s\,\text{obs.}}}{I_{s=100\,\text{obs.}}} - c,$$

where $I_{c\,\text{obs.}}$ is the intensity which would be observed if the proportionality were maintained. The results of the

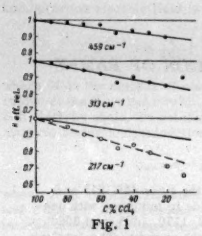

Fig. 1

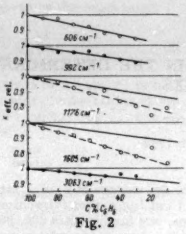

Fig. 2

Fig. 1. Dependence of the relative effective intensity coefficients of the lines of CCl_4 on concentration in the mixture CCl_4 + $(CH_3)_2CO$. Points—experimental data (the diameter of a circle corresponds to the mean square error). Lines—the calculated data.

Fig. 2. Dependence of the relative effective intensity coefficients of the lines of C_6H_6 on concentration in the mixture C_6H_6 + $(CH_3)_2CO$. The points and lines have the same significance as in Fig. 1.

comparison of the theory with experiment are shown in Figs. 1 and 2.

The data presented are, in general, in adequate agreement with the theory. Further development of the theory of the influence of the internal field on Raman intensities is indubitably of interest. From the results obtained we note that in all cases, a drop in intensity is observed when the refractive index of the medium decreases. The polarized lines 459 cm^{-1} of CCl_4 and 992 and 3063 cm^{-1} of C_6H_6 are affected by internal field to a lesser degree than the depolarized lines. For the lines 217 cm^{-1} of CCl_4 and 1176 and 1605 cm^{-1} of C_6H_6, the difference between the slopes of the experimental and theoretical curves is significant. In the latter case, this may possibly be connected with Fermi resonance.

I wish to express my thanks to O. P. Girin and N. G. Bakhshiev for fruitful discussions of the results of this investigation.

REFERENCES

1. L. Woodward and H. George, Proc. Phys. Soc. **64B**, 780 (1951).
2. D. Long, D. Milner, and A. Thomas, Proc. Roy. Soc. **237A**, 197 (1956).
3. V. M. Pivovarov, Opt. i Spektr. **6**, 101 (1959). Optics and Spectroscopy **6**, 60 (1959).
4. D. Rea, J. Opt. Soc. Am. **49**, 90 (1959).
5. V. M. Pivovarov and Ya. S. Bobovich, Opt. i Spektr. **3**, 134 (1957).
6. M. A. Kovner and B. N. Snegirev, Opt. i Spektr. **5**, 239 (1958).
7. M. V. Vol'kenshtein, "Stroenie i Fizicheskie Svoistva Molekul" (The Structure and Physical Properties of Molecules), Izd. Akad. Nauk SSSR, Moscow-Leningrad, 1955.
8. K. Denbigh, Trans. Faraday Soc. **36**, 939 (1940).
9. M. V. Vol'kenshtein, M. A. Elyashevich, and B. I. Stepanov, "Kolebaniya Molekul" (Molecular Vibrations), Vol. 2. Gosudarst. Izd. Tekh. Teoret. Lit., Moscow, Leningrad, 1949.
10. D. Long, T. Spencer, D. Waters, and L. Woodward, Proc. Roy. Soc. **240**, 499 (1957).

THE OSCILLATOR STRENGTH FOR THE δ-SYSTEM OF THE NO-BANDS

S. P. Erkovich and Yu. V. Pisarevskii

Received 11 March 1960

In preceding papers[1,2] we have calculated the oscillator strength, or the probability of electronic transitions, in the γ- and β-systems of the bands of the molecule NO, using the spectroscopic data of Marmo[3] and Mayence.[4] This communication presents the results of similar calculations for the δ-system of the NO-bands; the same data[3,4] are used. In carrying out the calculations, the method proposed in references 1 and 2 has been employed. We take this occasion to mention that we made a mistake in ref. 1, Eq. (15); the damping constant δ_0 should be obtained from the following relation (notation same as in ref. 1):

$$b_0=\frac{1}{4\pi c}\sum_{v_1'}A_{v',J',v'',J''}=\frac{16\pi^3\nu_0^3kT}{3B''hc^3}(2J''+1)R_e^2, \qquad (1)$$

where $A_{v',J',v'',J''}$ are the Einstein transition probabilities for emission. This error has been corrected in the results of ref. 2.

If Eq. (1) is used, the absorption function assumes the form

$$A=\frac{16\pi^3\nu_0^3i_{J'J''}}{3hcq}R_e^2\sum_{J'}f(|\nu_J-\nu_0|,\ a)\sqrt{\frac{2(v'-v'')\,kT}{B''hc}}. \qquad (2)$$

To calculate the transmission function of the spectrograph, $f(|\nu_J-\nu_0|, a)$, we used data from the analysis of the rotational band structure obtained by Lagerquist and Miescher.[5] The Hönl-London factors $i_{J'J''}$, were calculated by the method of Hill and Van Vleck.[6] In doing this, we have taken into consideration that, according to ref. 5, a $C^2\Pi - X^2\Pi$ transition takes place in the case of the δ-bands of NO; for the δ(0,0)-band, the upper state corresponds to Hund's case (b) while the lower state approximates Hund's case (a). For transitions of this kind the Hönl-London factors have the form:

$$i_{P_{11}}=\frac{[4(J'+1)^2-9](2J'-1)}{8(J'+1)(2J'+1)},\qquad i_{P_{21}}=\frac{[4(J'+1)^2-1](2J'-1)}{8(J'+1)(2J'+1)},$$

$$i_{P_{12}}=\frac{[4(J'+1)^2-9](2J'+3)}{8(J'+1)(2J'+1)},\qquad i_{P_{22}}=\begin{cases}\dfrac{[4(J'+1)^2-1](2J'+3)}{8(J'+1)(2J'+1)}, & J'>\dfrac{1}{2},\\ \dfrac{[4(J'+1)^2-1](2J'-1)}{8(J'+1)(2J'+1)}, & J'=\dfrac{1}{2}.\end{cases} \qquad (3)$$

$$i_{R_{11}}=\frac{4(J'^2-9)(2J'-1)}{8J'(2J'+1)},\qquad i_{R_{21}}=\frac{(4J'^2-1)(2J'-1)}{8J'(2J'+1)}, \qquad (4)$$

$$i_{R_{12}}=\frac{(4J'^2-9)(2J'+3)}{8J'(2J'+1)},\qquad i_{R_{22}}=\frac{(4J'^2-1)(2J'+3)}{8J'(2J'+1)}.$$

$$i_{Q_{11}}=\frac{9(2J'-1)}{8J'(J'+1)},\qquad i_{Q_{21}}=\frac{2J'-1}{8J'(J'+1)}, \qquad (5)$$

$$i_{Q_{12}}=\frac{9(2J'+3)}{8J'(J'+1)},\qquad i_{Q_{22}}=\frac{2J'+3}{8J'(J'+1)}.$$

The harmonic oscillator model was used to obtain the value of the Franck-Condon factor, q(0,0) = 0.165.

State of molecule	T_e (cm^{-1})	ω_e (cm^{-1})	$\omega_e x_e$ (cm^{-1})	B_e (cm^{-1})	r_e (A)
$X^2\Pi_{1/2}$ . . .	0	1904.03	13.97	1.7046	1.1508
$X^2\Pi_{3/2}$ . . .	121.1	1903.68			
$C^2\Pi$	52148	2395	15	2.002	1.062

The optical constants of the molecule used in the calculations are listed in the table (according to the data of Herzberg,[7] and Lagerquist and Miescher[5]). The experimental values of the absorption coefficients in the δ(0,0)-band were obtained from the data of ref. 3, and are shown in the figure (broken lines). The theoretical values are shown there by full lines; these values were obtained from Eq. (2), and have been adjusted to the experimental curves by a suitable choice of the quantity R_e^2. We have not taken the Q-branches into consideration, since according to (5), they should not make any appreciable contribution. It should be mentioned that in ref. 3 the intervals between the experimental points were of the order 28 cm^{-1} or more. It is because of this that the δ(0,0)-band presented in ref. 3 shows two peaks instead of four (see, for instance, the papers of Tanaka[8]).

From the normalization condition we obtain R_e =

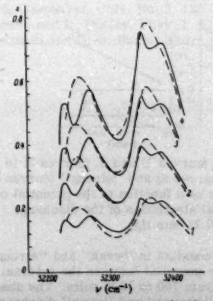

Absorption coefficient in the δ(0,0)-band of the NO-molecule at different gas pressures. Full lines: theoretical values for R_e = 0.128 at. units; broken lines: experimental values (according to ref. 3). NO pressure (in mm Hg): curves 1—1.33; curves 2—4.0; curves 3—7.9; curves 4—14.8.

0.128 at. units; this corresponds to an oscillator strength f = 0.0026. Mayence's data give somewhat different results: R_e = 0.142 at. units, f = 0.0032 (mean values from six measurements). This difference might be due to the circumstance that we had to determine the NO pressure used in the experiments described in ref. 4 in an indirect way (for details, see ref. 1). Besides, the data of ref. 4 refer only to the maxima of the band, which showed two peaks. The normalization was thus made difficult.

REFERENCES

1. S. P. Erkovich, Opt. i Spektr. 6, 297 (1959), Optics and Spectroscopy 6, 193 (1959).
2. S. P. Erkovich and Yu. V. Pisarevskii, Opt. i Spektr. 9, 21 (1960), Optics and Spectroscopy 9, (1960).
3. F. F. Marmo, J. Opt. Soc. Am. 43, 1186 (1953).
4. J. Mayence, Ann. Phys. 7, 453 (1952).
5. A. Lagerquist and E. Miescher, Helv. Phys. Acta, 31, 221 (1958).
6. E. Hill and J. H. Van Vleck, Phys. Rev. 32, 250 (1928).
7. G. Herzberg, "Molecular Spectra and Molecular Structure. I. Diatomic Molecules," 2nd ed. Van Nostrand, New York, 1950.
8. Y. Tanaka, Sci. Papers Inst. Phys.-Chem. Res. (Tokyo) 39, 456 (1942); 43, 28 (1949).

OPTICAL AND ELECTRICAL PROPERTIES OF "WEAK" AND "STRONG" HIGH FREQUENCY DISCHARGES IN NEON

L. P. Razumovskaya and O. P. Bochkova

Received 25 March 1960

It is known[1] that two stable forms, called "weak" and "strong" discharges,[2] exist in a high frequency discharge, under certain conditions. We have measured the optical and electrical properties of "weak" and "strong" discharges in Ne, excited under the same conditions by an alternating field having a frequency of 6 Mc.

A cylindrical discharge tube 150 mm long and 12 mm in diameter was used for this investigation. The tube had ring-shaped external electrodes spaced 70 mm apart. Under these conditions, both types of discharge can develop in pure neon only at pressures between 0.2 and 0.3 mm.

Figure 1 shows the values of electron temperature T_e and electron concentration n_e^0, which were measured by the double probe method[4,5] along the axis in the central part of the discharge tube. It is easy to see that the quantity T_e remains constant in "weak" and "strong" discharges when the potential between the external electrodes changes from 700 to 1300 volts. The absolute values of T_e for "strong" and "weak" discharges are 67,000°K and 81,000°K, respectively. Despite the good reproducibility of the results (within 3%), the difference between the values of T_e in "weak" and "strong" discharges may still be within the limits of accuracy of the measurement, which is approximately 15%. The concentration of electrons increases linearly with increasing potential in "weak" as well as in "strong" discharges, but in the latter, the concentration is several times greater. N_e is of the order of 10^9-10^{10} cm^{-3}. In general, the results obtained from our measurements agree with previously published data.[1,2]

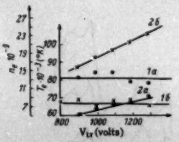

Fig. 1. T_e (curves 1) and n_e (curves 2) in "weak" (curves a) and "strong" (curves b) discharges as a function of the potential of the external electrodes of the discharge tube (p = 0.26 mm Hg).

Simultaneously with our double probe method measurements, we studied the optical properties of two forms of Ne discharge. The qualitative difference between them is that the integral brightness of a "strong" discharge is appreciably greater than that of a "weak" one. In the positive column of both "weak" and "strong" discharges only the arc lines are excited, but in the weak discharge, the lines with higher excitation potentials are relatively brighter. The results of the measurements of relative line intensities, obtained at V_{tr} = 1100 volts and p = 0.2 mm of Hg by the usual methods of heterochromatic photographic photometry, are given in Table 1. The intensity of the line 4712A ($2p^5\ 6d\ 8_3^0 \rightarrow 2p^5\ 3p^3\ D_4$) was taken as a unity.*

*Translator's note: The notation of transitron is taken from R. F. Bader and S. Goudsmit, "Atomic Energy States," (1932) which is obsolete. According to AEL by C. E. Moore Sitterly (1949) it should be $2p^5\ 6d(2\frac{1}{2})_3^0 \rightarrow 2p^5\ 3p(2\frac{1}{2})_3$.

Table 1

λ (A)	Transition	$\frac{I_\lambda}{I_{\lambda\ 4712}}$ "weak"	$\frac{I_\lambda}{I_{\lambda\ 4712}}$ "strong"
4712	$2p^5 6d 8_3^0 \rightarrow 2p^5 3p^3 D_3$	1	1
4704	$2p^5 6d 8_2^0 \rightarrow 2p^5 3p^3 S_1$	0.7	0.8
4708	$2p^5 4d 7_1^0 \rightarrow 2p^5 3p^3 S_1$	0.7	1.0
5330	$2p^5 4d 5_2^0 \rightarrow 2p^5 3p^3 S_1$	3.3	4.9
5341	$2p^5 4d 7_1^0 \rightarrow 2p^5 3p^3 S_1$	3.4	5.7
5400	$2p^5 3p^3 S_0 \rightarrow 2p^5 3s^3 P_1^0$	7.1	11

In Fig. 2, the dependence of the rate of change of the relative intensities on the potential on the tube, first considering and then neglecting the reabsorption of radiation, is presented for "weak" and "strong" discharges. It is

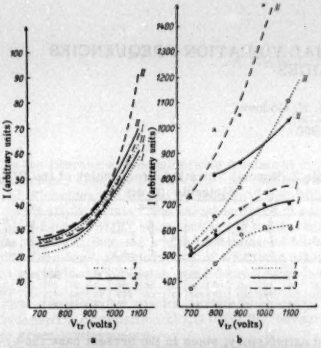

Fig. 2. The intensities of spectral lines in "weak" (a) and "strong" (b) discharges as function of the potential of the electrodes of of the discharge tube. The wavelength of the emission lines (in A): 1—5945; 2—6598; 3—6163. Conditions of measurement: curves I—neglecting, and curves II—considering the reabsorption of radiation.

easy to see that the reabsorption of radiation for the line which end on the $3P^0_{0,1,2}$ levels is appreciably higher for a "strong" discharge than for a "weak" one (for the line 6354A of Ne I it is almost 3.5 times greater). The N_i values of the concentration of excited atoms on the $3P^0_{0,1,2}$ and $1P^0_1$ levels are given in Table 2 and were obtained by reabsorption measurements at p = 0.2 mm of Hg and V_{tr} = 1000 volts. N_i values are also given as calculated from the usual formula:

$$N_i = \frac{g_i}{g^k} N_{k^0} e^{-\frac{E_i - E_k}{kT_e}}.$$

From these data, it is seen that the concentration of excited atoms on the same levels is 3-4 times higher in a "strong" discharge than in a "weak" one.

The ratios of the measured concentrations on the $3P^0_{0,1,2}$ levels in "weak" and "strong" discharges are

Table 2

Level	V_{exci} (ev)	$N_i \cdot 10^{-11}$ (obs)		$N_i \cdot 10^{-11}$ (calculated)	
		"weak"	"strong"	"weak"	"strong"
$2p^53s^1P^0_1$	16.79	0.5	2	11	7.4
$2p^53s^3P^0_2$	16.66	0.8	2	4.6	2.8
$2p^53s^3P^0_1$	16.62	2	6.8	14	8.5
$2p^53s^3P^0_0$	16.57	3.7	10.6	23	14

1 : 2.5 : 4.6 and 1 : 3.4 : 5.3, respectively, and differ very little from the ratio of the statistical weights of these levels, which is 1 : 3 : 5. However, the absolute values of the concentration of excited atoms for T_e, which we measured in this experiment, appeared to be two orders of magnitude lower than the calculated values (see the 5th and 6th columns in Table 2). From this it can be concluded that the excitation conditions are far from equilibrium in both cases.

A comparison of the results of the optical and double probe investigations shows that the difference between the optical properties of "weak" and "strong" discharges depends mainly on the difference in electron concentration. The observed change of T_e cannot appreciably influence the relative intensities of spectral lines.

When applying the high frequency discharge to the analysis of gases, the "weak" discharge can be used to increase the concentration sensitivity of the analysis for the difficulty excitable component of gas mixtures. Neglecting the possibility of the existence of two forms of high frequency discharges under the same conditions, having different optical properties, can lead to serious mistakes in the analysis.

The authors express their gratitude to S. E. Frish and Yu. M. Kagan for their help in the work and evaluation of the results.

REFERENCES

1. S. M. Levitskii, Zhur. Tekh. Fiz. **27**, 970 (1957).
2. S. D. Vagner, E. I. Vavilin, and A. M. Drukman, Zhur. Tekh. Fiz. **29**, 1264 (1959).
3. Yu. M. Kagan, V. I. Perel', and P. I. Ripatti, Vestnik Leningrad. Gosudarst. Univ. No. 8, 129 (1956).
4. E. O. Johnsen and L. Molter, Phys. Rev. **80**, 58 (1950).
5. L. O. Biberman and B. O. Panin, Zhur. Tekh. Fiz. **21**, 12 (1951).

APPROXIMATE PREDICTION OF THE NORMAL VIBRATION FREQUENCIES OF THE HAFNIUM HALIDES

A. M. Aleksandrovskaya and I. N. Godnev

Received 31 March 1960

The procedure previously described by us [1,2] may also be used for an approximate prediction of the normal vibration frequencies of the hafnium halides in the gaseous state.

The case under consideration, however, differs from those described earlier[1,2] in the absence of any data on the values of the interatomic distances and the frequencies. Therefore, in order to find out the former, we could not use the $r = f(Z_{periph.})$ curves and found the distances on the basis of the $r = f(Z_{centr.})$ curves instead. The results are presented in Table 1.

Table 1. Interatomic Distances r (Hf-X) (in A)

Molecule	$r = f(Z_{centr.})$
$HfCl_4$	2.41
$HfBr_4$	2.56
HfI_4	2.75

In order to determine the values of the reduced force constants k and the interaction coefficients k^*, we used, as before,[2] the $k = f(A_{centr.})$ and $k^* = f(A_{centr.})$ curves based on the points for all the elements of the fourth group.* The vibration frequencies presented in columns A and B of Table 2 were calculated on the basis of the values found for the coefficients k and k^* for the molecules $HfCl_4$, $HfBr_4$, and HfI_4. Unfortunately, in this case it is not possible to avoid an extrapolation; consequently, in order to check our calculations, we used curves of the type of Hildebrand's curves,[3] which, as shown by a test which we carried out, satisfactorily represent the dependence on r of the frequency values of XY_4 molecules when Y = const.* Study of these curves has also shown that it is better to plot them not as a function of r but as a function of the atomic number of the central atom $Z_{centr.}$. Such curves have been plotted separately for the chlorides, bromides, and iodides using the electronic configuration $Hf(d^2s^2)$, and with their help the frequencies of the HfX_4 molecules were found for $Z_{Hf} = 72$. Their values were for all molecules somewhat less than the average of columns A and B, but the deviation $\Delta\nu$ proved to lie within the limits of error indicated in ref. 1. Hence the agreement may be considered satisfactory, since in the present case the errors might be large on account of the extrapolation.

*We used the smoothed curves, since the separate plotting of the Ti-Zr-Hf branch is difficult.

*These curves must not be confused with Jolly and Latimer's curves,[4] which give the dependence of $\nu = f(r)$ when X = const.

Table 2. Normal Vibration Frequencies of the HfX_4 Molecule (in cm^{-1})

Frequency	$HfCl_4$ A	$HfCl_4$ B	$HfCl_4$ Average	$HfCl_4$ From method of ref. 3	$HfCl_4$ $\Delta\nu$	$HfBr_4$ A	$HfBr_4$ B	$HfBr_4$ Average	$HfBr_4$ From method of ref. 3	$HfBr_4$ $\Delta\nu$	HfI_4 A	HfI_4 B	HfI_4 Average	HfI_4 From method of ref. 3	HfI_4 $\Delta\nu$
$\nu_1(A_1)$	350	344	347	340	7	217	210	211	205	6	140	143	142	137	5
$\nu_2(E)$	87	89	88	85	3	58	58	58	54	4	39	39	39	34	5
$\nu_3(F_2)$	370	386	378	360	18	249	260	255	240	15	183	187	185	170	15
$\nu_4(F_2)$	94	91	93	90	3	64	62	63	60	3	46	46	46	42	4

The average values of the A and B frequencies were used to calculate the entropy of $HfCl_4$ in the ideal-gas state. The results of the calculation are presented in Table 3, where they are compared with the entropy values calculated by us on the basis of the value of the entropy of $HfCl_4$ in the solid state.[5] The calculation was carried out according to the formula

$$S_{\text{compare}} = S_{\text{tr.}} + \frac{\lambda}{T} - R \ln \frac{P}{P_1}.$$

Table 3. Entropy of $HfCl_4$ (in cal/deg-mole)

$\lambda_{subl.}$ (kcal/mole)	T (°K)	$S_{calc.}$	$S_{expt.}$
24.6	485	103.0	102.5*
	490	103.6	103.1*

*The correction for nonideality was disregarded on account of its smallness.

The latent heat of sublimation $\lambda_{subl.}$ was found from the vapor-pressure curve measured by Sun In-chou and Morozov.[6] It is easy to see that the agreement may be considered satisfactory.

REFERENCES

1. I. N. Godnev, A. M. Aleksandrovskaya, and I. V. Rigina, Opt. i Spektr. 7, 271 (1959), Optics and Spectroscopy 7, 172 (1959).
2. A. M. Aleksandrovskaya, I. V. Rigina, and I. N. Godnev, Opt. i Spektr. 7, 844 (1959), Optics and Spectroscopy 7, 495 (1959).
3. J. H. Hildebrand, J. Chem. Phys. 15, 727 (1947).
4. W. L. Jolly and W. M. Latimer, J. Am. Chem. Soc. 74, 5754 (1952).
5. S. S. Todd, J. Am. Chem. Soc. 75, 3035 (1953).
6. Sun In-chou and I. S. Morozov, Zhur. Neorg. Khim. 4, 492 (1959).

A NEW LUMINOR: $2Li_2O - WO_3(U)$

Yu. S. Leonov

Received 31 March 1960

In the literature, a considerable number of crystal phosphors are described which are activated by uranium.[1,2] Fluorides of calcium,[3,4] sodium,[5,6] and lithium,[7] halides of alkali metals,[8] and halophosphates of barium and magnesium,[9] which luminesce in the green region of the spectrum, possess a high luminescence intensity. On the other hand, the tungstates of alkali and alkaline earth metals[2] activated by uranium have a weak luminescence.

We have prepared a new tungstate luminor of the stoichiometric composition $2Li_2O \cdot WO_3(U)$, having an intense green luminescence.

For a more accurate determination of the thermal treatment of the luminor, we used Kurnakov's pyrometer to obtain the heating curve of a 2 : 1 mixture of lithium carbonate and tungstic oxide. The presence of two fundamental irreversible endothermal effects in the heating curve (in the 485-540° and 635-745° regions) indicated that the interaction of the components proceeds in two stages. For this reason we also conducted the thermal treatment of the charge in synthesizing the luminor first at 640°C (2 hr) and then at 1090°C (1 hr).* The optimal concentration of the uranium activator in the phosphor was ~ 1.3 mol.%.

*The second firing temperature is taken considerably higher than the temperature of the second endothermal effect in order to facilitate the diffusion of the uranium activator in the phosphor. The melting point of $2LiO_2 \cdot WO_3$ is 1190°C.

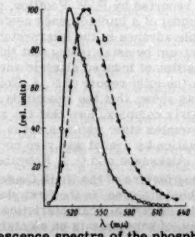

Luminescence spectra of the phosphors $2Li_2O \cdot WO_3(U)$ (curve a) and $Li_2WO_4(U)$ (curve b). Concentration of uranium activator in both phosphors 0.00044 mol.U/mol. base; excitation by light of wavelength $\lambda = 365$ mμ.

The above-described luminor is excited both by long wavelength ($\lambda = 365$ mμ) and short wavelength ($\lambda = 253.7$ mμ) ultraviolet light and also by x-rays, electrons, and neutrons.

The figure shows the luminescence spectrum of the luminor $2Li_2O \cdot WO_3(U)$ obtained on a photoelectric apparatus using an FEU-32 photomultiplier. Excitation was provided by long wavelength ultraviolet light ($\lambda = 365$ mμ). The luminescence spectrum is an unsymmetrical band with its maximum at 520 mμ. A second band is observed near 530 mμ.

The luminor stores a quantity of light on excitation with short wavelength ultraviolet light ($\lambda = 253.7$ mμ) and also on excitation with cathode rays (in the latter case, phosphorescence is observed at room temperature). The possibility of the occurrence of recombination processes in calcium tungstate was established in ref. 10. The luminescence is as bright as that of ZnS(Cu) on excitation by long wavelength ultraviolet light ($\lambda = 365$ mμ) and is comparable with the luminescence of $Zn_2SiO_4(Mn)$ on excitation by short wavelength ultraviolet light ($\lambda = 253.7$ mμ).

Intensity of Luminescence of Calcined Mixtures of Li_2O and WO_3 of Various Compositions Containing U. Concentration of Activator Uranium 0.0004 mol. U/mol. Li_2O.

No.	Ratio Li_2O/WO_3	Intensity of luminescence (rel. units)
1	9.00	15.0
2	5.66	23.0
3	4.00	13.5
4	3.00	23.0
5	2.33	49.0
6	2.00	100.0
7	1.50	26.5
8	1.22	19.0
9	1.00	0.0
10	0.66	0.0
11	0.50	0.0
12	0.33	0.0
13	0.11	0.0

The literature contains descriptions of the compound Li_2WO_4[11] and a luminor $Li_2WO_4(U)$[2] possessing a weak green luminescence, but it does not contain any data on the compound $2Li_2 \cdot WO_3$, which we prepared.

The luminors $2Li_2O \cdot WO_3(U)$ and $Li_2WO_4(U)$ differ in their luminescence spectra. For comparison, the figure shows the luminescence spectrum of $Li_2WO_4(U)$ (the phosphor was obtained by firing at 640° for 2 hr). The spectrum was obtained under the same conditions as the spectrum of $2Li_2O \cdot WO_3(U)$.* It is readily seen that the maximum of the luminescence band of the phosphor $Li_2WO_4(U)$ is situated near 538 mμ.

*The luminescence spectra of both phosphors were normalized.

The two tungstates also differ in their luminescence properties in the absence of the activator: $2Li_2O \cdot WO_3$, when excited by 253.7 mμ radiation at liquid nitrogen temperature, possesses a blue luminescence; Li_2WO_4 does not luminesce.

In order to determine the composition of the new luminor more accurately, we investigated the dependence of the intensity of luminescence of these preparations on their composition. The Table gives the brightness of calcined mixtures of Li_2CO_3 and WO_3 of different compositions. It is easily seen that the $2Li_2O \cdot WO_3(U)$ preparation gave a more intense luminescence* than any of the others.

*The luminescence intensity of the preparations was measured visually with the aid of a FM photometer.

To see whether the luminor obtained from a charge of composition $2Li_2CO_3 + WO_3$ consists of a single phase,

we observed the heating curve of a prepared luminor. The detection of thermal effects in this curve would show the multiphase character of the product obtained. The test showed that there were no thermal effects on the curve. The x-ray diagram of the new compound showed a system of lines which differed from those of Li_2WO_4 and also from those of the initial components or their decomposition products.

Thus, from the combined experimental data it follows that the new luminor must be assigned the composition $2Li_2O \cdot WO_3(U)$.

I wish to express my sincere thanks to M. A. Konstantinova-Shlezinger for guidance in this work.

REFERENCES

1. A. V. Moskvin, "Katodolyuminestsentsiya" (Cathodoluminescence). Part 2, Moscow, Leningrad, 1949.
2. F. A. Kröger, "Some Aspects of the Luminescence of Solids." Amsterdam, 1948.
3. P. P. Feofilov, Mater. V Soveshch. po Lyuminestsentsii (Proc. 5th Conf. on Luminescence), Tartu, 1957.
4. F. A. Kröger, Physica **14**, 488 (1948).
5. T. S. Dobrolyubskaya, Zhurn. Anal. Khim. **11**, 3(1956).
6. W. A. Runciman, Nature, **175**, 1082, 1955.
7. P. P. Feofilov, Opt. i Spektr. **7**, 842 (1959), Optics and Spectroscopy **7**, 493, 1959.
8. I. P. Shapiro, Opt. i Spektr. **7**, 126 (1959), Optics and Spectroscopy **7**, 78, 1959.
9. G. T. Anderson and R. S. Wells, J. Electrochem. Soc. **98**, 10 (1951).
10. V. L. Levshin, V. B. Gutan, and E. N. Karzhavina, Opt. i Spektr. **6**, 372 (1959), Optics and Spectroscopy **6**, 274, 1959.
11. A. G. Bergman, A. I. Kislova, and V. I. Posypaiko, Zhurn. Obshch. i Khim. **24**, 1935 (1954).

EVENTS

THE NINTH CONFERENCE ON LUMINESCENCE (CRYSTAL PHOSPHORS)

It is well-known that the conferences on luminescence are alternately devoted to molecular luminescence and to crystal phosphors. The latter was the subject of the Ninth Conference on Luminescence, which was held at Kiev during 20-25 June, 1960. The conference was attended by 325 participants, who came from 30 cities and presented about 120 papers. Approximately a third of the papers were devoted to phosphors of the zinc sulfide type, and a third to alkali halide phosphors. Space limitations permit us to report only on several papers of a physical character, without touching upon the numerous and very important papers on the chemistry of crystal phosphors.

The conference opened with an introductory address by V. L. Levshin, who stressed its significance in the development of luminescence as one of the important fields of optics, intimately connected with the needs of the national economy of the USSR.

There were only six theoretical papers; half of these were concerned with calculation of the impurity centers in crystals. K. K. Rebane and O. I. Sil'd, using the method of moments of Lax, gave a general solution of the problem of calculating the shapes of continuous electronic-vibrational bands and solved several concrete problems. A. M. Ratner and G. E. Zil'berman computed the shapes of the absorption and luminescence bands of an impurity center. They estimated the probability of radiationless transitions, taking account of the effect of a change of the vibration frequency along with the electronic transition. N. N. Kristofel' discussed the question of the interaction of an impurity center with local vibrations which were not completely symmetrical. The rest of the theoretical papers were concerned with the computation of kinetic schemes using the band model. V. V. Antonov-Romanovskii considered the kinetics of phosphor luminescence with traps of several kinds. K. S. K. Rebane analyzed a band scheme with three capture levels. V. E. Khartsiev communicated the results of computations on the kinetics of "photothermostimulated" phenomena.

The experimental papers were concerned both with the usual phosphors of the zinc sulfide type and alkali halide crystals with traditional activators and with a number of new or little-investigated substances and compositions. Several papers presented data on the luminescence of glasses. In a survey paper, M. T. Shpak presented interesting material on the luminescence of molecular crystals containing various impurities. The complex spectra of activated crystals are apparently connected with the different types of spatially distributed centers which may interact strongly on raising the concentration or on introducing certain impurities. Detailed spectroscopic and polarization investigation of the luminescence of uranium-activated lithium and sodium fluorides, reported by P. P. Feofilov, permitted formulation of a model of a luminescence center and made a considerable advance in the interpretation of a luminescence spectrum by establishing that this spectrum is a superposition of induced electric and magnetic radiation. In the joint report of N. A. Tolstoi and Lyu Shun-Fu, it was shown that the relaxation spectra of fluorides are fairly complex, i.e., that the excited centers are in a complex state which is not in thermal equilibrium. Activation by uranyl was also considered in papers by E. P. Alekseeva and G. I. Kobyshev.

A distinguishing feature of the Ninth Conference was the considerable extension, in the first place, of investigations of the electrical characteristics of phosphors and, secondly, of experiments on electrical effects on optical phenomena in phosphors. Among the former were papers by V. L. Levshin and P. A. Pipins, who studied the capture levels in alkali earth phosphors by the methods of exoelectron emission in combination with thermoluminescence; A. I. Belkind and Kh. F. Kyaembre, who investigated electron emission with excited ultraviolet radiation of alkali-halide crystals; I. K. Vitol and others, who measured the thermostimulated conductivity of ionic crystals; F. I. Vergunas and G. M. Malkin, who studied the role of the diffusion of electrons in the photodielectric effect (PDE), due to the conductivity; Ya. A. Oksman and A. V. Burlakov, who considered the possibilities offered by the methods based on the PDE of studying the electric and photoelectric properties of powders; the work of P. E.

Ramazanov, who measured the PDE in the thermoluminescence of the phosphor ZN^5-Cu, Fe; the investigations of I. K. Vitol and I. A. Tale on the photoelectric polarization of zinc sulfides and its connection with luminescence; the work of A. T. Bartanyan and L. D. Rozenshtein on comparison of the electrical resistance and phosphorescence of a number of organic compounds, and finally, the work of V. G. Dubinin on paramagnetic resonance in SrS-Eu, Sm. Great interest was aroused by the paper of V. M. Fridkin on the luminescence of electretized zinc sulfides.

The second group of "electrical" papers included 15 communications devoted to electroluminescence. A great impression was made by the paper of A. M. Bonch-Bruevich and V. A. Molchanov, who used the powerful modern methods of electronics to study the fundamental processes of electroluminescence, which enabled them to examine the pheonomena occuring in individual ten-micron regions of the crystal. A. I. Georgobiani and M. V. Fok presented interesting material on the temperature dependence of luminescence and the role of tunnel transitions in electroluminescence. V. E. Oranovskii investigated the local appearances of electroluminescence in single ZnS crystals. I. K. Vereshchagin established a relation between the surface properties of phosphors and their electroluminescence. The relation between the brightness and the applied voltage and current (with the use of combinations of rectangular impulses and dc voltage) was similarly the subject of the paper by V. N. Favorin and co-workers. Interesting possible ways of controlling the brightness of electroluminescent condensers with the aid of ferroelectrics were noted in the paper by I. N. Orlov et al. A comparison of electro- and photoluminescence was made in the papers of N. A. Vlasenko (on the sublimate phosphor Zn-Mn) and I. P. Shapiro and N. I. Kuznetsov (on the phosphor ZnS-Cu). Polarization effects and their influence on the anisotropy of the light pulses were discussed in the work of V. L. Rabotkin and V. A. Sokolov. Cathodoluminescence was discussed in the paper of Yu. M. Popov, who considered theoretically the processes possible in phosphors irradiated by a high-density electron beam, and also in a number of papers devoted to specific cathodoluminors and cathodoluminescent screens, in particular monocrystalline types (paper of M. A. Vasilyeva, V. V. Kuprevich, I. V. Stepanov and P. P. Feofilov).

T. P. Belikova and M. D Galanin showed that the difference between the duration of α-scintillations and photoluminescence in ZnS reduces to the difference in the density of the excitation.

The representatives of the "Tartu school" came forward with interesting papers devoted as a whole to the undoubted connection of the "alkali halide luminescence" with the "zinc sulfide luminescence." The most important results were summarized in the paper of Ch. B. Lushchik et al. As a result of the complex study of the mechanism of the processes of energy storage in ionic crystals, the role of electron-hole, exciton sensitized, ionic and dislocation processes in the storage of luminous energy was evaluated. Different important aspects of the optical mechanism of alkali halide phosphors were discussed in the papers of I. V. Yaek (on the quantum yield of recombination luminescence), R. I. Gindina (luminescence topography in crystals), K. K. Shvarts and G. K. Vale (resonance migration of energy), and others. An important contribution to the understanding of the connection between the structure of an elemental crystal cell and the spectral properties was made in the work of F. D. Klement and L. A. Teiss on the effect of isostructures on the spectra of mixed crystals.

Important material on the luminescence of alkali halide phosphors was also presented in the communications of N. I. Ivanova, N. P. Kalabukhov, M. L. Kats, L. M. Shamovskii, and their co-workers.

A considerable number of papers heard at the Ninth Conference were concerned with the properties of individual important phosphors. Of special mention are the papers of V. L. Levshin, Yu. V. Voronov, V. B. Gutan, S. A. Fridman, and V. V. Shchaenko on Zn-Ag, Sm. These papers discussed important details of the interaction of activators. I. S. Gorban', S. N. Ryzhova, and A. A. Shishlovskii and also Yu. I. Karkhanin, E. N. Bereznyakovskii, Yu. V. Vorobovyev and G. P. Peka presented important new data on the luminescent properties of cuprous oxide; in the first paper, new short wavelength luminescence bands of Cu_2O are related to oxygen vacancies and are used to explain the unusual time dependence of the afterglow and efficiency on the temperature; the second paper discusses the effect of the state of the acceptor centers on the luminescence of Cu_2O. Cadmium sulfide, as always, drew the attention of optics specialists. V. L. Broude and V. S. Medvedev investigated the excitation spectra of the blue luminescence of CdS. E. F. Gross, B. S. Razbirin, and M. A. Yakobson studied the line structure in the spectra of the absorption edge and the luminescence of CdS at helium temperatures. Extreme interest was aroused by the paper of A. A. Kaplyanskii on "piezospectroscopic phenomena" in unilaterally deformed monocrystals, which he studied in detail and interpreted. These investigations undoubtedly will play an important part in the optics of solids.

The effect of the dimensions of natural and crushed ZnS crystals on luminescence was the subject of the paper of V. L. Levshin and B. D. Ryzhikov. The phenomena arising in the compression of crystals on all sides were discussed by Ya. Ya. Kirs.

The mechanisms of flash phenomena were discussed in the papers of I. A. Parfianovich and N. A. Tolstoi and co-workers.

We are unable to consider here several important papers on practical applications that were presented at the Conference. As a whole, the Conference was a great success and undoubtedly had a stimulating effect on the further creative work of its participants.

In his concluding words, V. L. Levshin summed up the Conference, noting the numerous contributions which were made by Soviet physicists to the luminescence of crystal phosphors in the two years that had elapsed since the preceding Conference.

N. A. Tolstoi

ABBREVIATIONS FOR JOURNALS, PLACES, ETC. OFTEN REFERRED TO IN "OPTICS AND SPECTROSCOPY"**

Doklady Akad. Nauk SSSR - Proceedings of the Academy of Sciences of the USSR

Izvest. Akad. Nauk SSSR - Bulletin of the Academy of Sciences of the USSR
Ser. Fiz. - Physical Series
Ser. Mat. - Mathematical Series
Otdel Khim. Nauk - Chemical Sciences Section

Uspekhi Fiz. Nauk - Advances in Physical Sciences

Uspekhi Khim. - Advances in Chemistry

Zhur. Eksptl. i Teoret. Fiz. - Journal of Experimental and Theoretical Physics

Zhur. Tekh. Fiz. - Journal of Technical Physics

Zhur. Obshchei Khim. - Journal of General Chemistry

Zhur. Priklad. Khim. - Journal of Applied Chemistry

Zhur. Russ. Fiz.-Khim. Obshchestva - Journal of the Russian Physical-Chemical Society

Zhur. Fiz. Khim. - Journal of Physical Society

Trudy Fiz. Inst., Akad. Nauk SSSR, Fiz. Inst. im. P.N. Lebedev - Transactions of the Institute of Physics, Academy of Sciences of the USSR, named for P.N. Lebedev

Trudy Fiz.-Tekh. Inst., Akad. Nauk Uzbek. SSR - Transactions of the Physico-Technical Institute, Academy of Sciences of the Uzbek SSR

Trudy Inst. Krist., Akad. Nauk SSSR - Transactions of the Institute of Crystallography, Academy of Sciences of the USSR

Trudy Inst. Nefti, Akad. Nauk SSSR - Transactions of the Petroleum Institute, Academy of Sciences of the USSR

Trudy Gosudarst. Opt. Inst., Leningrad - Transactions of the Optical Institute in Leningrad

Trudy Inst. Fiz. i Astron., Akad. Nauk Eston. SSR - Transactions of the Institute of Physics and Astronomy, Academy of Sciences of the Estonian SSR

Trudy Inst. Fiz., Akad. Nauk Ukr. SSR - Transactions of the Institute of Physics, Academy of Sciences of the Ukrainian SSR

Trudy Vsesoyuz. Nauch.-Issledovatel. Inst. Metrol. - Transactions of the All-Union Scientific Research Institute of Meteorology

Vestnik Leningrad. Univ. - Bulletin of the Leningrad University
Ser. Fiz. i Khim. - Series on Physics and Chemistry

Vestnik Moskov. Univ. - Bulletin of Moscow University
Ser. Fiz.-Mat. i Estestven. Nauk - Series of Physical-Mathematical and Natural Sciences

Uchenye Zapiski Leningrad. Gosudarst. Univ. im. A. A. Zhdanov - Scientific Reports of the Leningrad State University named for A. A. Zhdanov
Ser. Fiz. Nauk - Series on the Physical Sciences
Ser. Khim. Nauk - Series on the Chemical Sciences

Uchenye Zapiski, Moskov. Gosudarst. Univ. im. M. V. Lomonosova - Scientific Reports, M.V. Lomonosov Moscow State University

Uchenye Zapiski Tomsk. Gosudarst. Univ. in. V. V. Kuibysheva - Scientific Reports of the Tomsk State University named for V. V. Kuibyshev

Opt. i Spektr. - Optics and Spectroscopy

Pribory i Tekh. Ekspt. - Instruments and Technique of Experiment

Astron. Zhur. - Astronomical Journal

Fiz. Metal. i Metalloved., Akad. Nauk SSSR, Ural. Filial - Physics of Metal and Metallography, Academy of Sciences of the USSR, Ural Branch

Priborostroenie - Instrument Manufacturing

Zavodskaya Lab. - Factory Laboratory

Radiotekhnika - Radio Engineering

Radiotekh. i Elektron. - Radio Engineering and Electronics

Inzhener.-Fiz. Zhur., Akad. Nauk Belorus. SSR - Engineering-Physics Journal, Academy of Sciences of White Russian SSR

Ukrain. Fiz. Zhur. - Ukrainian Physics Journal

Automat. i Telemekh. - Automatics and Telemechanics

Nauch.-Issledovatel. Fiz.-Tekh. Inst., Leningrad. Univ. - Scientific Research Institute of Physics and Technology, Leningrad University

Nauch.-Issledovatel. Radio-fiz. Inst., Gor'kii Univ. - Scientific Research Institute of Radiophysics, Gorki University

Gorkov. Issledovatel. Fiz. Tekh. Inst. - Gorki Research Institute of Physics and Technology

Gosudarst. Izd. Tekh.-Teoret. Lit. - State Publishers of Technical-Theoretical Literature

Gosudarst. Izd. Fiz.-Mat. Lit.- State Publishers of Physical-Mathematical Literature

**These abbreviations must be used by OIS translators in their translations. This list will be added to from time to time.

(FILLER MATERIAL - NOT IN RUSSIAN ORIGINAL)

Gosudarst. Opt. Inst. - State Optical Institute

Moskov. Fiz.-Tekh. Inst. - Moscow Physico-Technical Institute

Izd. Inostrannoi Lit. - Publishers of Foreign Literature

Izd. Akad. Nauk SSSR - Academy of Sciences Press

Inst. Fiz., Akad. Nauk Ukr. SSR, Kiev - Institute of Physics, Academy of Sciences of the Ukrainian SSR, Kiev

Inst. Fiz. i Astron., Akad. Nauk Eston. SSR, Tartu - Institute of Physics and Astronomy, Academy of Sciences of the Estonian SSR, Tartu

TRANSLITERATION OF CYRILLIC CHARACTERS

used by the Optical Society of America

А	а	a	Р	р	r
Б	б	b	С	с	s
В	в	v	Т	т	t
Г	г	g	У	у	u
Д	д	d	Ф	ф	f
Е	е	e	Х	х	kh
Ж	ж	zh	Ц	ц	ts
З	з	z	Ч	ч	ch
И	и	i	Ш	ш	sh
Й	й	i	Щ	щ	shch
К	к	k	Ъ	ъ	"
Л	л	l	Ы	ы	y
М	м	m	Ь	ь	'
Н	н	n	Э	э	e
О	о	o	Ю	ю	yu
П	п	p	Я	я	ya

(FILLER MATERIAL - NOT IN RUSSIAN ORIGINAL)

Superhigh-Frequency Absorption of CH_3GeF_3 . . . . . N. A. Irisova and E. M. Dianov 136 (261)
Luminescence of Ethanolamine Compounds of Platinum . . . . . A. M. Tkachuk and N. A. Tolstoi 136 (261)
Application of Perturbation Theory to the Calculation of the Ionic Refractions of Lanthanides and Actinides . . . . . L. N. Mazalov and S. S. Batsanov 137 (264)
Consideration of the Internal Field in the Determination of Raman Intensities . . . . . V. M. Pivovarov 139 (266)
The Oscillator Strength for the δ-System of the NO-Bands . . . . . S. P. Erkovich and Yu. V. Pisarevskii 141 (269)
Optical and Electrical Properties of "Weak" and "Strong" High Frequency Discharges in Neon . . . . . L. P. Razumovskaya and O. P. Bochkova 142 (271)
Approximate Prediction of the Normal Vibration Frequencies of the Hafnium Halides . . . . . A. M. Aleksandrovskaya and I. N. Godnev 144 (273)
A New Luminor: $2Li_2O - WO_3(U)$ . . . . . Yu. S. Leonov 145 (275)

EVENTS

The Ninth Conference on Luminescence (Crystal Phosphors) 146 (277)

EDITOR'S NOTE

Comments on the scientific content of the translated Russian articles published in OPTICS AND SPECTROSCOPY are invited. They should be addressed as a Letter to the Editor of the Journal of the Optical Society of America and forwarded to the Editor of that journal, Dr. W. R. Brode, National Bureau of Standards, Washington 25, D.C.

VOL. IX, NO. 2 AUGUST 1960

(Numbers in parentheses are original Russian page numbers)

Hyperfine Structure and Isotopic Shift in the Spectrum of Tl I ..... A. I. Odintsov 75 (137)

A Spectroscopic Determination of the Isotopic Composition of Carbon ..... A. N. Zaidel and G. V. Ostrovskaya 78 (142)

Intensity Distribution in the Bands of the α-System of the TiO Molecule ..... F. S. Ortenberg 80 (147)

Calculation of the Relative Transition Probabilities for Certain Band Systems of Oxides and Hydrides of the Group II Elements ..... F. S. Ortenberg 82 (151)

Rotational Analysis of Boron Monoxide Bands Located in the Vacuum Ultraviolet ..... Yu. Ya. Kuzyakov, V. M. Tetevskiy and L. N. Tunitsky 84 (156)

The Energy Levels and Wave Functions of the Disubstituted Benzene Molecule Calculated by the Method of the "Metal" Model ..... A. F. Terpugova 86 (162)

Partial Frequencies of Pyramidal Hydrides and Deuterides with Symmetry C_{3v} ..... G. I. Rybakova, B. I. Naugol'nikov, and V. P. Morozov 88 (166)

Intensities and Depolarizations in the Raman Spectra of Polymethybenzenes II. Numerical Calculation for Toluene ..... M. A. Kovner and B. N. Snegirev 90 (170)

Calculation of Intensities and Polarizations in the Vibrational Absorption Spectra of Polyatomic Molecules II ..... L. A. Gribov 93 (176)

Calculation and Interpretation of the Vibrational Spectra of Naphthenes IV. The Influence Constants of Cyclopentane ..... L. M. Sverdlov and N. I. Prokof'eva 97 (184)

Effect of Temperature on the Intensities of the Vibrational Absorption Bands of Liquid Bromoform ..... M. P. Lisitsa and Yu. P. Tsyashchenko 99 (188)

Vibration Spectra of the Silicates I. Infrared Spectra of Silicates with Anions of the Type $(Si_2O_7)^{-6}$ ..... A. N. Lazarev 103 (195)

Sensitized Fluorescence in Solutions ..... B. Ya. Sveshnikov, P. I. Kudryashov and L. A. Limareva 107 (203)

Variation in the Fluorescence of Naphthalene Derivatives as a Function of the Concentration of Hydrogen Ions in Solution ..... L. D. Derkacheva 110 (209)

Electronic-Vibrational Processes in the Luminescence Centers of Ionic Crystals ..... Ch. B. Lushchik, N. E. Lushchik, and K. K. Shvarts 113 (215)

The Nature and Kinetics of Radiation Processes in ZnS-Mn Phosphors During Excitation ..... V. L. Levshin and V. F. Tunitskaya 118 (223)

On the Scattering of Light by Dielectric Ellipsoids Comparable with the Wavelength II. Dependence of the Indicatrix of the Scattering on the Size, Form, and Orientation of the Ellipsoid. The Scattering Coefficient ..... A. V. Shatilov 123 (233)

Determination of the Size of Particles by the Scattering of Light. Nomograms for the Determination of the Size of Rod-shaped Particles ..... I. Ya. Slonim 127 (244)

Theory of Increasing the Transparency of Metallic Coatings ..... P. G. Kard 129 (248)

The Spectrovisor ..... M. M. Gurevich and K. I. Kolyadin 131 (253)

SHORT COMMUNICATIONS

The Theory of Spin-Lattice Relaxation of Nuclear Spins Surrounded by an Octahedral Complex ..... B. I. Kochelaev 133 (257)

On the Light Absorption Edge in Alkali-Earth Metal Oxides ..... V. P. Rombakh 134 (258)

Free Exciton Luminescence in a Molecular Crystal ..... Yu. M. Popov and A. S. Selivanenko 135 (260)

(Contents continued on inside back cover)